

UNCLASSIFIED

AD 267 616

*Reproduced
by the*

**ARMED SERVICES TECHNICAL INFORMATION AGENCY
ARLINGTON HALL STATION
ARLINGTON 12, VIRGINIA**



UNCLASSIFIED

NOTICE: When government or other drawings, specifications or other data are used for any purpose other than in connection with a definitely related government procurement operation, the U. S. Government thereby incurs no responsibility, nor any obligation whatsoever; and the fact that the Government may have formulated, furnished, or in any way supplied the said drawings, specifications, or other data is not to be regarded by implication or otherwise as in any manner licensing the holder or any other person or corporation, or conveying any rights or permission to manufacture, use or sell any patented invention that may in any way be related thereto.

VOLUME 1

DASA 1300

267 616

High Altitude Sampling Program

267 616

HASHP

**PURPOSE
&
METHODS**



Defense Atomic Support Agency
WASHINGTON 25, D.C.

ISOTOPES, INC.

DASA 1300

THE HIGH ALTITUDE SAMPLING PROGRAM

by

James P. Friend, Editor
Herbert W. Feely, Project Director
Philip W. Krey
Jerome Spar
Alan Walton

VOLUME I

HASP PURPOSE AND METHODS

The Final Report on Contract DA-29-044-XZ-609

Prepared for

Defense Atomic Support Agency
Washington 25, D. C.
August 31, 1961

ISOTOPES, INCORPORATED
123 Woodland Avenue
Westwood, New Jersey

ABSTRACT

The four major objectives of the High Altitude Sampling Program (HASP) were:

1. the direct measurement of stratospheric concentrations of debris from tests of nuclear weapons,
2. the determination of the stratospheric burdens of strontium-90 and of other potentially hazardous radionuclides,
3. the estimation of the stratospheric residence time of nuclear debris, and
4. the delineation of the mechanisms and rates of transfer of nuclear debris within the stratosphere and from the stratosphere to the troposphere.

To accomplish these objectives, high flying (to altitudes of 70,000 feet), long range Lockheed U-2 aircraft were used to collect filter samples of stratospheric air in a meridional sampling corridor. The samplers and the filter medium, IPC filter number 1478, were calibrated to permit accurate determination of the volumes of sampled air. About 3700 filter samples were collected and analyzed between August 1957 and June 1960. An ion-exchange technique was used to measure the first few hundred samples received, but carrier radiochemistry was used on all subsequent samples. Virtually all were analyzed for total beta activity and strontium-90 concentration. More than 300 analyses were made of each of the hazardous nuclides cesium-137 and plutonium. Shorter-lived fission products were also measured in all samples to determine the age and origin of the debris which they contained. Many samples collected before the beginning, in late 1958, of the ban on testing were assayed for barium-140. Almost all samples collected before mid-1959 were analyzed for strontium-89 or zirconium-95, and a few were also analyzed for yttrium-91. Measurements of cerium-144 were made on some samples collected during 1958 and 1959 and on most collected during 1960. One of the Hardtack tracers, tungsten-185 or tungsten-181, was measured in almost every sample collected after May 1958. Many samples collected during December 1959 - June 1960, and a few collected earlier, were analyzed for rhodium-102, the tracer for debris from an August 1958 rocket shot. Analyses of the cosmic ray product beryllium-7 were made on many samples collected during late 1959 and early 1960, and analyses of phosphorus-32 were made on a few, in order to trace stratospheric mixing processes.

The interpretation of the HASP data is restricted somewhat by the limitation of sampling to altitudes below 70,000 feet and to latitudes between 71° North and 57° South. However, using data from three B-52 sampling flights to the

North Pole and results from the USAEC Project Ashcan, the HASP data have been extrapolated to the remainder of the stratosphere.

Throughout the nearly three years of HASP sampling the stratospheric concentrations of nuclear debris were found to vary with altitude, latitude and time. Concentrations of all fallout nuclides were found to increase with altitude above the tropopause, but presumably all passed through a maximum and then decreased to zero in the highest regions of the atmosphere. In the tropical stratosphere the maximum concentrations of strontium-90 normally lay above 70,000 feet, but the maximum concentrations of tungsten-185 lay between 65,000 and 70,000 feet. In the polar stratosphere the maximum concentrations of strontium-90 were found below 70,000 feet during 1958 but, in the Northern Hemisphere at least, at or above 70,000 feet during 1959, apparently because of the influx of debris from high yield Hardtack shots, and during 1960, evidently as a result of influx of debris from the high altitude rocket shots. The maximum concentrations of tungsten-185 in the polar stratosphere were found at about 50,000 to 60,000 feet at all times after mid-1958.

Typically, maximum concentrations of nuclear debris were found near the latitude of injection. Thus, during 1957 and 1958 the highest concentrations of beta activity and of strontium-90 were found in the northern tropical and northern polar stratosphere. During 1959 high concentration persisted in the northern tropical stratosphere, but the rapid fallout of debris from Soviet injections eliminated the polar maximum. By 1960 the influx of debris into the polar stratosphere from the high tropical stratosphere produced concentrations in the polar regions which were the highest to be found below 70,000 feet, though still higher concentrations presumably existed in the high tropical stratosphere above the limits of HASP sampling. Higher concentrations of debris were found in the Northern Hemisphere than in the Southern, as expected. The Northern Hemisphere apparently contained about 75 percent of the stratospheric debris in late 1958, but less than 60 percent by mid-1960.

The stratospheric burden of strontium-90, from sources other than the high altitude rocket shots, was about 2.4 megacuries by the end of 1958, about 1.1 megacuries by mid-1959 and about 0.8 megacurie by mid-1960. About 0.08 megacurie of strontium-90 from the rocket shots had entered the lower stratosphere (below 40 millibars) by mid-1960. During 1958-1960 the ratio $Cs^{137}/Sr^{90} = 1.7 \pm 0.4$ in stratospheric debris and was virtually independent of latitude, altitude and time. The ratio $Pu/Sr^{90} = 0.017 \pm 0.007$, but varied somewhat with the source of the debris.

The apparent residence half time of nuclear debris in the stratosphere, calculated from changes in the stratospheric strontium-90 burden, was about 10 months during 1958-1959 and about 18 months during 1959-1960. The fallout rates from the lower stratosphere, below 40 millibars, were faster with a residence half time of about 6 months during 1958-1959 and about 12 months during 1959-1960.

At all times after its injection into the stratosphere in 1958, the highest concentrations of tungsten-185 were found in a layer which sloped from the equator toward the poles. The measurements of strontium-90 indicated a similar distribution of maximum concentrations of that nuclide, but the layer of maximum strontium-90 was at higher altitudes. These distributions are consistent with the concept of diffusion of debris poleward by large scale, quasi-horizontal turbulent mixing, together with vertical mixing in the polar stratosphere. The observed spread of tungsten-185 and of strontium-90 from specific shots indicates that the meridional horizontal mixing coefficient, K_y , is about $10^9 \text{cm}^2 \text{sec}^{-1}$ and the vertical mixing coefficient, K_z , is about $10^3 \text{cm}^2 \text{sec}^{-1}$ or less in the tropical stratosphere and about $10^4 \text{cm}^2 \text{sec}^{-1}$ in the polar stratosphere. If a meridional circulation exists in the stratosphere, it is a second order effect at best as far as the transfer of radioactive debris in the stratosphere is concerned.

The calculated rate of vertical mixing through the tropopause is considerably smaller than the observed fallout rate, and much of the loss of debris from the stratosphere must occur either by an organized downward movement of air through the polar tropopause or, more likely, by horizontal turbulent mixing or organized meandering of air currents through the tropopause gap region.

Measurements of fallout at the earth's surface indicate that between 0.4 and 0.5 megacurie of strontium-90 fell out during 1955-1956 and during 1956-1957, about 0.9 megacurie fell out during 1957-1958, 1.3 megacurie during 1958-1959 and 0.6 megacurie during 1959-1960. The surface burden of strontium-90 was about 2.3 megacuries in July 1958, about 3.6 megacuries in July 1959, and about 4.2 megacuries in July 1960. These estimates have an uncertainty of about $\pm 40\%$. Continued fallout after July 1960 should result in a maximum surface burden of about 4.5 megacuries in 1962-1963, which should subsequently decrease almost with the half life of strontium-90.

HASP data have played an important role in recent years in testing the validity of theories on world-wide fallout. The HASP estimates of the stratospheric burden of debris, despite their limitations, are the best that have yet been made. The principal remaining uncertainty concerns the exact concentration of debris at altitudes above 70,000 feet. The short stratospheric residence time of most debris from past nuclear weapons tests, indicated by HASP measurements, has been substantiated by other programs of fallout study. The HASP data have also served to disprove fairly conclusively the supposed primary importance of a meridional circulation in transferring debris within the stratosphere.

The short stratospheric residence time of nuclear debris which is indicated by HASP data probably resulted in the rapid attainment of maximum concentrations of strontium-90 in human bone in 1959. If biologic uptake of strontium-90 varies more directly with the rate of fallout than with the cumulative surface deposit, concentrations in newly formed bone will decrease rapidly in future years, unless weapon testing is resumed. The genetic dose rate from cesium-137 is only a

small percentage of the MPD, and may be of less significance than the dose rate from carbon-14 when the infinite time dose to many generations from artificial carbon-14 is considered. The short stratospheric residence time of nuclear debris results in a greater potential hazard from short-lived gamma emitters than was once realized. In addition the radiation dose delivered to the lungs, lymph nodes and gonads by plutonium, which enters the body mainly by inhalation, appears to constitute about the same fraction of the MPC as does the dose delivered to the bone tissue by strontium-90. Evidently the irradiation of the human population by world-wide fallout from weapons tests performed before 1959 has not reached and will not reach levels which, by current standards, would be considered hazardous.

Several supplementary studies were conducted during HASP. One of these involved the investigation of the physical and chemical properties of stratospheric dust. Particles collected by means of impactor probes were studied using optical and electron microscopy and electron diffraction. Particles collected in filter samples have been investigated by means of autoradiography and neutron activation. Most particles in impactor samples consisted of ammonium sulfate or ammonium persulfate, and varied in diameter between 0.2 and 1 micron. A small number of larger particles (up to 15 microns in diameter) of three types were observed. Neutron activation analysis of particles in filter samples gave upper limits for the possible concentration of a number of elements in stratospheric dust. The autoradiography of thin sections of filters indicated that less than 1.5 percent of the radioactive particles penetrated more than 90 percent of the way through the filters.

Other supplementary studies included the measurement of carbon-14 in tropospheric carbon dioxide and of tritium in precipitation in Bergen County, New Jersey, the delineation of the vertical distribution of fallout nuclides in some New Jersey and Kansas soils, and some measurements of plutonium concentrations in man and his environment. Carbon-14 concentrations in tropospheric carbon dioxide at Washington Township, New Jersey passed through a minimum in January 1961, probably due to transient local effects. Seasonal variations in the fallout rate of tritium were similar to those in the fallout rate of strontium-90, indicating that similar factors probably govern the removal of gaseous and particulate debris from the stratosphere and from the troposphere. The fallout rate of tritium seems to depend upon the latitude and conditions of the weapon detonation which produced it. In the typical New Jersey soils in 1960, about 55 percent of the total strontium-90 deposit was contained in the upper 2 inches, about 79 percent in the upper 4 inches, and about 96 percent in the upper 9 inches. Strontium-90 appeared to have penetrated to greater depths in the soil than had cesium-137. Ruthenium-106 appeared to have penetrated more completely through the upper few inches of the soil than had cerium-144, but this relationship was reversed below 2 inches. The permeability and drainage of the soil appear to be the major factors in controlling the vertical distribution of activity below the surface.

Average soil concentrations in New Jersey in July 1960 were 75 mc Sr⁹⁰/mi², 155 mc Cs¹³⁷/mi², 295 mc Ce¹⁴⁴/mi², and 160 mc Ru¹⁰⁶/mi². The combined activity of the three gamma-emitting nuclides was sufficient to produce a genetic dose rate which was less than 3 percent of the maximum permissible. Measurements of plutonium in foodstuffs and in human tissue indicated the concentration of this nuclide in the lungs, lymph system and gonads.

PREFACE

This is the Final Report of the High Altitude Sampling Program, and describes all techniques employed, all results obtained and all conclusions reached during that program. Included in it are all data presented earlier in the quarterly reports, annual reports and published papers prepared under Contract DA-29-044-XZ-609.

History of the High Altitude Sampling Program

The Joint Chiefs of Staff, realizing the seriousness and complexity of the problem of contamination of the entire world population by radioactive fallout from nuclear tests or atomic warfare, requested in the early fall of 1954 that the Defense Atomic Support Agency (then known as the Armed Forces Special Weapons Project) study and evaluate this problem on a continuing basis. After considerable study of the problem within DASA during 1955, it was determined that the largest uncertainty in the prediction of the distribution and concentration of world-wide fallout debris on the surface of the earth is the quantity of fission products in the stratospheric reservoir and the rate and mode of their transfer. Thus, DASA, early in 1956, initiated a research program to define and delineate the stratospheric reservoir of fission debris. This program became known as the High Altitude Sampling Program, or Project HASP. A contract was let in September 1956 with the Institute of Paper Chemistry, Appleton, Wisconsin for further development and calibration of the filtering medium, IPC filter paper No. 1478.

A contract was let in February 1957 with Isotopes, Inc., Westwood, New Jersey, to provide scientific direction and interpretation, and to perform the radiochemical analyses. Based on theoretical work by Professor E. G. Reid Stanford University, Lockheed Aircraft Corp. designed and built a filter sampler which was installed in the nose position as an integral part of each of six Lockheed U-2 aircraft assigned to DASA for carrying out Project HASP. The operational responsibility for carrying out HASP sampling was assigned to the Strategic Air Command (SAC), and sampling began after the assignment of the six DASA U-2's to the 4080th Strategic Reconnaissance Wing (4080th SRW) in August and September 1957.

In November 1957 a meridional sampling corridor was established along the 70° West meridian in the Northern Hemisphere and in September 1958 it was extended into the Southern Hemisphere along the 64° West meridian. From September 1959 to May 1960, sampling was again restricted to the Northern Hemisphere, but in May-June 1960 the Southern Hemisphere was resampled briefly before the program was terminated. Almost 4000 filter samples of stratospheric radioactivity were collected and analyzed radiochemically during the program, and this report is concerned mainly with these analyses. Other problems, related to the main objectives of HASP, were also studied, however, and the methods used during these studies and their results are also discussed here.

Organization of the Report

The work performed during HASP is presented in three parts in this report. Part I encompasses the radiochemical analysis of filter samples of stratospheric air. Part II describes the physical and chemical investigations of stratospheric particles. Part III contains the descriptions of several supplementary studies of fallout which were carried out during HASP.

The report is divided into five volumes because of its bulk. The first four volumes contain Part I and the fifth volume contains Part II and Part III. In Volume 1 are given some introductory remarks and a description of the procedures used in sampling and in performing radiochemical analyses. The results of the radiochemical analysis of the filter samples are given in tables and diagrams in Volume 2. Volume 3 contains a discussion of the analytical data in terms of the stratospheric distribution of nuclear debris and its meteorological significance. In Volume 4 the HASP data are applied to the problems of describing and explaining the world-wide distribution of fallout. The surface burden of strontium-90 is calculated, HASP data are compared to results of other programs, and future hazards from fallout are evaluated. A summary of the results and conclusions obtained from the filter analyses is given. Volume 5 contains Part II of the report, in which the methods of collecting and studying stratospheric particles are discussed and the resulting data are interpreted, and Part III, in which carbon-14 measurements of tropospheric air and tritium measurements of precipitation are reported, data on the vertical distribution of nuclear debris in soil are given, and the hazard from plutonium in man and in his environment is discussed.

Acknowledgements

This report has been prepared at Isotopes, Inc. by those senior research personnel and consultants who have been most directly involved in the performance of work on the program since its inception. In Part I of the report, Chapter 1 "Introduction," Chapter 2, "The Problem," Chapter 4, "Analytical Results," Chapter 5, "The Distribution of Nuclear Debris in the Stratosphere," Chapter 8, "Remaining Problems in World-Wide Fallout," and Chapter 10, "Summary and Conclusions," were written principally by H. W. Feely. Chapter 3, "Procedures," was written by H. W. Feely, J. P. Friend, and P. W. Krey. Chapter 6, "Meteorological Processes and Radioactivity," was written principally by Professor J. Spar. Chapter 7, "The Surface Burden of World-Wide Fallout," and Chapter 9, "The Hazards from Radioactive Fallout," were written by A. Walton. Part II of the report, "Studies of Stratospheric Particles," was written principally by J. P. Friend. In Part III, Chapter 1, "Measurements of Carbon-14 in Tropospheric Air," and Chapter 2, "Measurements of Tritium in Precipitation," were written principally by A. Walton. Chapter 3, "The Distribution of Radioactivity in Soils," was written by A. Walton and P. W. Krey. Chapter 4, "Plutonium in Man and Environment," was written by P. W. Krey. Appendix A, "Recalibration of the U-2 Particulate Samplers," was written by Professor E. G. Reid. F. Bazan, R. J. Lagomarsino, R. D. Sherwood and M. Trautman aided in the preparation of descriptions of analytical procedures.

Many organizations and individuals contributed to the success of HASP during its more than four years of existence. Many personnel of the Defense Atomic Support Agency, especially Dr. F. H. Shelton, Lt. Col. H. C. Rose,

Lt. Col. R. W. Swanson, Major L. E. Trapp, Major A. K. Stebbins, III, Cdr. R. S. Sullivan and Mr. J. W. Watson, played important roles in organizing and administering the program. We wish to acknowledge the important contributions to the technical aspects of the program which were made by Major Stebbins, in addition to thanking him for his initiative and resourcefulness in handling administrative problems.

The personnel of the 4080th SRW, of the Air Rescue Service and of other United States Air Force groups performed well the difficult tasks of the sampling program. We wish to thank the many Air Force personnel who facilitated the collection of special impaction samples and samples for neutron activation analysis during regular Crowflight missions.

The sampling program was possible only because of the cooperation of the Government of Argentina, which provided base rights at Ezeiza Airport, and of the Governments of Canada, Mexico, Venezuela, Brazil, Bolivia and Paraguay which provided overflight rights.

The work of Dr. J. A. Van den Akker of the Institute of Paper Chemistry on the development and calibration of IPG filter paper No. 1478, and the work of Professor E. G. Reid of Stanford University on the design and calibration of the Lockheed U-2 samplers was essential to the success of the program. The studies of stratospheric particles were aided immeasurably by the cooperation of Dr. C. Junge and Mr. J. Manson in supplying the impaction probe samplers which they had designed and built.

Help in planning the program of soil sampling and analysis was supplied by Dr. J. C. F. Tedrow of Rutgers University and by several employees of the United States Department of Agriculture.

Stimulating conversations with many scientists about the problems of measuring and interpreting world-wide fallout have been extremely helpful. We especially wish to thank L. Machta and R. List of the United States Weather Bureau, Professor W. F. Libby of the University of California, J. Van den Akker and L. Dearth of the Institute of Paper Chemistry, Lt. Col. I. Russell of the United States Air Force, M. Kalkstein, C. Junge and J. Manson of the Air Force Cambridge Research Laboratories, D. Lal of the Tata Institute, J. Harley of the U. S. A. E. C., New York Operations Office, L. Lockhart of the Naval Research Laboratory, and W. Broecker and A. Schulert of the Lamont Geological Observatory. We are also extremely grateful to all of the participants at the July 1960 Conference on Delayed Fallout in London for the ideas and information which they shared with us.

Many individuals at Isotopes, Inc. have contributed to the performance of HASP. Although we will mention here only the scientific personnel, many technicians, clerks and typists have also performed important tasks.

During the first year and a half of HASP the direction of the program was the responsibility of D. R. Carr and H. L. Volchok and then of J. L. Kulp. During the final few years of the program, H. W. Feely was the project director. Meteorological interpretation of the data was supplied by Professor J. Spar, who served as a consultant throughout the duration of the program. The design and direction of the program of radioclimical analyses was the responsibility of

P. W. Krey. J. P. Friend analyzed the data on the calibration of the samplers and of the filter medium for HASP and directed the studies of stratospheric particles. A. Walton interpreted data on surface fallout, including measurements of carbon-14 in tropospheric air and tritium in precipitation, for HASP, evaluated the potential hazard from fallout and directed the program of soil sampling.

Other scientific personnel who have made important contributions to HASP are C. R. Barnett, F. Bazan, D. Bogen, B. A. Caridi, E. M. Franz, E. French, R. Fried, P. A. Kluff, R. J. Lagomarsino, W. M. Martin, P. Rey, R. D. Sherwood, I. Schulz, and M. Trautman.

GENERAL TABLE OF CONTENTS

Volume 1. HASP Purpose and Methods

Abstract

Preface

Part I. Stratospheric Radioactivity

Chapter 1. Introduction

Chapter 2. The Problem

Chapter 3. Procedures

Appendix A. Recalibration of the U-2 Particulate Samplers

Volume 2. Results of Filter Analyses

Part I. (Continued)

Chapter 4. Analytical Results

Volume 3. Discussion of HASP Results

Part I. (Continued)

Chapter 5. The Distribution of Nuclear Debris in the Stratosphere

Chapter 6. Meteorological Processes and Radioactivity

Volume 4. The Application of HASP Data

Part I. (Continued)

Chapter 7. The Surface Burden of World-Wide Fallout

Chapter 8. Remaining Problems in World-Wide Fallout

Chapter 9. The Hazards from Radioactive Fallout

Chapter 10. Summary and Conclusions

Volume 5. Supplementary HASP Studies

Part II. Studies of Stratospheric Particles

Chapter 1. Introduction

Chapter 2. Physical Methods of Particle Studies

Chapter 3. Neutron Activation of Filter Samples

Chapter 4. Analytical Results

Chapter 5. Discussion and Conclusions

Part III. Measurements of Fallout in Man's Environment

Chapter 1. Measurements of Carbon-14 in Tropospheric Air

Chapter 2. Measurement of Tritium in Precipitation

Chapter 3. The Distribution of Radioactivity in Soils

Chapter 4. Plutonium in Man and Environment

VOLUME 1

TABLE OF CONTENTS

Abstract	
Preface	
Part I. Stratospheric Radioactivity	
Chapter 1. Introduction	1
Objectives of HASP	2
Methods Used to Achieve the Primary Objectives	3
Results Obtained During HASP	5
Chapter 2. The Problem	7
The Need for Stratospheric Sampling	8
The Desirability of Aircraft Sampling	11
References	12
Chapter 3. Procedures	15
The Sampling Program	16
The Basic Plan	16
Accomplishments of the Sampling Program	22
Representativeness of the Data	33
The U-2 Duct Samplers	43
Nose Sampler	43
Hatch Sampler	45
Operation of Samplers	45
Handling of Samples	47
The Filter Sampling Medium	48
Particle Retention	49
Pressure Drop-Flow Rate Characteristics	50
The Computation of Sample Volumes	61
Calibration of Duct Samplers	62
Construction of Flow Rate Calibration Curves	63
Determination of Flow Rates for Temperatures Different From the Standard Atmosphere	68
Method of Calculating HASP Sample Volumes	74
Reproducibility of HASP Sampling	76
The Distribution of Activity on the Filter	77
Reproducibility of Sampling	83
Sample Pretreatment	91
Total Beta and Gamma Analysis	91
Ashing and Dissolution	93

Ion Exchange Technique	97
Zirconium Separation	97
Mode of Operation	99
Carrier Radiochemistry	103
Sequential Radiochemical Separation of Beryllium-7, Phosphorus-32 and Rhodium-102	105
Sequential Radiochemical Separation of Sodium-27 and Calcium-45	106
Sequential Radiochemical Separation of Strontium-89, 90, Yttrium-91, Zirconium-95, Cesium-137, Barium-140 and Cerium-144	107
Beryllium-7 Purification Procedure	110
Sodium-22 Purification Procedure	112
Phosphorus-32 Purification Procedure	113
Calcium-45 Purification Procedure	115
Yttrium-90 Purification Procedure	117
Strontium-89, 90 Purification Procedure	118
Yttrium-91 Purification Procedure	119
Zirconium-95 Purification Procedure	121
Rhodium-102 Purification Procedure	127
Iodine-131 Purification Procedure	130
Cesium-137 Purification Procedure	133
Barium-140 Purification Procedure	135
Cerium-144 Purification Procedure	140
Tungsten-181, 185 Purification Procedure	142
Plutonium-239 Purification Procedure	145
Reagents	149
Radiometric Assay Techniques	153
Beta Counters	153
Alpha Counters	163
Gamma Counters	165
Counter Calibration and Accuracy	170
Quality Control	174
References	182
Appendix A. Recalibration of the U-2 Particulate Samplers.	185

VOLUME 1

LIST OF TABLES

3.1	Flight Tracks of Crowflight Missions	20
3.2	Distribution of Samples Collected during Phases 1 and 2	31
3.3	Distribution of Samples Collected during Phase 3.	31
3.4	Distribution of Samples Collected during Phase 4.	32
3.5	Distribution of Samples Collected during Phase 5.	32
3.6	Parameters Used to Determine Duct Flow Rates	64
3.7	Percent Standard Deviation From the Mean of Analyses of Samples for which Two or More Quadrants were Analyzed Separately.	80
3.8	The Total Beta Activity of 40 Disks Cut From Sample 3723	80
3.9	The Uniformity of Total Beta Activity Across a Filter.	84
3.10	Standard Deviation of Sample Pairs Collected Simultaneously	84
3.11	Comparison of Calculated With Measured Relative Collection Efficiencies of Hatch and Nose Samplers	86
3.12	Standard Deviation of Sample Pairs Collected on a Single Mission at the Same Latitude, Longitude and Altitude	88
3.13	Standard Deviation of Nose Samples Collected at Different Longitudes but the Same Latitude and Altitude during a Single Mission	89
3.14	Feasibility of the Nb ⁹⁵ growth Method for the Calculation of Zr ⁹⁵ Activity	126
3.15	Comparison of Zr ⁹⁵ Analyses by Radiochemical Separation with Gamma Ray Spectrum Analyses	126
3.16	Comparison of the Ba ¹⁴⁰ Assay by Direct Gamma Spectrum Analyses and by Radiochemical Separation and Analysis	139

3.17	Summary of Radioassay Techniques	173
3.18	Interlaboratory Calibration Number 1	178
3.19	Comparison of Quadrant Analyses Between Laboratories	179
3.20	Interlaboratory Calibration Number 2	179
3.21	Analyses of Standard Uranium-235 Fission Solution	181
3.22	Reproducibility of Radiochemical Analyses	181

VOLUME 1

LIST OF FIGURES

3.1	Flight Tracks for HASP Sampling	21
3.2	Types of Missions Flown during HASP	24
3.3	Section Along the Meridional Sampling Corridor	39
3.4	The Location of the U-2 Duct Samplers	44
3.5	Schematic Representations of the Duct Samplers	46
3.6	Characteristics of 14.3 Gram Filters	53
3.7	Filter Characteristics Found by Van den Akker	55
3.8	Schematic Relationship of Calibration Parameters to Sampler	65
3.9	Recorded Pressure Drop Across Filter (hatch)	66
3.10	Recorded Pressure Drop Across Filter (nose)	67
3.11	Standard Atmosphere Flow Rates (nose)	69
3.12	Standard Atmosphere Flow Rates (hatch)	70
3.13	Standard Flow Rates (nose)	71
3.14	Standard Flow Rates (hatch)	72
3.15	Location of Disks used to Determine Variation of Total Beta Activity Across Sample 3723	81
3.16	Mounting Small Disk on Brass Planchet	92
3.17	Tracerlab Filtering Apparatus	95
3.18	Brass Planchet	96
3.19	Diagrammatic Sketch of Ion Exchange Column	98
3.20	Automatic Fraction Collector.	100

3.21	Elution Curve of Cesium, Strontium, Cerium, and Barium Tracers.	101
3.22	Flow Diagram for the Analysis of Air Filter Samples, Ion Exchange Method	102
3.23	Baseline Subtraction of Zr ⁹⁵ -Nb ⁹⁵ Photoelectric Peak.	123
3.24	Zr ⁹⁵ -Nb ⁹⁵ Photopeak as a Function of Time	124
3.25	Empirical Decay of Separated Rhodium Samples	129
3.26	Iodine Distillation Apparatus.	132
3.27	La ¹⁴⁰ 1.6 Mev Gamma Ray of Standard Ba ¹⁴⁰ Sample	137
3.28	La ¹⁴⁰ 1.6 Mev Gamma Ray from HASP Sample No. 592	138
3.29	Electrodeposition Cell	147
3.30	Electroplating Cells and Apparatus	148
3.31	High Level Beta Counter	155
3.32	Low Level Beta Counter, Model CCL-4	156
3.33	Low Level Beta Counter, Model CCL-4C	158
3.34	Diagram of the Defined Geometry System of the Tracerlab T6C-2 Muller Tube	159
3.35	4 Pi Beta Counter.	162
3.36	Alpha Counter Head and Slide	164
3.37	Alpha Particle Spectrometer.	166
3.38	Bulk Spectrometry Facility.	169
3.39	Efficiency Curve for 100-Channel Gamma Ray Spectrometric . . .	171

THE HIGH ALTITUDE SAMPLING PROGRAM

PART I

STRATOSPHERIC RADIOACTIVITY

CHAPTER 1
INTRODUCTION

The High Altitude Sampling Program (HASP) was initiated by The Defense Atomic Support Agency (DASA) to permit direct measurement of the concentrations of strontium-90, cesium-137 and other potentially hazardous constituents of radioactive fallout in the stratosphere and to provide data from which the rates and mechanisms of diffusion of this debris through and out of the stratosphere might be deduced. The prediction of the future hazard to the human population from radioactive fallout from past and future tests of nuclear weapons requires an estimation of the amount of debris held in the stratosphere and its rate of release to the troposphere and thence to the ground. Indirect estimates of the stratospheric burden of fallout had been made using surface measurements of fallout rates and estimates of stratospheric injections of debris, but the results had frequently been inconclusive or mutually contradictory. Direct measurement of stratospheric concentrations was undertaken in HASP by radiochemical analysis of filter samples of stratospheric dust collected by means of Lockheed U-2 aircraft. The radiochemical data, together with other data which were gathered during the program, have been studied in the light of the known properties of nuclear debris and of stratospheric meteorology. Estimates have been prepared of the stratospheric burden of strontium-90, cesium-137, plutonium and other radionuclides and stratospheric residence times of such debris have been calculated.

OBJECTIVES OF HASP

The prime objectives of the High Altitude Sampling Program were:

1. the determination of the quantities of various radionuclides in the stratospheric reservoir and the distribution of this debris as a function of latitude, altitude and time,
2. the estimation of the residence times of these radionuclides in the stratospheric reservoir, and
3. the determination of the mechanisms and rates of mixing and transfer of this debris within the stratosphere and into and through the troposphere.

These objectives were to be accomplished by the measurement of radionuclide concentrations in filter samples of stratospheric dust collected by Lockheed U-2 aircraft. The sampling operation was designed to obtain the maximum amount of useful information from the available sampling capability. A mixing-transfer model was to be constructed using the information gained on the change with time of concentrations of debris in various regions of the stratosphere. This model was then to be used to assimilate all available information on world-wide fallout into a coherent picture.

A number of secondary objectives were adopted as work under HASP proceeded and it became evident that contributions could be made by studying other aspects of world-wide fallout. Physical and chemical measurements were made of particles of stratospheric dust collected on the filters and on special impaction probes designed by C. Junge of AFCRL. A number of radiochemical analyses were made of fission products in cores of soil to provide

information on the vertical distribution of fallout nuclides in soil. Such information is needed to assess the gamma dose rate to the human population from energetic gamma emitters in fallout. The concentrations of tritium in precipitation and carbon-14 in tropospheric air were monitored to give information on the fallout rate of gaseous nuclear debris. A small number of samples of human and animal tissue were analyzed for plutonium to assess the significance of the potential hazard from the presence of this long lived alpha emitter in fallout from nuclear weapon tests. Data from all of these studies have been used in analyzing the future hazard from fallout from past weapon tests and from possible future weapon tests.

Full descriptions of the work done toward the achievement of the secondary objectives are given in Parts II and III of this report. Part I of the report deals only with work done toward the accomplishment of the primary objectives.

METHODS USED TO ACHIEVE THE PRIMARY OBJECTIVES

•
•
•
•
The High Altitude Sampling Program became possible when the Lockheed U-2 aircraft was developed and was made available to DASA, for this aircraft alone had the range and altitude capability which were needed to sample a large part of the lower stratosphere. Also of great importance to the initiation of HASP were the development at the Institute of Paper Chemistry of a filter medium, I. P. C. 1478, of low resistance to air flow at high velocities but with high collection efficiency under flight conditions, and the theoretical and

experimental aerodynamic investigation by Professor E. G. Reid of Stanford which showed that the volume of air sampled by a filter under flight conditions could be accurately determined.

The program got underway when six Lockheed U-2 aircraft were assigned to the 4080th Strategic Reconnaissance Wing of S. A. C. during August and September 1957 to carry out Crowflight, the sampling operation of HASP. In November 1957 sampling was begun along a meridional network in the Northern Hemisphere and in September 1958 the sampling network was extended into the Southern Hemisphere. A more intensive sampling of the Northern Hemisphere was begun in September 1959 and in May and June 1960 the sampling program was completed with a brief resampling of the stratosphere of the Southern Hemisphere.

The filter samples collected during Crowflight were sent to Isotopes, Inc. in Westwood, New Jersey where they were analyzed radiochemically for total beta activity and for their concentrations of hazardous nuclides such as strontium-90, cesium-137 and plutonium. Analyses were also made for shorter lived fission products, such as barium-140, strontium-89, zirconium-95 and cerium-144, the relative concentrations of which indicate the age of the debris and the amount of fractionation it has undergone. Following the injection of large quantities of tungsten-185, tungsten-181 and rhodium-102 into the stratosphere by some weapons detonated during the Hardtack test series, these nuclides were also measured in some HASP samples. Finally, to provide additional information on stratospheric mixing processes, a series of samples were analyzed for beryllium-7 and phosphorus-32, which are produced by cosmic

ray interaction with air in the stratosphere.

The volume of air represented by each sample was calculated using flight data supplied by the 4080th S. R. W. The concentrations of the various radionuclides in stratospheric air were then calculated using these volumes and the radiochemical data. Meteorological data, obtained from the United States Weather Bureau and from the weather officers of the 4080th S. R. W. were used to reconstruct the meteorological conditions in the stratosphere at the time of the sampling and the radionuclide concentrations were interpreted in terms of these meteorological conditions.

RESULTS OBTAINED DURING HASP

The primary objectives of the High Altitude Sampling Program have all been accomplished satisfactorily, though many aspects of the behavior of nuclear debris in the stratosphere are still understood only vaguely. Still, an estimate of the stratospheric burdens of strontium-90 and cesium-137 has been made which is much more accurate and precise than those which were made in the past. It became clear as the program progressed that all of the widely accepted estimates of the stratospheric burden of strontium-90 were too high and that, as a result, calculated stratospheric residence times of nuclear debris were too long. Observations of the distribution of the various radionuclides in the stratosphere and the changes which have occurred in these distributions with time have been used to elucidate the paths and rates of mixing and transfer within

the stratosphere. Data on tungsten-185, injected by some surface bursts during Hardtack, have been especially useful in demonstrating the nature of lateral mixing within the lower stratosphere. Data on rhodium-102, injected at very high altitudes by rocket bursts during Hardtack, together with data on cerium-144 have given valuable information on the path followed by debris from high altitude injections. The seasonal character of the processes which affect the transfer and mixing of debris within the stratosphere have been made evident by observations of changes in the distribution of strontium-90. These concepts have been used to recalculate the probable future rates of fallout and the expected surface burdens of strontium-90 and other hazardous nuclides. In light of these predictions the future hazards from fallout from past nuclear weapon tests have been reevaluated.

The techniques used during the High Altitude Sampling Program, the results obtained and the conclusions reached are discussed in full detail in this report.

CHAPTER 2

THE PROBLEM

With the advent of high yield thermonuclear weapons in 1952 a new scientific problem, the behavior of long range radioactive fallout from such weapons became of intense interest. Even before Operation Ivy the first steps had been taken to assess the extent of the world-wide fallout of radioactive debris from nuclear weapon tests¹, for it had become evident that such fallout was of medical, sociological and political significance.

The fireballs which are produced by the explosion of nuclear weapons are extremely hot and, because of their buoyancy, they rise rapidly to great heights, cooling as they rise. When they reach thermal equilibrium with the surrounding air their ascent is stopped and the radioactive cloud into which they have evolved begins to spread laterally. The large hot fireballs from high yield weapons will often rise through the tropopause and penetrate the stratosphere before reaching equilibrium. Large particles of debris which condense in the cooling cloud fall back to the ground within a few hours or days regardless of the height of stabilization of the cloud, but the fallout rate of the fine particles, which remain in suspension, is dependent upon the meteorological processes which subsequently affect the air which contains them. Many months or years may be required for much of the nuclear debris which has been injected into the stratosphere to escape into the troposphere and fall back to the surface of the earth. These long residence times of debris in the stratosphere permit it to spread about the earth and to be deposited ultimately as "world-wide fallout". In 1957, when the High Altitude Sampling Program was initiated, neither the total burden nor the residence time of radioactive debris in the stratosphere was known with any degree of certainty. Consequently, two basic parameters needed for the estimation of the future hazard

from fallout produced by past and future tests were unknown. As it became increasingly clear that these parameters could not be determined accurately using only surface fallout measurements, the need for a program like HASP became evident.

THE NEED FOR STRATOSPHERIC SAMPLING

Many different techniques have been used to sample radioactive fallout in man, in his diet and in his immediate environment, and analyses of these samples have indicated the relative hazard from fallout at the time of sampling; but the prediction of future hazards cannot be accomplished without the sampling of regions such as the stratosphere which, though remote from man, play an important role in the ultimate distribution of fallout.

The most obvious object of investigation for the assessment of biological hazards from fallout is man himself. This was realized quite early in the "atomic era", and Project Sunshine¹ was begun to investigate the potential danger to man from strontium-90 by analyzing human tissues (and other materials) for their concentrations of this nuclide. Since 1953 many analyses have been made of strontium-90 in humans, especially in bones². Human tissue has also been analyzed for other potentially dangerous nuclides^{3, 4, 5}, such as cesium-137, iodine-131 and plutonium. As a result, a good deal of information is available on the concentrations of strontium-90 and cesium-137 in humans and on their dependence upon the subject's geographical location, culture, age, sex, etc. On the other hand, very little is still known about the occurrence of the other fallout nuclides in man. Moreover the biological effects which should result from the observed concentrations are only poorly defined. In spite of these limitations, it is possible to measure the present average body burden of at least two of the most

dangerous of the constituents of fallout and to relate them statistically to any changes in the rate of human maladies which might be attributable to increases in ionizing radiation in the body.

Two important aspects of fallout hazard are not illuminated by analyses of human tissue, however. The first of these is the amount of external radiation to which the body is subjected because of the fallout gamma emitters in the air and in the soil, and the second is the probable future rate of change of the levels of internal and external radiation.

Information pertinent to both of these questions is obtained by the analysis of environmental materials; the air which man breathes, the water he drinks, the food he eats and the soil on which he walks and on which he grows his food. There are several programs for the regular sampling of the radioactivity in ground level air^{6, 7} and a U. S. A. E. C. program for the periodic sampling of strontium-90 in soil⁸. One of the uses of the data from these programs is the calculation of the external gamma dose rate to the population. These data are also employed in the calculation of future hazards. The concentration of radioactivity in drinking water is monitored by many private water companies as well as by Federal agencies⁷, and the U. S. Atomic Energy Commission regularly analyzes the strontium-90 content of certain water supplies⁹. A number of investigations have been made of strontium-90 and other nuclides in the human diet^{10, 11, 5} and especially in milk¹². The information gained from all of these measurements may be combined to give a fairly good picture of the radiation doses to which the populations under study are being subjected at a particular time. It is not a simple matter to extrapolate this information to other populations which have a different culture, for the concentrations of strontium-90 which will be deposited in bone, for example, depend quite strongly on the chemical as well as the radiochemical composition of the diet. Thus the strontium-90 concentrations in human tissue are influenced by the amount of calcium available

in the diet. In a culture in which children do not regularly get milk, with its high calcium content and low strontium-90 to calcium ratio, their bones will be built with calcium from other sources, principally vegetable, and, as a result, will accumulate relatively high concentrations of strontium-90.

The prediction of future changes in the concentration of strontium-90 and other nuclides in the human diet, and the human body requires a knowledge of the amount of fallout which has been deposited on the surface of the earth and the rate at which it will be deposited during coming years. For several years the concentration of fallout in precipitation has been measured at a number of sites throughout the world¹³. The gummed-paper network of the U. S. A. E. C. gave rough data on fallout rates during the years that the rainfall collection network was being established¹⁴. The combination of precipitation and soil analyses permits the calculation of the present and past rates of fallout and, added to data on fallout concentrations in the diet, should permit the determination of the relative rates of uptake by plants of old and fresh fallout. The extent to which the "aging" of fallout decreases the tendency of plants to absorb it must be known if future concentrations in plants, animals and man are to be predicted.

The final parameters required for the calculation of future body burdens of fallout nuclides are the quantity of debris in the stratospheric "reservoir" and its mean residence time there. Prior to the direct measurement of stratospheric concentrations during HASP, this was accomplished mainly by the comparison of estimated injections of debris into the stratosphere with the estimated surface burden obtained from integration of soil and rainfall data¹⁵. By the time HASP was begun the U. S. A. E. C. Ashcan program¹⁶ of stratospheric sampling, using balloon-borne filter equipment, had been underway for almost a year. The Ashcan results were not readily accepted by most authorities on fallout because they disagreed with estimates made using surface fallout data and because of uncertainties

in the sample efficiencies which made the data suspect. More recently the accuracy and precision of the Ashcan data have improved and even the early results have generally been confirmed by later HASP data. Nevertheless, it became evident by 1956 that the use of U-2 aircraft to measure the distribution of fallout in the stratosphere would permit a great advance in the accuracy with which future fallout rates could be predicted.

THE DESIRABILITY OF AIRCRAFT SAMPLING

The use of manned aircraft has many advantages over the use of unmanned balloons for the collection of filter samples. The latitude and altitude of collection may be determined and controlled much more accurately when an aircraft is used. The control of altitudes is especially important because of the steep vertical concentration gradients which have characterized the tropical stratosphere. Aircraft are also able to collect a series of samples over a range of latitudes and/or altitudes, giving information on the spatial distribution of activity on the date of sampling. Finally the efficiency of a sampler borne by a high speed aircraft may be determined more accurately than the efficiency of the balloon-borne sampler through which air can be pumped only at relatively low velocities. Low velocity sampling may discriminate between particles depending upon their size. For all of these reasons aircraft sampling of the stratosphere was desirable and, indeed, was begun in Sweden and Britain¹⁷. But the development of the Lockheed U-2 made an extensive program of stratospheric sampling feasible for the first time, for only this aircraft has the range altitude capability required to reach a significant fraction of the stratospheric air mass. Thus, when six Lockheed U-2 aircraft became available to the Defense Atomic Support Agency in 1957 the High Altitude Sampling Program was begun.

REFERENCES

1. Rand Corp., "Worldwide Effects of Atomic Weapons; Project Sunshine", U.S.A.E.C. Report AECU-3. R-251-AEC (Amended) (1953)
2. Arden, J. W., Bryant, F. J., Henderson, E. H., Lloyd, G. D., and Morton, A. G., "Radioactive and Natural Strontium in Human Bone, U.K. Results for 1959, Part I", U.K. Atomic Energy Authority, AERE-R3246 (1960)

Kulp, J. L., Schulert, A. R., and Hodges, E. J., "Strontium-90 in Man IV", Science 132, 448-454 (1960)

Schulert, A. R., Hodges, E. J., Lenhoff, E. S. and Kulp, J. L., "Strontium-90 Distribution in the Human Skeleton", Health Physics, 2, 62-68, (1959)

U. S. A. E. C. "Fallout Program, Quarterly Summary Report", Health and Safety Lab. Report HASL-105, 112-113, (1961)
3. Langham, W. H. and Anderson, E. C., " Cs^{137} Biospheric Contamination from Nuclear Weapon Tests", Health Physics 2, 30-48 (1959)

Anderson, E. C., "Radioactivity of People and Milk:1957", Science 128, 882-886, (1958)

Maycock, G., Terry, S. W., Vennart, J., and Wise, M. E., "Measurements of Caesium-137 in Human Beings during 1958-59", Nature, 188, 355-357 (1960)

Rundo, J., "Radiocaesium in Human Beings", Nature, 188, 703-706, (1960)
4. Beierwaltes, W. H., Crane, H. R., Wegst, A., Spafford, N. R., and Carr, E. A., Jr., "Radioactive Iodine Concentration in the Fetal Human Thyroid Gland from Fall-Out," J. Am. Med. Assoc., 173, 1895-1902 (1960)
5. Krey, P. W., Bogen, D., and French, E., "Plutonium in Man and Environment", submitted for publication to Nature.
6. Lockhart, L. B., "Fission Product Radioactivity of the Air Along the 80th Meridian (West); NRL Problem AO2-13, Project No. NR571-003", U. S. Naval Research Laboratory, interim reports (1956-1961)

Lockhart, L. B., Jr., Patterson, R. L., Jr., Saunders, A. W., Jr., and Black, R. W., "Fission Product Radioactivity in the Air Along the 80th Meridian (West) During 1959", U. S. Naval Res. Lab., Phys Chem Branch; NRL Report 5528 (1960)
7. U. S. Dept. of Health, Education and Welfare, "Radiological Health Data", Public Health Service monthly reports (1960-1961)

8. Alexander, L. T., Jordan, R. H., Dever, R. F., Hardy, E. P., Jr., Hamada, G. H., Machta, L. and List, R. J., "Strontium-90 on the Earth's Surface", U. S. A. E. C. Report HASL-88, 195-229, (1960)
9. U. S. A. E. C., "Fallout Program, Quarterly Summary Report", Health and Safety Lab. Report HASL-111, 110 (1961)
10. *ibid.*, 109, 115, 116-122
11. Anon., "Strontium-90 in the Total Diet", Consumer Reports, 25, 289-293, (1960)
 U. S. A. E. C., "Fallout Program, Quarterly Progress Report", Health and Safety Lab. Report HASL-88, 184 -186, (1960)
 Anderson, E. C., Schuch, R. L., Fisher, W. R., and Langham, W. H., "Barium-140 Radioactivity in Foods", Science, 125, 1273-1278, (1957)
 Murthy, G. K., Goldin, A. S., and Campbell, J. E., "Zinc-65 in Foods", Science, 130, 1255-1256, (1959)
 Van Dilla, M. A., "Zinc-65 and Zirconium-95 in Food", Science, 131, 659-660, (1960)
12. U. S. A. E. C., "Fallout Program, Quarterly Summary Report", Health and Safety Lab Report, HASL-111, 106-108 (1961) and in other reports in this series
 Anon., "The Milk We Drink", Consumer Reports, 24, 102-111 (1959)
 Los Alamos Sci. Lab., "Tabulation of Gamma Radioactivity of People and Milk During 1960", U. S. A. E. C. Health and Safety Lab. Report HASL-95, 127-151, (1960)
13. U. S. A. E. C., "Strontium Program" and "Fallout Program", U. S. A. E. C. Health and Safety Lab. quarterly reports. (1957-1961)
14. Harley, J. H., Hallden, N. A., and Ong, L. D. Y., "Summary of Gummmed Film Results through December 1959", U. S. A. E. C. Health and Safety Lab. Report HASL-93, (1960)
15. Machta, L., and List, R. J., "Meteorological Interpretation of Strontium-90 Fallout", U. S. A. E. C. Health and Safety Lab. Report HASL-42, 282-309, (1958)
 Libby, W. F., "Radioactive Fallout Particularly from the Russian October Series", Proc. Nat. Acad. Sci, 45, 959-976, (1959)
16. Holland, J. Z., "Stratospheric Radioactivity Data Obtained by Balloon Sampling", U. S. A. E. C. Div. of Biol. and Med. Report TID-5555, (1959)

17. Peirson, D. H., Crooks, R. N., and Fisher, E. M. R., Radioactivity of the Atmosphere due to Distant Nuclear Test Explosions, "Nature, 186, 224-225 (1960)

Edvarson, K., "A Device for Air-Sampling in the Upper Atmosphere," The Research Institute of National Defence (Sweden), Avdelning 2, Dnr. 2407-2097, (1957)

CHAPTER 3

PROCEDURES

The main work accomplished during the High Altitude Sampling Program has been the collection and radiochemical analysis of filter samples of stratospheric air. The sampling and analytical procedures are described in detail below. The results obtained and their interpretation are given in subsequent chapters. An explanation is given of the design of the sampling net and the accomplishments of the various phases of the collection program are reviewed. The number of samples collected during each phase and the sampling density within the various parts of the stratosphere are enumerated. The assumptions made in averaging data and in extrapolating the data to the regions of the stratosphere which were not sampled are described. The aircraft and the filter samplers mounted on them are described and the preflight procedures for preparing the samplers and the inflight procedures for exposing the filter samples are outlined. The nature of the filter medium is described and a summary is given of the work done in deducing its flow characteristics. A description is given of the sampling duct calibration programs and the principles used in calculating sampling efficiency are explained. The radiochemical and radiometric procedures used in the analysis of the filter samples are described in detail and the accuracy and precision of the analyses are evaluated.

THE SAMPLING PROGRAM

Crowflight, the sampling operation of the High Altitude Sampling Program, was designed to provide as much information as possible on the stratospheric distribution of nuclear debris. Naturally, limits were imposed upon it by the range and altitude capabilities of the Lockheed U-2 aircraft, by the location of airfields which could be used and by the frequency of sampling flights which was possible. The initial planning was also hindered by the lack of information on the actual concentrations and distribution of debris in the stratosphere. As results from the early flights became available and a better idea was obtained of the behavior of debris in the stratosphere, the design of the sampling operation was modified. While it was desired that sampling continue in all regions of the stratosphere which could be reached it also seemed important to sample most intensively in the regions in which the most critical data on transfer processes could be obtained. Before the HASP data became available it was still widely believed that nuclear debris was well mixed throughout the stratosphere. As it became evident from the early HASP data that stratospheric mixing was incomplete and debris had only a relatively short residence time in the lower stratosphere, the sampling operations were replanned to permit better determination of variations in concentration from region to region and from one time to another in particular regions.

The Basic Plan

The fulfillment of the concept of the High Altitude Sampling Program became possible with the development of the Lockheed U-2 aircraft. This is essentially a soaring plane powered by a Pratt and Whitney J-57 turbojet engine capable of up to 10,000 pounds thrust. It has a thin skin and is lightly stressed.

The length is 49 feet, 8 inches and the wing span is 80 feet, 2 inches. One peculiar feature is its tandem landing gear and removable outriggers. Upon take-off, these outriggers drop from the aircraft. Wing tip skids prevent damage when landing. The aircraft is operated by one man and has very limited communication and navigation equipment aboard. Its 3000 mile range at a speed of 475 miles per hour (0.73 to 0.8 Mach) operating at altitudes up to 70,000 feet make it an ideal vehicle for sampling the lower stratosphere.

The sampling program was planned to obtain reliable data on concentrations of nuclear debris within all of the regions of the stratosphere which could be reached by the aircraft. Each of the aircraft could collect only four samples during each flight when the program began and only two missions, with flights by four aircraft during each, could be scheduled for a single week. Thus it was necessary to restrict the types of missions to be flown to allow enough repetition of each type to provide a measure of the reproducibility of the sampling.

It was decided that sampling should be carried out within a meridional corridor since, over a sufficiently long period of time, zonal circulation could be expected to carry all stratospheric air through such a corridor. Subsequent measurements bore out the validity of this plan for, with the exception of periods of weapon testing, measured concentrations of stratospheric debris were rather constant over extended intervals of time. This confirmed the relatively rapid mixing of stratospheric air parallel to zonal flow. It has been suggested that debris might be caught in a circulation about continental highs and might not reach the HASP sampling corridor. No evidence for such hold-up was found. Radioactive debris from both United States and United Kingdom tests in the Pacific and from the Soviet tests in the Arctic was intercepted by Crowflight aircraft within a week or two after its injection into the stratosphere. Debris

from individual tests within a series typically arrived at the sampling corridor in the same sequence as their shot dates. Within a month or two after the completion of a weapon test series it was commonly found that mixing had smoothed out stratospheric concentrations so that "hot clouds" were no longer discernible though the highest concentrations were still found at the approximate latitudes of debris injection.

Crowflight was carried out using six U-2 aircraft which had been assigned to the Defense Atomic Support Agency. These were divided between two detachments and each detachment scheduled two missions per week with two aircraft participating in each mission. When Crowflight began in August 1957 each aircraft was equipped with a filter sampler, capable of exposing four filter papers in succession, mounted in the nose position. Twice a week, normally on a Tuesday and on a Friday, four aircraft were flown and 16 samples were collected. In June 1959 additional samplers, mounted in a hatch in the aircraft and capable of exposing six filters in succession, were made available for the three aircraft stationed at Ramey Air Force Base. During September 1959 hatch samplers were also mounted on the other three Crowflight aircraft. A single aircraft, equipped with both types of filter, could collect ten samples during a flight. Thus after September 1959 the schedule called for the collection of 40 samples per mission or 80 samples per week.

The sampling program was carried out in five phases. The bases used and the latitudes and longitudes reached by the aircraft operating from those bases are indicated in Table 3.1 and Figure 3.1. Phase 1 was used for testing the equipment and training the pilots and ground personnel. During Phase 2 a meridional corridor was sampled in the Northern Hemisphere. During Phase 3 this meridional sampling corridor was extended into the Southern Hemisphere. A more intensive study of the stratosphere of the Northern Hemisphere was

undertaken during Phase 4. Finally, during Phase 5 a brief resampling of the stratosphere of the Southern Hemisphere was undertaken.

Crowflight operations were performed by personnel of the 4080th Strategic Reconnaissance Wing of S. A. C. which is based at Laughlin Air Force Base, Texas. Thus the testing and training missions of Phase 1 were flown from Laughlin. Detachments of the 4080th, generally stationed at other S. A. C. bases, were used during all of the other Crowflight Phases. The sampling corridor set up during Phase 2 was located along the Eastern Coast of North America because of the availability there of S. A. C. bases from which both Crowflight and Air-Sea Rescue operations were possible and of radiosonde stations which could provide data for flight weather forecasting and for meteorological analysis of the radiochemical data. Plattsburg Air Force Base, New York was chosen as the base for Detachment 4 sampling the northern section of the meridional corridor and Ramey A. F. B., Puerto Rico was chosen as the base for Detachment 3 sampling the southern section. Samples could be collected as far north as 67° North latitude from Plattsburg and as far south as 7° South from Ramey. During Phase 3, Detachment 4 was deployed to Ezeiza Airfield near Buenos Aires, Argentina. Monthly deployments to Plattsburg by Detachment 3 were planned to provide some data on the northern section of the sampling corridor while the sampling was concentrated in the southern section. Flights from Ezeiza collected samples from the region between 57° South and 10° South latitude. Thus during Phase 3 samples were collected along the 64° West meridian and mainly between 57° South and 38° North but with some samples collected as far north as 68° North. During Phase 4 only one detachment was available. However, three of the aircraft could be based at Laughlin A. F. B., so the detachment was deployed to Minot A. F. B. which is almost directly north of Laughlin. The sampling corridor had to extend northwest from Minot, however,

Table 3, 1 Flight Tracks of Crowflight Missions

Phase	Base	Limits of Sampling				
		Latitude	Longitude	Direction		
1	Laughlin, Texas	29°40' N	100°57' W	North	54°30' N	100°30' W
				South	14°00' N	100°30' W
				East	31°30' N	76°00' W
2	Plattsburg, New York	44°42' N	73°28' W	North	67°00' N	71°00' W
				South	21°00' N	71°00' W
	Ramey, Puerto Rico	18°25' N	66°00' W	North	39°00' N	69°00' W
				South	07°00' S	69°00' W
3	Plattsburg, New York	44°42' N	73°28' W	North	68°00' N	71°00' W
				South	38°00' N	64°00' W
	Ramey, Puerto Rico	18°25' N	66°00' W	North	07°30' S	64°00' W
				South	09°30' S	64°00' W
	Ezeiza, Argentina	35°00' S	58°30' W	North	57°00' S	64°00' W
				South		
4	Minot, North Dakota	48°15' N	101°20' W	Northwest	71°00' N	132°30' W
				South	32°30' N	99°40' W
	Laughlin, Texas	29°40' N	100°57' W	North	49°50' N	98°00' W
				Southeast	11°00' N	80°00' W
				South	08°00' S	67°00' W
5	Eielson, Alaska	65°00' N	147°30' W	Northwest	70°00' N	157°00' W
				Northwest	33°30' N	105°00' W
				Southeast	10°00' N	56°00' W
				South	58°00' S	64°00' W
	Laughlin, Texas	29°40' N	100°57' W	Northwest	70°00' N	157°00' W
				Northwest	33°30' N	105°00' W
	Ramey, Puerto Rico	18°25' N	66°00' W	Southeast	10°00' N	56°00' W
				South	58°00' S	64°00' W
	Ezeiza, Argentina	35°00' S	58°30' W	South	58°00' S	64°00' W

ISOTOPES, INC.

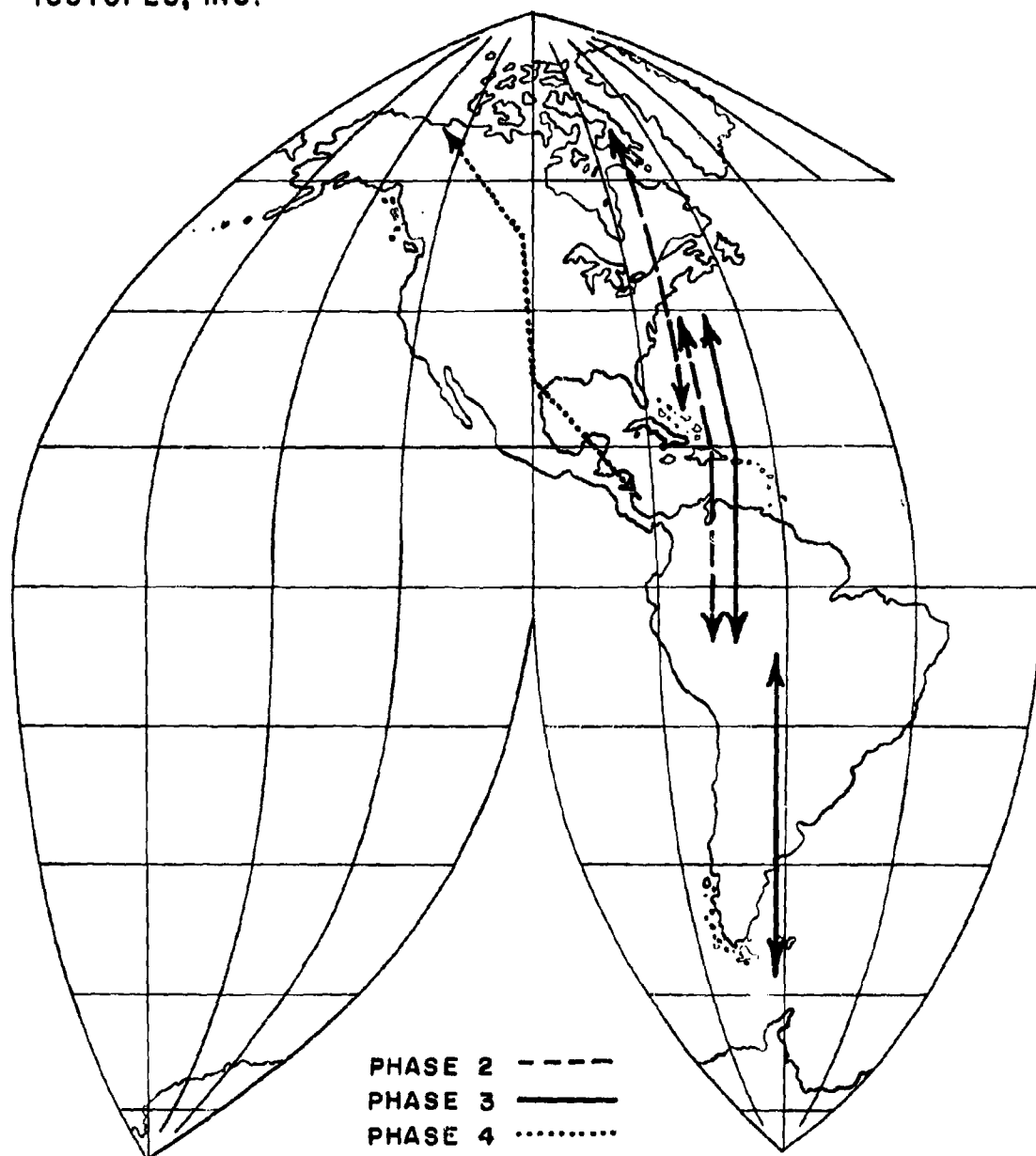


FIGURE 3.1 FLIGHT TRACKS FOR HASP SAMPLING

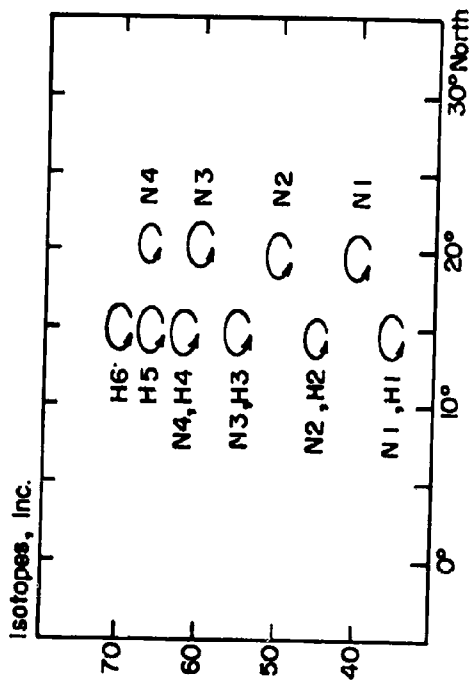
to prevent the aircraft from flying so near to the magnetic pole that their compasses would not function and to allow them to fly over populated areas wherein emergency rescue operations would be possible and wherein radiosonde stations were located. It was also necessary that the sampling corridor extend southeast from Laughlin to bring it into a region in which radiosonde stations were located and to avoid requiring the Air-Sea Rescue aircraft to cross the Mexican mountains. During Phase 5 a small number of samples were taken by three aircraft which deployed to Ezeiza. Some other samples collected by means of U-2 aircraft were supplied by the U. S. Air Force. Three sets of these were collected during flights out of Alaska, some in September-October 1958, some in April 1959 and some in May 1960. During May 1960 the Air Force also supplied a few samples collected in flights from Laughlin and Ramey. In addition three sampling missions to the North Pole were flown for HASP by the Air Force using hatch samplers mounted on B-52 aircraft.

Accomplishments of the Sampling Program

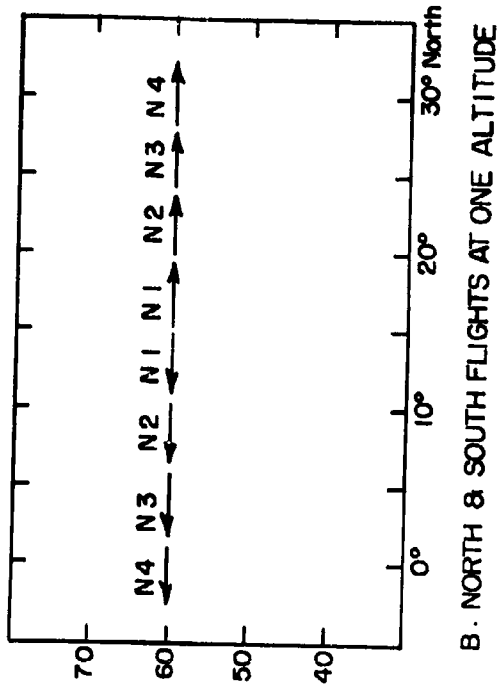
The accomplishments of HASP sampling may be summarized in terms of the various Crowflight phases and the purposes for which they were designed. During Phase 1, which began on 22 August 1957 and continued through 16 October 1957, the pilots and ground personnel were trained and the equipment was tested in flights from Laughlin A. F. B., Texas. Five missions were flown and twenty samples were collected. At this time the aircraft were equipped only with the nose samplers. Two of the missions were vertical soundings (or orbit flights) in which one sample was collected at each of four altitudes and three were horizontal flights in which all four samples were collected in succession at a single altitude. One horizontal flight was northward, one southward and one eastward from Laughlin. The various types of missions flown during Crowflight

are illustrated in Figure 3.2. Orbit flights are pictured in part A of Figure 3.2 and horizontal flights are pictured in part B.

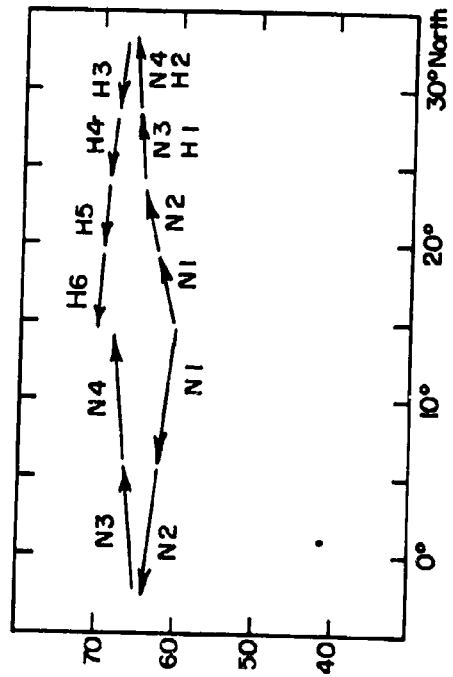
During Phase 2, which lasted from 5 November 1957 through 8 July 1958, three aircraft were based at Plattsburg A. F. B., New York and three at Ramey A. F. B., Puerto Rico. The sampling corridor was located approximately along the 70° West meridian. Most of the missions flown during Phase 2 involved the collection of four samples at a single altitude by each aircraft with one aircraft flying north and one south from each base. Some orbit missions were also flown as well as some climbing flights to maximum altitude, such as are shown in Figure 3.2, Part C. In these latter missions two samples were collected on the outbound leg and two on the inbound. Since flights south from Plattsburg sampled the same latitudes as flights north from Ramey, it was possible to check the reproducibility of the sampling when the two flights were at the same altitude or to obtain information on vertical as well as latitudinal concentration gradients when they were at different altitudes. One mission, flown on 25 March 1958 was designed specifically to test sampler reproducibility. Two aircraft flew south from Plattsburg collecting samples over identical latitude intervals at 60,000 feet and two flew north from Ramey at 65,000 feet, also collecting samples over identical latitude intervals. Once a month during February through May 1958 the region between Ramey and Plattsburg was sampled by all four aircraft, each flying at a different altitude. Occasionally the aircraft collected two samples outbound and two inbound, all at the same altitude, but usually all four samples were collected outbound. It was necessary to avoid long collection intervals for the samples in order to increase the accuracy of location of areas of especially high or especially low concentration and of transition regions. A total of 530 samples were collected during Phase 2. The number of samples collected in each 5000 foot altitude layer of each 10 degree latitude



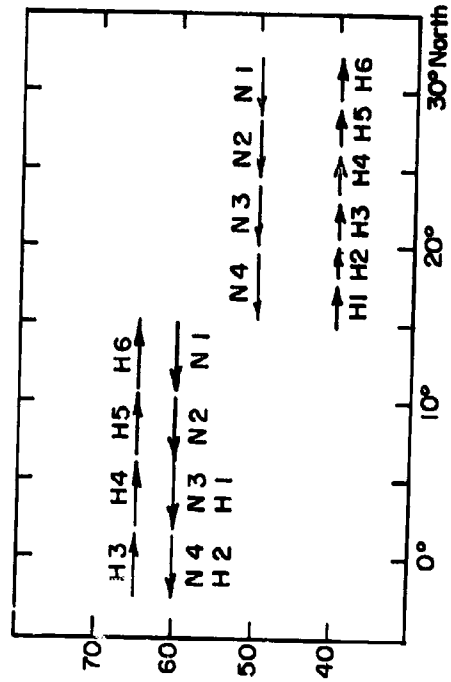
A. ORBIT FLIGHTS



B. NORTH & SOUTH FLIGHTS AT ONE ALTITUDE



C. CLIMBING FLIGHTS TO MAXIMUM ALTITUDE



D. OUTBOUND & INBOUND AT DIFFERENT ALTITUDES

FIGURE 3.2 TYPES OF MISSIONS FLOWN DURING HASP

band during Phases 1 and 2 is indicated in Table 3.2.

Detachment 4 left Plattsburg after the mission of 24 May 1958 to be deployed to Ezeiza for the beginning of Phase 3. They reached Ramey in early July but before they could continue on to Ezeiza all U-2 aircraft were temporarily grounded. During the six weeks before the redeployment of Detachment 4 only two aircraft from Detachment 3 were flying missions. Since the meridional network could not be sampled adequately by two aircraft they flew orbit flights predominantly to establish the vertical distribution of debris in the vicinity of Ramey.

During Phases 1 and 2 fresh debris from several test series was intercepted in the sampling corridor. During September through December 1957, debris from late 1957 Soviet tests was sampled. In late November 1957 and again in early February 1958 debris from the early November 1957 United Kingdom shot was sampled. Between mid March 1958 and early May 1958 Crowflight aircraft collected fresh debris from Spring 1958 Soviet tests. By late May 1958 the first traces of debris from United States Hardtack tests had appeared in HASP samples.

On 12 September 1958 the three U-2 aircraft of Detachment 4 were deployed to Ezeiza Airfield in Argentina. This marked the beginning of Phase 3 which was completed with the return of Detachment 4 to the Northern Hemisphere on 8 August 1959.

During September through December 1958 the collection rate at Ezeiza was temporarily reduced. Since it was not possible to sample the meridional corridor adequately at several different altitudes during this time, it was decided to concentrate on establishing week to week variations in

activity at a single altitude in the sampling corridor during the first months of Phase 3. Thus all flights from Ramey, except for deployments to Plattsburg, and all HASP flights from Ezeiza were scheduled for an altitude of 60,000 feet during September through November 1958. By December 1958 the flight plans were changed to provide periodic sampling at a series of altitudes, 55,000 through 70,000 feet in the tropical stratosphere and 48,000 through 65,000 feet in the southern polar stratosphere.

During the periodic deployments of Detachment 3 to Plattsburg each aircraft flew at a different altitude, 50,000, 55,000 and 60,000 feet on the first and 55,000, 60,000, and 65,000 feet on subsequent deployments. During all but the last of these monthly deployments only one northward mission, flown by two aircraft, could be scheduled for HASP. On the first such deployment, in September 1958, the malfunction of one aircraft caused the repetition of the mission, however, and on the second deployment, in November 1958, HASP received four samples from a special mission. No deployment was made in December 1958 and no flights from Plattsburg could be made because of weather conditions during the January 1959 deployment. Reluctantly the deployments to Plattsburg were canceled until April 1959 when weather conditions were better. Deployments were made in April, May, June and July 1959. Flights north from Plattsburg were scheduled for maximum altitude during the September and October deployments, for the higher altitude layers in this region had not been sampled well during Phase 2. By April 1959 these Plattsburg-north missions were rescheduled for lower altitudes in an attempt to find the expected large stratospheric burdens of fission products from the October 1958 Soviet tests. Beginning in April 1959 the missions flown from Ezeiza were again reduced in number and HASP no longer received as many samples as were desired from the Southern Hemisphere.

During June 1959 hatch samplers were installed on the aircraft assigned to Detachment 3. Hence during late June and all of July 1959 the sampling capability of these aircraft was greatly increased. Missions were planned to permit sampling outbound and inbound at different altitudes by these aircraft so that information could be obtained simultaneously on the vertical and horizontal distribution of debris. Such missions are illustrated in Figure 3.2, Parts C and D. In many flights some of the hatch filters were exposed simultaneously with some of the nose filters. These simultaneous collections permitted checking of the relative calibrations of the two samplers. When the aircraft flew at low altitudes, however, where the air was dense and measurable activities could be collected even when the flight track was sampled as six separate segments, the nose and hatch filters were exposed separately to provide the maximum amount of data.

The sampling corridor during most of Phase 3 was along the 64° West meridian, but the missions flown north from Plattsburg were along the 71° West meridian. A number of radiosonde stations were situated near this flight track in the Northern Hemisphere but few meteorological data were available from the Southern Hemisphere. Fortunately several radiosonde stations were operating in South America, mainly along the western coast, as part of the International Geophysical Year. DASA supplied funds to keep them going past their scheduled closing date and to the end of Phase 3. Some of these stations were quite far west of the Crowflight sampling corridor but there was no other source for the data they supplied.

Several series of special samples were supplied to HASP by the U. S. Air Force to augment the samples collected during Crowflight. During Phase 3 these included one set collected north of Alaska by U-2 aircraft during

September-October 1958 and a second set collected in the same area during April 1959. In addition a set of samples were collected by B-52 aircraft with hatch samplers and flying northward from 60° North to 90° North latitude and back during April 1959. This mission, designated Sea Fish Special No. 3, was duplicated in August 1959 by Sea Fish Special No. 7.

A total of 1423 samples were collected during Phase 3. In Table 3.3 are listed the number of samples collected in each 5000 foot altitude layer in each ten degree latitude zone. It was unfortunate that the northern polar stratosphere could not have been sampled more intensively during the first few months after the injection of debris into that region by the October 1958 Soviet tests, but it is obvious that the aircraft could not be everywhere at once and the sampling in the Southern Hemisphere did yield very valuable data.

The Crowflight aircraft were grounded during most of July and August 1958 when fresh debris from Hardtack tests was being carried through the sampling corridor. When Phase 3 began, however, concentrations of debris in the equatorial stratosphere were still quite high as a result of these tests, much higher than they had been in April 1958. Shortly after Phase 3 began, on 3 October 1958, debris from the United Kingdom test of 2 September 1958 entered the sampling corridor in the equatorial stratosphere. Debris from this test continued to be encountered in this region at 60,000 feet, the only altitude which was being sampled, until early November 1958. On 19 October 1958 debris from the autumn 1958 Soviet tests was encountered for the first time. These samples were obtained in the north temperate latitudes. Samples collected at altitudes above 50,000 feet in the northern polar stratosphere during September and October 1958 did not contain detectable quantities of this debris, though it was present at 50,000 feet in this region during November 1958. By late December 1958 mixing of the debris had been sufficient so that "hot clouds" of

debris were not encountered again. The moratorium on testing which began in November 1958 resulted in no new injections of debris into the stratosphere during Phase 3 (or during Phases 4 and 5). Thus the remainder of HASP was used to monitor subsequent redistribution of debris within the stratosphere due to mixing and transfer processes.

During September 1959 Detachment 9, with three aircraft, was deployed to Minot A. F. B., North Dakota and Detachment 10, with three aircraft, was set up at Laughlin A. F. B. Phase 4 began on 15 September 1959 with sampling along a corridor which ran northward and southeastward from Laughlin and northwestward from Minot. Missions in which one aircraft sampled north and one sampled south of Laughlin alternated with missions in which both sampled to the north. With only a few exceptions all missions from Minot had both aircraft sampling to the north of that base. Since all six aircraft were equipped with both nose and hatch samplers by the beginning of Phase 4, all flight plans called for the collection of samples outbound and inbound at different altitudes in missions similar to those pictured in Figure 3.2, Parts C and D. Orbit missions in which both nose and hatch samplers were employed, as portrayed in Figure 3.2, Part A, were also flown on a number of occasions. Monthly deployments of Detachment 10 to Ramey A. F. B. were made and two flights were made south from Ramey during each deployment. This permitted the extension of the sampling corridor south of 12° North latitude, which was as far south as flights from Laughlin could usually penetrate, to 8° South latitude. In October 1959 Sea Fish Special No. 8 again carried the sampling to the North Pole. Phase 4 ended with an orbit mission from Minot on 6 May 1960 and a southward mission from Ramey on 9 May 1960.

A total of 1689 samples were collected during Phase 4. The number collected in each 5000 foot altitude layer of each ten degree latitude band is

shown in Table 3.4. As is evident from the table, the sampling density was good within all regions of the stratosphere of the Northern Hemisphere which could be reached by the aircraft.

During Phase 4 no weapons of megaton yield were tested, though the French exploded two smaller weapons in the Sahara. No evidence of debris from these French bombs was found in any HASP samples. Presumably this debris did not enter the stratosphere at all or, at least, did not penetrate above 55,000 feet or so in the tropical stratosphere. Thus it was possible to monitor the changes which were occurring in the stratospheric distribution of the older debris in response to seasonal meteorological factors.

Basically Phase 5 consisted of a redeployment of three aircraft to Ezeiza and the collection of a small number of samples. In addition some samples collected by missions flown from Laughlin, Ramey, and Eielson A. F. B., Alaska at about the same time were supplied to HASP. Two samples, each with a short duration of exposure, were supplied from each Eielson mission. Each of these sample pairs was combined for radiochemical analysis since the individual samples did not have enough activity to make their separate analysis worthwhile. Many of the samples from Ramey and Laughlin contained too little activity to be worth analyzing radiochemically. A number of composites were also made of samples collected at Ezeiza and on flights between Ezeiza and Ramey in order to permit analyses for isotopes such as rhodium-102 and beryllium-7. Phase 5 began on 10 May 1960 with the collection of the first samples at Eielson, continued with the deployment of three U-2 aircraft to Ezeiza on 12 May 1960, and ended with their return to Ramey on 8 June 1960 and to Laughlin on 10 June 1960.

A total of 102 samples were collected during Phase 5. Their distribution with latitude and altitude is shown in Table 3.5. It is evident that the sampling

Table 3, 2 Distribution of Samples Collected during Phases 1 and 2,
August 1957 - July 1958

<u>Latitude</u>	<u>Altitude (Thousands of Feet)</u>						
	<u>40</u>	<u>45</u>	<u>50</u>	<u>55</u>	<u>60</u>	<u>65</u>	<u>70</u>
80°-90° N	0	0	0	0	0	0	0
70°-80° N	0	0	0	0	0	0	0
60°-70° N	0	3	1	13	2	3	0
50°-60° N	0	6	2	31	4	4	0
40°-50° N	3	13	7	41	7	5	1
30°-40° N	0	14	1	38	15	36	10
20°-30° N	0	9	3	36	19	33	11
10°-20° N	0	10	4	30	22	33	11
0°-10° N	0	3	3	16	9	7	2
0°-10° S	0	2	2	10	7	4	4

Number of Samples: 521 from Northern Hemisphere
29 from Southern Hemisphere
550 Total

Table 3, 3 Distribution of Samples Collected during Phase 3,
September 1958 - August 1959

<u>Latitude</u>	<u>Altitude (Thousands of Feet)</u>								
	<u>30</u>	<u>35</u>	<u>40</u>	<u>45</u>	<u>50</u>	<u>55</u>	<u>60</u>	<u>65</u>	<u>70</u>
80°-90° N	0	3	10	0	0	0	0	0	0
70°-80° N	0	4	4	0	5	0	4	5	0
60°-70° N	0	4	3	4	6	4	6	10	0
50°-60° N	0	0	0	5	9	8	10	8	0
40°-50° N	0	0	1	2	8	11	25	20	4
30°-40° N	0	0	0	0	7	11	50	52	1
20°-30° N	0	0	0	0	10	28	79	93	1
10°-20° N	0	0	0	0	9	25	53	45	23
0°-10° N	0	0	0	0	6	19	58	53	21
0°-10° S	0	0	0	0	3	9	32	32	7
10°-20° S	0	0	0	2	6	12	32	31	6
20°-30° S	0	0	0	1	5	9	16	17	1
30°-40° S	6	5	22	13	41	30	53	47	9
40°-50° S	0	1	8	6	21	20	33	22	1
50°-60° S	0	0	1	3	8	6	12	5	2

Number of Samples: 827 from Northern Hemisphere
596 from Southern Hemisphere
1423 Total

Table 3.4 Distribution of Samples Collected during Phase 4
September 1959 - May 1960

Latitude	Altitude (Thousands of Feet)								
	30	35	40	45	50	55	60	65	70
80°-90° N	0	1	5	0	0	0	0	0	0
70°-80° N	0	3	2	0	0	0	0	0	0
60°-70° N	3	6	38	27	27	62	60	57	12
50°-60° N	23	19	47	28	32	49	51	40	16
40°-50° N	11	0	34	34	92	44	66	103	21
30°-40° N	0	0	38	26	37	23	27	55	23
20°-30° N	0	0	9	7	1	3	32	50	21
10°-20° N	0	0	0	0	0	3	55	90	25
0°-10° N	0	0	0	0	0	0	28	44	25
0°-10° S	0	0	0	0	0	0	16	28	20

Number of Samples: 1625 from Northern Hemisphere
64 from Southern Hemisphere
1689 Total

Table 3.5 Distribution of Samples Collected during Phase 5
May - June 1960

Latitude	Altitude (Thousands of Feet)				
	50	55	60	65	70
80°-90° N	0	0	0	0	0
70°-80° N	0	0	0	0	0
60°-70° N	4	1	5	7	0
50°-60° N	0	0	0	0	0
40°-50° N	0	0	0	0	0
30°-40° N	0	0	0	0	0
20°-30° N	0	1	5	2	1
10°-20° N	2	0	5	8	1
0°-10° N	0	0	0	0	4
0°-10° S	0	0	0	4	4
10°-20° S	0	0	0	6	2
20°-30° S	0	0	0	6	2
30°-40° S	9	0	11	8	0
40°-50° S	0	0	0	1	1
50°-60° S	0	0	0	1	1

Number of Samples: 46 from Northern Hemisphere
56 from Southern Hemisphere
102 Total

was scattered but the data which were obtained from the Southern Hemisphere especially are valuable since no other samples of stratospheric debris had been collected there in almost a year.

Representativeness of the Data

It is inherently quite difficult to sample adequately a dynamic system like the stratosphere. Before data from the High Altitude Sampling Program became available it was assumed by some interpreters of fallout data that the stratospheric aerosol was essentially static; mixing was presumed to occur quite rapidly so that within a few weeks or months after the completion of a test series the concentration of individual isotopes was uniform everywhere within the stratosphere. Evidently the movement of fallout through the tropopause and into the troposphere was visualized as analogous to movement through a semipermeable membrane. This simplified model permitted calculations of stratospheric residence times using surface fallout measurements. If it were true it would greatly facilitate the determination of stratospheric burdens of debris, for only a few measurements would serve to define the concentrations in stratospheric air. This simple model never did satisfy meteorologists, however, for neither the stratosphere nor the tropopause has the properties which this model ascribes to them. Meteorologists pointed out that the tropopause was merely the lower limit of the stable air layers of the stratosphere and that mixing through it should be no less rapid than mixing down to it. Thus a vertical concentration gradient could be expected to exist in the lower layers of the stratosphere. This would complicate the determination of the stratospheric burden and residence time of nuclear debris. Moreover a meridional circulation of the stratosphere, which had been suggested by Brewer and accepted by Dobson, was applied by Stewart et al to the interpretation of surface fallout data. The

existence of such a transfer process could seriously limit the usefulness of HASP measurements, for extrapolation and interpolation of the data would be difficult. Thus it was not clear, at the commencement of HASP sampling, to what extent this program would be able to define the behavior of nuclear debris in the stratosphere.

Data from the first few HASP missions were sufficient to demonstrate that concentrations of debris are not uniform throughout the stratosphere and that all stratospheric regions which could be reached by the aircraft would have to be sampled to provide the information needed to calculate the total burden of strontium-90 and other nuclides. Both the Soviet Union and the United Kingdom were testing weapons at the time that HASP sampling was getting under way and it soon became evident that the stratospheric concentrations of debris changed with time as a result of fresh injections and of subsequent mixing. With the commencement of the moratorium on weapon testing in November 1958 it also became clear that, even without new injections, changes in the stratospheric distribution of nuclides occurred as a result of seasonal meteorological factors. Thus variations in concentration are found depending upon the latitude, altitude and time of sample collection. These must be taken into account in calculating the mean stratospheric distribution, burden and residence times of nuclear debris.

It has been expedient in the interpretation of HASP results to average data from many samples rather than to use data from individual samples in determining nuclide concentrations. There is always a possibility that large random errors may occur in data from a single sample or a small number of samples. From time to time serious errors have been found to have occurred in the recording of flight data, either during or after collection, in the labeling of samples, either before their shipment to the laboratory or during their

radiochemical processing, in the treatment of the samples, and in the calculation and transcription of the data from the analyses. Where such errors were evident the data were corrected, if possible, or discarded, if there was ample justification. Smaller errors which change the data by a factor of two or less are not readily detected since natural variations appear to be at least of this size. These natural variations themselves limit the significance of any observations based on only a few samples. Since the meteorological factors which may cause day to day variations in concentrations at any point in the stratosphere are still far from being understood thoroughly, attempts have not been made in this report to interpret short range fluctuations. By averaging as many samples as possible we have attempted to eliminate the effect of small random errors in the data and of short range fluctuations in stratospheric concentrations.

The data have been grouped by assigning each sample to a five or ten degree latitude band and a 5000 foot altitude layer, selected according to the midpoint of the sampling path. When only a small number of samples have been analyzed for a nuclide during any given time interval, the data have been divided using larger regions, such as the northern polar (30° North- 90° North), Tropical (30° South- 30° North) and southern polar (30° South- 90° South) stratosphere and the higher (62,500-70,000 feet), intermediate (47,500-62,500 feet) and lower (30,000-47,500 feet) stratosphere. Generally all samples collected in each of these specified regions during a designated time interval have been averaged. The time intervals chosen have been long, usually a year or a phase of Crowflight, when the average distribution of a nuclide in the stratosphere was being studied or short, commonly two months but sometimes one, three or four months, when seasonal changes in the distribution were to be shown. Often, when the activities of a nuclide were too low to be detected in a single sample, composites have been made of several samples and have been analyzed. Almost

all analyses for rhodium-102, beryllium-7 and phosphorus-32, as well as many analyses for strontium-89 and tungsten-185 were made on composites. Although it is rather unrealistic to assign data for such composites to a point in space this has been necessary to permit comparisons between samples, none of which represent identical sampling paths. The various groupings in space and time which have been used for the different nuclides have been chosen somewhat subjectively, reflecting the analysis which was made of the apparent distribution and behavior of each nuclide. The selection of groupings has been guided by data on the accuracy of definition of sampling tracks, on the uniformity of distribution of the nuclide and on the constancy with time of its concentration.

A more serious questioning of the validity of using HASP data to characterize the behavior of nuclear debris in the stratosphere may arise when these data are used to deduce the concentration of strontium-90 or other nuclides in regions which have not been sampled and to predict the future behavior of debris from such regions. Thus, though HASP sampling has been limited to one meridional corridor it has been assumed that these data were representative of the entire stratosphere. The Crowflight aircraft have not penetrated the polar stratosphere beyond 71° North latitude or 57° South latitude but the HASP data have been considered adequate for calculating the burden of debris in the entire polar region. Although much of the debris which has been injected into the stratosphere has probably penetrated above 70,000 feet, the ceiling of U-2 aircraft, it has been assumed that HASP data, extrapolated upward using information from Project Ashcan, may be used to deduce concentrations of nuclear debris in the upper stratosphere. The validity of each of these assumptions may be considered separately.

The general applicability of data from a meridional corridor to the entire stratosphere depends on the existence of an effective zonal circulation of

the entire stratosphere. The fate of debris from United States and United Kingdom weapon tests provides evidence on zonal circulation in the tropical stratosphere and the fate of debris from Soviet tests provides evidence on zonal circulation in the northern polar stratosphere. Clouds of debris from weapon tests have been observed to travel about the earth in the zonal circulation of the troposphere, maintaining some of their integrity through almost a complete circuit of the globe. When HASP began it was expected that clouds of debris in the stratosphere would be even more persistent and that they would make several complete circuits of the earth before their mixing with the air about them would leave them indiscernible. Although such behavior was never completely verified, the data obtained from missions flown subsequent to the November 1957 United Kingdom tests and the Spring 1958 and Autumn 1958 Soviet tests did suggest that at least two distinct passes of this debris through the HASP sampling corridor had been detected. The second interceptions were generally somewhat questionable, for within two months after shot date these clouds, though they might still be distinguishable because of the concentrations of short-lived nuclides within them, seldom displayed strontium-90 concentrations which were more than twice as high as those in the air masses surrounding the cloud. The fact that clouds of debris did pass through the sampling corridor more than once and that clouds from individual tests passed through in the same sequence as their shot dates does argue against any large scale diversion of stratospheric air out of the zonal circulation. Within a few months after the end of a test series the day to day and week to week variations in strontium-90 concentrations in samples collected in most regions became relatively small (± 50 percent). This is indicative of fairly good mixing in the zonal direction. The residual fluctuations in concentration were as likely caused by minor subsidence or upwelling of the air masses or by variations in the true altitude of the flight tracks (due to

discrepancies in altimeter calibration between aircraft) as by in homogeneities of concentration in the zonal direction, for strontium-90 has typically exhibited steep concentration gradients in the lower stratosphere. Moreover in regions such as the southern polar stratosphere which have received no direct injections of debris, the concentrations present at any time have depended upon the rates of influx and efflux of debris originating in other regions of the stratosphere. Thus constancy of concentration is unlikely since mixing may occur by fairly random motions which carry masses of air from the tropical stratosphere into the polar stratosphere or vice versa, or which shift air masses between the troposphere and stratosphere. The region of the tropopause gap, between about 30° and 45° latitude, may especially be subject to large variations in concentration for it is a transition zone between tropical stratosphere and polar stratosphere and between tropical troposphere and polar stratosphere. Nuclides such as tungsten-185 and rhodium-102, originating in a tropical source, may be expected to show wide fluctuations in concentration in the polar stratosphere, while beryllium-7, originating chiefly in polar sources, may be expected to show wide fluctuations in concentration in the tropical stratosphere. For the most part, however, measured nuclide concentrations have changed slowly and there is no reason to doubt that a meridional sampling corridor gives data representative of the entire stratosphere.

The extent to which the HASP meridional corridor has actually been sampled is indicated in Figure 3.3. A section through the corridor is pictured here with the sine of the latitude plotted against the pressure altitude in millibars. On this type of plot, areas on the diagram are proportional to the equivalent masses of air in the corridor. Typical tropopause positions are indicated on the diagram and, based upon them, a conservative estimate of the stratospheric mass has been made. It is evident that at least 54 percent of the

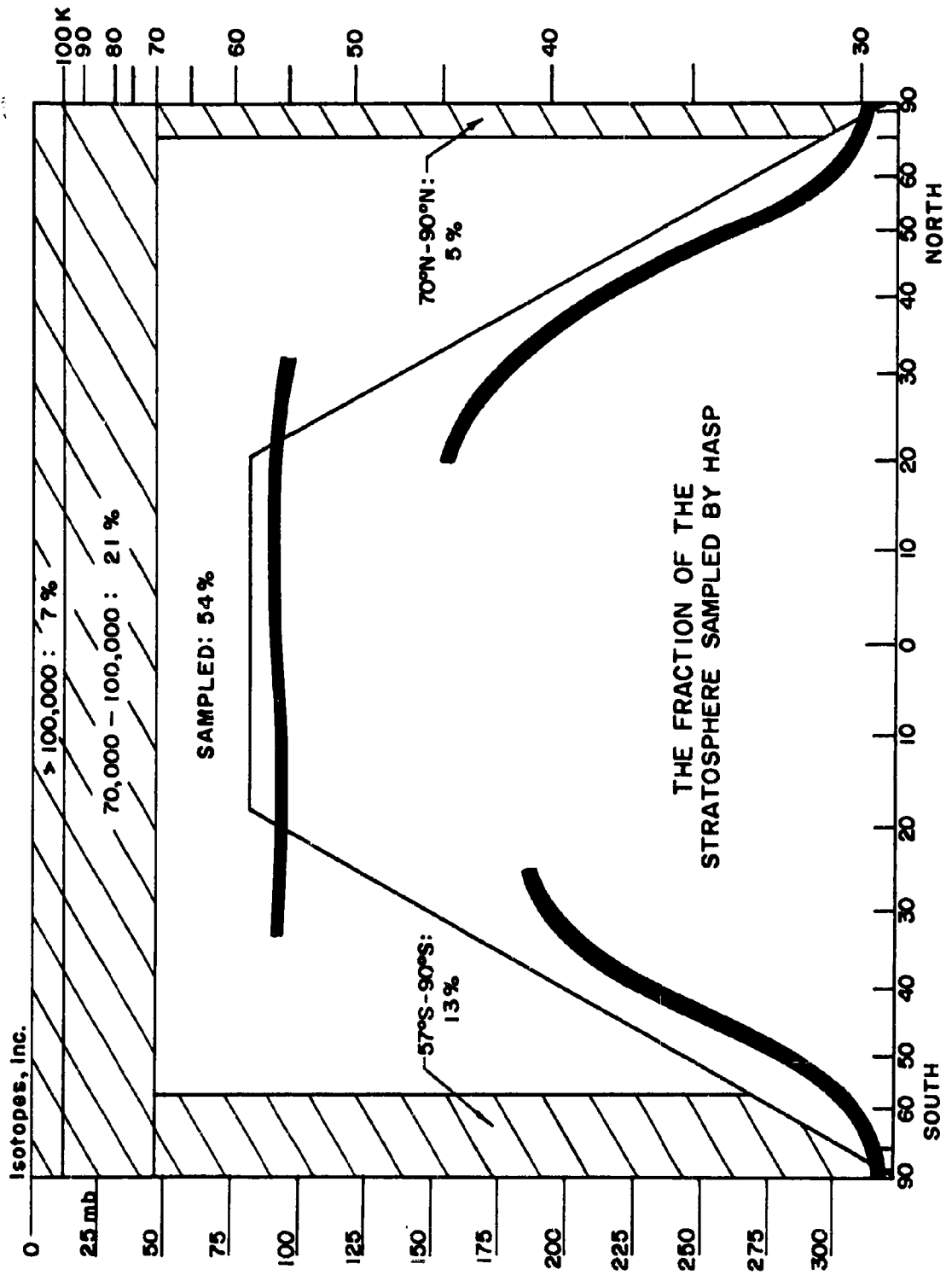


FIGURE 3.3 SECTION ALONG THE MERIDIONAL SAMPLING CORRIDOR

stratospheric air (including in the term "stratosphere" all air above the tropopause, including the mesosphere, etc.) has been sampled by HASP aircraft during one or another phase of Crowflight. About 5 percent of the stratosphere is north of the limits of U-2 sampling, 71° North, 13 percent is south of the limits, 57° South, and 28 percent is above the altitude capability, 70,000 feet, of the U-2. Actually the polar stratosphere is much less characterized by temperature stratification than is the tropical stratosphere and there is good reason to expect reasonably rapid lateral mixing within it. Thus it has been assumed that sampling poleward beyond 45° latitude would give data which could be applied to the air all the way to the pole. There remained the possibility that serious errors could be made in extrapolating HASP data to the North Pole if this were not true, for the Soviet Union has injected large quantities of debris into the lower northern polar stratosphere. To check this possibility, three sampling missions were flown to the North Pole by B-52 aircraft. The samples obtained showed a uniformity of concentrations from 60° to 90° North latitude. The existence of a similar uniformity in the southern polar stratosphere is quite likely, for no direct injections of nuclear debris have ever occurred there. Thus the air below 70,000 feet, which includes at least 72 percent of the stratosphere, should be well represented by HASP measurements.

The extrapolation of HASP data above 70,000 feet entails more uncertainties than does its extrapolation to other latitudes or longitudes below 70,000 feet. Nevertheless there are data available which permit this upward extrapolation to be made in a reasonable manner. The data from Project Ashcan, analyses of filters exposed at altitudes between 50,000 feet and 100,000 feet in balloon-borne samplers, can be used to extrapolate HASP data up to 100,000 feet. There has been a persistent uncertainty in the sampling efficiency of the

Ashcan samplers but this problem has apparently now been fairly well solved. The samples collected during this program have also tended to contain rather small amounts of debris, making their analysis difficult and subject to large errors. The steep vertical concentration gradients of debris in stratospheric air which have been observed during HASP indicate that the common uncertainty in actual altitude of Ashcan sample collection may also adversely affect the utility of the data. Nevertheless in regions where HASP and Ashcan have both collected samples, at 50,000 and 65,000 feet altitudes, the correspondence between data from the two programs has been fairly good. The general conclusions reached by correlating data from HASP and Ashcan can be checked by observing changes in the distribution of debris below 70,000 feet and calculating the corresponding changes which must be occurring above 70,000 feet, for the same processes affect the entire lower stratosphere. Thus, with the use of Ashcan data, HASP data may be extrapolated upward to 100,000 feet. Only 7 percent or less of the stratosphere is above this altitude and there is reason to think that its burden of strontium-90 and other nuclear debris may be estimated fairly well. Except for the rocket shots, Teak and Orange, few weapons have injected debris above 100,000 feet. Initially all of the debris from Teak and Orange was above this altitude and by estimating how much has since come down into and through the lower stratosphere we may estimate how much is still there. Considering the somewhat surprisingly short residence time of debris from Teak and Orange in the upper layers of the atmosphere it seems unlikely that any debris from surface shots, even that from very large weapons, has experienced really long detention times in the upper stratosphere. It is probably safe to conclude that the burden of nuclear debris in the stratosphere above 100,000 feet was quite small during HASP until the injection of fallout by Teak and Orange in August 1958.

Thus HASP data should be quite representative of stratospheric concentrations of radionuclides below 70,000 feet. There are some limitations resulting from the inability of the aircraft to be in all places at all times and by the possibility of minor concentration differences poleward beyond the limits of HASP sampling. Upward extrapolation of the data to altitudes above 70,000 feet may be done reasonably and gives the best available measure of the burden of nuclear debris in the high stratosphere. If the theories of atmospheric mixing and transfer used during HASP are correct, these extrapolations should be accurate to within a factor of two.

THE U-2 DUCT SAMPLERS

From the inception of the program each aircraft used in HASP missions was equipped with a duct sampler with the air intake located in the nose. By the start of Phase IV an additional duct sampler was installed in a hatch in each aircraft. Fig. 3.4 is a photograph of the U-2 aircraft showing the locations of these duct samplers. The duct has a gradually-increasing cross-section from the entrance where a damper valve is located to the plane of the filter paper which is mounted normal to the flow of air. Filters are rigidly secured in a ringholder with wire mesh fore and aft to prevent tearing of the paper. Following the filter paper the duct continues for a few feet before the filtered air is vented near a pressure minimum on the surface of the aircraft.

The sampling procedure consists of several steps. First, the filter paper is moved into sampling position. Secondly, neoprene seals are inflated around the filter holder to form an airtight seal. The pilot then opens the damper valve permitting ram air to enter the duct and pass through the sampler. Finally, after completion of the sampling, the damper valve is closed, the filter paper removed from the sampling position and a new filter installed.

Both the nose and hatch samplers operate in essentially the manner described above. However, there are some minor differences which are given in the detailed descriptions which follow.

Nose Sampler

A schematic diagram of the nose sampler is shown in Fig. 3.5a. The cross section of the duct is circular along the entire length. From the inlet to the plane of the filter paper the diameter gradually increases from four inches to ten inches in a distance of sixty inches along the centerline of the duct. Downstream

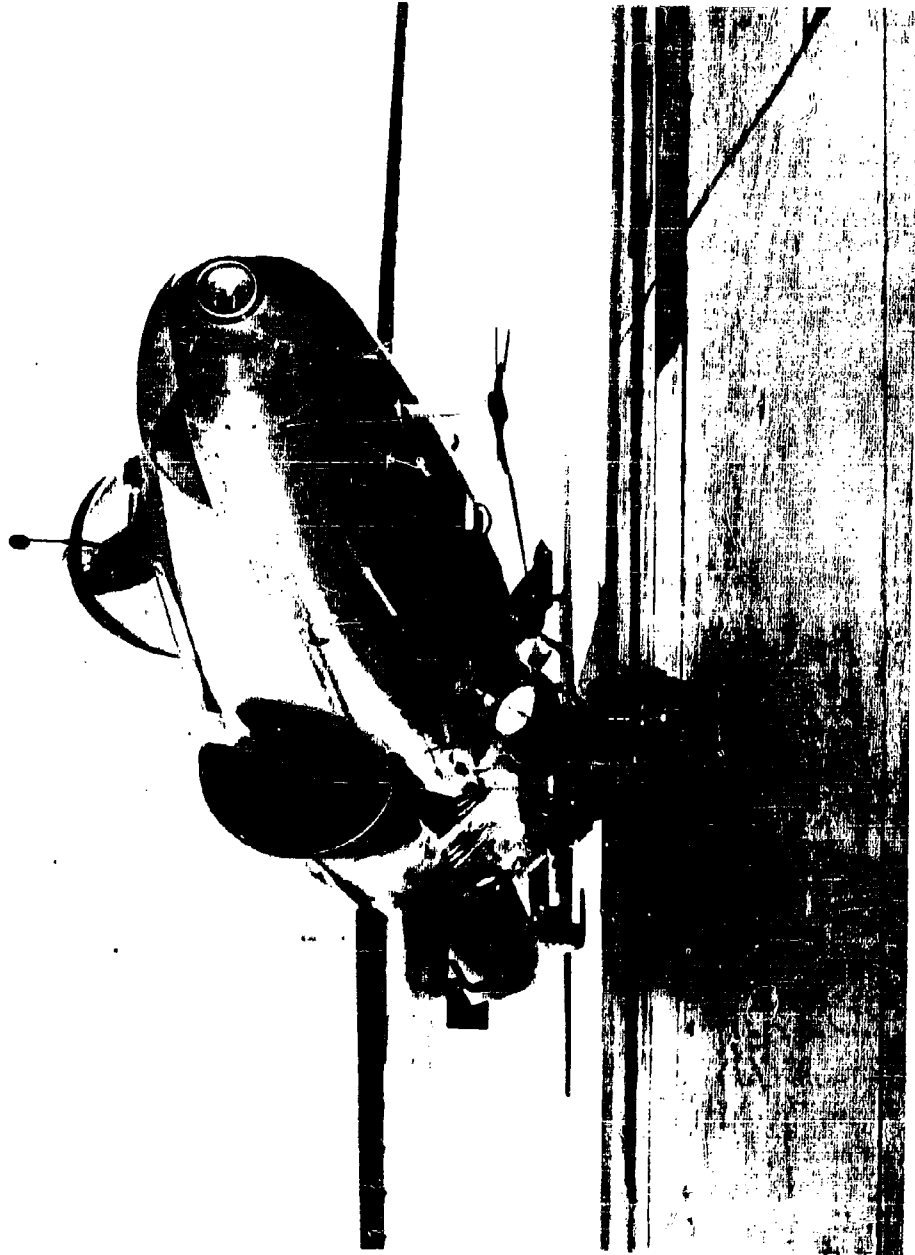


Figure 3.4

from the filter, the duct diameter decreases. The duct terminates about 2 1/2 feet downstream from the filter and flush with the skin in a central position on the bottom of the aircraft at a point which is near a pressure minimum.

Four filters, in their respective ringholders, are mounted in a circular rack which is pivoted at its center above the duct. By means of a switch the pilot can rotate the rack thereby sequentially placing each filter in the duct.

Hatch Sampler

This sampler is located just aft of the cockpit in a removable hatch which fits the underside of the fuselage. The duct is located off-center slightly to port in order not to sample air exhausted from the nose sampler. The schematic diagram of the hatch duct is shown in Fig. 3.5b. The entrance is elliptical and the cross section gradually changes to circular. The diameter of the filter paper is 15.9 inches. The duct is approximately six feet long with the plane of the filter paper about three feet from the entrance. The flow of exhausted air is approximately parallel with that of the intake air. As will be shown later in this chapter, in-flight pressure measurements revealed that the air sampled by the hatch is exhausted at pressures equal to or lower than those for the nose sampler. Thus the sampled air from the hatch is also exhausted at nearly free stream pressures.

The hatch sampler accommodates six filters which are changed sequentially by means of a spring loaded rack advancer. The filters are stacked together in the rack like a horizontal roll of coins. The filter holders are pivoted at the circumference on a rod above the duct. By means of a switch in the cockpit the pilot rotates a filter out of the duct; the rack advances; the next filter then rotates into the duct.

Operation of Samplers

During the sampling missions the sequence of events which occur in the

Isotopes, Inc.

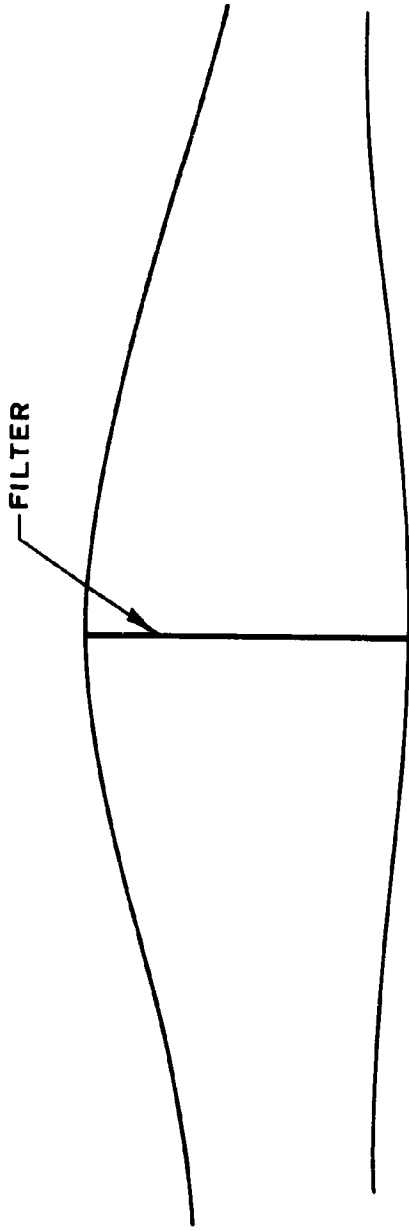


Fig. 3.5b
HATCH SAMPLER

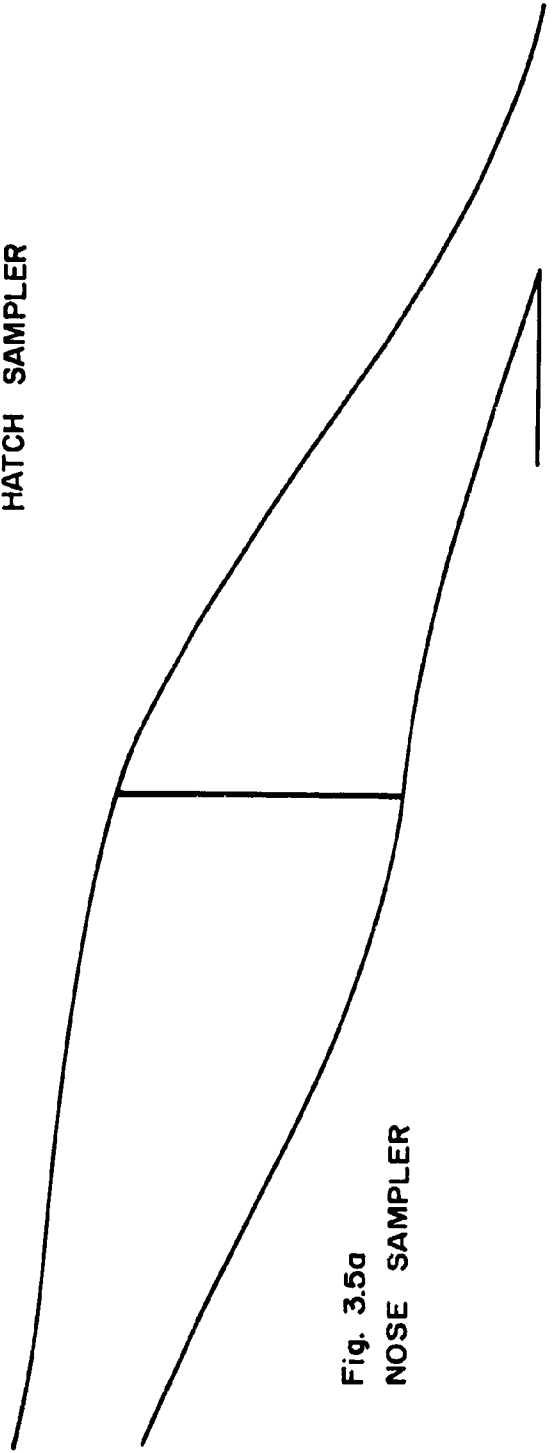


Fig. 3.5a
NOSE SAMPLER

operation of the samplers is the same for both hatch and nose equipment. Thus the description of the sampler operation given below is applicable to either sampler.

The aircraft takes off and flies to sampling altitude with filter number 1 in the duct and the damper valve closed. To begin sampling the pilot turns on a switch causing the damper valve to open. To change samples the pilot turns the switch off which results in, first, the closing of the damper valve, second, the deflation of the neoprene ring seals, third the changing of the filter in the duct and finally, reinflation of the ring seals. The whole process is then repeated until all filters have been exposed. The control panel for the sampler contains lights, one for each filter, which indicate when a given filter is in position in the duct and the ring seal is properly inflated. The pilot then knows that he may start the sampling procedure again.

A duplicate set of indicator lights is located in a bay just behind the pilot and above the hatch sampler. In addition to the lights are a duplicate altimeter, a clock, and an air temperature gauge. These instruments are arranged in a panel called an "A-O panel" (automatic observer), which is photographed every 15 seconds. Thus a complete record of the mission is obtained on film. The use of these records will be described in the section of this chapter dealing with the calculation of the volumes of air sampled.

Handling of Samples

The filter papers are packaged in polyethylene lined heat sealed envelopes which are stored in a relatively cool area. Four filters for the nose sampler are packaged in an envelope and six filters for the hatch sampler in an envelope. The holder for each filter is dismantled indoors on a clean wood top table. The filter is placed in the holder which is then carefully reassembled.

During the loading operations the filters are only handled by the outer edge which is clamped between the halves of the ringholder. The loaded holders are then installed in the racks of the sample changers. The exhaust ports of the samplers are kept covered with masking tape until just prior to take-off. After return of the aircraft to the hangar the masking tape is placed over the duct exhaust, the filter holders are removed and dismantled, the filters are folded twice and placed in individual manilla envelopes. Only the outer edges of the filter are held when it is folded and the filter is not creased flat until after it is inserted in the envelope. The envelopes containing the samples from the mission are then packaged along with flight data sheets and sent to Isotopes, Inc. for radiochemical analyses.

THE FILTER SAMPLING MEDIUM

The filter paper used in all HASP missions was IPC 1478. This paper was developed by the Institute of Paper Chemistry in 1949 for the express purpose of obtaining a sampling medium which would have the combined properties of high permeability, low ash content, low radioactivity content and high retention for small particles filtered from high velocity air streams. The objective was fulfilled by making the paper from lightly beaten second cut cotton linters, Grade 46, obtained from the Hercules Powder Company. The molded filter mat is backed by cotton scrim for additional strength. The finished filter paper is impregnated with "Kronisol" (di-butoxyethyl phthalate) which increases the retentivity for particles. The average basis weight of the filters used in HASP was 14.3 grams/ft². The range of basis weights was kept within about 13 to 15 grams/ft². The average fiber diameter is about 20 microns. The uncompressed

thickness of the mat is about one millimeter excluding the cotton scrim backing.

Particle Retention

Laboratory studies of the retention of IPC 1478 filter paper were carried out by Prof. J. A. Van den Akker of the Institute of Paper Chemistry¹.

The purpose of this investigation was to obtain some idea of the possible ranges of particle retention to be expected in HASP missions. At the time of initiation of the program nothing was known of the physical and chemical natures of stratospheric particles. It was guessed that the particles would have a density of about 2.5 g/cm^3 . A laboratory experiment was thus devised in which measurements of the retention of IPC 1478 filter paper for different aerosols could be made. Experiments were conducted in a wind tunnel in which HASP mission conditions were simulated in regard to temperature, pressure and velocity of the air stream. The aerosols tested were silicon dioxide, boron oxide, and aluminum oxide. The average ranges of test conditions were:

pressure downstream from filter	105.8-423.2 lb/ft ²
pressure drop across filter	12-150 lb/ft ²
harmonic mean air velocity in filter	15.5-72 ft/sec.
temperature of free air	-40° to +70°F

For both silicon dioxide and boron oxide the retention under all conditions was not found to be measurably different from 100% for particles as small as 0.0075 micron diameter. The filters exhibited retentions ranging from 30 to 75%, depending on conditions, for the aluminum oxide aerosol whose particles were estimated to be about 0.004 micron diameter. The aluminum oxide particles were too small to be observed in the electron microscope. The diffusion properties of silicon dioxide were studied and it was concluded that both silicon dioxide and boron oxide exhibited anomalously high diffusion coefficients which

account for their high retention in the filters. The aluminum oxide particles were found to behave in accord with filtration theory.

It is difficult to infer the retention of stratospheric particles in the HASP filters from the IPC results. There are, however, some results of independent investigations which shed light on the problem of the collection efficiency of the HASP filters for stratospheric radioactive particles. One experiment, performed by the United States Air Force, involved U-2 flights sampling stratospheric air with two ply filters inserted in the sampling duct of the U-2 aircraft. Radiochemical analyses showed that under these conditions greater than 95% of the radioactivity was retained by the upstream filter. Studies conducted under HASP at Isotopes, Inc. on stratospheric particles and on the distribution of radioactivity with depth in the filter mat of HASP samples also tend to support retentions of greater than 95%. The details of these latter studies and their meanings are presented in Part II of this report. In view of the results of the various retention studies, it is concluded that the assumption of 100% retention of stratospheric radioactive particles in HASP filters is justified and will not cause more than a five percent error in the determinations of concentrations of the various nuclides measured in HASP.

Pressure Drop-Flow Rate Characteristics

A relationship between a reduced pressure drop and a reduced face velocity of a filter was found by Reid^{2, 3} in 1949. This relationship was expressed in the form of a single curve and applies to a given filter paper over all measured pressures, pressure drops, temperatures and face velocities. The main features of Reid's analysis are reviewed here primarily as a basis for understanding the determination of volumes of air sampled in HASP. Reid reasons that the force on a filter in a duct is analogous to the drag force of a

solid body in an air stream. The pressure loss coefficient of a filter in a duct through which air is flowing is defined as

$$k = \Delta p/q \quad (3.1)$$

where

Δp = pressure drop across filter

$q = 1/2 \rho V^2$ = dynamic pressure

ρ = density of air at upstream filter face

V = velocity of air at upstream filter face.

The definition of k is analogous to that of the drag coefficient, C_D , of a solid body in an air stream:

$$C_D = D/S q \quad (3.2)$$

Where D/S is the drag force divided by the projected area of the body and, thus has dimensions equivalent to a pressure. The quantity q is the dynamic pressure, as in equation (3.1).

By analogy the pressure loss coefficient is a function solely of the Reynolds number associated with incompressible flow within the filter. Thus

$$k = f\left(\frac{\rho V t}{\mu}\right) \quad (3.3)$$

where

μ = the coefficient of viscosity of air at upstream face of filter

t = a length characteristic of the filter medium, e.g. fiber diameter.

Since t depends only on the filter and not on the dynamic quantities characterizing the air stream, a "pseudo-Reynolds number", $\sigma V/\omega$, is introduced which will serve as well as the Reynolds number. In this definition

σ = relative density of air at upstream filter face = ρ/ρ_0 .

ρ_0 = density of air at sea level in the standard atmosphere.

ω = relative viscosity of air at upstream filter face = μ/μ_0 .

μ_0 = coefficient of viscosity of air at sea level in the NACA standard atmosphere.

Equation (3.3) then becomes

$$k = f_1(\sigma V/\omega) \quad (3.4)$$

With the definition of k we have

$$k = \frac{\Delta p}{q} = \frac{\Delta p}{1/2 \rho V^2} = \frac{2\Delta p}{\rho_0 \sigma V^2} = f_1(\sigma V/\omega) \quad (3.5)$$

Thus by solving for Δp and multiplying both sides by σ/ω^2 we obtain

$$\sigma \Delta p / \omega^2 = \frac{\rho_0}{2} K (\sigma V/\omega)^2 = \frac{\rho_0}{2} (\sigma V/\omega)^2 f_1(\sigma V/\omega) \quad (3.6)$$

which is equivalent to

$$\sigma \Delta p / \omega^2 = f_2(\sigma V/\omega) \quad (3.7)$$

We have thus found that the quantity $\sigma \Delta p / \omega^2$, a reduced pressure drop, is also a function only of the pseudo-Reynolds number which may be viewed as a reduced velocity, since both σ and ω are dimensionless quantities. The validity of the analysis has been demonstrated quite thoroughly in experimental work by Reid³ and by Van den Akker¹. The important point to bear in mind is that each single filter is characterized by a particular function, $f_2(\sigma V/\omega)$, the function being different for different filters. The curve in Fig. 3.6 shows the results obtained by Reid for a filter of basis weight 14.3 g/ft² (which is the average basis weight of all HASP filters) in a plot of $\sigma \Delta p / \omega^2$ vs. $\sigma V/\omega$ with Δp in units of pounds/ft² (psf) and V in ft/sec (fps). The filter, whose characteristics are shown, was used in the duct flow rate calibration flights conducted in July 1960.

Van den Akker chose to express the filter characteristics in terms of average values of σ and V . The average density, $\bar{\sigma}$, is defined as

$$\bar{\sigma} = 1/2 (\sigma_1 + \sigma_2)$$

Where subscripts 1 and 2 refer to upstream and downstream faces of the filter.

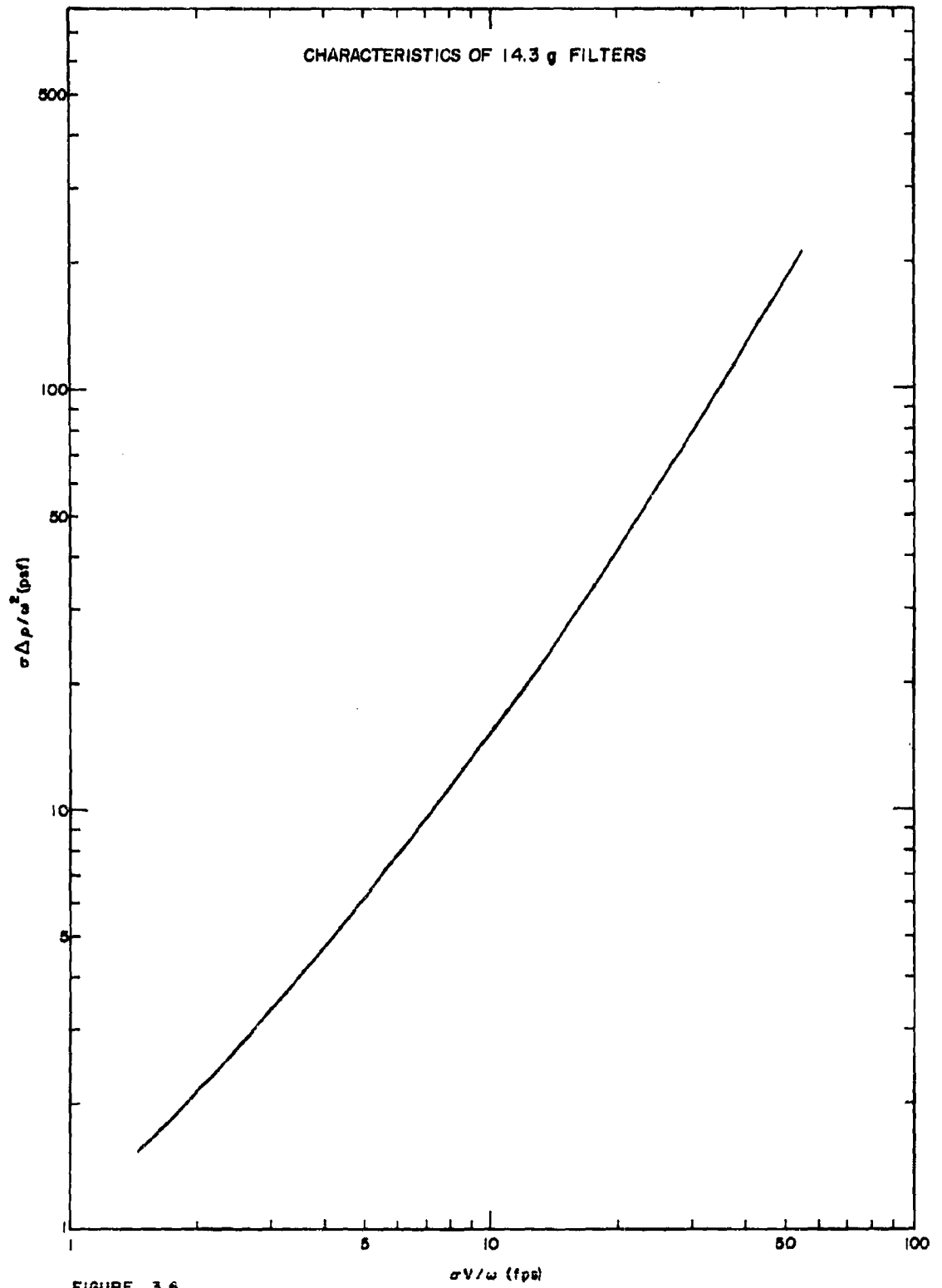


FIGURE 3.6

The average velocity, \bar{V} , which corresponds to the plane within the filter where the relative density is equal to $\bar{\sigma}$ is the harmonic mean velocity defined by

$$\frac{1}{\bar{V}} = \frac{1}{2} \left(\frac{1}{V_1} + \frac{1}{V_2} \right) .$$

In all cases under consideration the temperature at both faces of the filter is negligibly different from stagnation temperature. Thus there is essentially no difference between the relative viscosity at the upstream face and the average relative viscosity. We shall continue to use the symbol ω for relative viscosity in the discussion of average characteristics.

Since $\bar{\sigma}$ and \bar{V} refer to the same plane within the filter and $\bar{\omega} = \omega_1 = \omega_2 = \omega$ the equation of continuity gives

$$\bar{\sigma} \bar{V} / \omega = \sigma_1 V_1 / \omega_1 = \sigma_2 V_2 / \omega_2 .$$

Thus for filter characteristics in terms either of values referred to the upstream face or of average values the reduced velocities will be the same for any single set of conditions. The values of the reduced pressures, however, will be different, for $\bar{\sigma} \neq \sigma$, except when $\Delta p = 0$. For a single filter the two methods of expressing the characteristics yield two different curves.

Van den Akker performed his analyses on seventy different filter specimens tested over the ranges of conditions which he used for particle retention measurements and which were listed in the previous section of this chapter. The average basis weight of the seventy samples was 15.2 g/ft². A quadratic curve of $\bar{\sigma} \Delta p / \omega^2$ vs $\bar{\sigma} \bar{V} / \omega$ was fitted to 1450 data points. The standard deviation of the fit was 6%. The equation of the curve, which is shown in figure 3.7, is

$$\log(\bar{\sigma} \Delta p / \omega^2) = - 0.0388 + 1.0717 \log(\bar{\sigma} \bar{V} / \omega) + 0.1577 \log\left[\frac{\bar{\sigma} \bar{V} / \omega}{\bar{\sigma} \bar{V} / \omega}\right]^2 \quad (3.8)$$

Isotopes, Inc.

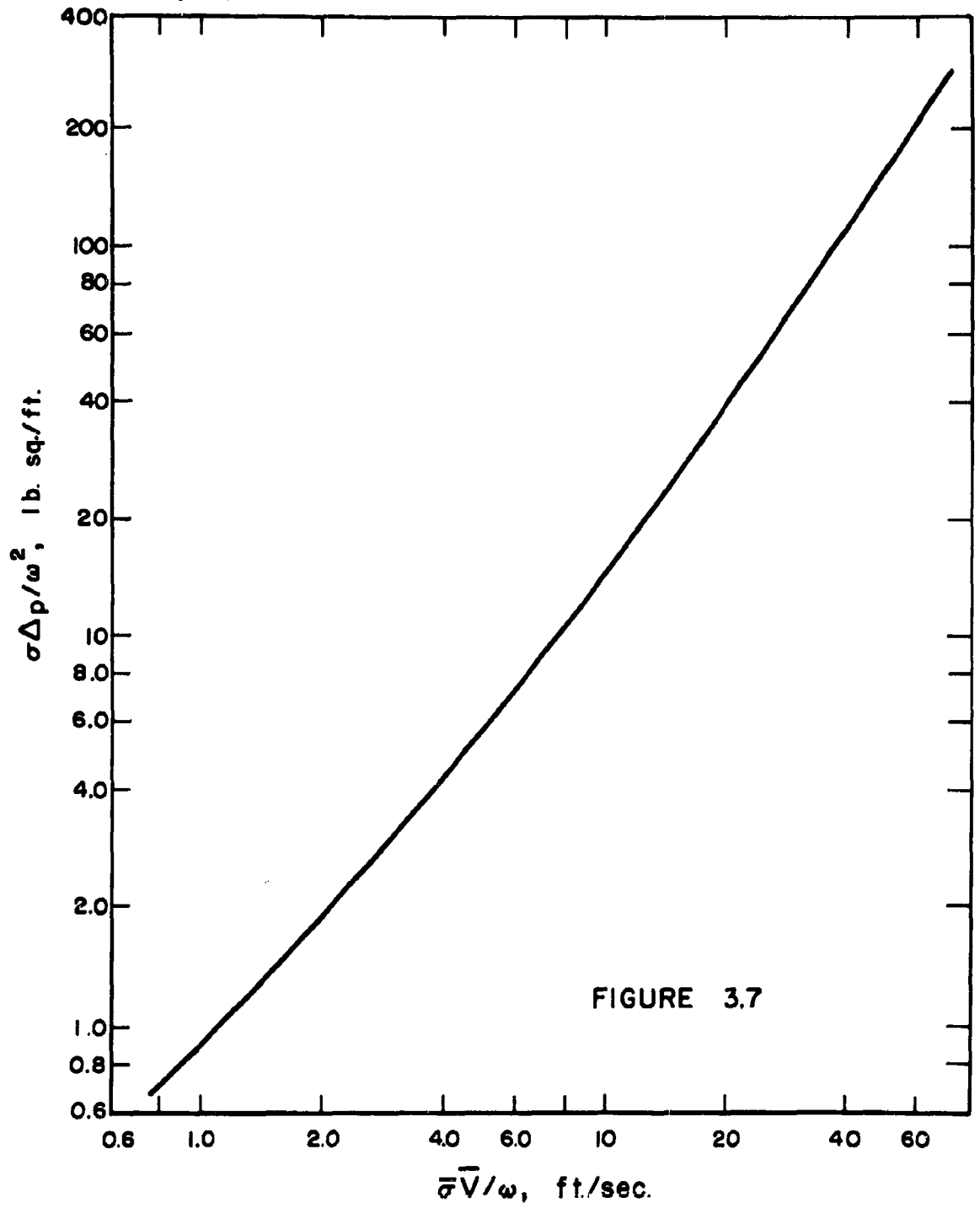


FIGURE 3.7

In the course of his work, Van den Akker found, for some single filters, that for low values of $\sigma V/\omega$ (<10 ft/sec) different conditions of pressure and temperature did not yield single valued curves when $\sigma_1 \Delta p/\omega^2$ was used as the ordinate. The use of $\bar{\sigma} \Delta p/\omega^2$ as the ordinate actually brought the points close to a single curve.

In Reid's wind-tunnel work the pressure could not be varied sufficiently at a given value of $\sigma V/\omega$ to give different values of $\sigma \Delta p/\omega^2$. The reason why the use of average characteristics tends to eliminate multivalued curves at low $\sigma V/\omega$ is probably that the filter tends to compact when the pressure drop across the filter becomes a substantial fraction of the pressure at the upstream face. This is the case for low pressure and high velocity a common situation in HASP sampling at the higher altitudes, e.g., at 70,000 feet and an indicated airspeed of 110 knots $\Delta p = 34$ psf and $p_1 = 132$ psf for the nose sampler with 14.3 g/ft² filters.

When a filter compacts in an air stream, the velocity profile through the filter mat changes. For equal values of $\sigma V/\omega$ in the compacted and uncompact cases it is to be expected that the velocity change at the average plane ($\sigma = \bar{\sigma}$) is less than that at the plane of the upstream face. Thus, while neither analysis of filter characteristics explicitly accounts for compaction effects in the filter, (in fact a rigid medium is implicitly assumed) the use of average values is inherently less sensitive to them.

The immediate concern in HASP over the presentation of filter characteristics will be made clear in the following section of this chapter. It is felt, however, that a discussion of the nature of filter characteristics is warranted since it may act as a guide in planning any air filtration studies.

In the limit of low velocity flow of a viscous fluid through a porous medium Darcy's law is applicable. This is an empirical law which states that

$$\Delta p = \frac{\mu h V}{B_0} \quad (3.9)$$

where h = thickness of porous medium in the direction of fluid flow.

B_0 = specific permeability coefficient

When applied to flow through a thin filter, Δp , μ , and V are as previously defined. The specific permeability coefficient of the filter, B_0 , is a property only of the filter and is constant in the absence of compaction. Equation (3.9) is equivalent to

$$\sigma \Delta p / \omega^2 = K (\sigma V / \omega) \quad (3.10)$$

with $K = \mu_0 / B_0$. Thus, it is expected that the limiting slope of a log-log plot of $\sigma \Delta p / \omega^2$ vs $\sigma V / \omega$ should be unity. Examination of figures 3.6 and 3.7 and equation 3.8 shows that this is the case for IPC 1478 filter paper. Many attempts have been made to understand the details of flow in porous media.⁴ Most often the end result has been a modification of Darcy's law which adequately defines the relationship of Δp to V for particular fluids in particular porous media, but which give little or no physical insight into the mechanisms causing the relationship.

In their work on IPC 1478 in connection with the balloon borne samplers of Project Ashcan, Stern, Zeller and Scherman⁵ were successful in showing that for low face velocities (up to about 4 ft/sec) Darcy's law could be modified to account for slip flow. A modified Cunningham slip correction term, C_a , was found by observing the apparent viscosity, μ , in plots of Δp vs V at different pressures and equating C_a to the ratio of μ to the viscosity in the absence of slip flow, μ_0 . Thus

$$C_a = \mu / \mu_0$$

Stern, et al found that C_a could be expressed as a function of pressure, viz.

$$C_a = 1 + 13.75/p \quad (p \text{ in millibars}) \quad (3.11)$$

and that the modified Darcy's law equation was

$$\Delta p = \frac{\mu_0 h V}{C_a B_0} \quad (3.12)$$

a plot of $C_a \Delta p$ vs V giving a straight line.

When this approach is applied to Van den Akker's data, in which $V > 15$ ft/sec, it fails to reduce the multi-valued curves to a single curve. Again a rigid porous medium is assumed.

To date there has not been found a model of a porous medium which adequately accounts for the effects of compaction of the fibers in a filter and the effects of slip flow around the fibers. To illustrate the nature of the problem to be solved we present here a short treatment of the drag theory of permeability. (See also Scheidegger⁴.)

The drag coefficient as given in equation (3.2) can be applied to the flow of a fluid through a filter paper by letting D be the drag force per unit volume of filter paper on the fibers located within the unit volume. Thus

$$D = C_D S q = 1/2 C_D \rho V_p^2 S \quad (3.13)$$

where S is the projected area of all of the fibers in a unit volume and V_p is the velocity of the fluid in the average pore. The total length of fiber, L , in a unit volume of filter paper is given by

$$\pi \delta^2 \frac{L}{4} = \rho_p / \rho_f = 1 - P \quad (3.14)$$

where δ = fiber diameter
 ρ_p = bulk density of filter
 ρ_f = fiber density
 P = porosity of filter

Thus the projected fiber area per unit volume of filter is:

$$S = \delta L = \frac{4(1-P)}{\pi \delta} \quad (3.15)$$

Substitution of equation (3.15) into equation (3.13) yields

$$D = \frac{4}{\pi} \frac{C_D Re}{2} \frac{1-P}{\delta^2} \mu V_p \quad (3.16)$$

where

$$Re = \text{local Reynolds number} = \frac{\rho V_p \delta}{\mu}$$

It is commonly assumed that the seepage velocity, V_s , defined as the volumetric flow rate divided by the macroscopic cross-sectional area of the filter is given by:

$$V_s = V_p P. \quad (3.17)$$

This is known as the Dupuit-Forchheimer assumption which considers V_p to be an actual statistical average over all local velocities⁴. We will adopt this assumption for simplicity with the realization that it may not be adequate in describing flow through IPC 1478 filter paper.

It can be shown⁴ that if V_s is referred to the arithmetic mean pressure in the porous medium, the drag equation expressing Δp in terms of q is applicable to compressible flow. Van den Akker¹ has shown that \bar{V} , the harmonic mean velocity, refers to the arithmetic mean pressure in the filter. We may thus identify \bar{V} with the seepage velocity V_s . Substitution of equation (3.17) into equation (3.16), placing $V_s = \bar{V}$, yields

$$D = \frac{4}{\pi} \left(\frac{C_D Re}{2} \right) \left(\frac{1-P}{P} \right) \frac{\mu \bar{V}}{\delta^2} \quad (3.18)$$

The drag force per unit volume can be equated to the pressure drop per unit length. Thus the pressure drop across a filter of thickness h is given by:

$$\Delta p = \frac{4h}{\pi} \left(\frac{C_D Re}{2} \right) \left(\frac{1-P}{P} \right) \frac{\mu \bar{V}}{\delta^2} \quad (3.19)$$

This equation can be expressed in terms of average filter characteristics by multiplying both sides by $\bar{\sigma} / \omega^2$, giving

$$\bar{\sigma} \Delta p / \omega^2 = \frac{2h \rho_0}{\pi \delta} \left(\frac{1-P}{P^2} \right) C_D (\bar{\sigma} \bar{V} / \omega)^2, \quad (3.20)$$

when the local Reynolds number is given as

$$Re = \frac{\rho V_p \delta}{\mu} = \frac{\rho_0}{\mu_0} \frac{\delta}{P} (\bar{\sigma} \bar{V} / \omega).$$

If compaction of the porous medium is an important effect, the porosity, P , becomes a variable. A mere plot of $\bar{\sigma} \Delta p / \omega^2$ vs $\bar{\sigma} \bar{V} / \omega$ is not sufficient for determining the dependence of porosity upon Reynolds number, for the drag coefficient, C_D , is also dependent upon the Reynolds number. The experimental fact that $\bar{\sigma} \Delta p / \omega^2$ is a unique function of $\bar{\sigma} \bar{V} / \omega$ indicates that the quantity $\left(\frac{1-P}{P^2} \right) C_D$ is a unique function of $\bar{\sigma} \bar{V} / \omega$ as well. What is required to unravel the drag coefficient from the porosity term in equation (3.20) is a model which yields the individual dependencies of the two terms on $\bar{\sigma} \bar{V} / \omega$. The model should yield an expression for the drag coefficient of an average fiber imbedded in a medium surrounded by neighboring fibers. In addition, the model should account for a variable porosity caused by compaction of the fibers under the influence of the drag force.

The effects of slip flow further complicate the picture of pressure drop-velocity relationships. Modification of the drag theory might be accomplished to account for slip flow by substitution of a modified viscosity following a method similar to that of Stern, et al⁵.

As a final note to this discussion of pressure drop-flow rate characteristics we mention here that an equation fitting Van Den Akker's experimental curve (Figure 3.7) was found:

$$\bar{\sigma} \Delta p / \omega^2 = a \left[\bar{\sigma} \bar{V} / \omega + b \left(\bar{\sigma} \bar{V} / \omega \right)^2 + c \right] \quad (3.21)$$

with $\left. \begin{array}{l} a = 0.966 \\ b = 0.0500 \\ c = -0.125 \end{array} \right\} \Delta p \text{ in pounds/ft}^2 \text{ and } \bar{V} \text{ in ft/sec.}$

This equation fits the experimental curve within about 5% over the whole range of experimental points and within 1% for values of $\bar{\sigma} \bar{V} / \omega > 7$. While this equation is certainly not more accurate than that obtained by Van den Akker (equation 3.8), it is perhaps in a form more readily used in computations of flow rates to be expected in planning specific experiments or programs utilizing IPC 1478 filter paper.

THE COMPUTATION OF SAMPLE VOLUMES

The flight data for HASP missions were supplied as films of the A-O panel (described in a previous section of this chapter) and on flight data cards containing observations recorded by the pilots. These data provide the following parameters of the flight during exposure of a single sample:

<u>Parameter</u>	<u>Source</u>
Indicated air speed (IAS)	Pilot
Outside air temperature	A. F. Weather Service Forecasts
Stagnation temperature	A-O Panel
Altitude	Pilot and A-O Panel
Time (at sampling end points)	Pilot and A-O Panel
Latitude and Longitude (at sampling end points)	Pilot

In principal, the only additional information required for computation of the volume of air which passed through the sampler is the volumetric flow rate of the air in the sampling duct under the particular conditions of air speed, altitude, and temperature. Ideally, the volumetric flow rate should have been measured for each sample. This, however, would have involved the use of considerable instrumentation and created additional problems in maintenance and calibration of instruments. Such an impractical procedure (virtually impossible for routine missions) was obviated by a series of special calibration flights. In these flights, the volumetric flow rates of a hatch sampler and a nose sampler, with filter papers of average basis weight in the ducts, were determined for a range of air speeds at different altitudes. The flow rates so obtained and corrected for temperature are considered to be applicable in the computations of the volumes of all HASP samples collected in different samplers and with filters of different basis weights. The spread in basis weight of the filters used in HASP was about $\pm 7\%$ of the average basis weight.

An estimation of the effect of variable basis weight on the computed nuclide concentrations is given in the following section of this chapter. It is assumed that each nose sampler is identical in construction and in aerodynamic characteristics with the nose sampler used in the calibration flights. A similar assumption is made for the hatch samplers.

Calibration of Duct Samplers

In July 1960 a series of flights was conducted at Edwards Air Force Base for the purpose of calibrating the air flow rates in the U-2 duct samplers. The basic plan of the calibration program was to obtain volumetric flow rates in each duct sampler (hatch and nose) for a series of air speeds at different altitudes. The envelope of altitude-air speed range attained in the calibration flights completely encompassed the HASP sampling envelopes. Each calibration flight consisted of two phases - high fuel weight and low fuel weight. The purpose of the different weights of fuel was to ascertain the effect of angle of attack on the flow rates through the sampling ducts. Filter papers with known pressure drop-flow rate characteristics were placed in the ducts. In-flight measurements of altitude, air speed, pressures at upstream and downstream filter faces, and stagnation temperature, all with calibrated instruments, sufficed to determine the required flow rate-altitude-air speed relationship.

The details of the instrumentation, the flight plans, and data reduction are given in Appendix A, which is Prof. E. G. Reid's report of the calibration program. An outline of the method employed to obtain the flow rate calibration curves is given here so that the reader may more readily understand the method of calculation of the sample volumes for HASP missions.

Construction of Flow Rate Calibration Curves

The following quantities, measured at each altitude and air speed, were used to calculate flow rates:

1. Altitude
2. Indicated air speed
3. Pressure at upstream filter face (p_f)
4. Pressure at downstream filter face (p_d)
5. Indicated temperature (stagnation temperature) (T_s)

The quantities determined from the recorded data are listed in Table 3.6 with the basis of the calculation. Figure 3.8 shows schematically the relationship of the parameters to the filter in the sampling duct.

The reduced pressure drop, $\sigma_f \Delta p_f / \omega_f^2$ is computed from the parameters obtained from the calibration data. The curve of filter characteristics (Figure 3.6) referred to the upstream filter face gives the value of $\sigma_f V_f / \omega_f$ corresponding to the reduced pressure drop. From this the flow rate, Q , through the duct is readily computed.

$$Q = \rho_f V_f A = \rho_o \sigma_f V_f A \quad (3.22)$$

where A = cross sectional area of filter. The mass flow rate, or equivalently, the flow rate of air referred to sea level conditions, Q_o , is given by:

$$Q_o = \sigma_f V_f A \quad (3.23)$$

The high fuel weight resulted in a pressure drop across the hatch filter which was less than 5% higher than when the fuel weight was low. Toward low air speeds the curves of indicated air speed vs. Δp_f cross as shown in Figure 3.9. The HASP missions above 66,000 feet were flown with low fuel weights. For the purpose of constructing the calibration curves the averages of the Δp_f 's for high and low weights were used except for altitudes above 66,000 feet where low weight data were used. The nose sampler exhibited essentially no effect due to weight, as shown in Figure 3.10.

Table 3.6 Parameters Used to Determine Duct Flow Rates

<u>Parameter</u>	<u>Symbol</u>	<u>Basis of Calculation</u>
Pressure	p	Altitude corresponding to p.
Ram pressure	q	$q = 1/2 \rho_0 V^2$ where V is velocity corresponding to IAS.
Mach number	M	Determined from value of $\frac{p}{p+q}$.*
Outside air temperature	T	Determined from M and stagnation temperature, T_s .* (checked by local radiosonde observations).
Relative viscosity at filter face (upstream)	ω_f	$\omega_f = \frac{T_f}{T_0}^{3/2} \frac{T_0 + 110.4}{T_f + 110.4}$ T_f, T_0 in ° K. (Sutherland's formula)
Relative density at filter face	σ_f	$\sigma_f = \frac{P_f}{P_0} \frac{T_0}{T_s}$
Pressure drop across filter	Δp_f	$\Delta p_f = p_f - p_d$

* The ratios $\frac{p}{p+q}$ and T/T_s are determined solely by Mach number. These are listed in NACA Report 1135, Equations, Tables, and Charts for Compressible Flow (1953).

Isotopes, Inc.

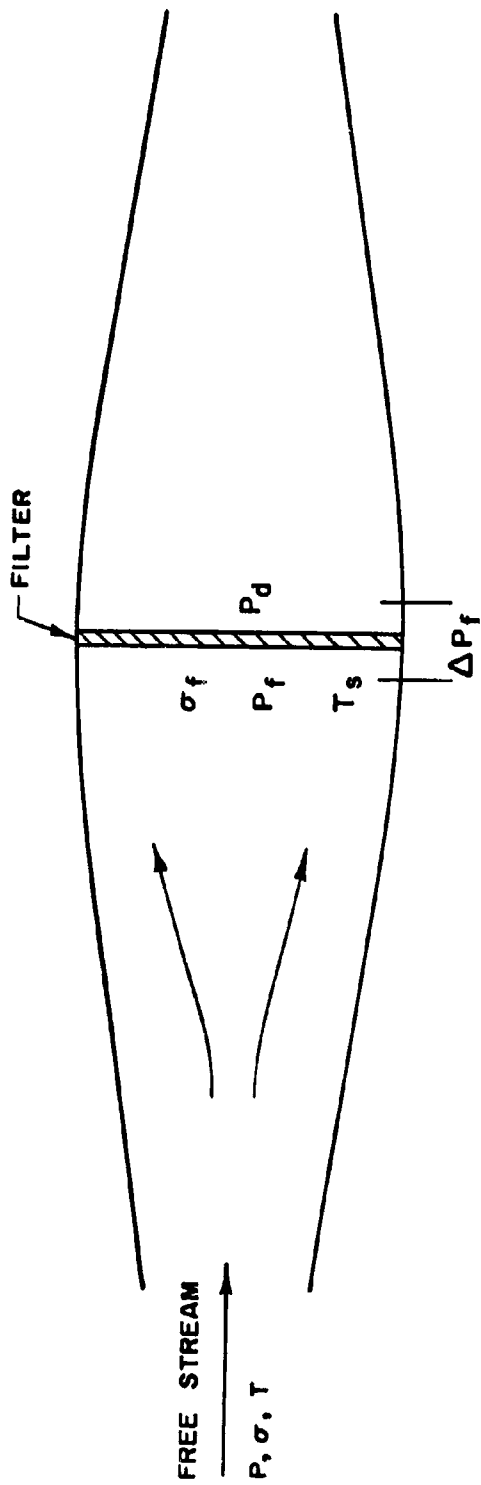


FIG. 3.8 SCHEMATIC RELATIONSHIP OF CALIBRATION PARAMETERS TO SAMPLER

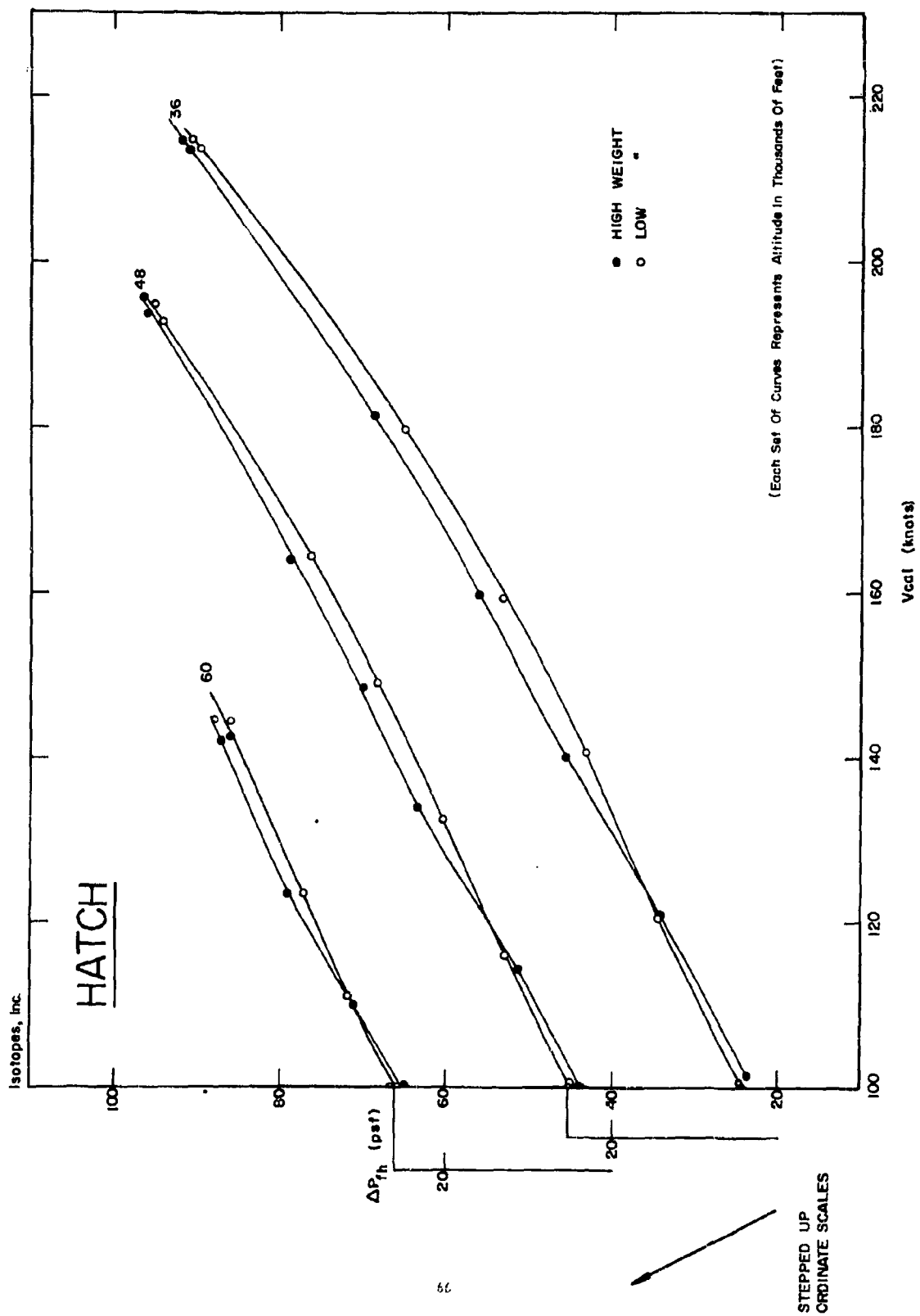


FIGURE 3.9 RECORDED PRESSURE DROP ACROSS FILTER

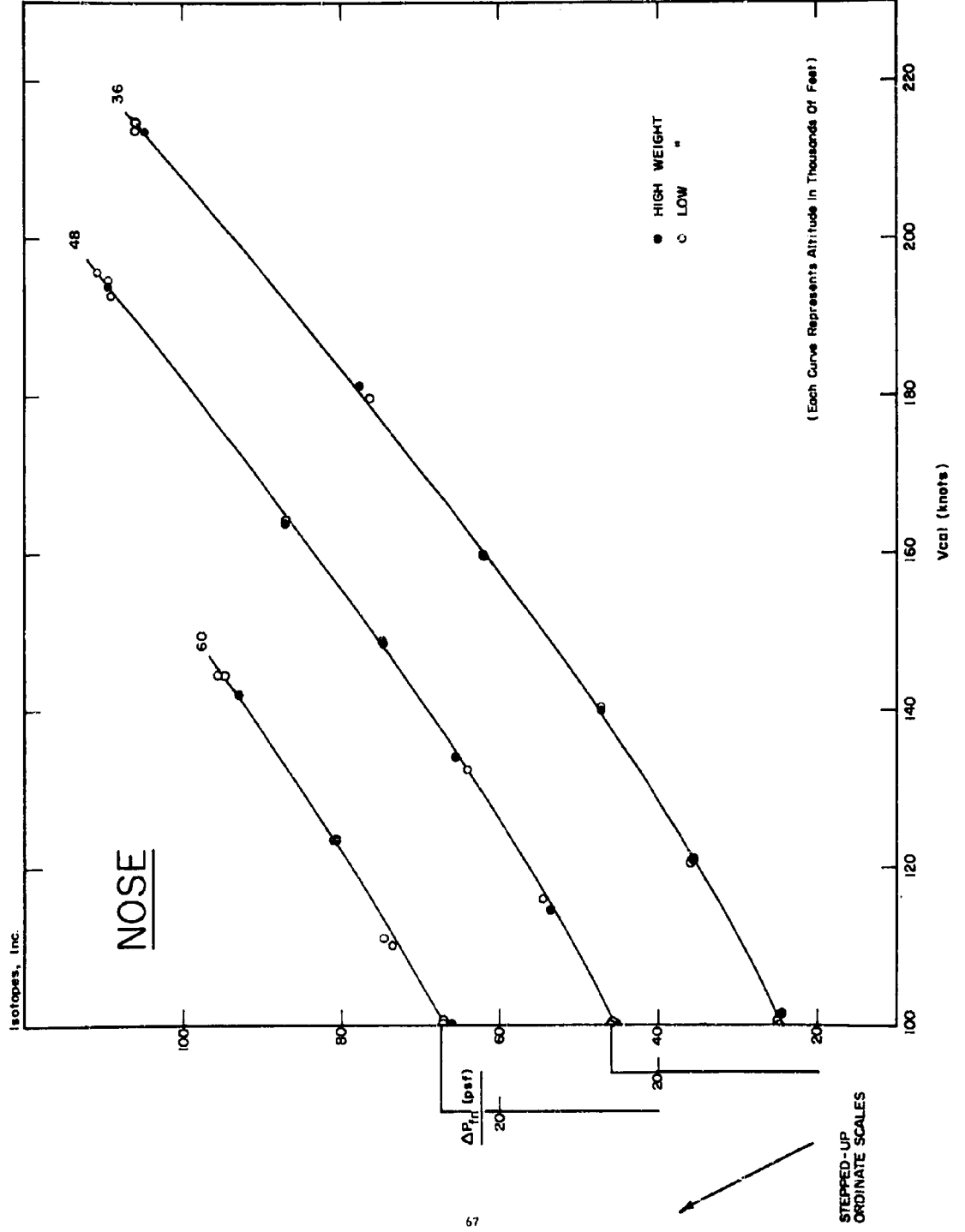


FIGURE 3.10 RECORDED PRESSURE DROP ACROSS FILTER

Since the calibration flights were carried out in air whose temperatures did not coincide with those of the standard atmosphere, the values of ω_f and σ_f were adjusted for each data point to correspond to standard atmosphere temperatures. The resulting flow rates (that is, Q , in ambient cubic feet per minute) were first plotted as a family of curves as a function of indicated air speed with each curve representing a single altitude. The families of curves for the nose and hatch samplers are shown in Figures 3.11 and 3.12 respectively. From these curves, the working calibration curves, plotted as Q vs altitude for each of a series of indicated air speeds, were constructed. The working curves are shown in Figures 3.13. and 3.14 for nose and hatch samplers respectively.

Determination of Flow Rates for Temperatures Different From the Standard Atmosphere,

The standard atmosphere (ARDC model atmosphere, 1959) has a tropopause height of 36,500 feet above which the stratosphere is isothermal with a temperature of 216.66 °K. Most HASP missions through the tropical stratosphere encountered temperatures lower than the standard value, sometimes down to about 192 °K. In a few cases, in the polar stratosphere, temperatures a few degrees warmer than 216 °K were encountered. It was thus necessary to determine the effect of temperature upon the flow rates. The method employed is outlined below.

The principal assumption made is that for flight at a given altitude and a given air speed, the pressure drop across the filter, Δp_f , does not vary with temperature. Though this is not strictly so, it appears to be reasonable, for the flight data show that, for the schedule of air speeds and altitudes employed in HASP, at constant indicated air speed and different densities (altitude) the pressure drop across the filter varies less than 10 percent with a density change

Isotopes, Inc.

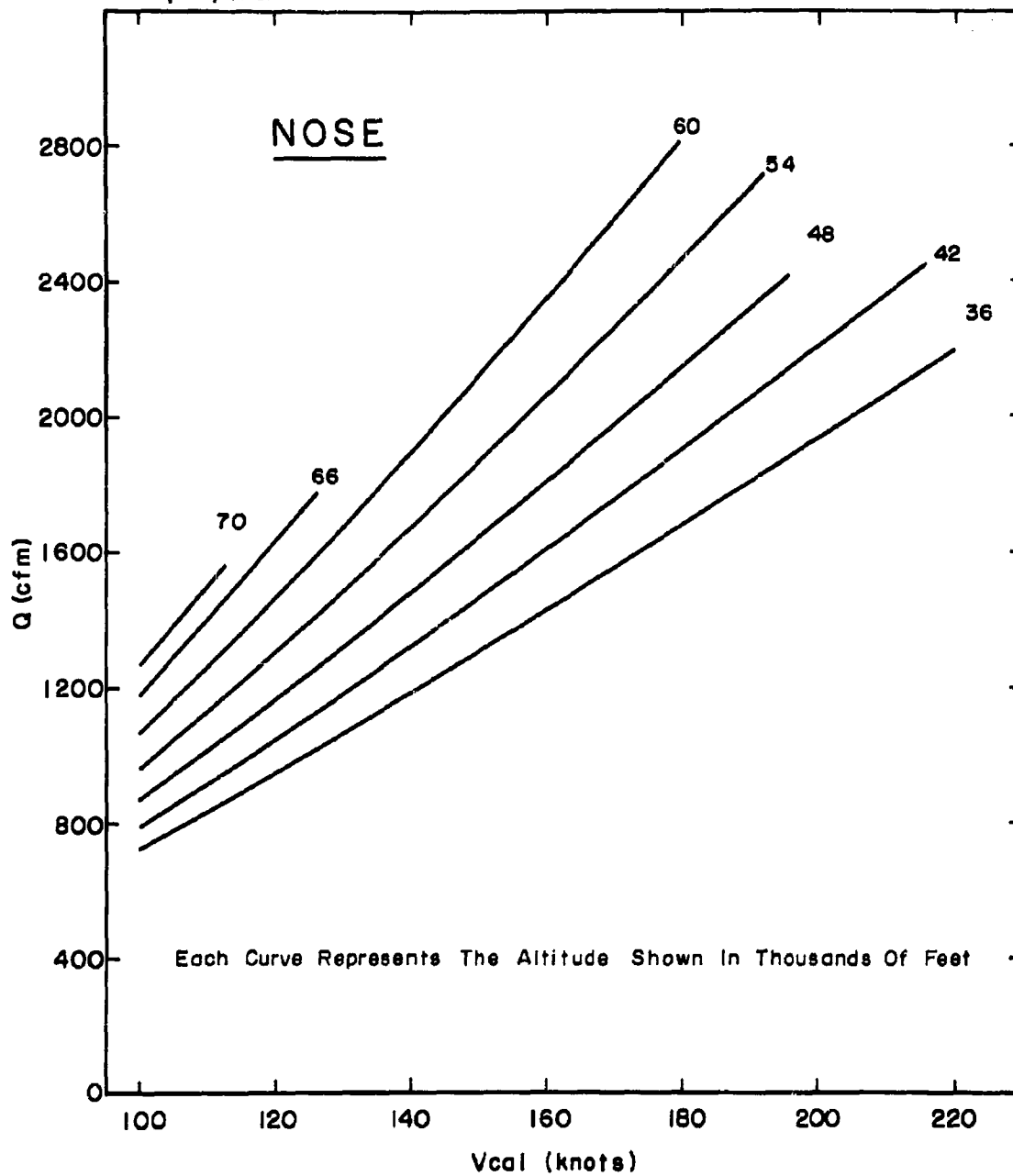


FIG. 3.11 STANDARD ATMOSPHERE FLOW RATES

Isotopes, Inc.

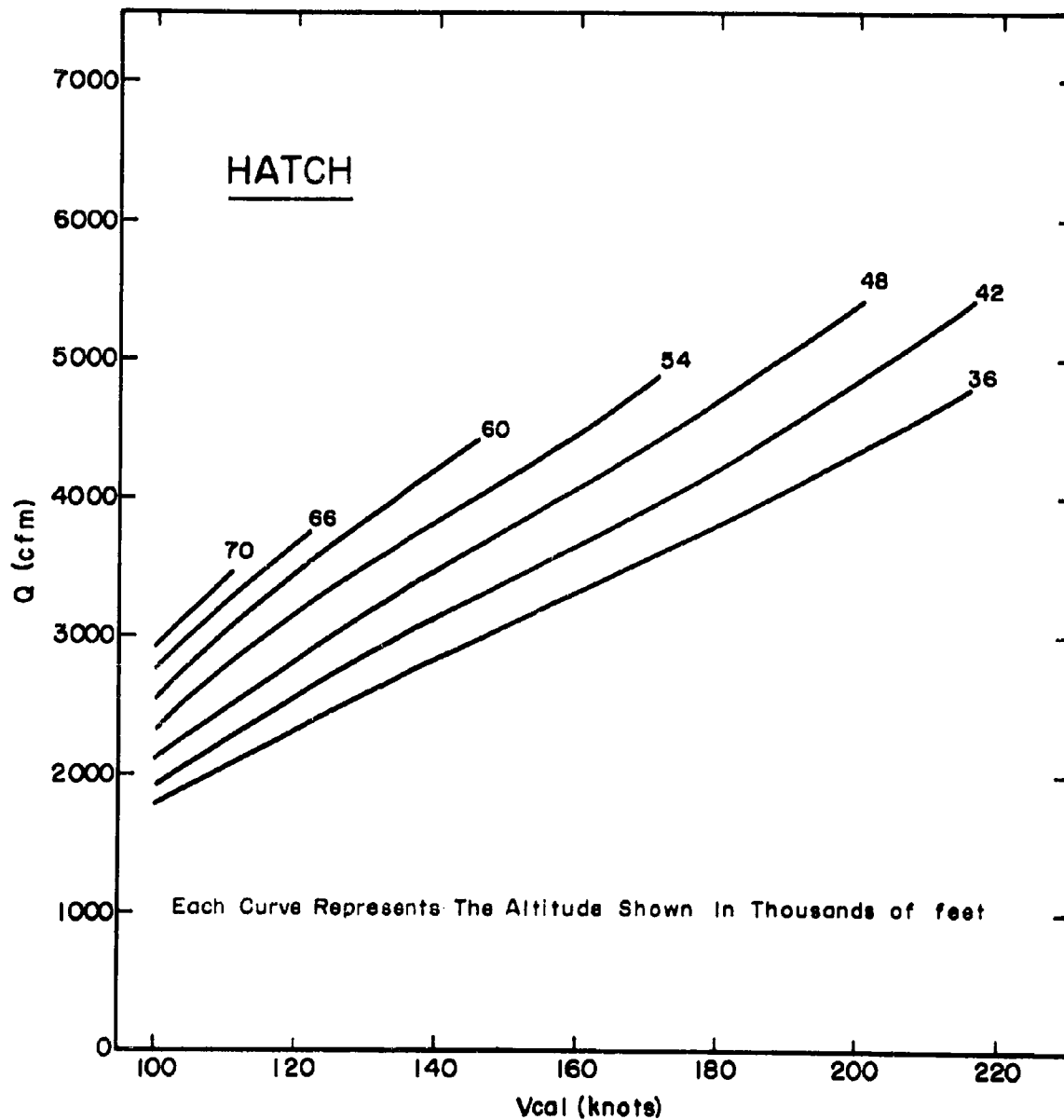


FIG. 3.12 STANDARD ATMOSPHERE FLOW RATES

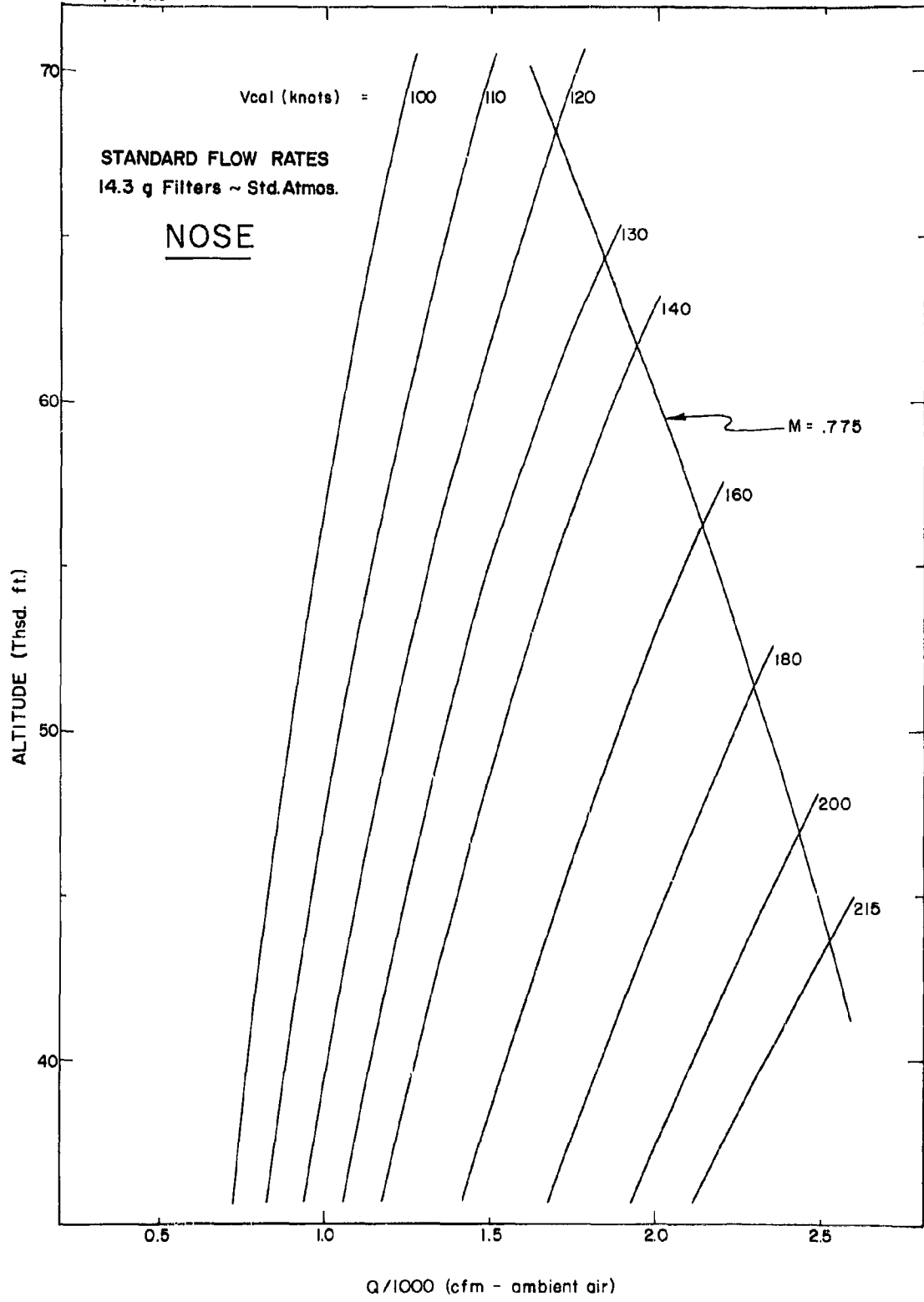


FIGURE 3.13

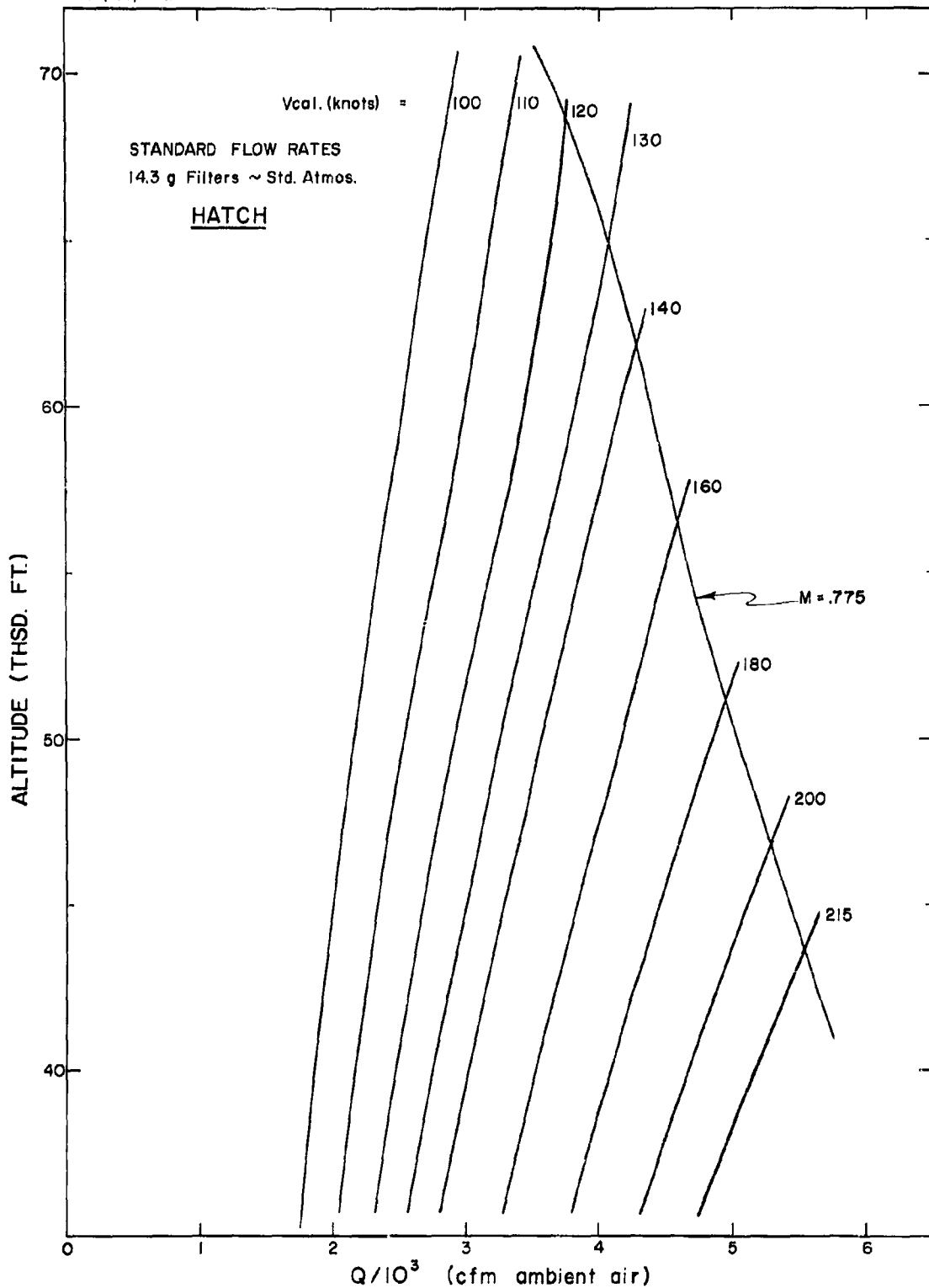


FIGURE 3.14

of 100%.

For simplicity we drop the subscript f since all quantities are referred to the upstream filter face. Further we denote quantities referring to flight in the standard atmosphere by the subscript o . For flight at a particular altitude and a particular air speed in air with a particular temperature, different from that of the standard atmosphere, we encounter a reduced pressure drop given by

$$\sigma_1 \Delta p / \omega^2 = (\sigma_o \Delta p / \omega_o^2) \left[\frac{\omega_o^2}{\sigma_o} \frac{\sigma_1}{\omega_1^2} \right] \quad (3.24)$$

where subscript 1 refers to the conditions caused by the temperature. The pressure drop across the filter has been assumed to be constant. The value of $\sigma_1 V_1 / \omega_1$, which corresponds to $\sigma_1 \Delta p / \omega_1^2$ is found by reference to the known filter characteristics (Fig. 3.6). The new standard flow rate, Q_{o1} , is found by

$$Q_{o1} = \sigma_1 V_1 A = \left(\frac{\sigma_1 V_1}{\omega_1} \right) [\omega_1 A] \quad (3.25)$$

In order to apply equations (3.24) and (3.25) we must determine the temperature dependence of the quantities in brackets. First let us note that under the conditions where only temperature varies, the ratio of stagnation temperatures (T_{s1} / T_{so}) is equal to the ratio of outside air temperatures (T_1 / T_o). Since pressure (altitude) is the same,

$$\sigma_1 / \sigma_o = T_{s1} / T_{so} = T_1 / T_o \quad (3.26)$$

The ratio of relative viscosities is given by Sutherland's equation:

$$\omega_1 / \omega_o = (T_{s1} / T_{so})^{3/2} \left(\frac{T_{so} + 110}{T_{s1} + 110} \right) \quad (3.27)$$

The stagnation temperature, T_{s1} , is given by

$$T_{s1} = T_{so} \frac{T_1}{T_o}$$

With reference to equation (3.24) we may define a "temperature coefficient" $R(T_s)$ to be: $R(T) = \frac{\omega_o^2}{\sigma_o} \frac{\sigma_1}{\omega_1^2}$,

and now

$$\sigma_1 \Delta p / \omega_1^2 = R (T) \quad \sigma_0 \Delta p / \omega_0^2 \quad (3.28)$$

Equations (3.26) and (3.27) give

$$R (T) = \left(\frac{T_{so}}{T_{s1}} \right)^4 \left(\frac{T_{s1} + 110}{T_{so} + 110} \right)^2 \quad (3.29)$$

Utilizing equations (3.28), (3.29) and Figure 3.6 and knowing the values of T_1 , T_0 , T_{so} , $\sigma_0 \Delta p / \omega_0^2$, and ω_0 we calculate $\sigma_1 \Delta p / \omega_1^2$ to find $\sigma_1 V_1 / \omega_1$ which then gives Q_{o1} through equation (3.25).

The magnitude of the "correction" due to flight in non-standard atmosphere is largest at the highest altitude, giving a standard flow rate at 70,000 feet which is 2% higher per 10°C decrease in temperature compared to the standard atmosphere. The correction is -0.42% / 10°C lower at 35,000 feet and is zero at about 43,000 feet. These corrections are given for the scheduled indicated air speeds at each altitude. The entire schedule will be given below.

Method of Calculating HASP Sample Volumes

As indicated at the beginning of this section the flight data provide altitude, indicated air speed, outside temperature, stagnation temperature and time of exposure for each sample. The sample volumes are calculated in a straightforward manner by:

1. finding the standard flow rate on the calibration charts corresponding altitude and indicated air speed,
2. correcting the standard flow rate for temperature as outlined above and
3. multiplying by the exposure time.

For the calculation of the volumes of the nearly four thousand samples in HASP, flow rate tables were used in order to eliminate time consuming and

tedious graph reading and interpolation. Two sets of tables, one set for the nose sampler and one set for the hatch sampler, were constructed. Each set consisted of five tables of flow rates for the ranges of indicated air speed and altitude. Each table within the set corresponded to a particular temperature, viz. 193.2°K, 198.5°K, 204.5°K, 210.5°K, and 216.6°K.

Since the aircraft flew according to a schedule of altitude and indicated air speed, it was not necessary to cover the entire range of aircraft capabilities in the flow rate charts. The schedule is given below:

<u>Altitude (ft)</u>	<u>IAS (knots)</u>
35,000	173
40,000	170
45,000	165
50,000	160
55,000	150
60,000	135
65,000	121
70,000	108

The tables were constructed to give the flow rates at each altitude for three air speeds - the scheduled air speed, 5 knots above, and 5 knots below scheduled air speed. The altitudes were taken in 1000 foot intervals from 35,000 to 70,000 feet. In the calculation of sample volumes, linear interpolation between altitudes, air speeds, and temperatures was employed when necessary.

REPRODUCIBILITY OF HASP SAMPLING

In the preceding pages the design, operation and calibration of the filters and the filter samplers which were used during HASP have been described. With the aid of the information which is available from the calibration experiments it should be possible to determine accurately the quantity of air which was sampled during each mission and, with the data from the radiochemical analyses, to calculate the concentrations of the various radionuclides in stratospheric air. The reliability of the radiochemical analyses is discussed later in this chapter. But the reliability of the final results is also influenced by several other factors which affect the precision of the sampling operation. Thus we must assume the aerodynamic equivalence of all of the filters and of all of the filter samplers used during the collection of HASP samples, and the representativeness of the aliquots of the samples used in the analyses. Since all samplers of a single type are identical in construction they should be aerodynamically equivalent, at least within the limits set by the precision of the flight data and of the radiochemical analyses. Moreover the nose samplers and hatch samplers were calibrated simultaneously. Although differences in basis weight, which should cause differences in air flow rates, have been observed between individual sheets of the filter medium, the errors which such variations in basis weight can introduce into the calculations of atmospheric activity should be less than 5 percent. The samplers were designed to give a symmetrical flow of air through the filters and, in the absence of pronounced variations in basis weight from one area of the filter to another, all areas of the filter should collect the same amount of activity.

To some extent the validity of the various assumptions which have been made about the reproducibility of the sampling may be checked by comparing analytical data for certain of the HASP samples. Thus, the uniformity of the distribution of activity across the filters has been investigated in two ways: two or three quadrants of a number of filter samples were analyzed separately to provide data on the representativeness of a single quadrant, and a number of disks were cut from a single filter and their beta activities were measured to permit the elucidation of any non-uniformity in the distribution of activity on the filter. The reproducibility of the entire sampling-analyses program has been checked by comparing the results of analyses of nose and hatch samples collected simultaneously by the same aircraft, of samples collected simultaneously by two different aircraft, and of samples collected in the same region of the stratosphere on the same day by the same or by different aircraft. The observed variations in activity between such samples may be compared with the possible variations due to analytical errors alone to assess the importance of the errors associated with the sampling techniques.

The Distribution of Activity on the Filter

It is important to verify the uniformity of the distribution of activity on the filter samples, for only one half or one quarter of each filter was used in analyzing the samples for any nuclide or series of nuclides. Such verification was attempted throughout the program by selecting an occasional sample, more or less at random, and analyzing two or three quadrants of it for each of a series of nuclides. The results of these analyses are summarized in Table 3.7

in which are listed the percent standard deviation from the mean of the concentrations of each nuclide in each pair of filters. For most of these samples the standard deviation is similar to or slightly higher than that which would have been expected had two aliquots of a sample solution been analyzed (see Table 3.22). For some samples, however, the standard deviations are quite high and it is possible that different quadrants did not collect the same concentrations of activity. This explanation cannot be applicable to all samples, however, for some, such as 1402, 1462, 1765 and 1839 show good agreement among quadrants for some nuclides but poor agreement for others. This might be attributable to the random arrangement of a few large particles of high activity on the filter for samples such as 327 through 330 and 347 through 358, which collected fresh debris from recent tests. The other filters all collected debris which had been in the stratosphere for some months, however, and there is no evidence that "hot" particles contributed a major fraction of their activity. There is reason to suspect that analytical errors caused many of the extreme variations. Sample 1839, for example, displayed fairly good agreement among three quadrants for tungsten-185 and cerium-144 and good agreement between two quadrants for strontium-90 and strontium-89, but one quadrant which was analyzed for strontium-90 did not agree with the others and thus produced a large standard deviation for the strontium-90 analyses. Similarly the large error on the strontium-90 analyses of sample 1765 was caused by data from one quadrant which failed to agree with data for two others, though all three agreed in tungsten-185 concentration.

In any event there is no systematic variation in the data which would indicate that lack of symmetry in the sampler or inhomogeneities in the filter medium had caused the observed variations. They must be attributed either to fractionation of debris among the collected particles or to analytical errors.

In order to delineate the distribution of activity across the face of a filter, 40 disks were cut from a single sample and were beta counted. This filter, sample 3723 had been collected at an altitude of 60,000 feet at 46°N latitude on 28 April 1960, and thus contained debris which has been in the stratosphere for well over a year. The location of the disks is shown in Figure 3.15 and the counting data (in counts per minute) are given in Table 3.8. Two series of measurements were made on the disk. During the first, carried out on 14 and 15 June 1960, the disks were counted in order according to their location on the filter. Each disk was counted for 15 minutes. A second series of measurements was made on 24 and 27 June 1960. Again each disk was counted for 15 minutes, but this time they were counted in random order to eliminate any anomalies which could result from systematic changes in counter performance. One disk, number 2d, was counted a number of times during and between both series of measurements to indicate any effect from decay of the activity. No such effect was observed because of the long effective half life of this old debris.

The data for the individual disks have been averaged in Table 3.9. In Part A of the table the disks have been assigned to octants and the percent deviation of each octant from the mean activity of the paper has been calculated.

Table 3.7 Percent Standard Deviation From the Mean of Analyses of Samples for Which Two or More Quadrants Were Analyzed Separately

Sample	Percent Standard Deviation						
	Sr ⁹⁰	Sr ⁸⁹	Zr ⁹⁵	W ¹⁸⁵	Cs ¹³⁷	Co ¹⁴⁴	Pu
323	2.9	----	----	----	----	----	----
327	2.4	1.8	0.7	----	----	----	----
328	6.8	0.2	9.6	----	----	----	----
329	7.7	13.6	9.6	----	----	----	----
330	16.1	20.8	2.7	----	----	----	----
347	----	----	----	----	----	----	----
348	9.6	----	----	----	----	----	----
349	0.1	----	----	----	----	----	----
350	0.5	----	----	----	----	----	----
351	2.1	9.8	----	----	----	----	----
352	2.9	10.5	10.6	----	----	7.6	----
353	13.0	2.1	7.0	----	----	----	----
354	8.9	8.3	23.7	----	----	----	----
355	11.2	11.2	0.1	----	----	----	----
356	6.8	3.1	5.2	----	----	4.9	----
357	3.4	2.0	3.3	----	----	1.3	----
358	6.9	4.2	----	----	----	12.6	----
594	----	----	30.8	----	----	----	----
1192	5.4	8.6	----	8.3	12.8	----	----
1402	4.1	3.9	----	40.5	75.5	----	----
1430	11.0	5.1	----	8.5	10.4	----	----
1462	0.2	12.1	----	4.4	5.7	----	----
1473	3.6	7.0	----	1.3	4.7	8.9	----
1528	6.6	14.5	----	7.4	43.8	----	----
1570	22.5	11.8	----	104	128	----	----
1594	5.0	29.5	----	3.3	24.0	----	----
1620	5.2	14.1	----	2.4	7.3	----	----
1765	26.4	14.1	----	2.8	----	----	----
1839	20.2	4.7	----	6.3	----	2.1	7.3
1896	8.5	6.8	----	9.9	----	----	----
1980	7.9	17.7	----	19.9	----	----	----
Average	7.9	9.5	9.4	16.8	34.7	6.2	7.3

Table 3.8 The Total Beta Activity of 40 Disks Cut From Sample 3723

Disk	Beta Activity (cpm)			Disk	Beta Activity (cpm)		
	1st Count	2nd Count	Mean		1st Count	2nd Count	Mean
1 a	53.7 ± 2.0	54.2 ± 2.0	54.0 ± 1.4	5 a	59.6 ± 2.1	59.1 ± 2.1	59.4 ± 1.5
1 b	58.8 ± 2.1	55.3 ± 2.0	57.1 ± 2.5	5 b	55.5 ± 2.0	53.8 ± 2.0	54.7 ± 1.4
1 c	59.2 ± 2.1	60.0 ± 2.1	59.6 ± 1.5	5 c	57.9 ± 2.1	54.1 ± 2.0	56.0 ± 2.7
1 d	60.4 ± 2.1	58.1 ± 2.1	59.3 ± 1.6	5 d	52.8 ± 2.0	53.7 ± 2.0	53.3 ± 1.4
1.2	58.1 ± 2.1	57.6 ± 2.1	57.8 ± 1.5	5.6	57.4 ± 2.1	55.1 ± 2.0	56.3 ± 1.6
2 a	53.7 ± 2.0	56.2 ± 2.0	55.0 ± 1.8	6 a	50.9 ± 1.9	55.1 ± 2.0	53.0 ± 3.0
2 b	59.6 ± 2.1	59.2 ± 2.1	59.4 ± 1.3	6 b	56.2 ± 2.0	54.9 ± 2.0	55.6 ± 1.4
2 c	59.0 ± 2.1	59.1 ± 2.1	59.1 ± 1.5	6 c	54.1 ± 2.0	53.5 ± 2.0	53.8 ± 1.4
2 d*	60.4 ± 2.1	63.3 ± 2.2	61.9 ± 2.1	6 d	55.9 ± 2.0	54.1 ± 2.0	55.0 ± 1.4
2.3	60.4 ± 2.1	56.3 ± 2.1	58.4 ± 2.9	6.7	53.6 ± 2.0	51.8 ± 2.0	52.7 ± 1.4
3 a	58.0 ± 2.1	59.3 ± 2.1	58.7 ± 1.5	7 a	53.6 ± 2.0	54.7 ± 2.0	54.2 ± 1.4
3 b	56.5 ± 2.1	57.3 ± 2.1	56.9 ± 1.5	7 b	52.1 ± 2.0	54.4 ± 2.0	53.3 ± 1.6
3 c	55.4 ± 2.0	56.2 ± 2.0	55.8 ± 1.4	7 c	52.1 ± 2.0	48.1 ± 1.9	50.1 ± 3.0
3 d	60.5 ± 2.1	60.8 ± 2.1	60.7 ± 1.5	7 d	58.1 ± 2.1	58.0 ± 2.1	58.1 ± 1.5
3.4	63.0 ± 2.1	65.2 ± 2.0	59.6 ± 4.8	7.8	57.6 ± 2.1	54.8 ± 2.0	56.2 ± 2.0
4 a	54.7 ± 2.0	60.9 ± 2.1	57.8 ± 4.4	8 a	56.3 ± 2.0	56.4 ± 2.1	56.4 ± 1.5
4 b	58.9 ± 2.1	61.9 ± 2.1	60.4 ± 2.1	8 b	53.8 ± 2.0	55.3 ± 2.0	54.6 ± 1.4
4 c	60.6 ± 2.1	60.3 ± 2.1	60.5 ± 1.5	8 c	52.8 ± 2.0	56.7 ± 2.1	54.8 ± 2.8
4 d	56.4 ± 2.1	56.8 ± 2.1	56.6 ± 1.5	8 d	60.1 ± 2.1	52.6 ± 2.0	56.4 ± 5.3
4.5	54.9 ± 2.0	56.5 ± 2.1	55.7 ± 1.5	8.1	55.6 ± 2.0	54.4 ± 2.0	55.0 ± 1.4
Mean	56.7 ± 2.9	56.4 ± 3.0	56.6 ± 2.6				

* Disk 2 d was used as a decay standard during both series of counts. Individual counts on it were: 60.4 ± 2.1 (6-14-60), 58.5 ± 2.1 (6-15-60), 61.5 ± 2.1 (6-16-60), 59.0 ± 2.1 (6-17-60), 61.9 ± 2.1 (6-20-60), 56.6 ± 2.1 (6-21-60), 62.4 ± 2.1 and 61.0 ± 1.8 (6-22-60), 60.8 ± 2.1, 64.9 ± 2.2 and 64.7 ± 2.2 (6-24-60), and 62.9 ± 2.2 (6-27-60).

Isotopes, Inc.

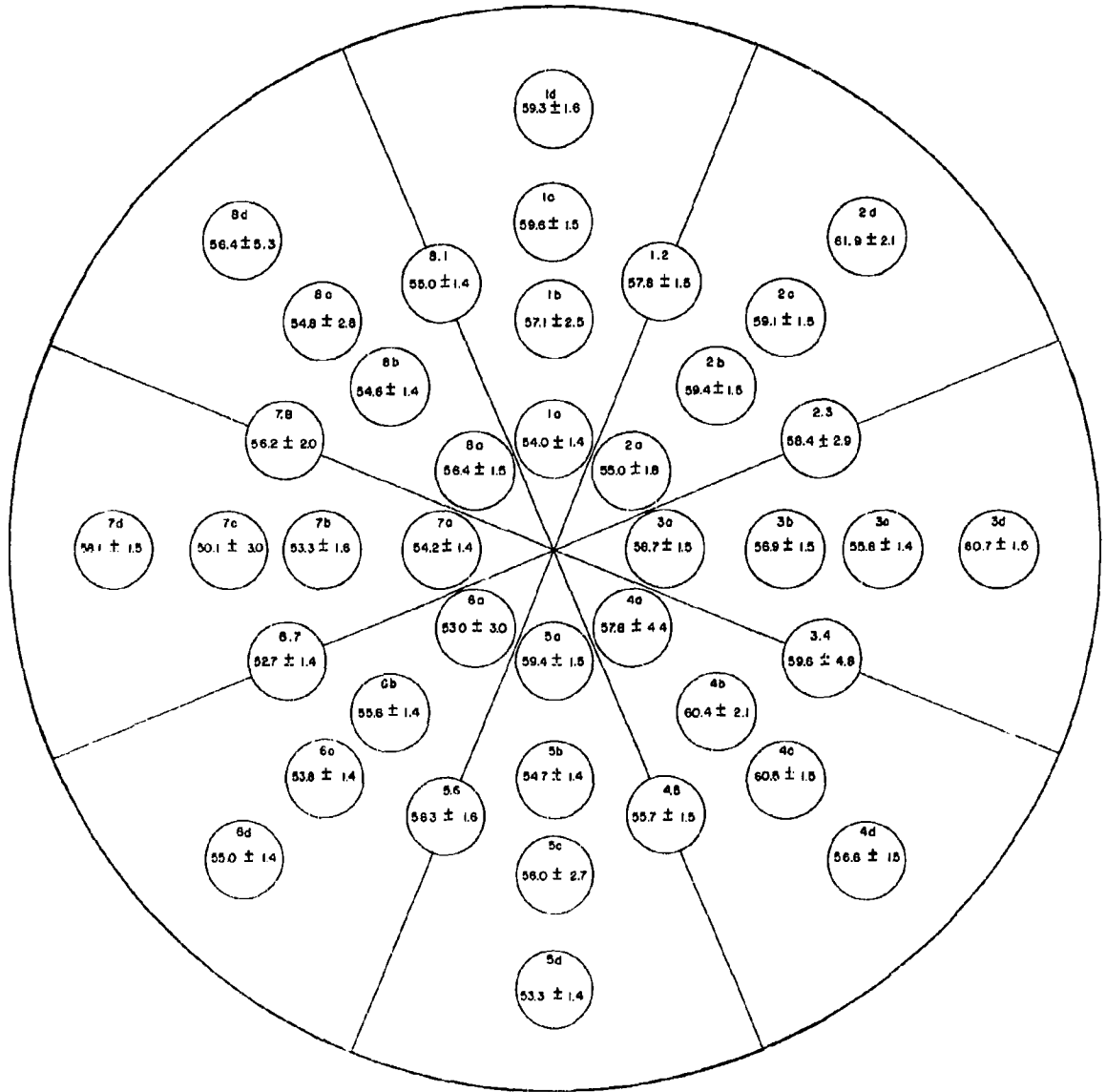


FIGURE 3.15 LOCATION OF DISKS USED TO DETERMINE VARIATION OF TOTAL BETA ACTIVITY ACROSS SAMPLE 3723

In Part B the octants have been combined into quadrants and the same calculation has been made. Obviously there is a real difference in the activity collected by the two halves of the filter and an error could be introduced if only an octant or a quadrant of the paper were used in the radiochemical analysis. The error would not be excessively large for this filter, however, since the greatest deviation of a single octant from the mean is only 4.6 percent and of a single quadrant only 3.2 percent. Were half of the filter used in an analysis an error of about 3 percent would result if the half contained octants 1, 2, 3 and 4 or 5, 6, 7 and 8, but no error would result if it contained octants 3, 4, 5 and 6 or 7, 8, 1 and 2. Thus, if the variations in activity from quadrant to quadrant shown by sample 3723 are typical, little error results from the analysis of only a quadrant of the filter and even less from the analysis of a half.

In Part C of Table 3.9 the disks have been grouped according to their distance from the center of the filter. The outermost ring seems to contain slightly more activity than the rest of the filter, but the difference may not be real. In any event the radial distribution of the activity appears as uniform as could be reasonably expected. This substantiates the belief that lack of uniformity between quadrants is more likely due to variations in basis weight from place to place in the filter than to asymmetrical flow of air caused by the sampler. If this is true the measurement of the distribution of activity on only one sample is inadequate for evaluating the extent to which variations in activity can occur among quadrants. The data in Table 3.7 do give a measure of these variations, however, and, as is noted above, they appear to be no larger than the variations which result from analytical errors.

Reproducibility of Sampling

It was assumed throughout HASP that the sampler calibration data were equally applicable to all samplers which were used. Although this assumption is quite reasonable for the most part, it was desirable that some checks be made by comparing the relative activities of samples which were collected simultaneously, or at least during the same day, in the same air mass. Such data are available for the comparison of both the nose and hatch samplers carried by U-2 aircraft and for the hatch samplers carried by B-52 aircraft during "Sea Fish Special."

On 25 March 1958 a mission was flown from Ramey and Plattsburg specifically to gather information on the reproducibility of the sampling operation. The two aircraft from each base flew together, exposing filters over identical time and latitude intervals. The standard deviations of the individual samples from the mean values for simultaneously exposed pairs are given in Table 3.10, Part A. Two quadrants of each sample were analyzed separately in duplicate, so most of the observed variations should be real and not due to analytical errors. They may be attributable to the presence in these samples of "hot" particles of fractionated debris which had been injected into the stratosphere by Soviet tests only a month before.

The only other missions during which simultaneous collection of similar samples occurred were the "Sea Fish Special" B-52 flights to the North Pole. Data for hatch samples collected simultaneously by the several samplers mounted beneath the wings of these aircraft are given in Part B of Table 3.10. Some differences in collection efficiency among these samplers are quite likely, for

Table 3.9 The Uniformity of Total Beta Activity Across A Filter

A. Variation in Activity Between Octants of the Filter

Octant	1st Count	2nd Count	Ave	% Deviation of Octant from Mean of Filter
1	57.8 ± 2.6	56.7 ± 2.3	57.3 ± 2.4	+ 1.2%
2	58.4 ± 2.7	59.0 ± 2.8	58.7 ± 2.6	+ 3.7%
3	58.4 ± 2.6	58.0 ± 2.0	58.2 ± 2.2	+ 2.8%
4	57.9 ± 2.3	59.3 ± 2.5	58.6 ± 2.4	+ 3.5%
5	56.4 ± 2.6	55.3 ± 2.3	55.9 ± 2.4	- 1.2%
6	54.5 ± 2.2	54.2 ± 0.8	54.4 ± 1.5	- 3.9%
7	54.3 ± 2.6	53.7 ± 3.6	54.0 ± 3.0	- 4.6%
8	55.9 ± 2.8	55.1 ± 1.7	55.5 ± 2.2	- 1.9%
Mean	56.7 ± 1.7	56.4 ± 2.2	56.6 ± 1.9	

B. Variations in Activity Between Quadrants of the Filter

Quadrant	1st Count	2nd Count	Ave	% Deviation of Quadrant from Mean of Filter
1-2	58.1 ± 2.5	57.8 ± 2.7	58.0 ± 2.5	+ 2.5%
3-4	58.2 ± 2.6	58.6 ± 2.3	58.4 ± 2.4	+ 3.2%
5-6	55.5 ± 2.6	54.8 ± 1.6	55.1 ± 2.1	- 2.7%
7-8	55.1 ± 2.8	54.4 ± 2.7	54.8 ± 2.7	- 3.2%
Mean	56.7 ± 1.7	56.4 ± 2.1	56.6 ± 1.9	

C. Variation in Activity from the Center of the Filter Toward the Periphery

Ring	Mean Distance	1st Count	2nd Count	Ave	% Deviation of Rings from Mean of Filter
a	3.4 cm	55.1 ± 2.8	57.0 ± 2.5	56.0 ± 2.7	1.1%
b	7.4 cm	56.4 ± 2.6	56.5 ± 2.8	56.5 ± 2.6	0.2%
c	9.8 cm	57.6 ± 3.0	55.3 ± 2.2	56.5 ± 2.7	0.2%
d	11.3 cm	56.4 ± 3.2	56.0 ± 4.1	56.2 ± 3.6	0.7%
d	15.2 cm	58.1 ± 2.8	57.2 ± 3.7	57.6 ± 3.2	1.8%
Mean		56.7 ± 1.2	56.4 ± 0.8	56.6 ± 0.6	

Table 3.10 Standard Deviation of Sample Pairs Collected Simultaneously

A. Nose Samples Collected by Two Different U-2 Aircraft

Samples	Total Beta	Percent Standard Deviation				
		Sr ⁹⁰	Sr ⁸⁹	Zr ⁹⁵	Ce ¹⁴⁴	Pu
347:351	23.9	20.8	----	----	6.4	22.1
348:352	2.6	7.4	22.0	25.4	3.9	2.1
349:353	37.3	3.1	41.2	----	28.8	4.7
350:354	8.2	0.5	6.4	3.6	15.1	4.5
327:355	13.9	5.9	26.8	13.3	4.7	----
328:356	2.4	1.2	8.7	4.8	7.8	----
329:357	2.7	15.0	16.3	9.7	7.6	----
330:358	4.3	8.3	15.2	2.4	1.9	----
Average	11.9	8.0	12.4	9.9	9.5	8.4

B. Hatch Samples Collected by a Single B-52 Aircraft

Samples	Total Beta	Percent Standard Deviation							
		Sr ⁹⁰	Sr ⁸⁹	W ¹⁸⁵	Zr ⁹⁵	Ce ¹⁴⁴	Pu	W ¹⁸¹	Ca ¹³⁷
1357-1360:1361	4.3	20.6	3.1	12.0	0.5	20.6	13.0	----	----
1359:1360	28.9	15.1	9.7	22.8	17.3	26.4	11.3	----	----
2070,2071:2341	0.4	19.5	----	----	----	----	----	----	----
2072:2320	6.4	2.8	68.7	----	----	----	51.0	----	----
2073,2074:2342	2.4	5.3	76.7	----	----	----	----	----	----
2310,2311:2343	19.7	10.6	----	----	----	----	----	5.3	----
2312:2313	18.1	13.8	----	----	----	29.0	106	52.5	31.2
Average	11.4	12.5	39.6	17.4	8.9	25.3	45.3	28.9	31.2

various other instruments were mounted in front of some of the samplers on the fuselage of the aircraft.

After June 1959, a large number of simultaneous collections by hatch and nose samplers, mounted on a single aircraft, were made. Data from these filters, which may be used to test the intercalibration of the two types of sampler are presented in Table 3.11. The ratio of the concentrations in the hatch samples relative to these in the nose samples indicate that the hatch samples collected 2.5 times the activity collected by the nose samples. This is also the ratio between the areas of the two filters. The calibration data indicate that the hatch samples should have collected only 2.25 times the activity collected by the nose samples. (Analyses of two pairs of filters used in the calibration experiment indicated hatch/nose ratios of 2.24 and 2.32.) The 10 percent difference between the predicted and observed hatch: nose activity ratios may have resulted from the greater care taken in sealing the samplers before the calibration flights than before routine sampling missions. Since it was not evident whether the discrepancy was caused by the data for the nose sampler, those for the hatch sampler or both, no attempt to correct either set of data was made.

It is also of interest to compare results for filters which, though not exposed simultaneously, did collect debris from the same region of the stratosphere on the same day. A list of such sample pairs, collected at the same latitude and altitude during a single mission, is given in Table 3.12. The percent standard deviation of the individual samples from the mean value for the pairs is given for total beta and strontium-90 analyses. The number of the sample which displayed the higher beta activity is indicated followed by the number of the sample which displayed the higher strontium-90 activity, unless

Table 3.11 Comparison of Calculated with Measured Relative Collection Efficiencies of Hatch and Nose Samplers

(The standard deviation from each average and, in parentheses, the number of samples included in each average are given).

Altitude	SCF	Ratio of Hatch/Nose				dpm Ce 144
		dpm total B	dpm Sr 90	dpm W 185	dpm Ce 144	
70,000	2.28 ± 0.02(29)	2.51 ± 0.36(29)	2.44 ± 0.27(28)	2.43 ± 0.34(15)	2.37 ± 0.24(10)	
65,000	2.28 ± 0.02(125)	2.48 ± 0.31(124)	2.44 ± 0.28(122)	2.45 ± 0.41(56)	2.48 ± 0.22(26)	
60,000	2.26 ± 0.04(97)	2.50 ± 0.36(90)	2.54 ± 0.34(89)	2.52 ± 0.43(39)	2.58 ± 0.36(14)	
55,000	2.20 ± 0.04(30)	2.57 ± 0.44(29)	2.44 ± 0.37(28)	2.54 ± 0.55(6)	2.49 ± 0.41(10)	
50,000	2.21 ± 0.09(44)	2.54 ± 0.35(41)	2.50 ± 0.33(38)	2.44 ± 0.46(12)	2.50 ± 0.39(13)	
45,000	2.23 ± 0.01(9)	2.41 ± 0.25(9)	2.34 ± 0.49(9)	2.38 ± 0.60(4)	2.55 ± 0.31(3)	
40,000	2.26 ± 0.01(3)	2.53 ± 0.38(3)	2.59 ± 0.43(3)	2.58 ± 0.41(2)	3.18 ----(1)	
30,000	2.26 ± 0.01(4)	-----	2.00 ± 0.23(2)	2.80 -----(1)	-----	
Average	2.26 (341)	2.50 (325)	2.47 (319)	2.47 (135)	2.50 (77)	

both were displayed by the same sample. Nose samples collected by the same aircraft, hatch samples collected by the same aircraft, nose samples collected by two different aircraft and hatch samples collected by two different aircraft are included in Parts A, B, C and D respectively in Table 3.12. It appears to make little difference in sampling reproducibility whether the filters were collected by the same or by different aircraft. Moreover, the variations in activity between these sample pairs, frequently collected hours apart and many miles apart, are not noticeably larger than those between samples collected simultaneously by a single aircraft or by aircraft flying within sight of each other.

Finally we may consider the variations in activity between samples collected on the same day at the same latitude and altitude but at different longitudes. A few such collections were made during Phase 2 of Crowflight, when missions were flown north from Ramey along the 69°W meridian and south from Plattsburg along the 71°W meridian, and one was made during Phase 4 when a Laughlin north mission along 98°W was flown on the same day as a Minot south mission along $100^{\circ}30'\text{W}$. The variations in concentration displayed by these sample pairs are greater, on the average, than those shown by samples collected under similar conditions at the same latitude. This could be expected, especially since these samples were all collected near the "tropopause-gap" region. These data are shown in Table 3.13.

In summary we may state that small errors did result from using only an aliquot of a filter rather than the whole filter for an analysis and that some variability was introduced into the data through the use of many different

Table 3.12 Standard Deviation of Sample Pairs Collected on a Single Mission at the Same Latitude, Longitude and Altitude

A. Nose Samples Collected by a Single Aircraft

Samples	% Std. Deviation			Samples	% Std. Deviation		
	Total Beta	Sr ⁹⁰	Sample with Higher Activity		Total Beta	Sr ⁹⁰	Sample with Higher Activity
237:238	0.4	10.1	238	1390:1391	0.14	2.1	1390
239:240	1.2	4.4	240,239	1418:1419	24.0	3.8	1418
249:250	3.4	23.9	249,250	1421:1422	35.9	20.5	1422
251:252	0.1	19.9	251	1439:1440	1.0	2.5	1439
324:326	2.5	5.7	324	1456:1457	15.3	22.1	1457
376:377	41.2	13.5	376	1458:1459	7.4	1.0	1458
380:381	20.0	8.9	380	1488:1489	5.0	7.2	1489
383:386	1.6	2.2	386	1516:1517	23.6	3.1	1517
384:385	19.0	7.6	384	1540:1541	7.5	19.0	1541, 1540
387:390	12.1	5.8	390, 387	1542:1543	2.3	5.0	1542
388:389	4.9	17.3	389	1566, 1567:			
969:972	2.5	3.4	969	: 1568	5.2	23.2	1566-1567, 1568
970:971	16.2	4.6	971, 970	1729:1730	2.6	2.0	1729
1115:1118	10.6	4.8	1118	1731:1732	11.1	44.3	1732
1116:1117	14.6	4.0	1117, 1116	1753:1754	10.2	13.2	1754
1293:1294	44.2	15.0	1294	1798:1799	19.8	17.0	1799
1297:1298	2.2	7.0	1298, 1297	1800:1801	13.2	17.8	1800
1315:1316	17.7	3.7	1315	1938:1939	---	29.7	1938
1317:1318	10.0	14.7	1318	1940:1941	15.1	24.9	1940
1321:1322	4.7	15.7	1322, 1321	1989:1990	10.5	0.6	1990
1325:1326	2.7	3.9	1326, 1325	2047:2048	20.7	6.5	2-47
1342:1343	8.1	0.2	1342	2049:2050	18.0	17.0	2050
1368:1370	0.6	41.0	1368, 1370	2051:2052	0.5	0.5	2051, 2052
				3212:3213	2.0	3.4	3212, 3213
				Average	10.9	11.4	

B. Hatch Samples Collected By a Single Aircraft

Samples	% Std. Deviation			Samples	% Std. Deviation		
	Total Beta	Sr ⁹⁰	Sample with Higher Activity		Total Beta	Sr ⁹⁰	Sample with Higher Activity
1639:1640:				2797:2798	11.2	2.4	2798
1641:1642:				2868:2869	8.9	8.4	2869
1643:1644	6.9	3.3	1639, 1644	2946:2947	12.7	10.1	2946, 2947
1645:1646:				3292:3293	17.7	6.1	3293
1647:1648:				3423:3424	9.6	1.4	3424, 3423
1649:1650	17.6	3.7	1650	3431:3432	4.4	20.6	3431, 3432
2394:2395	17.1	1.6	2395				
2666:2667	3.2	10.2	2666, 2667	Average	10.9	6.8	

C. Nose Samples Collected By Two Different Aircraft

1394:1398	1.3	9.8	1398, 1394	3298:3304	15.5	17.6	3304, 3298
1948:1956	4.1	5.6	1956, 1948	3850:3866	8.1	0.4	3850, 3866
2265:2268	11.1	9.8	2268	3974:3982	0.6	8.5	3982
2483:2487	13.7	19.1	2487	3975:3983	3.4	5.0	3983
3074:3083	25.5	28.5	3074	3976:3984	1.8	3.2	3976, 3984
3222:3227	18.8	24.9	3222	3977:	5.2	6.9	3985
				Average	9.1	11.6	

D. Hatch Samples Collected By Two Different Aircraft

1952:1960	3.4	11.4	1952, 227	3978:3986	9.2	12.2	3986
3078:3087	8.5	6.6	3087	3979:3987	7.2	11.5	3979
3080:3090	10.6	3.2	3090	3980:3988	18.5	12.2	3988
3356:3363	9.6	7.6	3365, 3363	3981:3989	2.4	1.1	3989, 3981
3854:3870	11.8	0.5	3854				
				Average	9.0	7.3	

Table 3.13 Standard Deviation of Nose Samples Collected at Different Longitudes but the Same Latitude and Altitude During a Single Mission

A. Samples Collected by the Same Aircraft

Samples	% Stnd. Deviation		Sample with Higher Activity
	Total Beta	Sr ⁹⁰	
7:8:9:10	7.7	17.6	7

B. Samples Collected by Different Aircraft

53:59	32.9	3.4	53, 59
80:93	15.8	9.5	80
81:94	12.1	7.4	81, 94
82:95	35.4	4.1	82
69:73	9.1	5.4	69
102, 103:105	9.9	6.4	105:102, 103
122:140	34.6	1.8	122, 140
123:139	20.0	21.3	123, 139
124:138	6.1	34.2	124, 138
135:147	25.8	16.8	135, 147
136:146	39.5	28.9	136
194:216	71.3	27.8	194
195:215	5.5	--	215
3612:3623	64.5	80.8	3612
Average	27.3	19.1	

samplers, which did not perform identically, during the course of the program. On the whole, however, this variability was not significantly greater than that caused by errors in the flight data and analytical data and does not significantly detract from the validity of the program.

The estimation of the overall error in the reported concentration of a single nuclide in a single HASP sample is difficult because of the complex relationships between the parameters which control the volume of air actually sampled. Perhaps an error of about ± 10 percent may be expected in a typical radiochemical analysis. (The errors given with the analytical data in Chapter 4 are generally less than 10 percent, but these represent only the counting error. Uncertainties in the basis weight of the individual filters used to collect samples and in the altitude (and therefore air density) of sample collection predominate in determining the random error of calculated flow rates and sample volumes. Although there are no data which would permit exact evaluation of these errors, it is probably reasonable to assume a random error of ± 15 percent in the calculated air volumes. A non-random error in the calibration data for the samplers is evident in the average discrepancy of about 10 percent between calculated nuclide concentrations in simultaneously exposed nose and hatch filters. To evaluate the uncertainty in the data for a single sample which is caused by this calibration error, we may arbitrarily treat it as a random error of ± 5 percent. The combined effect of these three major sources of error is an overall random error of slightly less than ± 20 percent in the concentrations reported for a typical sample. Nevertheless, this estimate is only approximate, and the actual errors for many samples are much higher and for others much lower than this average.

SAMPLE PRETREATMENT

Upon its arrival at Isotopes, Inc., each filter paper was given a code number and the collection data accompanying the filter were recorded. Two types of samples were taken routinely from each filter paper within a few hours after its arrival: (a) small (2.86 cm diameter) disks for total beta and gamma assay and (b) a quadrant (1/4) or a half (1/2) of the entire filter paper for a sequential radiochemical analysis. By this method at least fifty percent of each filter paper was usually reserved for possible future studies such as: (a) re-analysis of a particular sample, (b) analysis for a nuclide lost or discarded in the routine run, (c) inter-calibration with other laboratories, and (d) autoradiography, particle examination, etc. As discussed in a later section the entire filter paper and even composite samples were sometimes analyzed for certain nuclides.

The removal of disks and quadrants from the filter paper was carried out by reproducible techniques from identical locations on each paper. The orientation of the paper was set relative to a reference point made at the top of the paper by personnel at the sampling sites. (See Figure 3.16)

Total Beta and Gamma Analysis

The major value of the total activity analyses was the rapid indication of the level and average age of the radioactivity of each sample. Within an hour or two after arrival, the first total beta and gamma assays were completed. Subsequent recounts of each of the samples permitted the construction of a total activity decay curve which was useful in estimating the age of the debris.

For total beta analysis one of the small disks was mounted on a brass planchet, covered with a thin sheet of Pliofilm and secured with a brass ring.



Figure 3.16
Mounting Small Disk on Brass Planchet

These were then counted, utilizing an end window halogen filled geiger counter (Anton Electronics Laboratory Model No. 1007 T).

For total gamma analysis one or more disks were cut into five strips and placed in a test tube for counting by the NaI(Tl) well crystal of the 100 channel gamma-ray spectrometer.

Ashing and Dissolution

Depending on the activity level estimated from the total beta and gamma analyses, one quarter or one half of each filter paper was taken for the chemical analysis. The paper was cut into small squares approximately one half inch on a side and placed in a 150 ml platinum ashing dish. The sample was ashed for a minimum of 3 hours at 450° C. At this temperature the recovery of all the volatile tracers of interest was quantitative. For example, it was demonstrated by spike experiments that there were no losses of cesium-137 at 450°C and only a 4 percent loss of ruthenium-106 at 475-500°C.

The ashed filter paper sample was dissolved in 2 ml of concentrated HF and 2 ml of 70 percent HClO₄. The solution was evaporated on a hot plate until all the HF was distilled off and approximately 1 ml of HClO₄ remained. The solution was transferred to a 25 ml volumetric flask with a dropping pipette, and the platinum dish was thoroughly washed with hot concentrated HNO₃ and water. The washes were added to the volumetric flask. Aliquots were removed for sequential analysis or for the analysis of individual nuclides.

The platinum dish was dried and monitored with a Tracerlab TGC-2 Geiger-Mueller tube. This measurement was used to determine if any significant amount of activity remained in the dish. If greater than 3% of the original activity was retained, the platinum dish was again "scrubbed" with a mixture of HF-HClO₄ acids followed by a hot HNO₃ rinsing. The washes were added to the

original sample solution. The procedure of monitoring and "scrubbing" the platinum dish was repeated as many times as necessary to reduce the activity in the platinum dish to less than 3% of the original activity which was determined prior to ashing.

Two approaches were used in the analysis of HASP samples: (a) Ion-exchange technique and (b) carrier radiochemistry.

The ion exchange technique is based on the quantitative separation and recovery of carrier-free nuclides by a cation exchange resin. It was used in the initial stages of the program in the analysis of samples 1-300.

The carrier radiochemical method employs the use of carriers and such chemical steps as precipitations and extractions to effect the separation of the desired nuclides. The flexibility and economy offered by this method made it a preferred and suitable analytical tool for the thousands of HASP samples which were to be processed. Some samples that were analyzed via the ion exchange technique were cross-checked via carrier sequential analysis. The data proved the two methods of analysis to be comparable.

After the chemical purifications had been performed, each radioactive nuclide of interest was prepared for counting. This was accomplished by precipitating the nuclide plus its carrier as an appropriate insoluble compound, filtering this precipitate, using a 2.8 cm diameter disk of filter paper in a Tracerlab filtering apparatus (See Figure 3.17), and mounting the paper and precipitate on a Tracerlab brass planchet (See Figure 3.18). The filter paper was weighed before and after filtration of the precipitate if an estimate of the chemical yield of the purification was required. A thin sheet of Pliofilm, a plastic film of 1.1 mg/cm^2 , was placed over the precipitate before the brass ring of the planchet permanently locked the sample in place.

This method of mounting afforded a permanent sample with maximum

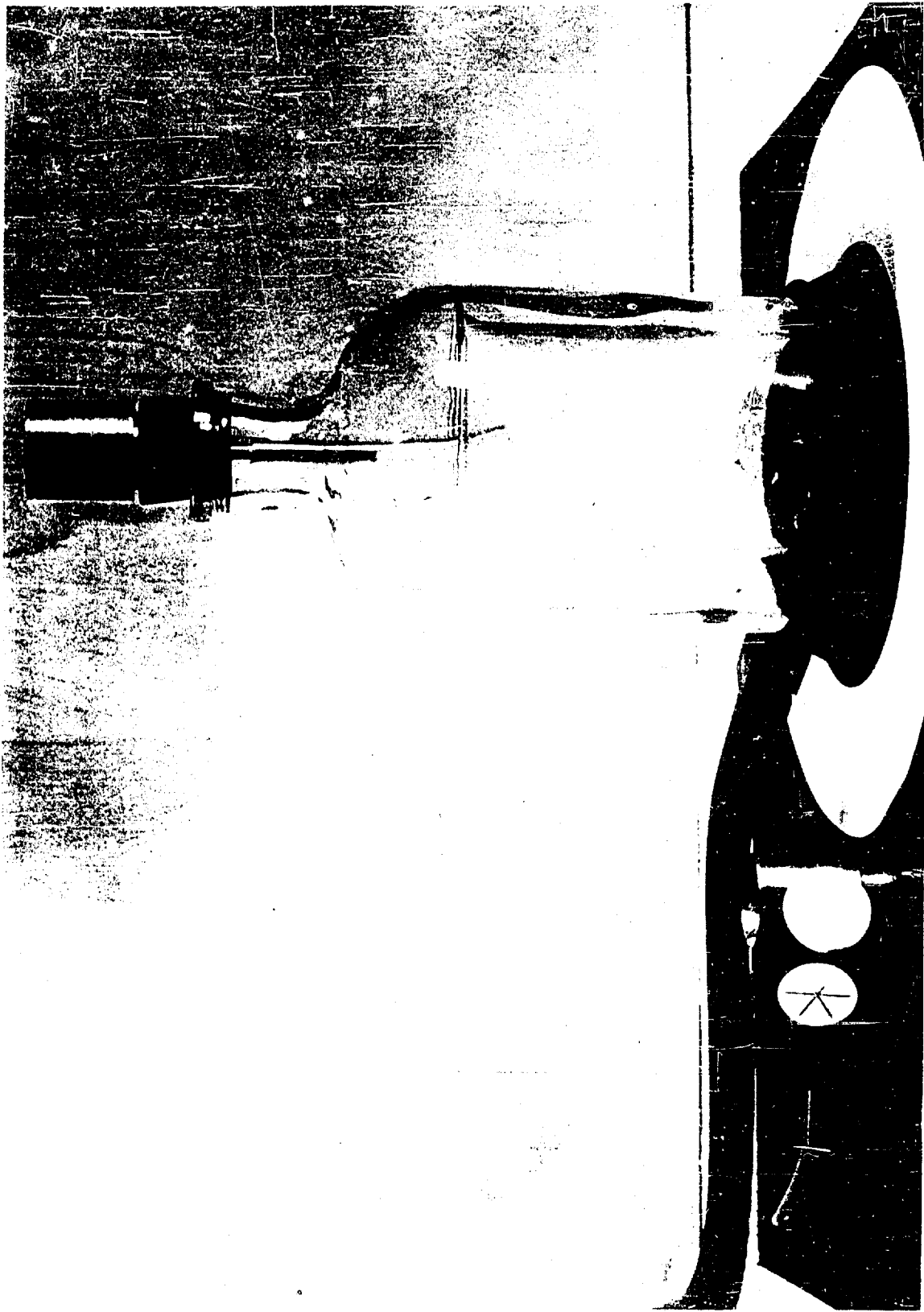


Figure 3.17. Tracerlab Filtering Apparatus

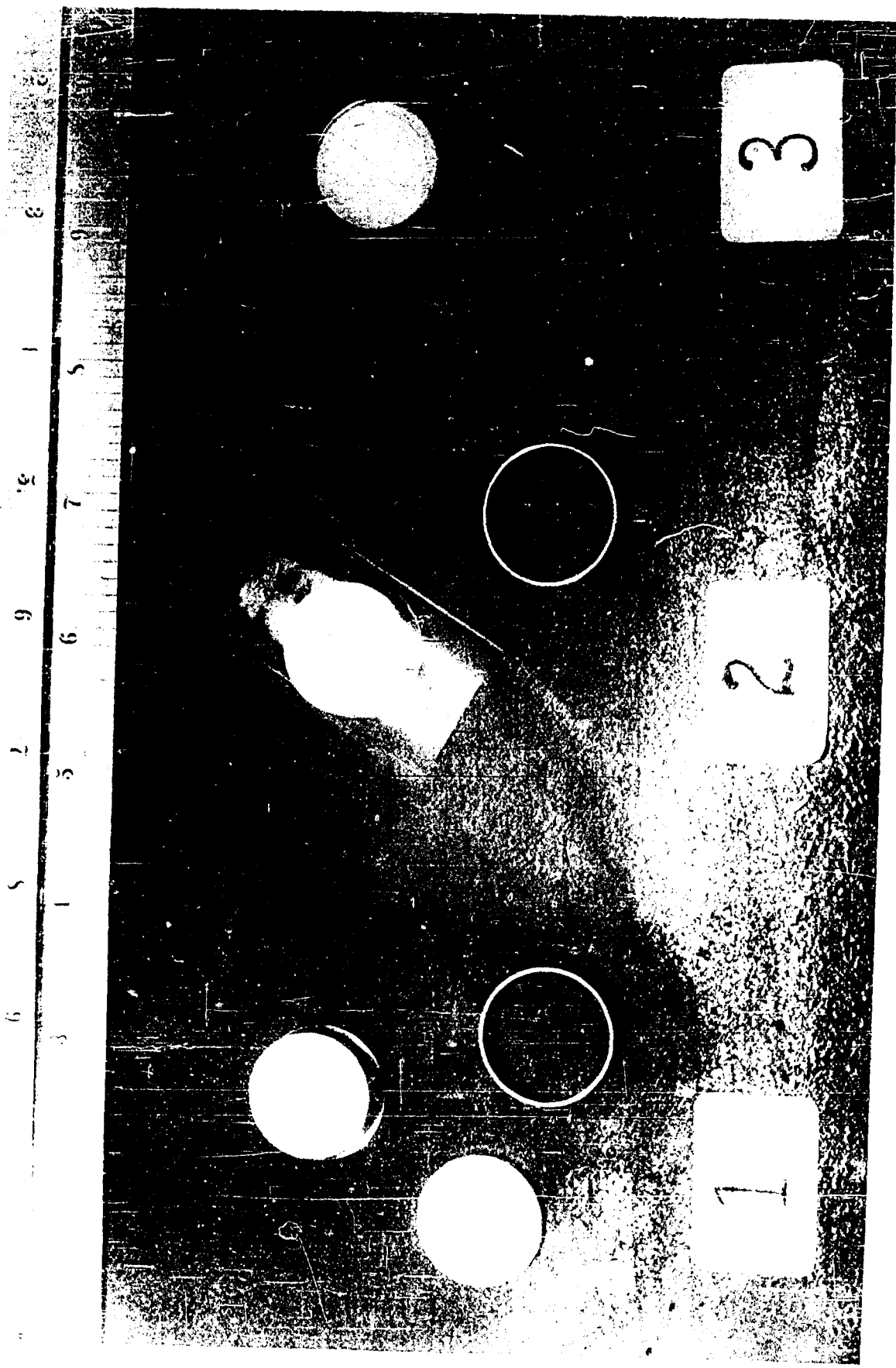


Figure 3.18. Brass Planchet

backscattering for beta particles and gamma rays. The maximum backscattering feature was advantageous in assaying samples which had a low level of activity.

ION EXCHANGE TECHNIQUE

This method of analysis was used for the separation of ruthenium-106, cesium-137, strontium-90 and a combined fraction of barium-140 cerium-144. Because of its erratic behavior in ion exchange, zirconium-95 had to be removed by precipitation in advance. Each one of the above fractions was subsequently purified and prepared for radiometric assay.

Zirconium Separation

Prior to introducing the solution of the filter paper ash to the ion exchange column, zirconium was separated by adding 10 mg of zirconium carrier as $ZrOCl_2 \cdot 8H_2O$ and precipitating it as Zirconium phenylarsonate with 5 ml of saturated phenylarsonic acid.

The zirconium phenylarsonate precipitate was centrifuged and reserved for zirconium-95 analysis. The supernate was decanted into a 100 ml beaker and evaporated to dryness. The dry residue was dissolved in about 5 ml of water; strontium-85 spike was added for subsequent radiometric yield determination and the solution was introduced to the ion exchange column.

The ion exchange column (see Figure 3.19) consists of a Pyrex glass tube, 1330 mm long and 8 mm (I. D.) with a stopcock at one end to control the flow rate and a reservoir flared to about 25 mm diameter at the other end to provide a constant hydrostatic head.

The column was filled to a height of 1170 mm with a bed of 120 to 200 mesh⁶ Amberlite CG-120 cation resin. The resin was converted to the hydrogen form by washing alternately with 6 M hydrochloric acid and water, after each wash

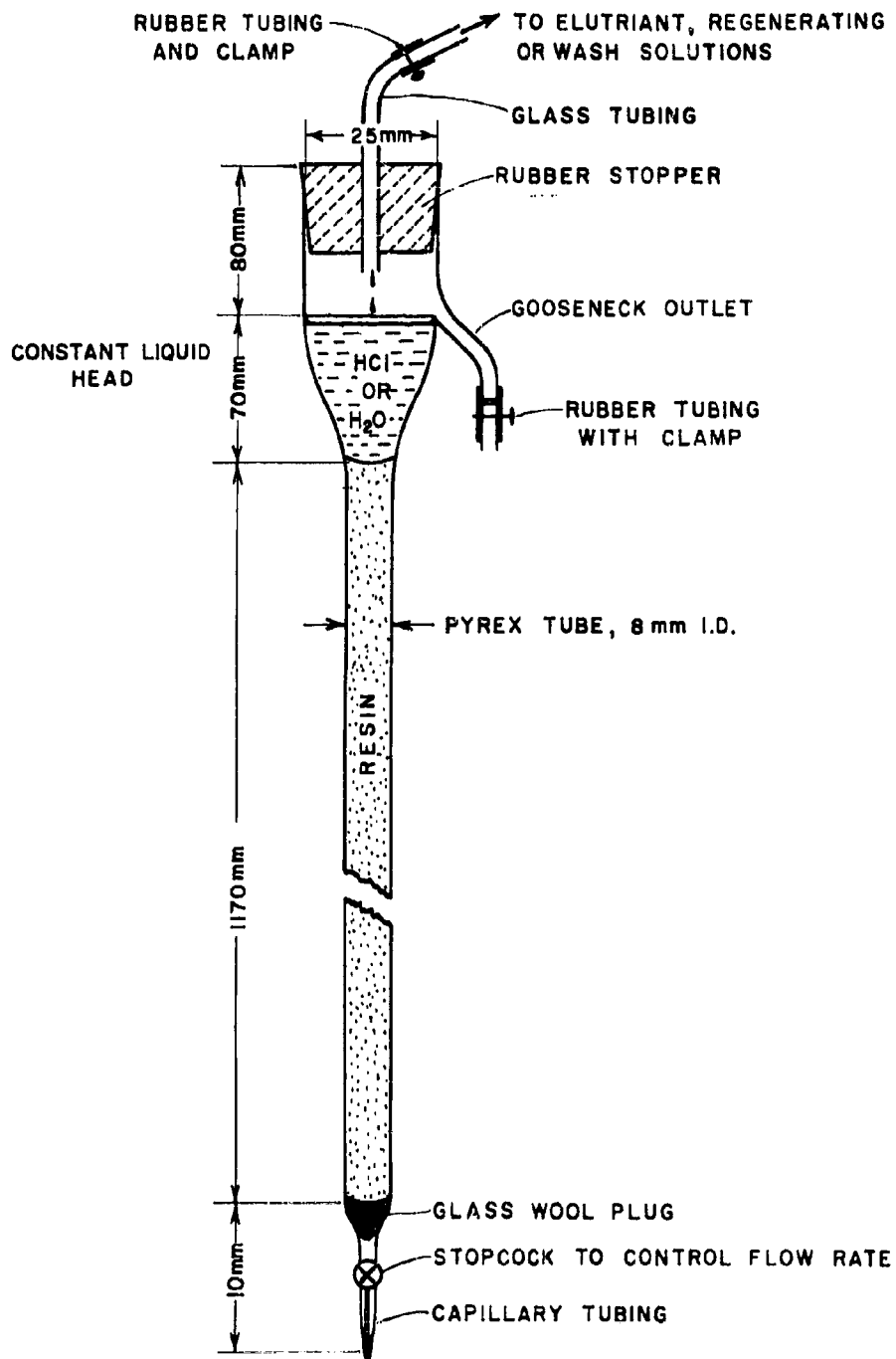


FIGURE 3.19 - DIAGRAMMATIC SKETCH OF ION EXCHANGE COLUMN

the fine particles which did not settle immediately were decanted. This cyclic process was repeated 6 to 8 times, and the resin was then stored in water until needed.

Mode of Operation

The sample was added to the resin column with a dropping pipette and the liquid level permitted to fall until it coincided with the top of the resin. The column was then washed with distilled water. The wash solution was reserved for ruthenium analysis. The column was then eluted with 5.5 M hydrochloric acid^{7, 8, 9, 10}

Elution was performed at room temperature with a flow rate of 0.2 to 0.3 ml per minute and 2 ml fractions were collected in small test tubes utilizing an automatic collector. A Packard Instrument Co. (Model 230) was modified at Isotopes, Inc. so that the turntable could accommodate 600 test tubes (13 x 100 mm) for simultaneous collection from six columns. (see Figure 3.20)

At the termination of the elution process which required from 140-160 test tubes for each sample, the nuclides of interest were identified by counting the test tubes in a NaI(Tl) well-type scintillation counter. Thus, the eluate was divided into the following four fractions: (1) the ruthenium fraction, (2) the cesium fraction, (3) the strontium fraction, and (4) the barium-cerium fraction. Since each fraction was collected in a number of test tubes, the solutions from all the test tubes in any one fraction were combined and the tubes were thoroughly rinsed with 5.5 M hydrochloric acid. The rinsings were added to their respective fractions. Each fraction was then evaporated to between 10 and 50 milliliters and further chemical purification of the pertinent nuclide was performed. These chemical purifications as well as the zirconium purification, are given in detail in the next section.

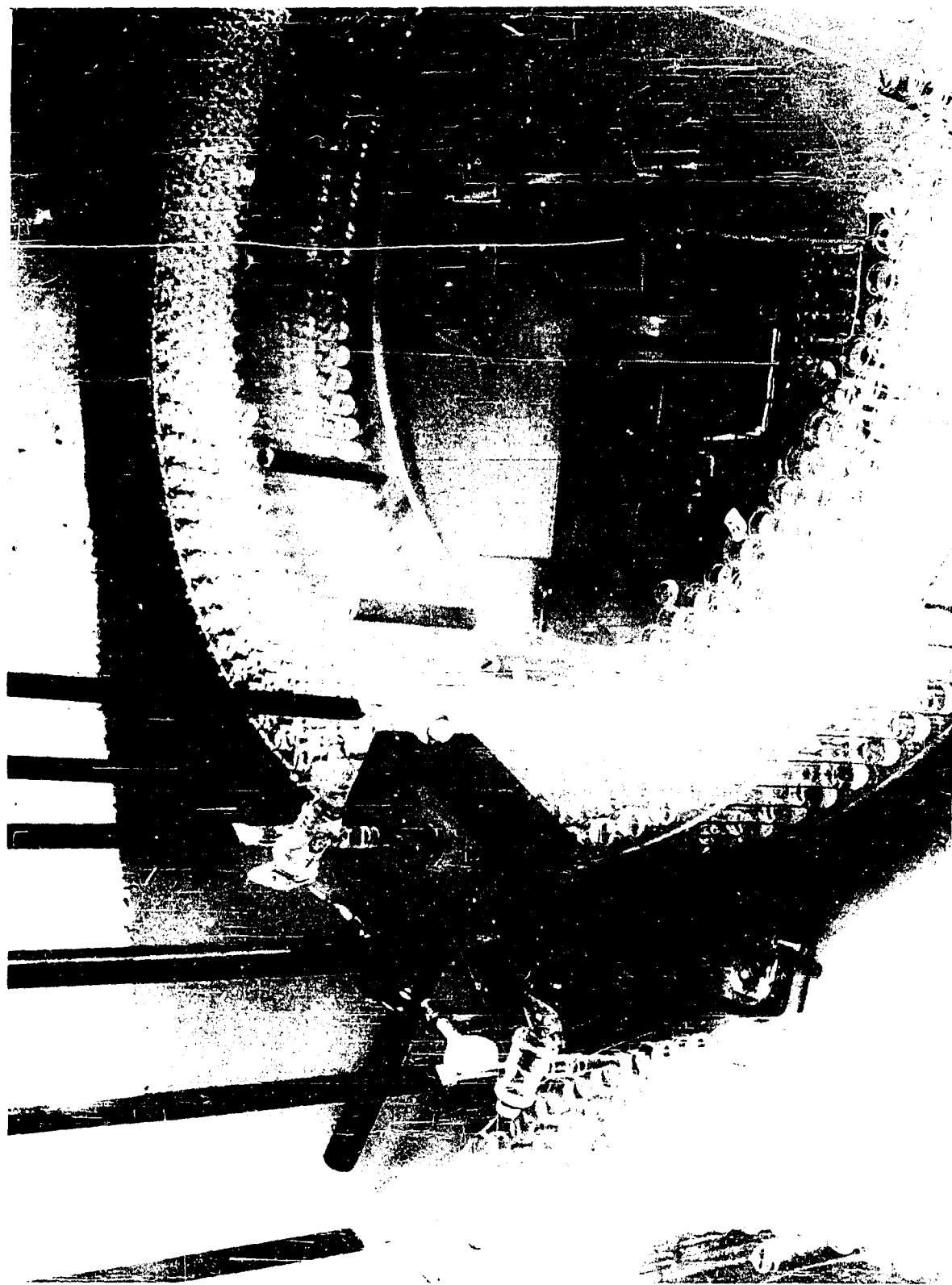


Figure 3.20. Automatic Fraction Collector

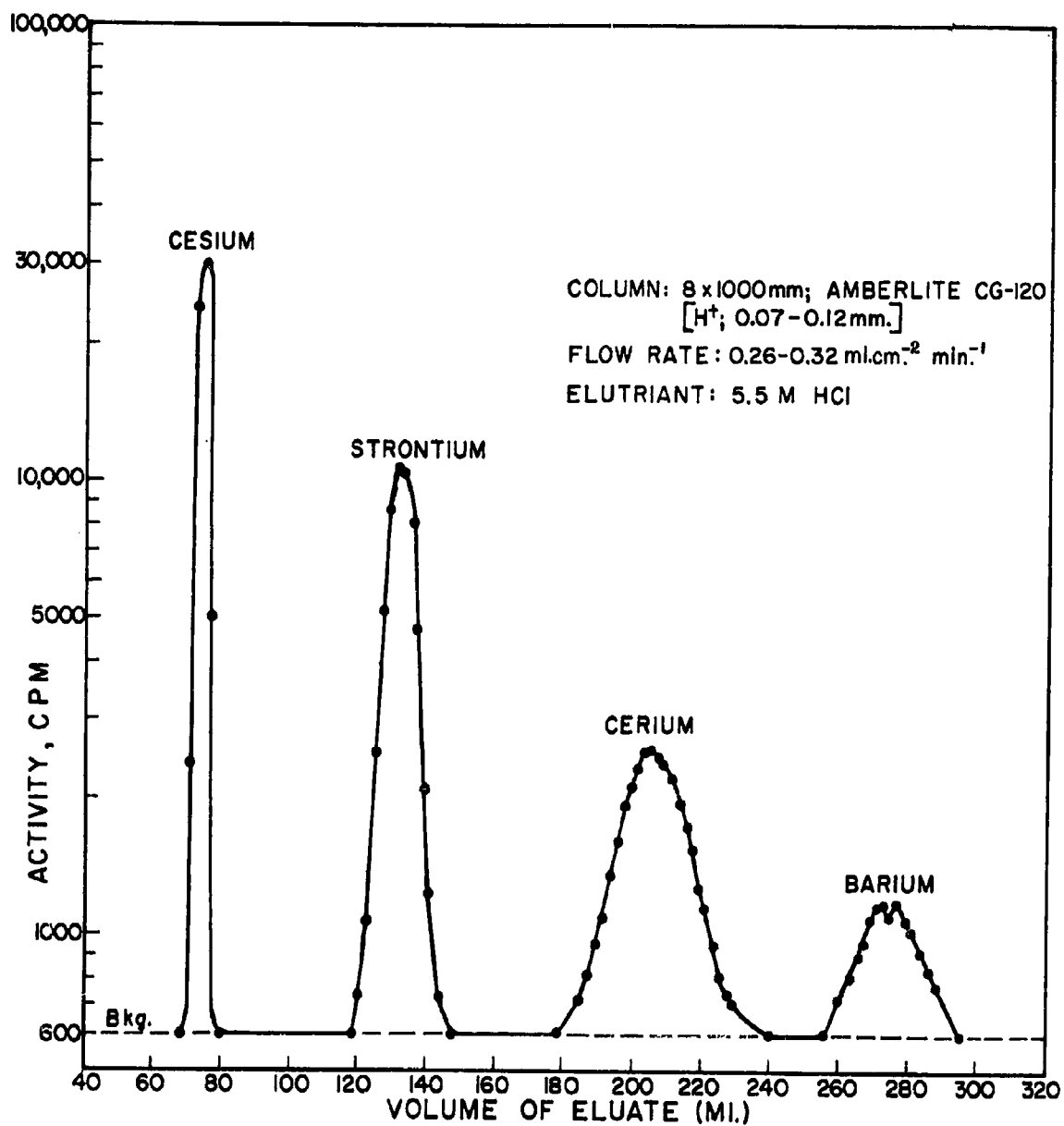
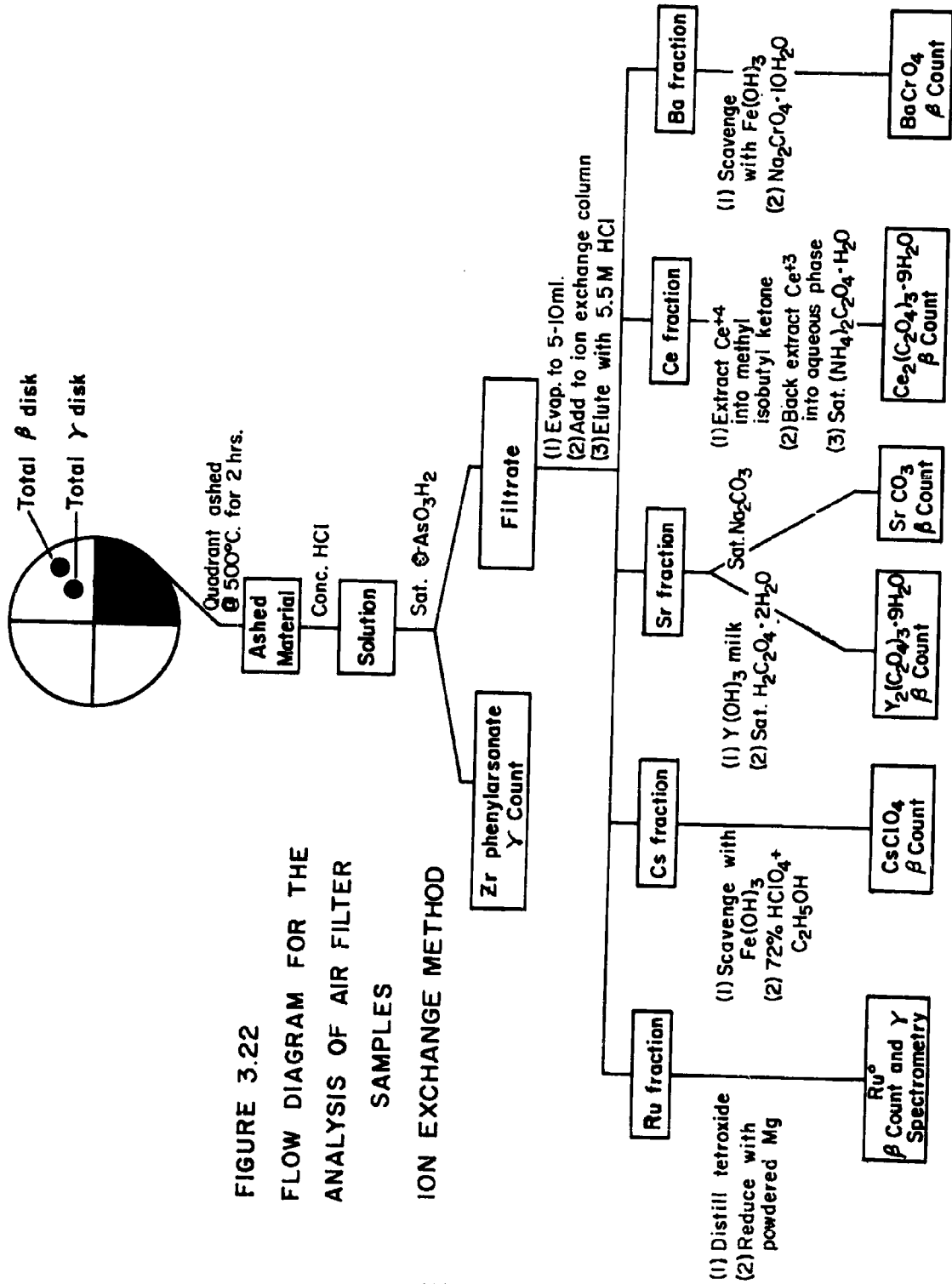


FIGURE 3.21 - ELUTION CURVE OF CESIUM, STRONTIUM, CERIUM, AND BARIUM TRACERS

(RUTHENIUM SEPARATES FROM OTHER NUCLIDES SINCE IT PASSES THROUGH THE CATION EXCHANGE RESIN PRIOR TO ELUTION.)



An actual separation of the nuclides of interest by the ion exchange technique is shown in Figure 3.21. The ruthenium fraction is not shown because it passes through the column with the washes indicated earlier. These data were obtained by spiking a solution with strontium-85, cesium-137, barium-140, and cerium-144 and passing the solution through the column under the conditions of a normal run. By plotting the activity versus volume of the eluate, four peaks were obtained. Each of these peaks represented a single nuclide as shown in Figure 3.21.

The entire procedure of analysis via ion exchange technology is shown in flow form in Figure 3.22.

CARRIER RADIOCHEMISTRY

The second approach to the analysis of radionuclides in filter paper samples was carrier radiochemistry. This technique entails the quantitative addition of radio-activity-free carrier to the sample solution at the beginning of the analysis and the gravimetric recovery of the same carrier in the form of a chemical compound at the end of the analysis. By selecting the appropriate nuclides, it is possible to develop a scheme by which group separations from a single aliquot of the sample can be effected by precipitations and extractions. Based on this principle, the following sequential radiochemical procedures were developed:

- I Beryllium-7, Phosphorus-32, and Rhodium-102
- II Sodium-22 and Calcium-45
- III Strontium-89, 90, Yttrium-91, Zirconium-95, Cesium-137, Barium-140, Cerium-144.

Analytical procedures were also developed for the analysis of iodine-131, tungsten-185 and plutonium. Depending on the level of activity or concentration

of the above mentioned nuclides in the collected samples, it was necessary to vary the amount of samples used for analysis at different stages of the HASP project. It varied from 1/4 of the filter paper for nuclides of group separation scheme III at the beginning of the project to the entire filter paper and even composite samples for nuclides of group separation schemes I and II in the latter stages of the project.

Regardless of the amount of sample needed for analysis, the same ashing and dissolution procedures, as described earlier, were followed. After dilution to a known volume, usually 25 ml, aliquots were removed for any or all of the above mentioned sequential type analyses. The separated nuclides were subsequently purified and prepared for radiometric assay.

Sequential Radiochemical Separation of Beryllium-7, Phosphorus-32 and Rhodium-102

1. To an aliquot of the sample solution (Note 1) contained in a 100 ml beaker, add 10 mg of beryllium carrier, 30 mg of rhodium carrier and 5 mg of phosphorous carrier with thorough mixing.
2. Add 4 ml of concentrated HNO_3 , 5 ml of ammonium molybdate reagent, several drops of Aerosol solution and heat for 5 minutes on a hot plate (the temperature should not exceed 50°C).
3. Transfer the mixture from step (2) to a lusteroid tube, centrifuge and reserve the supernate for beryllium-rhodium separation.
4. Wash the precipitate with 5 ml of 3% HNO_3 , centrifuge and repeat washings with 5 ml portions of 3% HNO_3 until the characteristic red rhodium color is no longer evident in the precipitate. Combine washings with the supernate for beryllium-rhodium separation and reserve the precipitate for phosphorus-32 analysis.
5. To the supernate from step (3) and washings from step (4), add 20 ml of pyridine, stir the solution for several minutes and then heat to boiling; make basic with 50% NaOH and stir for 5 minutes.
6. Transfer the solution to a 125 ml separatory funnel with 5 ml of H_2O and separate the aqueous (lower) phase into a clean 40 ml. centrifuge tube. Reserve the pyridine phase for step (d) of the rhodium-102 purification procedure.
7. Acidify the aqueous phase from step 6 with concentrated HCl and render the solution strongly basic with concentrated NH_4OH . Centrifuge and discard the supernate; wash the $\text{Be}(\text{OH})_2$ precipitate with 5 ml of H_2O containing 5 drops of concentrated NH_4OH , centrifuge and discard the wash. Reserve the precipitate for step (c) of the beryllium-7 purification procedure.

Notes:

1. Perchloric and hydrofluoric acids present from the dissolution of the filter paper ash are distilled off and the residue from the aliquot taken for analysis is dissolved in 25 ml of water.

Sequential Radiochemical Separation of Sodium-22 and Calcium-45

1. To an aliquot of the sample solution contained in a 40 ml centrifuge tube, add 10 mg of sodium carrier, 20 mg of calcium carrier.
2. Render the solution basic with concentrated NH_4OH and heat in a hot water bath for 5 minutes; add 10 ml of saturated $(\text{NH}_4)_2\text{CO}_3$ to precipitate CaCO_3 and digest until the precipitate settles. Cool, centrifuge and reserve the supernate for sodium-22 analysis and the precipitate for calcium-45 analysis.

Sequential Radiochemical Separation of Strontium-89, 90, Yttrium-91
Zirconium-95, Cesium-137, Barium-140 and Cerium-144

1. To an aliquot of the sample solution contained in a 40 ml centrifuge tube, add 20 mg of cesium, cerium, barium and strontium carriers and 10 mg of zirconium and yttrium carriers.
2. Add 1 ml of 5M $\text{NH}_2\text{OH}\cdot\text{HCl}$ dropwise from a pipette and stir carefully during addition. (Note: effervescence should occur at this point but if it does not, heat the solution on a hot water bath and carefully add 3 to 4 drops of concentrated HNO_3 .)
3. Place in a hot water bath for 20 minutes and stir occasionally.
4. Raise the pH to greater than 8.5 by the addition of 5 ml of 50% NaOH; heat the solution in a water bath and add 10 ml of a saturated solution of Na_2CO_3 with stirring; allow to digest for 5 to 10 minutes.
5. Cool to room temperature in a water bath, add several drops of Aerosol solution, centrifuge and decant the supernate into a 100 ml beaker; wash the precipitate with 5 ml of water, centrifuge and add washings to the beaker. Reserve the solution for the cesium purification procedures.
6. Dissolve the precipitate from step (5) with 5 ml of 6M HNO_3 and boil over a flame for several minutes to remove all CO_2 .
7. Dilute the solution to 10 ml with water and add 2 ml of saturated phenylarsonic acid solution.
8. Place in a hot water bath until the precipitate of zirconium phenylarsonate settles out and then cool to room temperature in a water bath.
9. Add a drop of Aersol reagent, centrifuge thoroughly and decant the supernate into a clean 40 ml centrifuge tube. Reserve the precipitate for the zirconium purification procedure.
10. To the supernate from step (9) add 10 drops of meta cresol purple indicator and adjust the pH to 7.2 - 7.4 with 6M NH_4OH ; i. e. until just one drop causes a color change from yellow to violet (Note 1); place in a hot water bath for several minutes, cool to room temperature in a water bath, centrifuge and decant the supernate into a clean 40 ml centrifuge tube.
11. Using a stirring rod, slurry the precipitate with 3 ml of water, centrifuge and add washings to the supernate from step (10).
12. Dissolve the hydroxide precipitate from step (11) in 25 ml of concentrated HNO_3 and reserve for yttrium-91 and cerium-144 purification procedure.
13. To the combined supernate from steps (10) and (11), add 5 mg of iron (ferric) carrier; to dissolve the resultant $\text{Fe}(\text{OH})_3$ precipitate, add concentrated HCl dropwise until the solution clears and then make basic with concentrated

NH_4OH until the $\text{Fe}(\text{OH})_3$ precipitate reappears (if the precipitate is slow in forming, place in a hot water bath). Centrifuge and transfer the supernate to a clean 40 ml centrifuge tube; discard the precipitate.

14. Repeat step (13) adding 5 mg of iron (ferric) carrier.
15. Heat the supernate from the second $\text{Fe}(\text{OH})_3$ scavenging; add 7 to 8 drops of phenolphthalein indicator and adjust the pH to greater than 8.5 with concentrated NH_4OH (solution will turn deep red at a pH greater than 8.5).
16. Add 10 ml of a saturated Na_2CO_3 solution, with stirring, to precipitate barium and strontium carbonate. Heat in a hot water bath until the precipitate settles out; cool to room temperature in a water bath, centrifuge and discard the supernate.
17. To the carbonate precipitate from step (16), add 5 ml of 6M HNO_3 and boil over a flame for about 2 minutes to remove all CO_2 .
18. Cool solution to room temperature and then add 4 to 5 drops of alizarin indicator; stir and adjust the pH to about 6.8 with 6M NH_4OH until a color change from yellow to violet occurs.
19. Add 5 ml of barium buffer solution (20% 6M HOAc - 80% 3M NH_4OAc) and heat nearly to boiling; add 1 ml of 1.5M Na_2CrO_4 (via a pipette), with stirring, and digest in a hot water bath until the BaCrO_4 settles out.
20. Cool the solution in a water bath, centrifuge and decant the supernate into a clean 40 ml centrifuge tube. Reserve the precipitate for the barium purification procedure.
21. To the supernate from step (20) add 5 ml of concentrated NH_4OH with stirring; heat in a hot water bath for several minutes and then add 10 ml of saturated Na_2CO_3 with stirring.
22. Digest in a hot water bath for 10 to 15 minutes until the SrCO_3 precipitate settles; cool to room temperature in a water bath, centrifuge and discard the supernate.
23. Wash the precipitate with 5 ml of water, slurring well with a stirring rod; centrifuge and discard the wash.
24. Dissolve the precipitate in 5 ml of 6M HNO_3 and boil over a flame to remove all CO_2 ; add 5 mg of iron (ferric) carrier and make basic with concentrated NH_4OH until the $\text{Fe}(\text{OH})_3$ precipitate appears. Centrifuge and transfer the supernate to a clean 40 ml centrifuge tube; discard the precipitate. Record time and date of this $\text{Fe}(\text{OH})_3$ scavenging as "separation time" for subsequent yttrium-90 growth calculations. Render the supernate acidic with concentrated HNO_3 ; add, via a pipette, 10 mg of yttrium carrier (Note 2).
25. Allow solution to stand for at least 3 days to permit sufficient yttrium-90 growth; add 7 to 8 drops of meta cresol purple indicator, shake well and make basic with 6M NH_4OH until just one drop causes a color change from yellow

to violet (Note 1).

26. Digest in a hot water bath for about 10 minutes and then cool to room temperature in a water bath; immediately centrifuge the $Y(OH)_3$ precipitate and decant the supernate into a clean 40 ml centrifuge tube. Record time and date of "milking" - i. e. when the supernate strontium fraction is decanted.
27. Wash the $Y(OH)_3$ precipitate with 3 ml of water, using a stirring rod to slurry the precipitate; centrifuge and combine supernate with the strontium fraction from step (26). Reserve the supernate for the strontium purification procedure and the precipitate for the yttrium-90 purification procedure.

Notes:

1. In order to prevent the precipitation of any strontium, the pH must be carefully controlled so that it will not exceed 7.6.
2. Strontium-85 spike may also be added at this point in order to monitor any loss of strontium carrier in succeeding steps. However, experimental evidence has shown that the use of strontium-85 spike is not necessary. Also, the spike interferes with the measurement of low levels of strontium-89 activity.

Beryllium-7 Purification Procedure^{11, 12}

- (a) To an appropriate aliquot of the filter paper solution contained in a 40 ml centrifuge tube, add 10 mg of beryllium carrier and 5 mg of lanthanum carrier.
- (b) Using concentrated NH_4OH , make the solution strongly ammoniacal; centrifuge and discard the supernate; wash the hydroxide precipitates with 5 ml of water containing 5 drops of concentrated NH_4OH , centrifuge and discard the wash.
- (c) To this precipitate or the precipitate from step 7 of sequential radiochemical separation I add 10 ml of 3M NaOH and digest in a hot water bath for not more than 5 minutes (Note 1); cool, centrifuge and decant the supernate into a clean 40 ml centrifuge tube. Repeat washing with another 10 ml of 3M NaOH, combining supernates; discard the $\text{La}(\text{OH})_3$ precipitate.
- (d) Neutralize the solution with dropwise addition of concentrated HCl and then make strongly ammoniacal with concentrated NH_4OH (Note 2).
- (e) Digest the solution in a hot water bath for 10 minutes, cool, centrifuge the $\text{Be}(\text{OH})_2$ and discard the supernate.
- (f) Dissolve the $\text{Be}(\text{OH})_2$ in 3 ml of 6M HCl and dilute to 10 ml with water; add 0.5 ml of molybdenum and tellurium carriers (10 mg/ml) and heat in a hot water bath for 5 minutes.
- (g) Bubble hydrogen sulfide gas through the solution for 5 minutes and then heat for an additional 5 minutes; filter the solution through a Whatman No. 42 filter paper (9 cm diameter) in a 2", 60° glass funnel and collect the filtrate in a clean 40 ml centrifuge tube.
- (h) Heat the filtrate in a hot water bath for 5 minutes and repeat step (g).
- (i) Boil the filtrate over a flame to expel H_2S ; make ammoniacal with concentrated NH_4OH , centrifuge the $\text{Be}(\text{OH})_2$ and discard the supernate.
- (j) Dissolve the $\text{Be}(\text{OH})_2$ in 2 ml of 6M HCl and dilute to 10 ml with water; transfer the solution to a 60 ml cylindrical separatory funnel; wash the centrifuge tube with two 5 ml portions of water and add washings to the separatory funnel.
- (k) Add 2 ml of "acetate buffer solution" (2M HOAc - 4M NH_4OAc) and 2 ml of 10% EDTA solution; adjust the pH to 5.5 - 6.0 by the dropwise addition of concentrated NH_4OH ; add 2 ml of acetylacetone and stir mechanically for several minutes.
- (l) Add 7 ml of benzene and stir mechanically for two minutes; withdraw the aqueous (lower) layer into a clean 40 ml centrifuge tube and transfer the organic phase into a second 60 ml separatory funnel; transfer the aqueous fraction back into the original separatory funnel and adjust the pH to 5.5-6.0.

if necessary, with concentrated NH_4OH .

- (m) Repeat step (l) twice and combine the benzene fractions in the second separatory funnel.
- (n) Wash the benzene fraction with 10 ml of "acetate wash solution" (0.25M HOAc, 0.5M NH_4OAc and 1% EDTA) the pH of which has been carefully adjusted to 5.7 with 6M NH_4OH ; withdraw and discard the wash solution.
- (o) To the benzene fraction, add 7 ml of 6M HCl; mechanically stir for several minutes and withdraw the HCl layer into a 125 ml Erlenmeyer flask.
- (p) Repeat step (o) twice combining the HCl fractions in the Erlenmeyer flask; discard the benzene layer.
- (q) Evaporate the HCl fraction almost to dryness; add 5 ml of concentrated HNO_3 and evaporate just to dryness.
- (r) Dissolve the $\text{Be}(\text{NO}_3)_2$ residue in 2 ml of 6M HCl and dilute with 5 ml of water; transfer the solution to a clean 40 ml centrifuge tube. Wash the flask with three 3ml portions of water and add washings to the centrifuge tube.
- (s) Make the solution strongly ammoniacal with concentrated NH_4OH , centrifuge and discard the supernate; wash the $\text{Be}(\text{OH})_2$ twice with 5 ml of water, centrifuge and discard the washings.
- (t) Dissolve the precipitate in a minimum of concentrated HCl and transfer the solution to a 10 ml test tube (12 x 100 mm); make the solution strongly ammoniacal with concentrated NH_4OH and reprecipitate $\text{Be}(\text{OH})_2$. Centrifuge, discard the supernate and gamma count the $\text{Be}(\text{OH})_2$ precipitate in the well of the NaI crystal of the gamma ray spectrometer. The absolute disintegration rate is obtained by subtracting the background from the 0.477 Mev photopeak and using a 17.25% counting efficiency and an 11% branching ratio for the gamma ray.
- (u) After completion of the radiometric assay, slurry the $\text{Be}(\text{OH})_2$ with a minimum of water and filter onto a Whatman No. 40 filter paper (9 cm diameter) in a 2", 60° glass funnel. Rinse the tube with two successive 5 ml portions of anhydrous "anhydrol" and transfer the washings to the filter paper.
- (v) Place the filter paper with precipitate into a previously weighed porcelain crucible (with cover) and heat cautiously until all of the filter paper is charred. Transfer to an electric muffle furnace and ash at 800 °C for one hour; weigh and record chemical yield of BeO_2 .

Notes:

1. It has been observed that digesting for longer than 5 minutes may result in some dissolution of the $\text{La}(\text{OH})_3$.
2. The addition of HCl will cause the precipitation of $\text{Be}(\text{OH})_2$; the solution is neutral when the $\text{Be}(\text{OH})_2$ redissolves.

Sodium-22 Purification Procedure¹³

- (a) To the supernate from step 2 of sequential radiochemical separation II. reserved for sodium analysis, add concentrated HCl until the solution is $\text{Ph} < 1$ and boil over a flame for several minutes to remove all CO_2 .
- (b) Add 2 drops of iron carrier, make just basic with concentrated NH_4OH and then add three drops in excess. Centrifuge and transfer the supernate to a 125 ml Erlenmeyer flask; discard the precipitate.
- (c) To the supernate, add 1 ml of concentrated HCl, and evaporate to near dryness with constant swirling over a Fisher burner. Cool, add 1 ml of 6M NH_4OAc and 100 ml of sodium precipitating reagent.
- (d) Stir vigorously for 20 minutes using a magnetic stirrer and then centrifuge portion-wise in a 40 ml centrifuge tube; discard the supernate.
- (e) Wash the precipitate with 20 ml of "sodium wash solution" centrifuge and discard the wash.
- (f) Dissolve the precipitate in several drops of concentrated HCl, dilute to 15 ml with H_2O , add 2 drops of iron carrier and make the solution just basic with concentrated NH_4OH adding 3 drops in excess. Centrifuge and transfer the supernate to a clean 40 ml centrifuge tube; discard the precipitate.
- (g) To the supernate from step (f) add concentrated HCl to make the solution 3N, add 5 drops of copper carrier, and saturate with H_2S gas for 5 minutes. Centrifuge and transfer the supernate to a clean 40 ml centrifuge tube; discard the precipitate.
- (h) Evaporate the solution to dryness, dissolve the resultant precipitate in several drops of H_2O and add 20 ml of concentrated HCl-ethyl ether (1, 1 ratio) reagent. Cool in an ice bath with vigorous stirring, centrifuge and discard the supernate.
- (i) Dissolve the NaCl precipitate in a minimum amount of H_2O , add 20 ml of concentrated HCl-ethyl ether reagent and again precipitate NaCl as in step (h). Centrifuge and discard the supernate.
- (j) Suspend the precipitate in 10 mls of cold absolute ethanol and filter onto a tared No. 42 Whatman filter paper using cold absolute ethanol as transfer agent. Dry in an oven at 110°C for 10 minutes, cool to room temperature in a desiccator and weigh for chemical yield; Mount on a brass planchet and beta count; chemical yield of NaCl is approximately 50%.

The NaCl mount is counted in a low level beta counter. Radiochemical purity is determined by counting without an absorber and then with an aluminum absorber of 14.59 mg/cm^2 thickness. The ratio of the two count rates is compared to the ratios obtained by counting absolute standards under the same conditions. If the sample ratio agrees with the standard ratio within the prescribed counting statistics, the sample is accepted as radiochemically pure. The Na-22 content of the sample is calculated by applying self absorption-self scattering, chemical yield and counting efficiency corrections.

Phosphorus-32 Purification Procedure^{14, 15}

- (a) Dissolve the precipitate of NH_4PMoO_4 from step (4) of sequential radiochemical separation I in 0.5 ml of concentrated NH_4OH (Note 1), add 10 ml of H_2O , 10 drops of 30% H_2O_2 and stir thoroughly.
- (b) Add 10 ml of concentrated HCl , 20 mg of zirconium carrier; digest in a hot water bath for 5 minutes, centrifuge and discard the supernate.
- (c) Wash the precipitate with 5 ml of H_2O , centrifuge and discard wash.
- (d) Dissolve the precipitate in 2 drops (Note 2) of concentrated HF , add 10 ml of H_2O , 0.5 ml of 1N HCl , 5 mg of cadmium carrier and a few drops of aerosol solution.
- (e) Heat in a hot water bath for 15 minutes while bubbling H_2S gas through the solution.
- (f) Filter the mixture containing the sulfide precipitate through a Whatman No. 42 filter paper (9cm diameter) in a 2", 60° glass funnel and collect the filtrate in a clean lusteroid tube.
- (g) Add 20 mg of lanthanum carrier (or until no more precipitate forms), centrifuge and transfer the supernate to a clean 40 ml glass centrifuge tube.
- (h) To the supernate from step (g) add 4 ml of concentrated HNO_3 , 5 ml of ammonium molybdate reagent, several drops of Aerosol solution and heat in a water bath for 5 minutes (temperature should not exceed 50°C). Centrifuge and discard the supernate.
- (i) Wash the precipitate with 5 ml of 3% HNO_3 , add a few drops of Aerosol solution, centrifuge and discard the wash.
- (j) Dissolve the NH_4PMoO_4 precipitate in 1 ml of concentrated NH_4OH (Note 3) and add 2 ml of citric acid solution.
- (k) Slowly add 10 ml of magnesia mixture with stirring and concentrated NH_4OH (dropwise) until the solution is just alkaline; then follow with an additional 10 drops of concentrated NH_4OH .
- (l) Stir for 1 minute after the formation of the precipitate and then add 4 ml of concentrated NH_4OH ; allow the mixture to stand for 4 hours with occasional stirring.
- (m) Filter the precipitate on a Whatman No. 42 filter disc using 1:20 NH_4OH and 15 ml of anhydrous "anhydrol" as transfer agents.
- (n) Dry in an oven at 100°C for 10 minutes, cool to room temperature in a desiccator and mount.
- (o) The MgNH_4PO_4 mount is counted in a low level beta counter. An aluminum

absorber of 71.58 mg/cm² thickness is placed directly on top of the sample in order to eliminate all P³³ activity. The sample is counted at three day intervals until a representative straight line can be drawn through a semi-logarithmic plot of the data. If the empirically determined half life is 14.3 ± 0.7 days, the sample is radiochemically pure.

- (p) The chemical yield is determined, upon completion of radiometric assay, by placing the filter paper, pliofilm and precipitate into a previously weighed porcelain crucible (with cover) and heating cautiously with a Fisher burner until the filter paper is charred. Transfer the crucible to an electric muffle furnace and slowly raise the temperature (Note 4) to 1050 °C; maintain this temperature for 1 1/2 hours. Weigh and record the chemical yield of Mg₂P₂O₇, which normally ranges between 60-70%.

Notes:

1. If a white or brownish precipitate remains after the yellow precipitate has dissolved, centrifuge and decant the supernate into clean lusteroid tube; discard the precipitate.
2. If the precipitate does not completely dissolve, add 1 extra drop of concentrated HF. CAUTION: excess HF will retard the precipitation of NH₄PMoO₄.
3. If the precipitate does not completely dissolve, centrifuge and decant the supernate into a clean 40 ml glass centrifuge tube.
4. All carbon should be burned off before 900 °C.

Calcium-45 Purification Procedure 16, 17, 18

- (a) Dissolve the precipitate from step 3 of sequential radiochemical separation II reserved for calcium analysis in 2 ml of 6N HCl, dilute to 10 ml with H₂O and add 6 drops of iron carrier. Heat over a flame for several minutes to remove all CO₂ and precipitate Fe(OH)₃ by the dropwise addition of concentrated NH₄OH.
- (b) Cool, centrifuge, transfer the supernate to a clean 40 ml centrifuge tube and discard the precipitate.
- (c) Acidify the supernate with concentrated HCl and repeat step (b) twice.
- (d) Render the supernate after the last Fe(OH)₃ scavenge strongly ammoniacal with concentrated NH₄OH, heat in a hot water bath and add 10 mls of saturated (NH₄)₂CO₃ solution. Digest until the precipitate settles, cool, centrifuge and discard the supernate.
- (e) Dissolve the CaCO₃ precipitate in 2 mls of 6N HCl, dilute to 10 mls with H₂O and boil over a flame for several minutes to expel CO₂.
- (f) Transfer the solution to a 100 ml beaker, dilute to 40 mls with H₂O and add 1N NaOH to pH of 12.
- (g) Add one-half of a murexide indicator tablet, stir until dissolved, and then add dropwise, with stirring, 7.5% EDTA solution until the color changes from red to blue.
- (h) Carefully adjust the pH to 5.5 with 1N HCl and transfer the solution, without washing, to a 60 ml separatory funnel, the stem of which is directly over an ion exchange column (13mm O. D.) containing sodium-cycled "Dqwex-50" cation exchanger. (Note 1).
- (i) Adjust the flow from the separatory funnel and column to 1 drop/second, collecting the effluent in a 250 ml beaker.
- (j) Elute the column with 150 mls of calcium wash solution and collect the eluent in the same 250 ml beaker.
- (k) Evaporate on a hot plate to approximately 50 mls and transfer to a 100 ml beaker with several washings; evaporate just to dryness.
- (l) Cautiously add 30 mls of fuming HNO₃ and evaporate just to wet dryness. Add another 20 mls of fuming HNO₃, evaporate to 5 mls and cool the beaker in a cold water bath for 5 minutes.
- (m) Decant the mixture into a 40 ml centrifuge tube, centrifuge and discard the supernate.
- (n) Dissolve the Ca(NO₃)₂ residue in the beaker with a minimum amount of H₂O and add to the centrifuge tube. Wash the beaker with two 5 ml portions of H₂O and add to the tube.

- (o) Render the solution strongly ammoniacal with concentrated NH_4OH , heat to boiling over a flame and precipitate $\text{CaC}_2\text{O}_4 \cdot \text{H}_2\text{O}$ by the dropwise addition of 3 mls of 4% $(\text{NH}_4)_2\text{C}_2\text{O}_4$ solution. Centrifuge and discard the supernate.
- (p) Dissolve the precipitate in 2 mls of concentrated HNO_3 , add 2 mls of 1M NaBrO_3 and evaporate to 1 ml over a flame.
- (q) Add 6 drops of iron carrier and dilute to 15 mls with H_2O . Add concentrated NH_4OH until $\text{Fe}(\text{OH})_3$ precipitates; centrifuge and discard the precipitate.
- (r) Acidify the solution with concentrated HNO_3 and repeat the scavenge.
- (s) Precipitate $\text{CaC}_2\text{O}_4 \cdot \text{H}_2\text{O}$ as in step (o) and filter onto a weighed Whatman No. 42 filter disk. Wash twice with two 10 ml portions of H_2O and once with a 10 ml portion of anhydrous "anhydrol". Dry in an oven at 100°C for 15 minutes, cool to room temperature in a desiccator and weigh for chemical yield. Mount on a brass planchet and beta count; chemical yields for calcium are about 60%.

The $\text{CaC}_2\text{O}_4 \cdot \text{H}_2\text{O}$ mount is counted in a low level beta counter. Radiochemical purity is ascertained by counting without an absorber and then with an aluminum absorber of 6.26 mg/cm^2 thickness. The ratio of the two count rates is compared to the ratio obtained by counting an absolute standard under the same conditions. If the sample ratio agrees with the standard ratio within the prescribed counting statistics, the sample is accepted as radiochemically pure. Self-absorption self-scattering corrections are applied to all Ca^{45} samples in converting to disintegrations per minute.

Notes:

1. The resin is conditioned by three alternate washings with 5% HCl solution and 5% NaCl solution in a 400 ml beaker. The resin is allowed to settle and the fine particles decanted off after the addition of each wash solution. The resin is finally washed free of NaCl with several H_2O washings. Approximately 10 ml of wet resin is placed in the column.

Yttrium-90 Purification Procedure¹⁹

- (a) Dissolve the $Y(OH)_3$ precipitate from step 27 of sequential radiochemical separation III in 2 ml of 1M HCl and add with a pipette 1.5 ml of 6M HNO_3 .
- (b) Heat the solution to boiling and add 5 ml of a saturated $(NH_4)_2C_2O_4 \cdot H_2O$ solution; stir for several minutes and add gradually 10 ml more of saturated $(NH_4)_2C_2O_4 \cdot H_2O$.
- (c) Digest in a hot water bath for 20 minutes with intermittent stirring; cool to room temperature and filter the $Y_2(C_2O_4)_3 \cdot 9H_2O$ onto a previously washed and weighed Whatman No. 42 filter disk using water and finally anhydrous "anhydrol" as transfer agents.
- (d) Dry in an oven at 100°C for 10 minutes and cool to room temperature in a desiccator; weigh, record chemical yield of $Y_2(C_2O_4)_3 \cdot 9H_2O$, and mount on a brass planchet for beta counting.

If the initial activity was greater than 10 counts per minute above background, the yttrium oxalate mount was counted with an Anton 1007 T halogen-filled Geiger tube no sooner than 10 hours after purification and then about every 24 hours for at least 3 successive days. The samples were counted to 1000 counts or for a maximum period of 30 minutes. The delay of 10 hours before the initial counting permits decay to insignificant levels of radon-220 and its daughter products present in the sample. These contaminants are introduced during the filtration and air drying of the final precipitate on the filtration apparatus because of their natural occurrence in ground level air. The logarithm of the activity is plotted against time; if the empirical half life is 65 ± 5 hours, the sample is accepted as radiochemically pure. The counting statistic, expressed as a percent, of the first empirical point falling on the best straight line through the points or the closest empirical point to the line is reported as the counting precision for the extrapolated "milking" time activity of yttrium-90.

If the initial activity is less than 10 counts per minute above background, the sample is subsequently counted 3 times on a low-level beta counter at approximately 48 hour intervals. The counting time for each measurement is 8 hours. The activity at each counting time is corrected back to milking time of Y^{90} using the theoretical Y^{90} half life of 64 hours. If the corrected activities agree to within one standard deviation of the counting error, the sample is considered radiochemically pure.

If the criteria of radiochemical purity are not met, the Sr fraction is dismounted, purified, and the "milking" and counting cycles repeated. The activity at milking time of the radiochemically pure sample is divided by the counting efficiency and the chemical yields of both the Y and Sr carriers to give the Y^{90} or Sr^{90} dpm in the sample aliquot. Under the counting conditions employed, there are no significant self-absorption self-scattering corrections applied to the Y^{90} activity.

Strontium-89, 90 Purification Procedure²⁰

- (a) Heat the combined strontium supernate from steps (26) and (27) of sequential radiochemical separation III for several minutes in a hot water bath; adjust the pH to greater than 8.5 with concentrated NH_4OH .
- (b) Add 10 ml of a saturated Na_2CO_3 solution with stirring and allow solution to stand until it has cooled to room temperature.
- (c) Centrifuge and discard the supernate. Add 10 ml of water to the SrCO_3 precipitate and slurry with a stirring rod.
- (d) Filter the precipitate onto a previously washed and weighed Whatman No. 42 filter disk using water and finally acetone as transfer agents.
- (e) Dry in an oven at 100°C for 30 minutes and then cool to room temperature in a desiccator; weigh, record chemical yield of SrCO_3 and mount on a brass planchet for beta counting.

The Sr^{89} activity in a sample is obtained from the beta measurements of the SrCO_3 mount and the Y^{90} dpm of the sample. The SrCO_3 is counted shortly after the Y^{90} separation, and then twice at 2 week intervals. At the first beta counting, the fractional contribution of the Y^{90} to the total activity should be small because little time has elapsed from the time of the Y^{90} separation. Two weeks later, the Y^{90} has grown back into complete equilibrium with Sr^{90} while the Sr^{89} has decayed. During the final 2 weeks before the last beta counting, only the Sr^{89} has decayed. The Sr^{89} is calculated from each of the 3 counts by subtracting out the appropriate activities of Sr^{90} and Y^{90} . If the calculated Sr^{89} activities corrected back to a common time agree with each other to within 10%, the sample is accepted as radiochemically pure.

Yttrium-91 Purification Procedure^{21, 22}

- (a) Transfer the yttrium-91 and cerium-144 fraction from step 12 of sequential radiochemical separation III to a 125 ml separatory funnel; rinse the centrifuge tube with 5 ml of concentrated HNO_3 and add washings to the separatory funnel.
- (b) Add 10 ml of TBP reagent (Note 1) and shake for 5 minutes. Withdraw the aqueous phase into a clean 100 ml beaker and wash the TBP phase twice with two 15 ml portions of concentrated HNO_3 ; add washings to the beaker. Reserve the aqueous phase for the cerium-144 purification procedure.
- (c) Strip the "yttrium" from the TBP by shaking with three separate 10 ml portions of water for one minute each. Combine the extracts in a 40 ml centrifuge tube and add 10 drops of meta cresol purple indicator; discard the organic phase.
- (d) Adjust the pH to 7.2-7.4 with 6M NH_4OH , i. e. until just one drop causes a color change from yellow to violet; digest in a hot water bath for about 10 minutes and then cool to room temperature in a water bath for approximately 15 minutes. Centrifuge and discard the supernate; slurry the $\text{Y}(\text{OH})_3$ precipitate with 5 ml of water and then centrifuge and discard the wash.
- (e) Dissolve the $\text{Y}(\text{OH})_3$ precipitate in 25 ml of concentrated HNO_3 and transfer to a 125 ml separatory funnel; rinse the centrifuge tube with 5 ml of concentrated HNO_3 and add washings to the separatory funnel.
- (f) Repeat steps (b), (c) and (d).
- (g) Dissolve the precipitate in 2 ml of 6M HCl and dilute to 15 ml with water; heat solution over a flame to just boiling and add 5 ml of a saturated $(\text{NH}_4)_2\text{C}_2\text{O}_4 \cdot \text{H}_2\text{O}$ solution; stir for several minutes and add an additional 10 ml of $(\text{NH}_4)_2 \cdot \text{C}_2\text{O}_4 \cdot \text{H}_2\text{O}$.
- (h) Digest in a hot water bath for about 20 minutes with intermittent stirring; cool to room temperature and filter the $\text{Y}_2(\text{C}_2\text{O}_4)_3 \cdot 9\text{H}_2\text{O}$ onto a previously washed and weighed Whatman No. 42 filter disk using water and finally anhydrous "anhydrol" as transfer agents.
- (i) Dry in an oven at 100°C for 10 minutes and then cool to room temperature in a desiccator; weigh, record chemical yield of $\text{Y}_2(\text{C}_2\text{O}_4)_3 \cdot 9\text{H}_2\text{O}$ and mount on a brass planchet.

The sample is set aside for three weeks before beta counting in order to allow decay of any yttrium-90 that may be present. The yttrium oxalate mount is counted without an absorber and then with a 71.6 mg Al/cm^2 absorber. If the ratio of the count rates agrees with the ratio obtained by counting an absolute standard under the same conditions, the sample is said to be radiochemically pure. The yttrium-91 activity is obtained by applying the chemical yield and counting efficiency correction factors.

Notes:

1. The TBP reagent is prepared by combining 48 ml of tributyl phosphate and 32 ml of ligroin (petroleum ether). The mixture is equilibrated by shaking with an equal volume of concentrated HNO_3 (this mixture is sufficient for the analysis of 4 samples).

- (a) Transfer the Zr phenylarsonate precipitate from step 9 of the sequential analyses into a 40 ml lusteroid tube by slurring with 6M HCl. After the transfer is complete, wash the precipitate with 3 ml of water. Discard all washes.
- (b) Dissolve the Zr phenylarsonate in 2 ml of concentrated HF; stir vigorously if precipitate fails to go completely into solution.
- (c) Add 5 mg La carrier, 2 ml of water and stir thoroughly. Digest in a hot water bath until the LaF₃ coagulates; centrifuge briefly.
- (d) Add another 5 mg of La carrier on top of the previous precipitate and centrifuge thoroughly. Decant the supernate into another lusteroid and discard the precipitate.
- (e) Repeat steps c and d twice.
- (f) After a total of 6 LaF₃ precipitates, add 50 mg of Ba carrier per 5 ml of supernate solution. Stir well and digest in hot water bath for several minutes. Centrifuge and discard the supernate.
- (g) Slurry the BaZrF₆ precipitate with 4 ml of a saturated H₃BO₃ solution and stir vigorously until the precipitate is finely divided. It is important to get a finely divided slurry.
- (h) Add 2 ml of concentrated HNO₃ and 10 to 12 ml of water; stir vigorously until a clear solution is obtained. See Note 1.
- (i) Reprecipitate the BaZrF₆ with 2 ml of Ba carrier and 2 ml of concentrated HF. Centrifuge, discard the supernate, and dissolve the precipitate as in steps g and h.
- (j) Precipitate the BaZrF₆ again with 2 ml of Ba carrier and 2 ml of concentrated HF; centrifuge and discard the supernate.
- (k) Dissolve the precipitate by vigorously stirring with 4 ml saturated H₃BO₃ solution and then adding 4 ml concentrated HCl plus 10 ml of water.
- (l) Add several drops of 9M H₂SO₄ and let stand for 15 minutes. Add a drop of Aerosol solution, centrifuge, and decant supernate into a 40 ml glass centrifuge tube; discard the BaSO₄ precipitate.
- (m) Add 12M NaOH until the solution is distinctly basic; digest in hot water bath until the Zr(OH)₄ precipitate settles out. Centrifuge and discard the supernate. Wash the precipitate with water and discard the wash.
- (n) Dissolve the Zr(OH)₄ in 2 ml of concentrated HCl (added via pipette); add 1 ml water and heat until a clear solution is obtained. Add 4 ml of 16% mandelic acid (via pipette) and heat in a hot water bath for 20 minutes with occasional stirring. See Note 2.

- (o) Add a drop of Aerosol solution, cool, centrifuge, and discard the supernate. Wash the precipitate with 5 ml of a 2% HCl-5% mandelic acid solution. Centrifuge and discard the supernate.
- (p) Slurry the Zr mandelate precipitate with anhydrol and filter through a previously washed, dried, and weighed Whatman number 42 filter disk. Air dry on filtering apparatus for several minutes, oven dry at 100 °C for 10 minutes and cool in desiccator. Weigh, record chemical yield of Zr mandelate and mount on a brass planchet.

The separated zirconium mandelate is counted on the total gamma counter or the 100 channel gamma rayspectrometer. The spectrometer is used when the Zr^{95} activity is low compared to the high background of the total gamma counter. The brass planchet on which the sample is mounted is placed face down on the center of the NaI(Tl) crystal. Each sample is counted once a week for 4 weeks and extrapolated back to separation time according to the theoretical growth of Nb^{95} . The theoretical growth of Nb^{95} can be used without applying counter efficiencies because the gamma ray energies of Zr^{95} and Nb^{95} are practically the same, 0.75 and 0.76 Mev, respectively. If the 4 activities corrected to separation time agree with each other to within one standard deviation of the counting statistics, the sample is accepted as radiochemically pure. The average value of the 4 is reported with the standard deviation of the individuals from the average.

When the 100 channel gamma ray spectrometer is used to monitor the Zr^{95} separated zirconium mandelate, the area under the combined Zr^{95} - Nb^{95} photoelectric peak is used to estimate the activity in the sample. However, the Nb^{95} growth calculations are the same. The activities at separation time are converted to dpm by calibration experiments with standard samples of Zr^{95} - Nb^{95} .

A Zr^{95} determination can be made from an analysis of the total gamma spectrum of the 3 disks which are removed from the untreated filter paper before ashing. This method consists of drawing a baseline of constant slope from the beginning of the Zr^{95} - Nb^{95} photoelectric peak through 16 channels and calculating the area encompassed by the baseline and the photoelectric peak (See Figure 3.23). This baseline subtraction effectively removes the background and the Compton contribution in this energy region from other gamma emitting nuclides such as Ba^{140} - La^{140} and Ru^{106} - Rh^{106} . Such measurements are repeated 3 times at approximately 10 day intervals and are plotted in units of cpm per 16 channels as a function of time. This technique is illustrated in Figure 3.24 for HASP sample number 592. The theoretical growth curve of Nb^{95} (dotted line in Figure 3.24) is fitted to the empirical points and the Zr^{95} cpm at the effective date of zero Nb^{95} activity is read at the ordinate.

This method applies to mixtures of Zr^{95} - Nb^{95} sources in different stages of equilibrium. To test this method, calculations were made of the behavior with time of the gross activity of varying mixtures of a pure Zr^{95} source and a source of Zr^{95} - Nb^{95} in complete equilibrium. The gross activity for each mixture was plotted as a function of time and the points fitted to the theoretical growth curve of Nb^{95} . The Zr^{95} activity at the effective date of

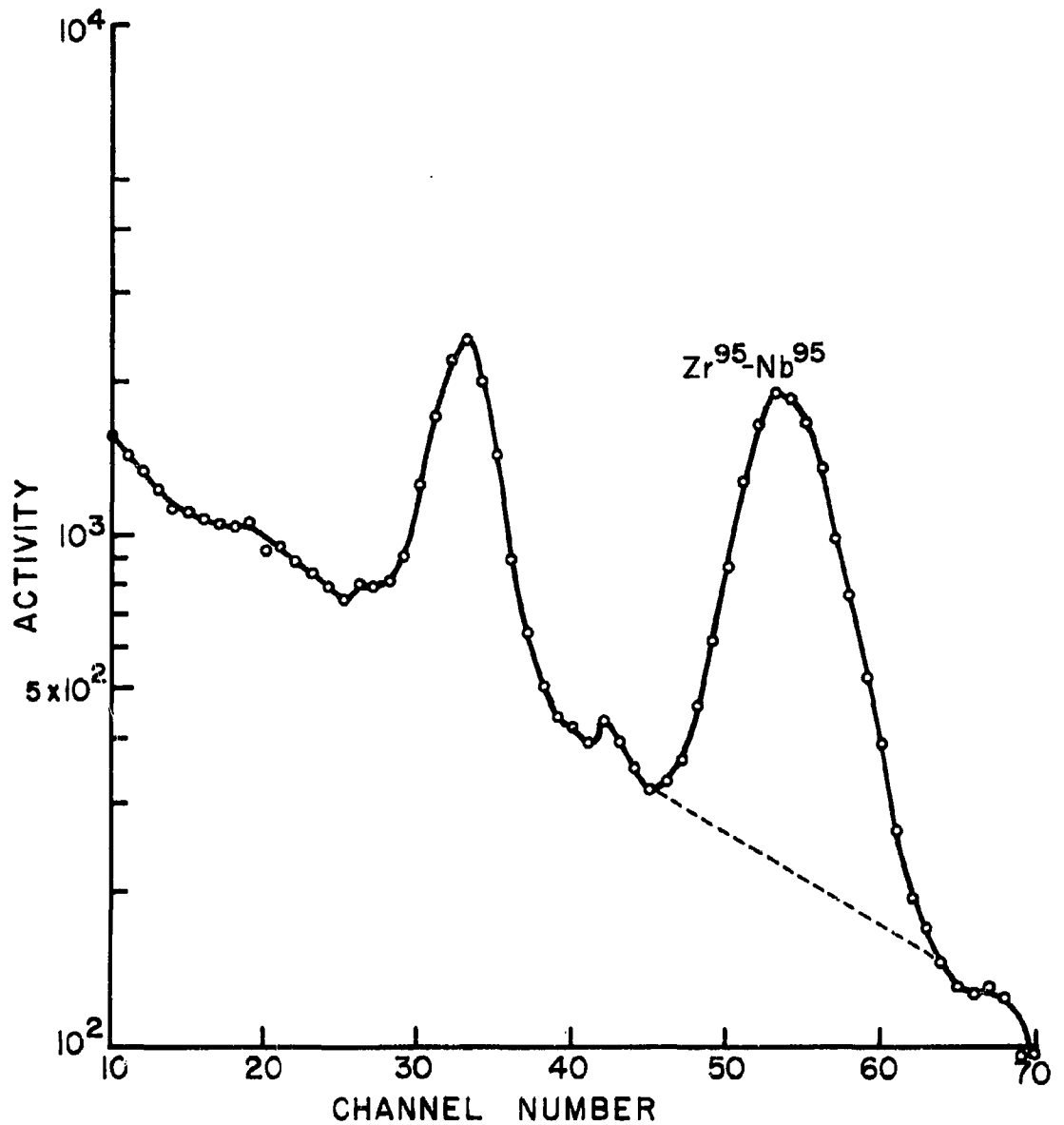


FIGURE 3.23 - BASELINE SUBTRACTION OF $Zr^{95}-Nb^{95}$
PHOTOELECTRIC PEAK IN TOTAL GAMMA
SPECTRUM OF UNTREATED HASP FILTER #552

ISOTOPES, INC.

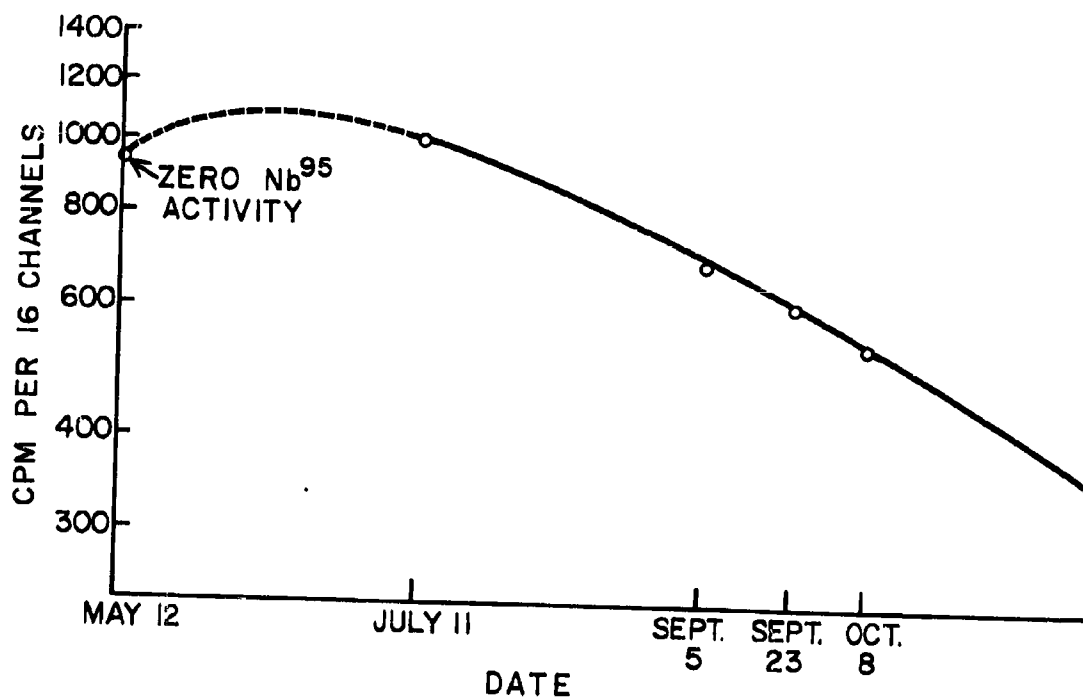


FIGURE 3.24 - Zr⁹⁵ - Nb⁹⁵ PHOTOPEAK AS A FUNCTION OF TIME

zero Nb^{95} activity was read at the ordinate, and a decay correction was made to obtain the activity of Zr^{95} present in the hypothetical mixture at the time of the mixing. Table 3.14 gives the results of these calculations and shows that the Nb^{95} growth method is applicable to mixtures of Zr^{95} - Nb^{95} sources in various stages of equilibrium. The small discrepancies in Table 3.14 probably arise from graphing and interpolation errors.

Several samples were analyzed for Zr^{95} both by radiochemical separation and by the gamma ray spectrum analysis. Table 3.15 gives the results of these analyses and illustrates the good reproducibility between the methods.

Notes:

1. If a large portion of the precipitate does not dissolve, add 1 to 2 more ml of saturated H_3BO_3 and stir well. If some precipitate still remains, centrifuge and decant supernate into another lusteroid. Discard the precipitate.
2. The zirconium mandelate forms slowly, but is quantitative in about 20 minutes.

Table 3.14 Feasibility of the Nb⁹⁵ Growth Method for the Calculation of Zr⁹⁵ Activity

<u>Mixture</u>	<u>Zr⁹⁵ cpm in Mixture</u>	<u>Zr⁹⁵ cpm in Mixture Calculated from Nb⁹⁵ Growth</u>
3 parts Zr ⁹⁵ -Nb ⁹⁵ : 1 part Zr ⁹⁵	1947	1915
1 part Zr ⁹⁵ -Nb ⁹⁵ : 1 part Zr ⁹⁵	1316	1320
0.5 parts Zr ⁹⁵ -Nb ⁹⁵ : 1 part Zr ⁹⁵	1158	1174

Table 3.15 Comparison of Zr⁹⁵ Analyses by Radiochemical Separation With Gamma Ray Spectrum Analyses

<u>HASP Sample No.</u>	<u>Radiochemical Separation</u>	<u>Gamma Spectrum Analyses</u>
548	33.0 × 10 ³ dpm	32.6 × 10 ³ dpm
592	372. × 10 ³ dpm	382. × 10 ³ dpm
571	23.7 × 10 ³ dpm	23.7 × 10 ³ dpm
552	37.4 × 10 ³ dpm	42.2 × 10 ³ dpm
567	14.7 × 10 ³ dpm	13.6 × 10 ³ dpm

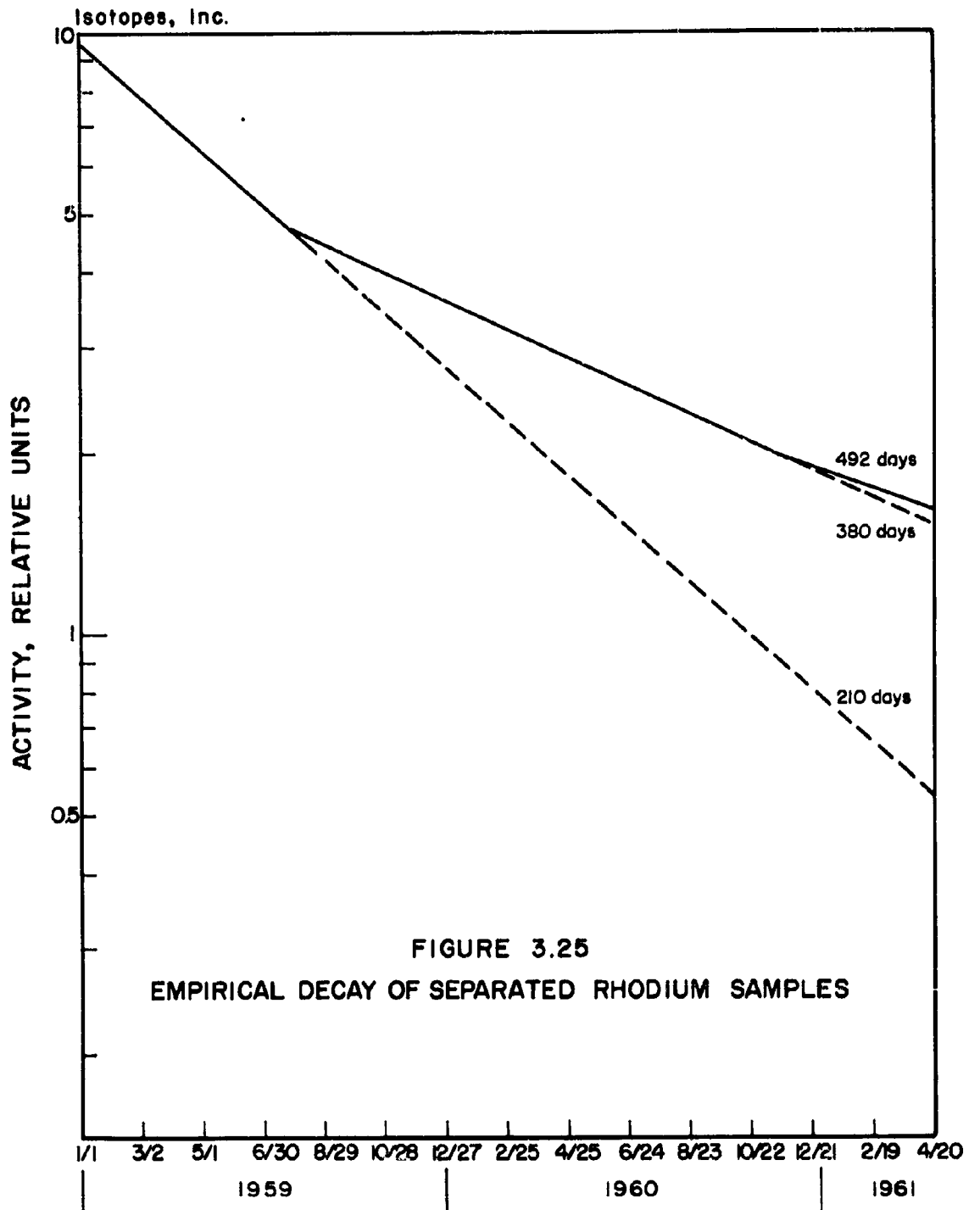
Rhodium-102 Purification Procedure 24

- (a) To an appropriate aliquot of the filter paper solution contained in a 40 ml centrifuge tube, add 30 mg of rhodium carrier with thorough mixing and then 10 ml of pyridine.
- (b) Stir the solution for several minutes and then boil over a flame for approximately two minutes; make basic with saturated Na_2CO_3 and stir for two minutes.
- (c) Transfer the solution to a 60 ml separatory funnel with 5 ml of water and separate the aqueous (lower) phase from the pyridine fraction; discard the aqueous phase.
- (d) Wash the pyridine fraction from step (c) above or from step 6 of sequential radiochemical separation I with two 10 ml portions of 12M NaOH and discard the washings; transfer the pyridine fraction to a 40 ml centrifuge tube, add several drops of 6M NaOH and evaporate to dryness in a sand bath.
- (e) Dissolve the residue from step (d) in 10 ml of water; heat in a water bath for 10 minutes and then bubble hydrogen sulfide gas through the solution for 3 minutes to precipitate rhodium sulfide.
- (f) Cool and carefully add 1 ml of 6M HCl with stirring; centrifuge and discard the supernate. Wash the precipitate with two 10 ml portions of 6M HCl and discard the washing.
- (g) To the sulfide precipitate add 4 ml of concentrated HCl, 2 ml of concentrated HNO_3 and heat in a water bath for 15 minutes.
- (h) Cool the solution, filter through a glass fiber filter paper (9 cm diameter) in a 2", 60° glass funnel to remove elemental sulfur and collect the filtrate in a clean 40 ml centrifuge tube; wash the filter paper with 10 ml of water and combine the washings with the filtrate.
- (i) To the filtrate add 10 mg of zirconium carrier; heat in a hot water bath for 10 minutes and add 2 ml of saturated phenylarsonic acid with stirring.
- (j) Digest the solution in a hot water bath for 10 minutes, cool in a water bath, and add 2 drops of aerosol reagent. Centrifuge the zirconium phenylarsonate precipitate and transfer the supernate to a clean 50 ml beaker. Wash the precipitate with 5 ml of water, centrifuge and add washings to the supernate; discard the precipitate.
- (k) Evaporate the solution to near dryness and add 15 ml of concentrated HCl.
- (l) Prepare two anion exchange columns using 13 mm OD glass tubing and a 1.5 inch resin bed of 100 to 200 mesh, 2% cross linkage, Dowex 1 anion exchange resin.

- (m) Condition one column with concentrated HCl and the other with 6M HCl; deposit the rhodium solution on the concentrated HCl column and collect the effluent in a clean 125 ml Erlenmeyer flask.
- (n) Rinse the beaker with 3 ml of concentrated HCl and add the washings to the column; wash the resin immediately with 10 ml of concentrated HCl collecting the combined effluents in the Erlenmeyer flask from step (m).
- (o) Boil the concentrated HCl effluent to a volume of 5 ml, cool and deposit on the 6M HCl anion exchange column, collecting the effluent in a clean 30 ml beaker.
- (p) Rinse the flask with 5 ml of 6M HCl and add the washings to the column; wash the resin immediately with 10 ml of 6M HCl collecting the combined effluents in the 30 ml beaker from step (o).
- (q) Evaporate the 6M HCl effluent to 5 ml and add 3 ml 70-72% HClO₄, 1 ml concentrated HNO₃ and several drops of Ru carrier; boil to fumes of HClO₄ and continue heating for 10 minutes to distill off the Ru.
- (r) Repeat step (q) three times.
- (s) Transfer the solution to a 125 ml Erlenmeyer flask with 20 to 30 ml of water; add powdered magnesium in small portions, heating and swirling between each addition until the reduction to the rhodium metal is complete as indicated by a colorless solution.
- (t) After the reduction is complete, boil the solution with 5 ml of concentrated HCl to destroy any excess magnesium; transfer to a 40 ml centrifuge tube, centrifuge the rhodium metal and discard the supernate.
- (u) Wash the rhodium metal with about 5 ml of hot HCl followed by two washings with 5 ml of water; slurry with water and filter onto a previously washed and weighed Whatman No. 42 filter disk.
- (v) Wash the precipitate with three 5 ml portions of anhydrous "anhydrol"; dry in an oven for 15 minutes at 100°C; cool in a desiccator. Weigh, record chemical yield of rhodium metal and mount on a brass planchet for x-ray counting.

Rhodium -102 was assayed by counting the separated element in contact with the thin NaI(Tl) x-ray crystal in conjunction with the 100 channel pulse height analyzer. The area beneath the 81 Kev ruthenium x-ray photopeak was converted to DPM after the appropriate background subtraction.

Kalkstein²⁵ has shown that there are three rhodium isotopes in the stratospheric debris, rhodium-101 m, rhodium-102 and rhodium-102 m. These isotopes contribute to the 81 Kev photopeak and the composite photopeak cannot be directly resolved into its individual components. Kalkstein has prepared an empirical curve by measuring a number of stratospheric rhodium samples which describes the total photopeak activity and the rhodium-102 photopeak activity as a function of time (See Figure 3, 25). All the rhodium samples separated in HASP have been corrected by this curve to yield only the DPM of rhodium-102.



Iodine-131 Purification Procedure²⁶

1. Cut a quadrant of the filter paper into 1/2 inch squares and place in a distilling flask (Note 1), the side arm of which is stoppered. Chill the flask in an ice bath and add 5 ml of concentrated HCl, 14 mg of iodate carrier with stirring (Note 2) and 10 mg of iodide carrier; add 45 ml of chilled, fuming HNO₃ and stopper immediately. Allow solution to stand in the hood overnight so that the filter paper is completely dissolved and a clear solution is obtained.
2. Place 25 ml of 6M NaOH and 5 ml of 1M NaHSO₃ in the receiving tube of the distillation apparatus; set air flowing through the bubbler tube at 1 to 2 bubbles/second.
3. Connect the distilling flask to the receiving tube and dilute the contents of the flask to 100 ml with water; add 10 ml of 2M NaNO₂ and insert the air inlet tube immediately.
4. Heat gently at first and then more strongly until all of the iodine is distilled into the receiving tube and no iodine crystals remain in the side arm.
5. Remove the receiving tube, washing down the side arm with water into the receiving tube.
6. Neutralize the solution in the receiving tube with concentrated HNO₃ and add 3 ml of 6M HNO₃ in excess; transfer the solution to a 250 ml separatory funnel containing 20 ml of CCl₄.
7. Add 1 ml of 2M NaNO₂ and extract the iodine into the CCl₄ layer with shaking (the CCl₄ layer should be violet).
8. Transfer the organic (lower) phase to a clean 125 ml separatory funnel; discard the aqueous phase.
9. Add 15 ml of water and 1 ml of 1M NaHSO₃ and shake; discard the CCl₄ layer (which should now be colorless).
10. Add 2 ml of 6M HNO₃, 15 ml CCl₄, and 1 ml of 2M NaNO₂ and shake; transfer the organic phase to another 125 ml separatory funnel.
11. Repeat steps (9) and (10) and then step (9) again.
12. Transfer the aqueous phase (from step (11)) to a clean 40 ml centrifuge tube; add 3 drops concentrated HCl and heat to boiling. (Note 3).
13. Add 15 ml of anhydrous "anhydrol" and add 20 mg of palladium carrier; cool to room temperature, centrifuge the PdI₂ and discard the supernate.
14. Wash the precipitate with 10 ml of anhydrous "anhydrol", centrifuge and discard the wash solution.
15. Suspend the PdI₂ precipitate in 10 ml of anhydrous "anhydrol" and filter onto a previously washed and weighed glass-fiber filter disk; dry in a vacuum

desiccator for one-half hour and weigh. Record chemical yield of PdI_2 and mount on a brass planchet for beta counting.

The iodine-131 is followed for beta decay and is accepted as radiochemically pure if its empirically determined half-life agrees to within ± 0.4 days with the theoretical half life of 8.1 days. The disintegration rate is obtained by applying chemical yield, and counting efficiency corrections.

Notes:

1. The distilling flask consists of a 200 ml round-bottom flask with a $\frac{1}{2}$ 19/38 outer joint neck and side arm with a 90° bend, the end of which is fitted with a $\frac{1}{2}$ 10/30 inner joint. (See Figure 3.26)
2. Iodine-131 may also be present on the filter paper in the form of iodate and hence iodate carrier is added before the iodide carrier in order to establish equilibrium with any radioiodate. The iodate is then quantitatively converted in strong HNO_3 solutions and in the presence of iodide, to the iodide (or tri-iodide) and then to iodine.
3. Boiling is necessary to insure the removal of SO_2 which interferes with the precipitation of the iodide.

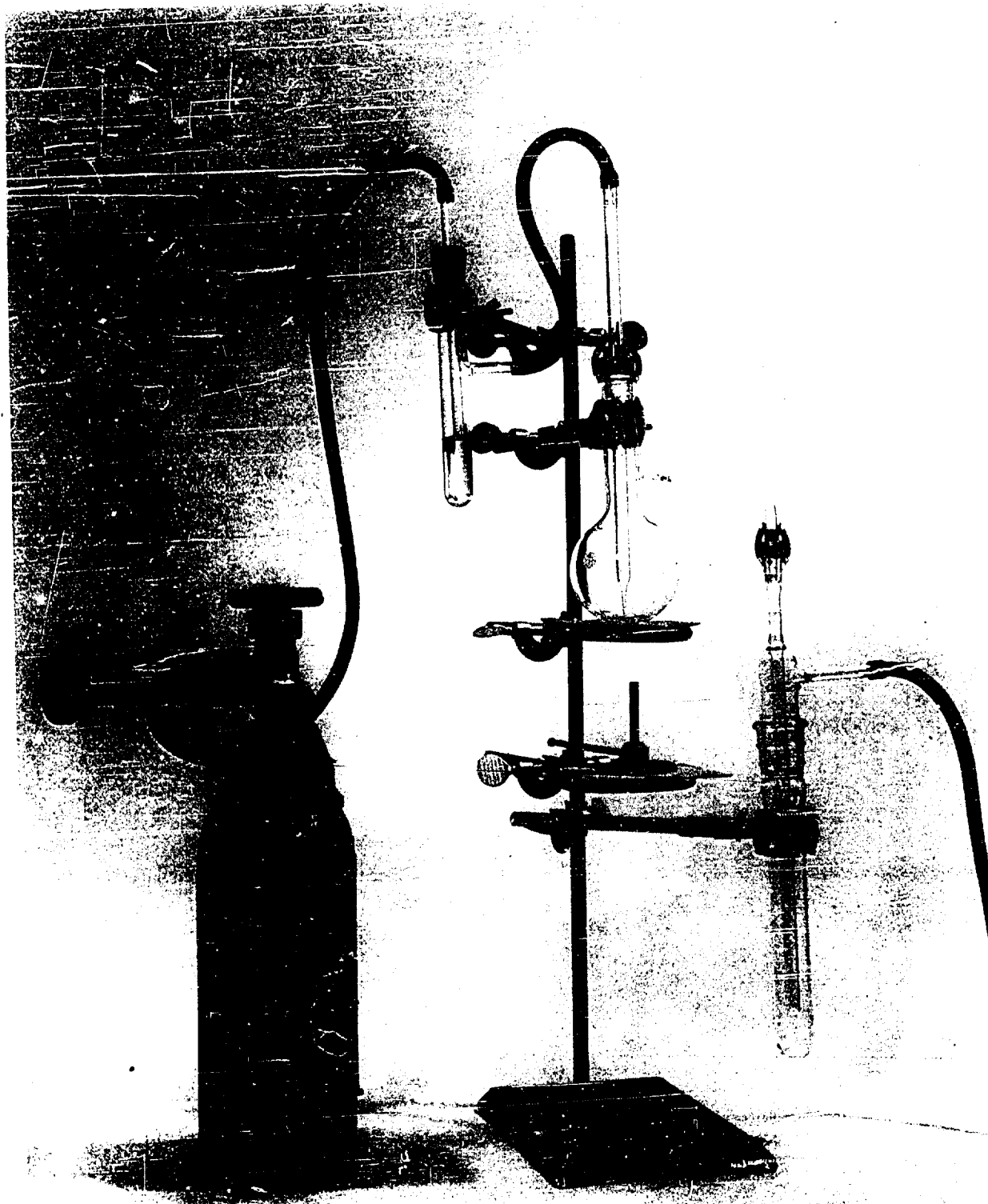


Figure 3.26
Iodine Distillation Apparatus

Cesium-137 Purification Procedure^{27, 28}

- (a) To the cesium fraction from Step 5 of sequential radiochemical separation III add 3 drops of meta cresol purple indicator and carefully neutralize with concentrated HCl; add an excess of 15 ml of 6M HCl.
- (b) Evaporate the solution on a hot plate until "salts" just begin to appear; cool to room temperature and then dilute with enough water to obtain a clear solution.
- (c) Transfer 30 ml of the solution to a 40 ml centrifuge tube and add 5 ml of 0.13M silicotungstic acid and 3 drops of Acrosol solution.
- (d) Digest the precipitate in a hot water bath for 10 minutes, centrifuge the cesium silicotungstate and discard the supernate.
- (e) Transfer, with washings, the remaining solution from step (b) to the centrifuge tube containing the previously precipitated cesium silicotungstate; proceed as in steps (c) and (d).
- (f) To the precipitate add 3 ml of 6M NaOH and heat over a flame until the precipitate is completely dissolved.
- (g) Add 20 ml of 6M HCl and digest in a hot water bath for 10 minutes; centrifuge the silica and tungstic acid and transfer the supernate to a clean 100 ml beaker.
- (h) Wash the precipitate twice with two 5 ml portions of 6M HCl and combine the washings in the beaker; discard the precipitate.
- (i) To the solution add 3 drops of meta cresol purple indicator and neutralize with 50% NaOH; transfer to a 125 ml separatory funnel containing 10 ml of citrate buffer solution (1M $\text{Na}_3\text{C}_6\text{H}_5\text{O}_{17}$, 0.5M HNO_3).
- (j) Add 25 ml of 0.05M sodium tetraphenyl boron-amyl acetate solution to the funnel, shake for 30 seconds and allow to stand for 3 minutes. (Note 1).
- (k) Withdraw the aqueous (lower) phase and collect in another 125 ml separatory funnel; extract again with 15 ml of 0.05M sodium tetraphenyl boron - amyl acetate solution.
- (l) Withdraw and discard the aqueous phase and combine the two portions of the organic phase in a separatory funnel.
- (m) Strip the cesium from the organic phase by extracting twice with two 10 ml portions of 3M HCl; combine the strips in a clean 100 ml beaker and heat on a hot plate for 30 minutes to distill off all traces of the amyl acetate.
- (n) Remove solution from hot plate, add 3 drops of meta cresol purple indicator and neutralize with 6M NaOH. Add 2 ml of 10% chloroplatinic acid very slowly, via a pipette, and stir vigorously during the addition; allow to stand for 30 minutes.

- (o) Filter the precipitate onto a previously washed and weighed glass fiber filter disk without applying suction (Note 2); wash the precipitate with two 5 ml portions of anhydrous "anhydrol" applying suction each time. Oven dry at 100°C for 10 minutes, cool in a desiccator, weigh as the cesium chloroplatinate for chemical yield and mount on a brass planchet for beta counting.

The cesium-137 mount is counted both without an absorber and with an absorber thickness of 13.3 mg Al/cm². The ratio of the counting rates is compared with the ratio from an absolute standard counted under the same conditions to ascertain purity of the sample. Self-scattering and self-absorption, and counting efficiency correction factors are applied to calculate the cesium-137 content of the sample.

Notes:

1. An insoluble precipitate, cesium tetraphenyl boron, will form at the bottom of the amyl acetate layer, obscuring the interface. The aqueous phase may be readily separated by draining until the white precipitate just begins to appear in the bore of the stopcock.
2. The Cs₂PtCl₆ precipitate is a very fine powder and filtering without suction deposits the precipitate evenly on the surface of the filter disk with no tendency for seepage around the edge of the filtering column.

Barium-140 Purification Procedure²⁹

- (a) Wash the BaCrO_4 precipitate from step 20 of sequential radio chemical separation III with 10 ml of hot water, centrifuge and discard the wash. Dissolve the precipitate in 1 ml of 6M HCl.
- (b) Add 15 ml of HCl-ethyl ether reagent and stir for 1 to 2 minutes. Centrifuge and decant the supernate. (Note: No open flames should be allowed in the laboratory during the preparation of the HCl-ethyl ether reagent; all handling of the reagent should be done under the fume hood.)
- (c) Dissolve the BaCl_2 precipitate in 5 ml of water and add 10 mg of Fe carrier; precipitate $\text{Fe}(\text{OH})_3$ with 2 ml of 6M NH_4OH . Centrifuge and discard the precipitate; record the time of the $\text{Fe}(\text{OH})_3$ scavenging as the separation time for subsequent lanthanum-140 growth calculations.
- (d) Neutralize the supernate with concentrated HNO_3 and add, via pipettes, 1 ml of 6M HOAc and 4 ml of 3M NH_4OAc . Heat the solution nearly to boiling and add 1 ml of 1.5M Na_2CrO_4 dropwise with stirring.
- (e) Digest in a hot water bath until the BaCrO_4 settles to the bottom of the tube. Cool and filter through a previously washed, dried, and weighed Whatman No. 42 filter disk. Wash with three 5 ml aliquots of water and then with two 5 ml aliquots of Anhydrol.
- (f) Air dry for several minutes and then oven dry at 100°C for 30 minutes; cool in a desiccator; weigh as BaCrO_4 for chemical yield determination and mount on a brass planchet for beta counting.

Generally, the purified BaCrO_4 mount is counted by means of the Anton 1007 T GM tube about 10 to 24 hours after separation. It is counted three additional times at intervals approximately 24 to 36 hours apart. These activities are corrected back to separation time according to an empirically determined growth curve of a standard Ba^{140} mount. If these corrected activities agree with each other to within one standard deviation of the counting statistics, the sample is accepted as radiochemically pure. The average of the corrected activities is reported with the standard deviation from the average of the individual values. When the counting schedule can not be maintained or the radiochemical purity cannot be confidently determined from measurements of the La^{140} growth, the samples are monitored beginning 7 days after separation time. By this time the La^{140} is in complete equilibrium with the Ba^{140} ; if the mixture decays with a 12.8 ± 0.5 day half life, the sample is accepted as radiochemically pure. Self-absorption self-scattering corrections are applied in correcting the activity of a pure sample to dpm.

A Ba^{140} determination can also be made from an analysis of the total gamma spectrum of the 3 disks which are removed from the untreated filter paper before ashing. The La^{140} daughter of Ba^{140} has a 1.6 Mev gamma ray which, if present in any significant quantities, produces a clearly visible photopeak in the total spectrum of the sample essentially unaffected by other nuclides which are usually present in the HASP samples. Figure 3, 27

illustrates this 1.6 Mev photopeak of La^{140} from a standard Ba^{140} mount. Figure 3.28 illustrates a similar curve from the total spectrum of HASP sample number 592. To obtain dpm from these measurements, the 1.6 Mev photopeak is extrapolated to yield a full Gaussian distribution. A baseline is drawn in from the point of obvious departure from the Gaussian distribution at the higher channel number side of the photopeak to the extrapolated lower channel number side of the photopeak. This procedure is illustrated in Figures 3.27 and 3.28. The area encompassed by the Gaussian curve and the baseline is then converted to DPM.

When the above procedure is performed on samples of significant Ba^{140} content, the baseline usually extends through 13 channels of the spectrum. For low Ba^{140} content samples, the extrapolation of the Gaussian curve to yield a 13 channel intersection with the baseline amounts to estimating over 50% of the total area and consequently 50% of the La^{140} activity in the samples. For such low level samples the best estimate of the photopeak is made and the baseline drawn regardless of the number of channels included.

The final dpm values for such low-level samples are expressed as equal to or less than the disintegration rates corresponding to the areas obtained. In many cases, there is no observable activity in the total gamma spectrum which is attributable to La^{140} . In the absence of any La^{140} activity, a value equal to or less than 120% of the statistical error of the background in these channels is reported.

To compare the gamma spectrum analysis for Ba^{140} with the radiochemical analysis for that nuclide many samples have been analyzed by both methods. Table 3.16 gives the results of these analyses and shows that the gamma spectrum method agrees very well with the radiochemical separation technique.

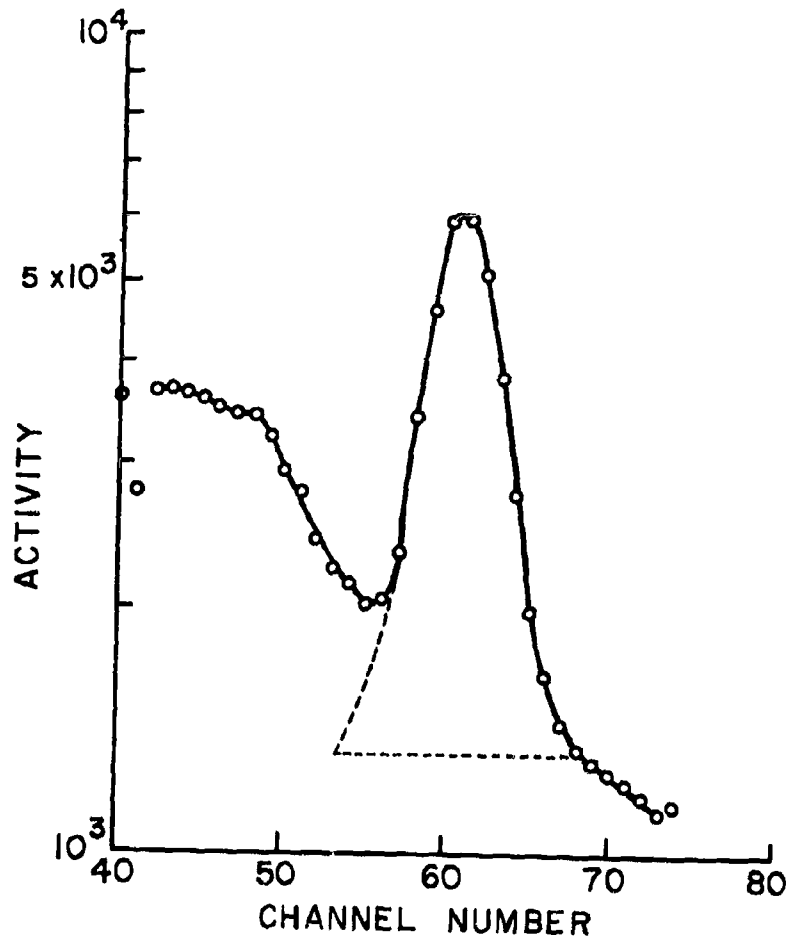


FIGURE 3.27 - La¹⁴⁰ 1.6 MEV. GAMMA RAY OF STANDARD Ba¹⁴⁰ SAMPLE

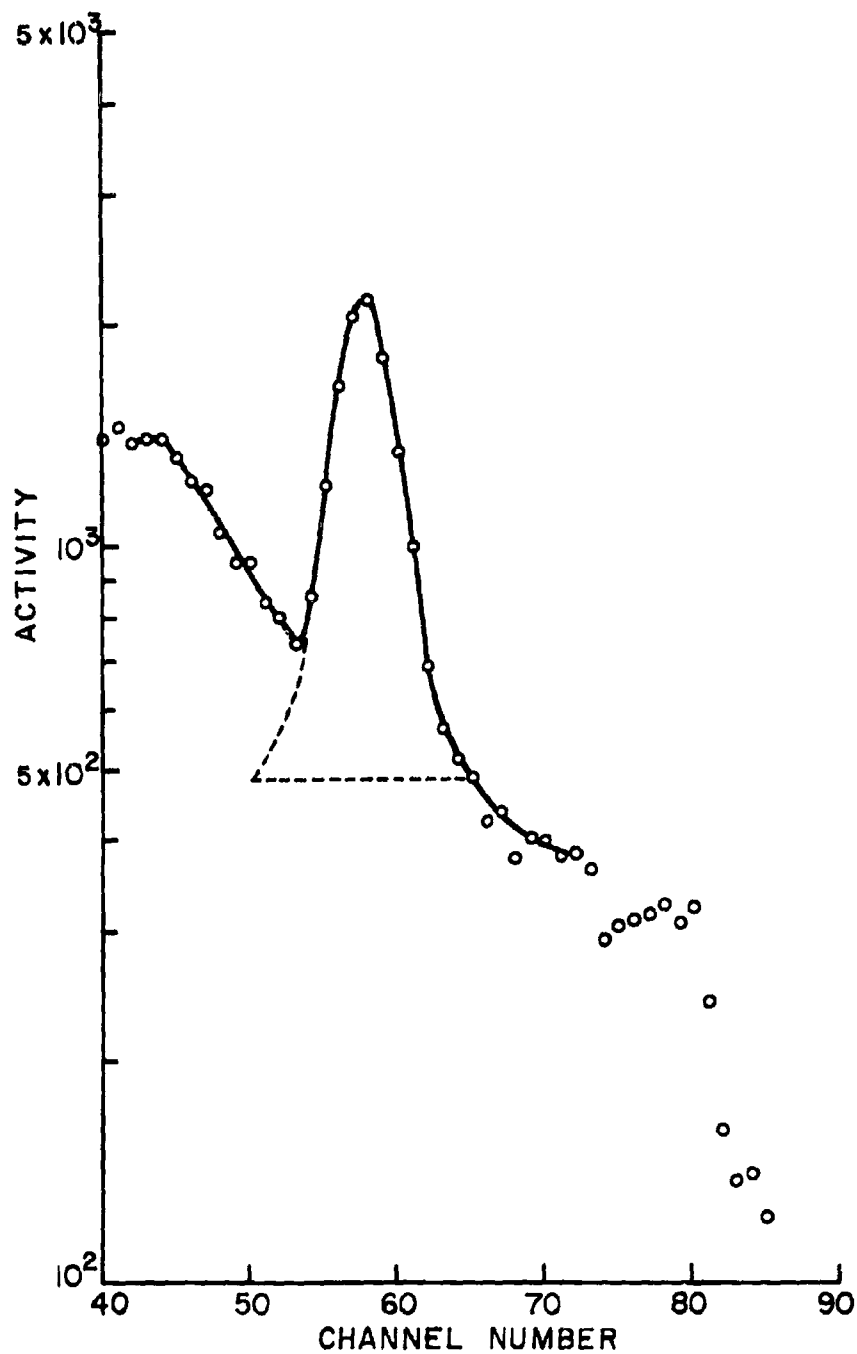


FIGURE 3.28 La^{140} 1.6 MEV. GAMMA RAY
FROM HASP SAMPLE #592

Table 3.16 Comparison of the Ba¹⁴⁰ Assay by Direct Gamma Spectrum Analyses and by Radiochemical Separation and Analysis

<u>HASP Sample</u>	<u>Gamma Spectrum Analyses</u>	<u>Radiochemical Separation</u>
535	27.2 x 10 ³ dpm	27.6 x 10 ³ dpm
539	≤ 5.88 x 10 ³ dpm	6.34 x 10 ³ dpm
544	≤ 12.0 x 10 ³ dpm	11.6 x 10 ³ dpm
548	≤ 5.74 x 10 ³ dpm	5.9 x 10 ³ dpm
552	≤ 3.54 x 10 ³ dpm	3.59 x 10 ³ dpm
563	≤ 2.98 x 10 ³ dpm	2.94 x 10 ³ dpm
592	384. x 10 ³ dpm	381. x 10 ³ dpm
654	2380. x 10 ³ dpm	2440. x 10 ³ dpm
668	1250. x 10 ³ dpm	1190. x 10 ³ dpm
674	1304. x 10 ³ dpm	1440. x 10 ³ dpm
675	1440. x 10 ³ dpm	1430. x 10 ³ dpm
732	2580. x 10 ³ dpm	2580. x 10 ³ dpm

Cerium-144 Purification Procedure³⁰

- (a) Evaporate the solution containing the cerium fraction (step (b) of the yttrium-91 purification procedure) to 10 ml and transfer to a 40 ml centrifuge tube. Wash the beaker with 5 ml of 6M HNO₃ and add the washings to the tube.
- (b) Carefully neutralize with concentrated NH₄OH and add 5 drops in excess; allow the Ce(OH)₃ precipitate to coagulate. Cool, centrifuge, and discard the supernate.
- (c) Slurry the precipitate with 10 ml of water; centrifuge and discard the washing. Dissolve the precipitate in 5 ml of 9M HNO₃ and transfer to a 125 ml separatory funnel containing 50 ml of freshly equilibrated methyl isobutyl ketone (Note 1).
- (d) Wash the tube with 6.5 ml of concentrated HNO₃, then with 2 ml of 2M NaBrO₃ and finally with 4.5 ml of water, and add washings to the separatory funnel; shake for 15 to 30 seconds.
- (e) Withdraw the aqueous (lower) phase and wash the methyl isobutyl ketone phase twice with 10 ml of 9M HNO₃ containing a few drops of 2M NaBrO₃ (Notes 1 and 2).
- (f) Back-extract the cerium by shaking the methyl isobutyl ketone phase with 5 ml of water containing 3 drops of hydrogen peroxide (Notes 1 and 3).
- (g) Withdraw the aqueous phase into a clean 40 ml centrifuge tube and neutralize by adding 3 to 5 ml of concentrated NH₄OH until a precipitate just appears; acidify with 1.5 ml of 6M HNO₃.
- (h) Dilute the solution to a volume of 15 ml with water and heat just to boiling; add 5 ml of saturated (NH₄)₂C₂O₄ · H₂O, stir for several minutes and add gradually 10 ml more of saturated (NH₄)₂C₂O₄ · H₂O.
- (i) Digest the solution in a hot water bath for about 10 minutes, cool to room temperature and filter through a Whatman number 42 filter disk.
- (j) Wash the filtered precipitate three times with 5 ml portions of water and three times with 5 ml portions of acetone.
- (k) Oven dry the precipitate at 100 °C for 20 minutes and then cool to room temperature in a desiccator. Mount the cerium oxalate precipitate on a brass planchet for beta counting.
- (i) The chemical yield is determined, upon completion of the radiometric assay, by igniting the cerous oxalate, along with filter disk and pliofilm, at 850 °C for 1 hour in an electric muffle furnace. Weigh and record chemical yield of CeO₂; customary yields range from 60 to 80 percent.

Several factors are to be considered before the radiochemical and radiometric analyses of cerium-144 can be carried out. There are 3 cerium isotopes present in a mixture of fission products several days after fission. These are: cerium-141 with a 32 day half-life, cerium-143 with a 32 hour half-life, and cerium-144 with a 290 day half-life. Within a period of 20 days after the time of fission, the cerium-143 decays away and is less than 0.2 percent of the total cerium activity. It would require approximately 200 days for the cerium-141 to decay to an activity level relatively insignificant compared to that of cerium-144. For most of the HASP samples, the exact time of fission which generated the cerium activities was not accurately known. In addition, most HASP samples contained debris from several nuclear detonations.

Consequently, the following procedure was adopted: The cerium purification was not begun until at least 20 days after the time of sampling. The cerium oxalate mount was beta counted first through a 234 mg/cm² aluminum absorber to discriminate against cerium-141 and cerium-144. Only the 2.98 Mev. beta emission of praseodymium-144, which is in secular equilibrium with cerium-144, was recorded. Then, the cerium oxalate mount was counted through a 409 mg/cm² aluminum absorber. If the ratio of the count rates agreed with that obtained by counting an absolute standard, the sample was accepted as radiochemically pure. The disintegration rate of any cerium sample was calculated from the counting rate through the 218 mg/cm² aluminum absorber, after making the necessary corrections for chemical yield and counting efficiency.

Notes:

1. The equilibration of methyl isobutyl ketone (enough for 10 samples) is performed in the following manner; to 400 ml of methyl isobutyl ketone add 400 ml of 9M HNO₃ containing 16 ml of 2M sodium bromate and shake or stir for 5 minutes. Caution: In extractions of strong HNO₃ solutions (6 to 12M) with methyl isobutyl ketone considerable amounts of HNO₃ pass into the organic phase. It has been observed that such solutions of HNO₃ in methyl isobutyl ketone are unstable and will undergo a vigorous reaction after standing for a few hours. The methyl isobutyl ketone phases remaining after back-extraction with 5 ml of water were observed to react similarly but only after standing for about 3 days. It is recommended, therefore, that the methyl isobutyl ketone not be equilibrated with HNO₃ until just before use and that it be washed thoroughly with water (three times with an equal volume) soon after use. It is also recommended that HNO₃ solutions which have been in contact with methyl isobutyl ketone be neutralized with NH₄OH before storing or discarding.
2. Combine the aqueous phase and washings and neutralize with NH₄OH before discarding.
3. Wash the methyl isobutyl ketone three times with 50 ml of water before discarding; also neutralize washings before discarding.

Tungsten-181, 185 Purification Procedure³¹

1. To an appropriate aliquot of the filter paper solution, contained in a 40 ml centrifuge tube, add concentrated NH_4OH dropwise until a pH of 8.0 to 8.5 is reached. (Note 1).
2. Add 20 mg of tungsten carrier, stir well to effect exchange between tungsten carrier and radioactive tungsten and then add 10 ml of concentrated HNO_3 ; digest in a hot water bath for approximately 10 minutes.
3. Remove solution, cool to room temperature in a water bath, centrifuge the tungstic oxide and discard the supernate.
4. Dissolve the tungstic oxide precipitate by the addition of 6 to 8 drops of concentrated NH_4OH followed by the addition of 15 ml of water.
5. Add 1 g of solid NH_4NO_3 and with stirring, three drops of iron (ferric) carrier and two drops of Aerosol reagent; centrifuge and decant the supernate into a clean 40 ml centrifuge tube. Discard the $\text{Fe}(\text{OH})_3$ precipitate.
6. To the supernate from step (5), add 6 drops of saturated tartaric acid solution, 5 drops of concentrated H_2SO_4 , 10 drops of bismuth carrier and 1 drop of molybdenum carrier.
7. Place the solution in a hot water bath for approximately 5 minutes and then bubble hydrogen sulfide gas through the solution for two minutes.
8. Allow the mixture to digest for 10 minutes in a hot water bath to enhance coagulation of the sulfides.
9. Filter the hot mixture containing the sulfide precipitates through a Whatman No. 42 filter paper (9 cm diameter) in a 2", 60° glass funnel and collect the filtrate in a clean 40 ml centrifuge tube.
10. Wash the original centrifuge tube with three one ml water washings, each time pouring the wash through the filter funnel and combining with the filtrate from step (9).
11. To the filtrate add 10 ml of concentrated HNO_3 , 3 drops of concentrated HCl and allow to digest in a hot water bath for at least 10 minutes. (Caution: when the mixture is heated a vigorous reaction may occur due to the evolution of oxides of nitrogen from the reaction between the tartaric acid present in solution and the HNO_3 added.)
12. Remove, cool to room temperature, centrifuge the tungstic oxide and discard the supernate.
13. Repeat steps (4) through (12).
14. Dissolve the tungstic oxide precipitate in 6 to 8 drops of concentrated NH_4OH ; transfer the solution to a 60 ml separatory funnel using 10 ml

of water as a transfer agent; add 8 to 10 drops of saturated tartaric acid solution and shake briefly.

15. Add 10 drops of concentrated HCl, 1 ml of niobium carrier and 10 ml of chloroform; shake briefly and add 3 ml of freshly prepared 6% cupferron reagent. (Note 2).
16. Shake again for about 30 seconds and allow to stand for 1 to 2 minutes; drain off the chloroform layer (lower layer) and discard. Extract again with 5 ml of chloroform and again discard the chloroform layer. Drain water layer into a clean 40 ml centrifuge tube; wash the separatory funnel by shaking with two 5 ml portions of water and combine washings with the water layer.
17. Repeat steps (6) through (12) except for the addition of the tartaric acid solution.
18. To the tungstic oxide precipitate obtained in step (17), add 6 drops of concentrated NH_4OH and 15 ml of water.
19. Add 6 drops of glacial acetic acid and 5 to 6 ml of buffer solution (1M HOAc-3.6M NaOAc); heat to boiling and add 1 ml of 5% 8-hydroxyquinoline reagent dropwise and then 1 to 2 drops of Aerosol reagent.
20. Digest for about 30 minutes in a hot water bath; allow to stand for several minutes and then filter the precipitate onto a previously washed and weighed Whatman No. 42 filter disk.
21. Wash the precipitate with water and then finally with anhydrous "anhydrol". Dry in an oven at 100°C for 10 minutes and then cool to room temperature in a desiccator; weigh, record chemical yield of the 8-hydroxyquinoline derivative and mount on a brass planchet for beta counting.

The tungsten quinolate mount is beta counted at approximately 10 day intervals until a representative straight line can be drawn through a semi-logarithmic plot of the data. If the empirically determined half-life is 74 ± 5 days, the sample is accepted as radiochemically pure. Self-absorption self-scattering, chemical yield, and counting efficiency corrections are applied in converting the counting rate to disintegration rate of tungsten-185 in the sample.

The radiometric assay of tungsten-181 was performed by folding the filter paper containing the tungsten quinolate precipitate into a small packet and inserting it into the NaI(Tl) well crystal of the gamma ray spectrometer. The area beneath the 67 Kev x-ray photopeak was measured and converted to disintegrations per minute. The analysis of tungsten-181 was also performed by a gamma spectrum analysis of the three disks which were removed from the untreated filter paper prior to ashing. The background was subtracted from the 67 Kev photopeak and a standard tungsten-181 spectrum was used to correct for contributions to the photopeak by Compton scattering and back scattering from higher energy gamma rays. Ten samples were analyzed for tungsten-181 by a gamma spectrum

analysis of both the three untreated disks and the radiochemically separated tungsten quinolate mount. The results of these analyses indicated agreement between the methods to within ± 10 percent.

Notes:

1. Add the NH_4OH dropwise by allowing it to run down a stirring rod into the solution. This precaution is necessary for there is an initial vigorous reaction.
2. The cupferron reagent should be kept in a cool place at all times; when needed, remove only the amount intended to be used. Under refrigeration, the reagent can be kept for about 1 week without serious decomposition.

Plutonium-239 Purification Procedure ³²

1. To an appropriate aliquot of the filter paper solution, contained in a 40 ml centrifuge tube, add 10 mg of iron (ferric) carrier and neutralize the solution with concentrated NH_4OH .
2. Centrifuge, and discard the supernate; dissolve the $\text{Fe}(\text{OH})_3$ precipitate by the dropwise addition of concentrated HNO_3 and add 1 ml of 5% $\text{NH}_2\text{OH}\cdot\text{HCl}$; allow to stand for 1 hour.
3. To the solution add 2 to 3 ml of concentrated HNO_3 and transfer to a 30 ml beaker using 7M HNO_3 as the transfer agent.
4. Evaporate the solution on a hot plate to approximately two-thirds of its original volume; cool to room temperature and transfer the solution to an anion exchange column (Note 1); wash the beaker twice with 2 ml portions of 7M HNO_3 and add washings to the column.
5. After the feed solution has been added, the column is washed with 200 ml of 7M HNO_3 at a flow rate of 2 ml/minute; the plutonium is then stripped from the resin by the addition of 20 ml of 1M HNO_3 followed by 45 ml of 5% $\text{NH}_2\text{OH}\cdot\text{HCl}$, both at a flow rate of 2 ml/minute.
6. The effluent, which is collected in a 100 ml beaker, is evaporated carefully until a rapid exothermic reaction destroys the $\text{NH}_2\text{OH}\cdot\text{HCl}$.
7. Transfer the solution to a 30 ml beaker washing three times with 2 ml portions of 1M HNO_3 ; evaporate the solution to near dryness, pick up with 1M HNO_3 , and evaporate to several drops.
8. Add 1 ml of 1M HNO_3 and 1 ml of 2% $\text{NH}_2\text{OH}\cdot\text{HCl}$ and allow to stand for 1 hour.
9. To the solution add 8 ml of H_2O and transfer to the electroplating cell (Note 2) using 2 ml of 0.1M HNO_3 as transfer agent.
10. The solution is electroplated for 1 hour at a current of 0.5 amp; the plutonium is deposited on a one inch diameter stainless steel disc which serves as the cathode.
11. Immediately prior to shutting off the current, 1 ml of concentrated NH_4OH is added to the electroplating solution to prevent any dissolution of the plutonium from the disk.
12. The disk is removed from the electroplating cell with forceps, flamed to red heat for a few seconds, cooled to room temperature and then alpha counted.

The plutonium-239 activity of the sample is obtained by applying chemical yield and counting efficiency corrections. Because the plutonium analysis is a carrier-free procedure, the chemical yield is not determined for each

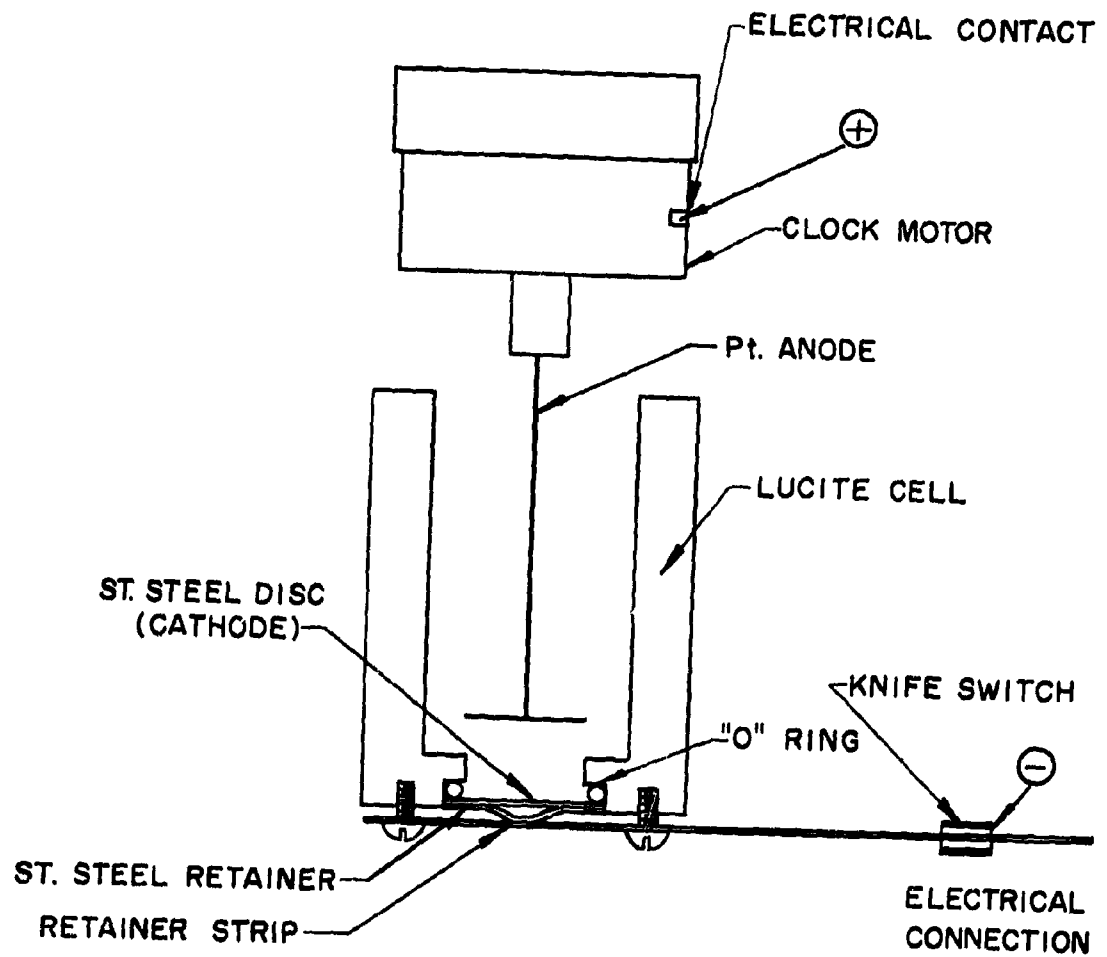
sample. However, by running blank samples spiked with plutonium-239 an average chemical yield can be obtained. This correction factor is applied to all samples run through the same procedure.

Notes:

1. The 100-200 mesh Dowex 1-X2 resin is washed with 4 portions water and 3 portions of concentrated HCl alternating each. After each wash, the resin is allowed to settle for 2-3 minutes and the fine particles in suspension are decanted. The resin is added into a 1-centimeter diameter column to a height of 6-7 centimeters and the resin is cycled with the following solutions allowing the resin to run dry before the addition of each solution:
 - (a) 100 ml of 7N HNO₃
 - (b) 20 ml of 1N HNO₃
 - (c) 30 ml of NH₂OH·HCl
 - (d) 20 ml of 1N HNO₃
 - (e) 100 ml of 7N HNO₃
 - (f) Repeat the cycle.

2. The electrodeposition equipment is shown in Figures 3.29 and 3.30. The anode is a platinum wire with its upper end attached to the shaft of a 1 r. p. s. clock motor and its lower end wound in a horizontal spiral. During the deposition, the anode also serves as a stirrer for the solution. The cathode onto which the plutonium is deposited is a 1 inch diameter stainless steel disk made from 26 gage (0.0185 inch) sheet stock with a number 4 finish. The cathode disk is held against an o-ring which forms a seal between the plastic plating cell and the cathode. During deposition, the plutonium is evenly deposited on the cathode in a circle with a diameter of 13/16 inches.

Isotopes, Inc.



ELECTRODEPOSITION CELL
FIGURE 3.29

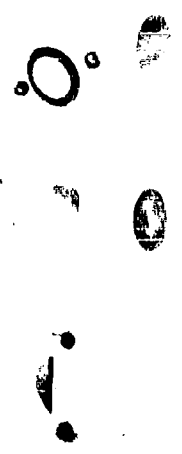
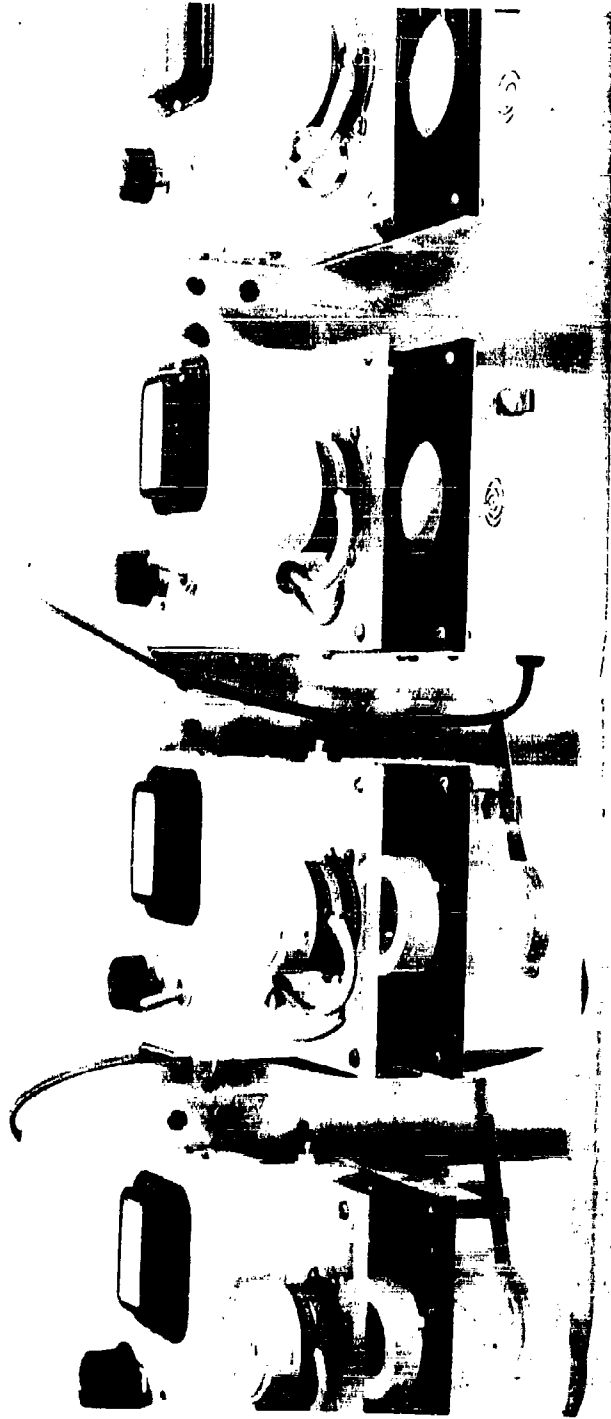


Figure 3.30
Electroplating Cells and Apparatus

REAGENTS

(1) Carriers

- (a) Cesium (CsCl), 20 mg Cs/ml
- (b) Cerium (CeCl_3), 20 mg Ce/ml
- (c) Barium ($\text{BaCl}_2 \cdot 2\text{H}_2\text{O}$), 20 mg Ba/ml
- (d) Strontium ($\text{SrCl}_2 \cdot 6\text{H}_2\text{O}$), 20 mg Sr/ml
- (e) Zirconium ($\text{ZrOCl}_2 \cdot 8\text{H}_2\text{O}$), 10 mg Zr/ml
- (f) Yttrium (Y_2O_3), 10 mg Y/ml
- (g) Lanthanum ($\text{La}(\text{NO}_3)_3 \cdot 6\text{H}_2\text{O}$), 5 mg La/ml
- (h) Tungsten (H_2WO_4), 20 mg W/ml
- (i) Bismuth ($\text{Bi}(\text{NO}_3)_3 \cdot 5\text{H}_2\text{O}$), 10 mg Bi/ml
- (j) Molybdenum [$(\text{NH}_4)_6\text{Mo}_7\text{O}_{24} \cdot 4\text{H}_2\text{O}$], 10 mg Mo/ml
- (k) Niobium (NbCl_5 in 1M oxalic acid), 10 mg Nb/ml
- (l) Rhodium (RhCl_3), 10 mg Rh/ml
- (m) Ruthenium (RuCl_3), 20 mg Ru/ml
- (n) Beryllium ($\text{BeSO}_4 \cdot 4\text{H}_2\text{O}$), 1 mg Be/ml
- (o) Tellurium (TeO_2), 10 mg Te/ml
- (p) Iodate (NaIO_3), 20 mg IO_3 /ml
- (q) Iodide (NaI), 10 mg I/ml
- (r) Palladium ($\text{PdCl}_2 \cdot 2\text{H}_2\text{O}$), 20 mg Pd/ml
- (s) Iron ($\text{FeCl}_3 \cdot 6\text{H}_2\text{O}$), 5 mg Fe/ml
- (t) Phosphorus [$(\text{NH}_4)_2\text{HPO}_4$] 5 mg P/ml
- (u) Cadmium ($\text{Cd}(\text{NO}_3)_2 \cdot 4\text{H}_2\text{O}$) 10 mg Cd/ml
- (v) Sodium (NaCl) 10 mg Na/ml
- (w) Copper ($\text{Cu}(\text{NO}_3)_2 \cdot 6\text{H}_2\text{O}$) 10 mg Cu/ml
- (x) Calcium ($\text{Ca}(\text{NO}_3)_2 \cdot 4\text{H}_2\text{O}$) 20 mg Ca/ml

- (2) HNO_3 (concentrated, fuming, 9M, 7M, 6M, 1M, 0.1M)
- (3) HCl (concentrated, 6M, 3M, 1M)
- (4) H_2SO_4 (concentrated, 9M)
- (5) HF (concentrated)
- (6) NH_4OH (concentrated, 6M)
- (7) NaOH (12M, 6M, 3M, 50%)
- (8) Perchloric acid (70-72%)
- (9) Mandelic acid (16%)
- (10) Chloroplatinic acid (10%)
- (11) Silicotungstic acid (0.13M)
- (12) Glacial Acetic acid
- (13) Phenylarsonic acid (saturated)
- (14) Tartaric acid (saturated)
- (15) Boric acid (saturated)
- (16) Hydroxylamine hydrochloride (5M, 5%, 2%)
- (17) Sodium tetraphenyl boron (0.05M) in amyl acetate
- (18) Methyl isobutyl ketone
- (19) Acetone
- (20) Chloroform
- (21) Carbon tetrachloride
- (22) Pyridine
- (23) EDTA solution (10%)
- (24) Acetylacetone
- (25) Benzene
- (26) Cupferron (6%)
- (27) 8-hydroxyquinoline (5%)
- (28) TBP reagent (tributyl phosphate, petrolcum ether, concentrated HNO_3)

- (29) "Citrate buffer solution" (1M $\text{Na}_3\text{C}_6\text{H}_5\text{O}_7$ - 0.5M HNO_3)
- (30) "Barium buffer solution" (6M HOAc - 3M NH_4OAc)
- (31) "Acetate buffer solution" (2M HOAc - 4M NH_4OAc); (1M HOAc -3.6M NaOAc)
- (32) "Acetate wash solution" (0.25M HOAc , 0.5M NH_4OAc , 1% EDTA)
- (33) "Mandelic acid wash solution" (2% HCl - 5% Mandelic acid)
- (34) Meta cresol purple indicator
- (35) Phenolphthalein indicator
- (36) Alizarin indicator
- (37) $(\text{NH}_4)_2\text{C}_2\text{O}_4 \cdot \text{H}_2\text{O}$ (saturated)
- (38) Na_2CO_3 (saturated)
- (39) NaBrO_3 (1.5M), 1M)
- (40) Na_2CrO_4 (1.5M)
- (41) NaHSO_3 (1M)
- (42) NaNO_2 (2M)
- (43) H_2O_2 (30%)
- (44) NH_4NO_3
- (45) Magnesium metal (powered)
- (46) H_2S gas
- (47) "Aerosol" solution (1%; a wetting agent)
- (48) Anhydrous "anhydrol" (commercial product of denatured 95% ethyl alcohol available from C. P. Chemical Solvents, Inc., Newark, N. J.)
- (49) Anion exchange resin (Dowex-1, 100 - 200 mesh)
- (50) "Ammonium Molybdate Reagent": 200 g $(\text{NH}_4)_6\text{Mo}_7\text{O}_{24} \cdot 4\text{H}_2\text{O}$, 800 ml H_2O and 160 ml of concentrated NH_4OH
- (51) "Magnesia Mixture": 50 gm $\text{MgCl}_2 \cdot \text{H}_2\text{O}$, 100 gm NH_4Cl , 3-5 drops concentrated HCl and 500 ml of H_2O

- (52) "Sodium Precipitating Reagent": 45 gm of $\text{UO}_2 (\text{C}_2\text{H}_3\text{O}_2)_2 \cdot 2\text{H}_2\text{O}$, 300 gm $\text{Mg}(\text{C}_2\text{H}_3\text{O}_2)_2 \cdot 4\text{H}_2\text{O}$, 60 ml glacial acetic acid in 800 ml H_2O , diluted to 1 liter. Stir the mixture mechanically for two hours, let it stand for 2 hours and filter.
- (53) "Sodium Wash Solution" 35 ml of glacial acetic acid, 405 ml of anhydrous ethyl acetate and 460 ml of anhydrol
- (54) Concentrated HCl - ethyl ether reagent (1:1)
- (55) "Calcium Wash Solution" (1% citric acid - 0.75% EDTA)
- (56) Ammonium carbonate (saturated solution)
- (57) "Murexide tablet" (Ammonium Purpurate)
- (58) Ammonium oxalate (4% solution)
- (59) Cation Exchange Resin (Dowex 50, 100-200 mesh)
- (60) Ethanol (absolute)
- (61) Ammonium Acetate (6M)
- (62) Citric Acid Solution (500 gm/liter)

RADIOMETRIC ASSAY TECHNIQUES

The final phase of a radiochemical analysis is the assay of the purified element and the verification of its radiochemical purity. The absence of radioactive contamination in each purified sample was established by following the radioactive decay rate of the sample, by aluminum absorption counting to define the energy of the beta emission, or by a spectral analysis of the nuclear emissions. The assay of each sample was corrected for chemical recovery, counting efficiency under the conditions of the assay including self-absorption self scattering effects when necessary, radioactive decay to a fixed point in time, and the aliquot of the entire sample which was removed for analysis. The extensive scope of HASP necessitated the use of several types of alpha, beta and gamma detecting instrumentation each of which is described in the following sections.

Beta Counters

For routine beta measurements, the activity of the sample determined the equipment to be used. Samples with activities greater than 10 counts per minute were assayed by Anton 1007T Geiger "pancake" counters with a 1 1/8 inch window diameter and mica window thicknesses between 1.4 and 2 mg/cm². These counters were used with conventional electronic equipment such as an Atomic Regulated High Voltage Power Supply and Glow Tube Scaler. The Anton counter is a halogen quenched, infinite-life tube with a 20 microsecond dead time which permits counting at rates of 60,000 counts per minute with coincidence losses as little as 2 percent. The background with 2 inches of lead shielding was 7 counts per minute

The Anton counter was mounted in a polystyrene stage as illustrated in Figure 3.31. Samples were inserted in a recess in the plastic slide which was then positioned 0.064 inches below the counter window. This close proximity of the counter and sample plus the brass planchet sample mount provided maximum physical geometry and backscattering for maximum counting efficiency. As a point of reference, the counting efficiency for the 2.2 Mev beta of Y^{90} was about 25 percent. In general, samples were counted for a total of 1000 counts or for a period of 1/2 hour if less than 1000 counts had accumulated during that time.

Samples with activities less than 10 counts per minute were assayed in multiple low-level beta counters, Model numbers CLL-4 and CLL-4C, which were designed and constructed at Isotopes, Inc. The counting periods for these samples were usually 8 hours. Model number CLL-4 consists of 4 central Anton 1007T "pancake" counters surrounded by, and in anticoincidence with, a ring of cosmic ray counting tubes*. (See Figure 3.32). The overall length of the cosmic ray counting tube is 15 1/8 inches; the active anode length is 12 inches. The samples were placed in receptacles in lucite slides which positioned the samples 0.08 inches from the mica windows of the central Anton counters. With a 2 inch lead shield and the anticoincidence ring in operation, the background of these counters was 2 to 3 counts per minute. Since the sample detecting unit was the central Anton counter its efficiency for counting Y^{90} was the same as reported above, i. e. about 30 percent. A bank of 4 multiple units with associated electronics is shown in Figure 3.32.

* Obtained from H. W. Leighton Laboratories, Glen Ridge, New Jersey.



Figure 3.31: High Level Beta Counter

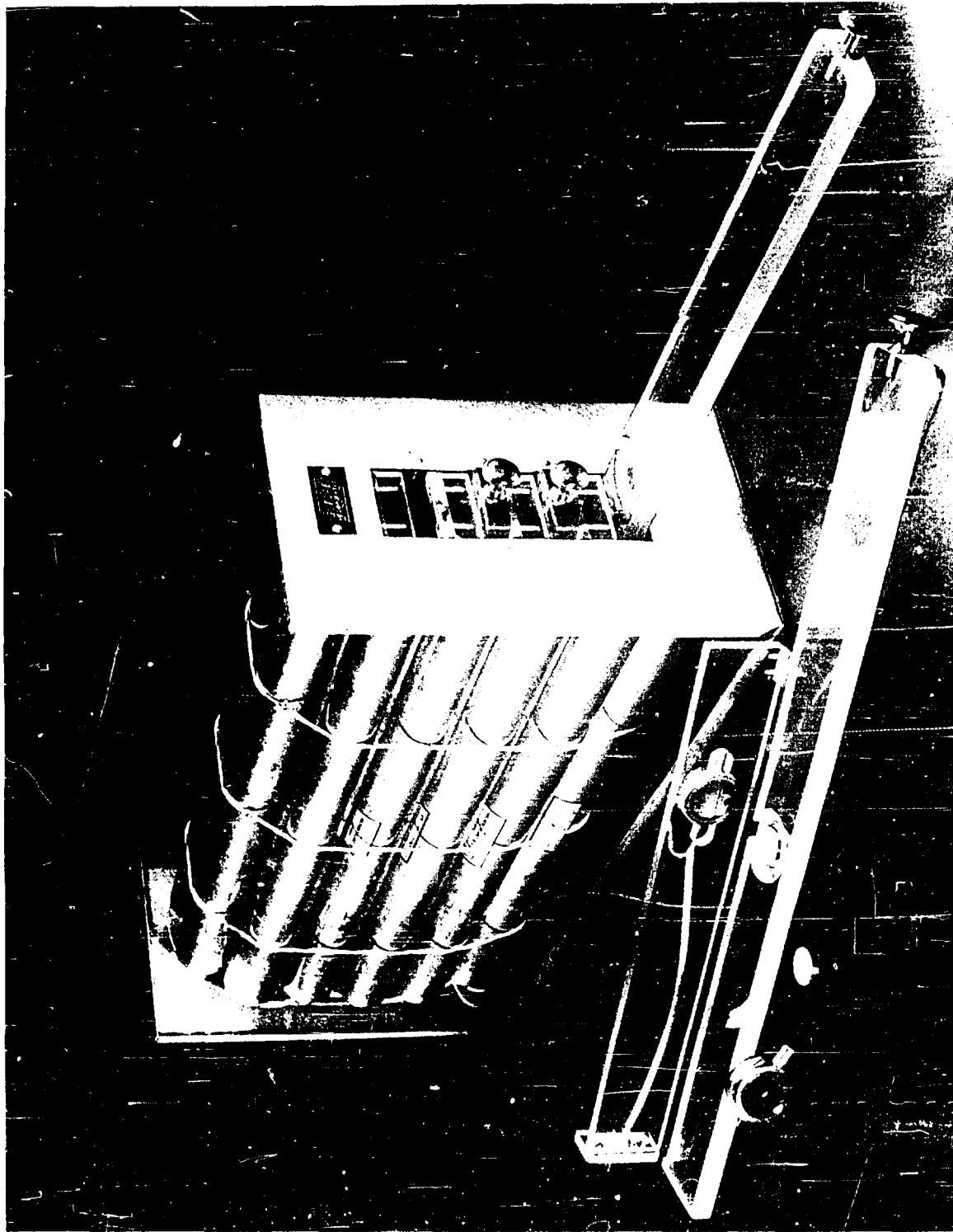


Figure 3. 32
Low Level Beta Counter, Model CCL-4

The Low-Level Beta Counter, Model CLL-4C, is a more recent and improved design for the assay of minute quantities of activity. It is a unit of 4 counters each with an anticoincidence gas flow guard detector (See Figure 3.33). Each counter is a 1 1/4 inch diameter gas flow Geiger tube with a 1 mg/cm² aluminized mylar window. The counting gas is a mixture of 99.5 percent helium and 0.5 percent isobutane. Each anticoincidence guard detector is a 6 inch x 6 inch x 3/4 inch multi-anode counter positioned directly above its respective Geiger counter. With 4 inches of lead shielding, the background was about 0.3 counts per minute and the efficiency for yttrium-90 was about 45 percent. The sample positioning in these counters is the same as for model CLL-4. For all low level beta counting employing either model, two plastic inserts are provided for each lucite slide. The larger insert or plug permits normal radioassay with the sample 2mm from the counter window. The second smaller insert drops the sample 0.15 inches to permit counting through an aluminum absorber. These plastic inserts are also shown in Figure 3.33.

Two other types of beta counters were employed in HASP not for routine sample measurement, but for calibration of standard radionuclide solutions. The first of these was an end-window (2 mg/cm²) Tracerlab TGC-2 Geiger counter mounted in a defined geometry system shown diagrammatically in Figure 3.34. This system employed a heavy brass plate with a machined hole coaxial with the anode wire of the counter to define accurately the physical geometry, or "view," of the counter. To reduce scattering, the edge of the hole was bevelled at an angle which made it parallel to the paths of the beta

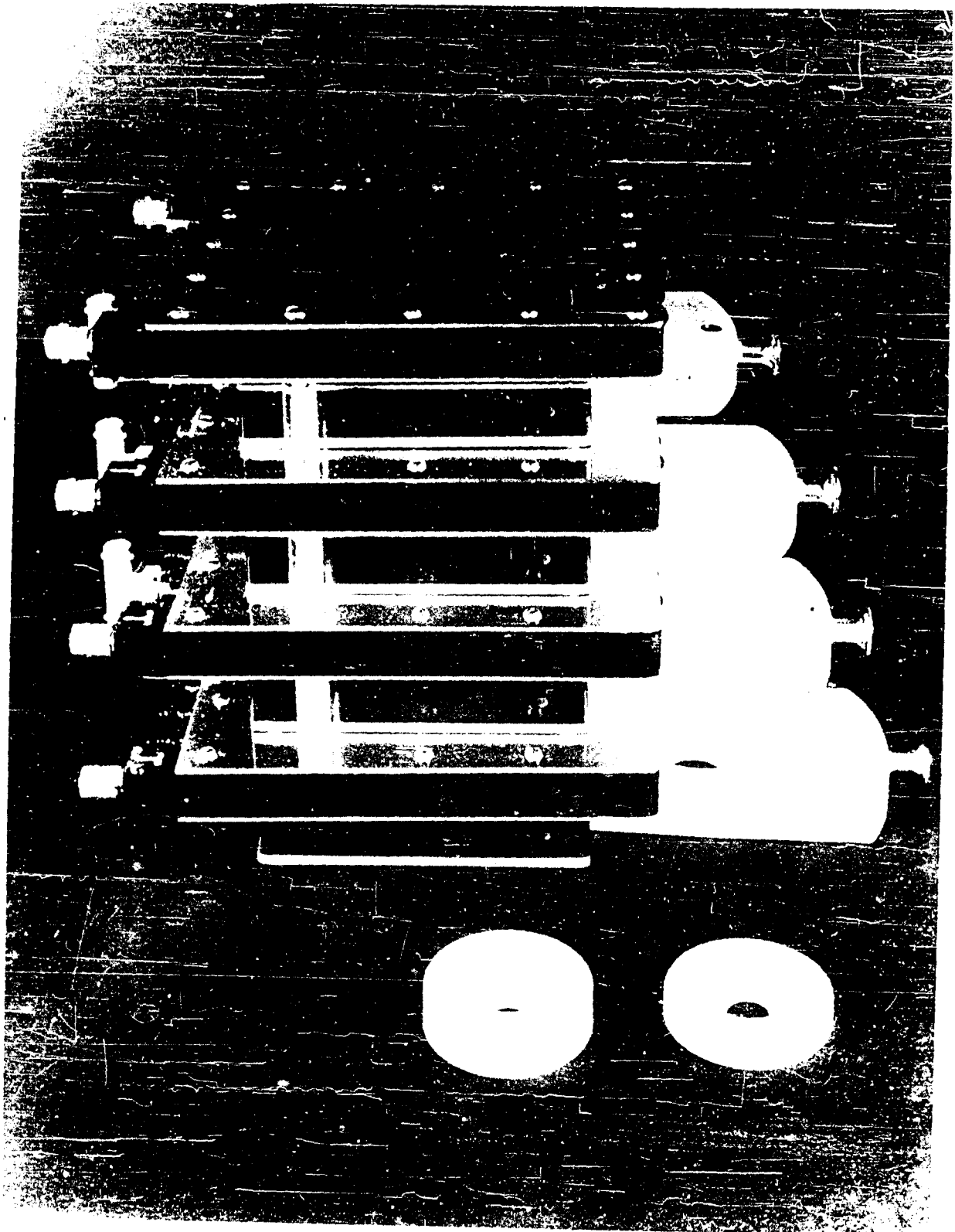


Figure 3.33
Low Level Beta Counter, Model CCL-4C

ISOTOPES, INC.

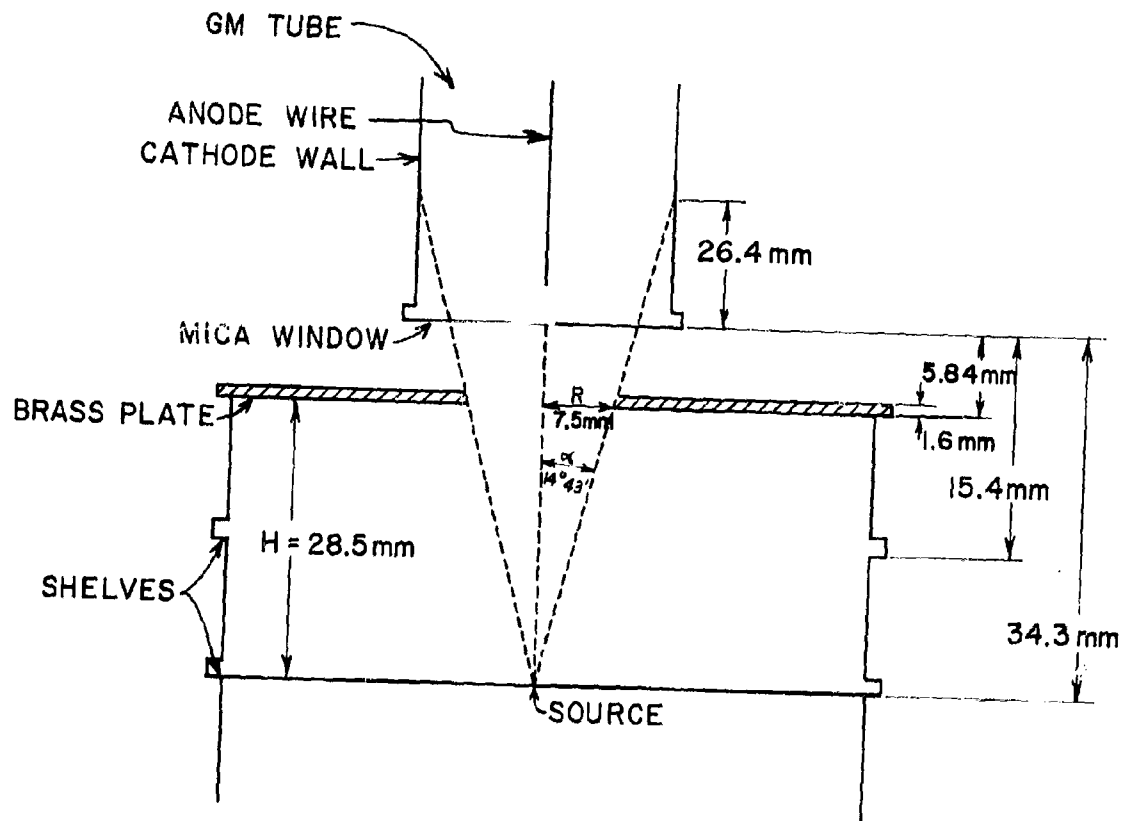


FIGURE 3.34 DIAGRAM OF THE DEFINED GEOMETRY SYSTEM OF THE TRACERLAB T6C-2 GEIGER-MULLER TUBE

particles originating from the point source. The hole was smaller than the tube window so that beta particles from the point source could penetrate the counter only at the core of the sensitive volume and not in the relatively insensitive regions near the cathode wall. The physical geometry, G , of this system is expressed by the equation:

$$G = 0.5 \left[1 - \frac{H}{\sqrt{H^2 - R^2}} \right] \quad 3.30$$

In the present instance:

$$R = 7.5 \text{ mm}$$

$$H = 28.5 \text{ mm and}$$

$$G = 0.0403$$

When carrier-free point sources with diameters less than 5 mm were prepared on thin Mylar sheets and assayed by this system, the absolute beta activity of the source was determined by the equation:

$$D = \frac{n}{G F_w} \quad 3.31$$

where:

D = Disintegrations per minute

n = Observed counts per minute corrected for coincidence losses, gamma contribution, and normal background.

F_w = Mass absorption correction factor for air and mica window.

When the source diameter was greater than 5mm, the physical geometry could be calculated from the Blackman equation³⁴. The mass absorption correction factor was calculated by:

$$F_w = e^{-\mu_0 t} \quad 3.32$$

where:

μ_0 = Mass absorption coefficient near zero absorber thickness in cm^2/mg , and

t = absorber including air and mica window between sample and sensitive volume of counter in mg/cm^2 .

Gleason³³ reported an expression which relates the mass absorption coefficient (μ_0) near zero absorber thickness to the maximum beta energy (E_{max} in Mev) through the range 0.15 to 3.5 Mev:

$$\mu_0 = 0.017 E_{\text{max}}^{-1.43} \quad 3.33$$

The second beta counting system employed for the calibration of standard radionuclide solutions was a 4π counter designed and constructed at Isotopes, Inc. (See Figure 3.35). This gas flow Geiger counter (99.5 percent helium, 0.5 percent isobutane mixture) consisted of a pre-flush chamber and a detection volume with upper and lower compartments. A carrier free source was evaporated to dryness on 0.5 mil aluminized Mylar film which was then positioned between the upper and lower counting compartments after a 5 minute preflush. The effective cathode dimension of each counting compartment was 1 1/8 inch diameter by 0.550 inch depth. With a 2 inch lead shield, the background was about 20 counts per minute. Radionuclide sources with energies greater than 0.50 Mev carefully prepared and counted in this system were assayed with a 100 ± 3 percent efficiency. Below 0.5 Mev corrections had to be made for attenuation through the aluminized Mylar backing.

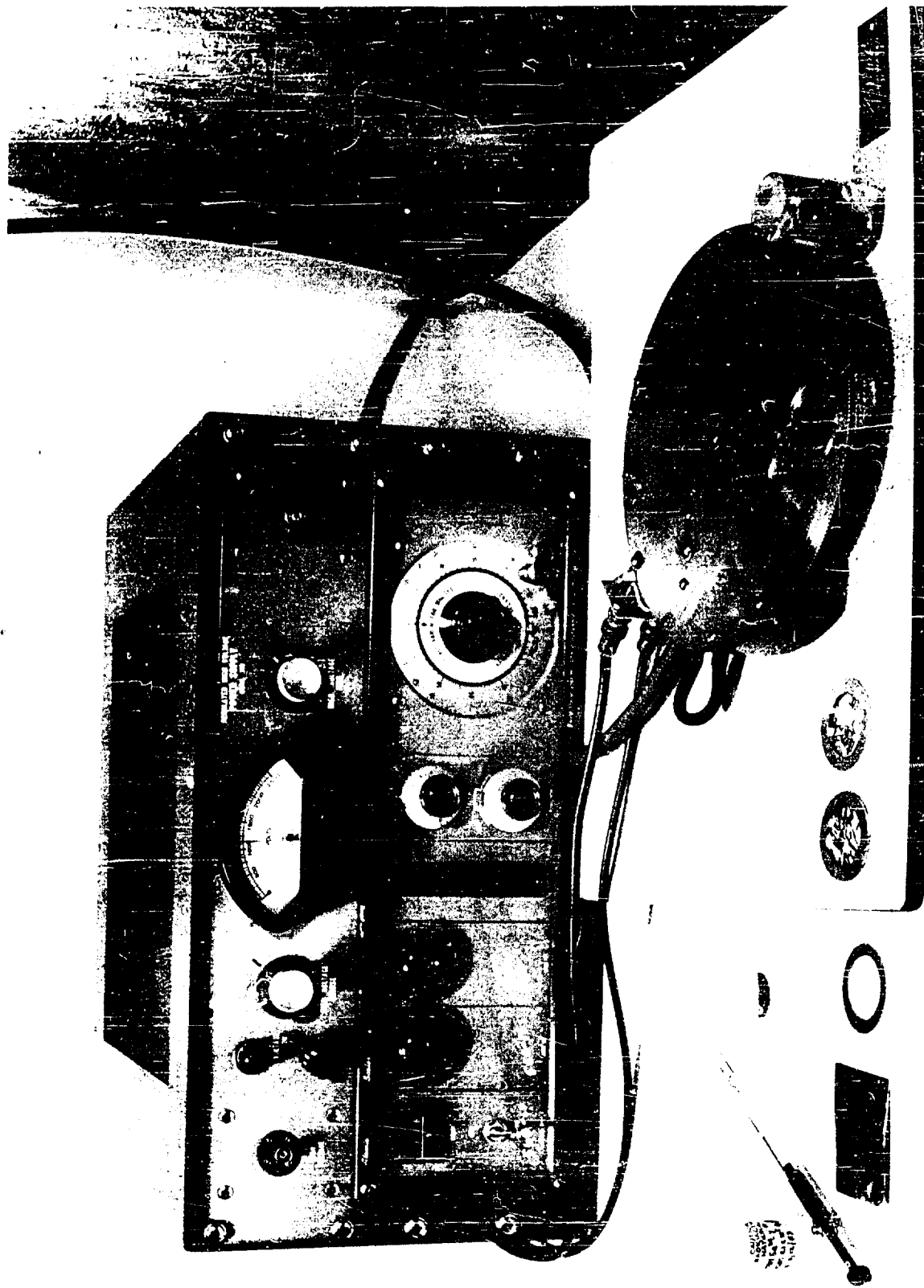


Figure 3.35. 4π Beta Counter

Alpha Counters

The routine radioassay of plutonium samples in HASP was performed by zinc sulfide scintillation counting. The plutonium was electroplated on one inch diameter steel disks which were then placed in the slide of the alpha counter shown diagrammatically in Figure 3.36. With the slide in counting position, the disk was 1/8 inch below the activated zinc sulfide coated surface of an RCA 6199 multiplier phototube. The slide assembly and counter housing was made light tight with a felt flock on the inside surface of the slide holder. The counting efficiency of this system for plutonium-239 was about 40 percent with a background of 6 counts per hour.

Alpha particle scintillation spectroscopy was performed on some samples as a qualitative and quantitative verification of the zinc sulfide counter radioassay. The technique employed was essentially the one described by Martines and Senftle³⁵. The detector was a truncated cone of thallium activated cesium iodide* with a height of 0.560 inches, and with diameters of the upper and lower bases of 0.500 and 1.293 inches, respectively. The crystal was optically coupled to a 2 inch diameter Dumont 6292 multiplier phototube with +0.000 centistoke silicone oil. The sample disks were placed face down on an annular stage which centered the active surface of the disk 0.005 inches from the CsI(Tl) crystal. The entire assembly was contained in a light-tight housing which was evacuated to about 0.1 mm pressure. The vacuum minimized the degradation of the alpha particle energy by collision with air molecules between the source and crystal. This

* The CsI(Tl) crystal was obtained from Crystals Division of Isotopes, Inc.

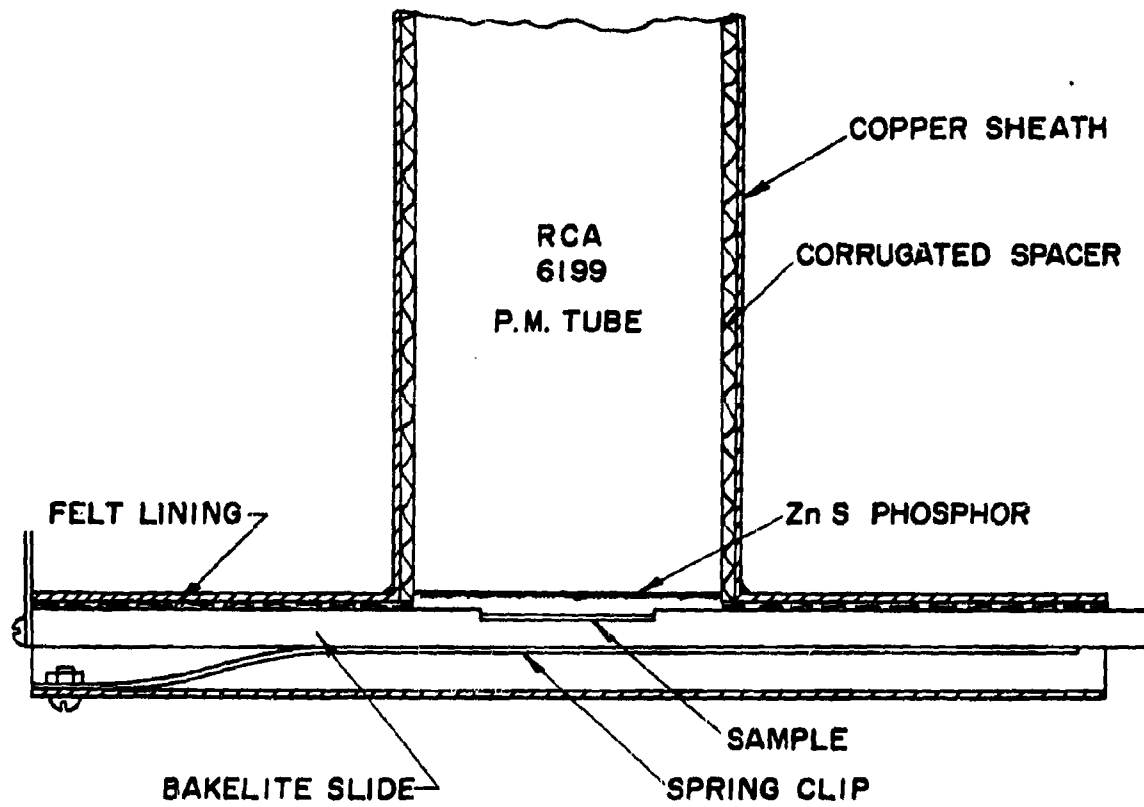


FIGURE 3.36 ALPHA COUNTER HEAD AND SLIDE

assembly is shown in Figure 3.37.

The detection head and pre-amplifier were coupled to a Penco 100 Channel Pulse Height Analyzer, Model PA-4; the high voltage to the multiplier phototube was supplied by a Baird-Atomic Super Stable High Voltage unit, Model 312. The pulses from the multiplier phototube were amplified by a Baird-Atomic Non-Overloading Amplifier, Model 215. The spectrum was recorded in magnetic cores in the analyzer, and then printed out by a Victor Recorder, Model 706054.

The resolution of the plutonium-239 5.15 Mev. alpha photopeak with a one inch diameter electroplated disk was 13.2 percent. However, with a point source of plutonium-239 the resolution reduced to 4.9 percent. The counting efficiency in the plutonium photopeak for the electroplated disk was 28.6 percent with a corresponding background of about 0.1 counts per minute.

Gamma Counters

Integral gamma counting and gamma ray spectroscopy were utilized in the analytical phase of the HASP program. The integral gamma counter was a Harshaw 1 3/4 inch diameter by 2 inch NaI(Tl) well crystal; the well dimensions were 1/2 inch diameter by 2 inches deep. The crystal was optically joined to a 2 inch diameter Dumont 6292 multiplier phototube with Dow Corning silicone grease and taped with black electrical tape to prevent any light leaks. A mu metal magnetic shield surrounded the phototube and the entire unit was shielded with a 2 inches of lead. The background of this system was about 150 counts per minute.

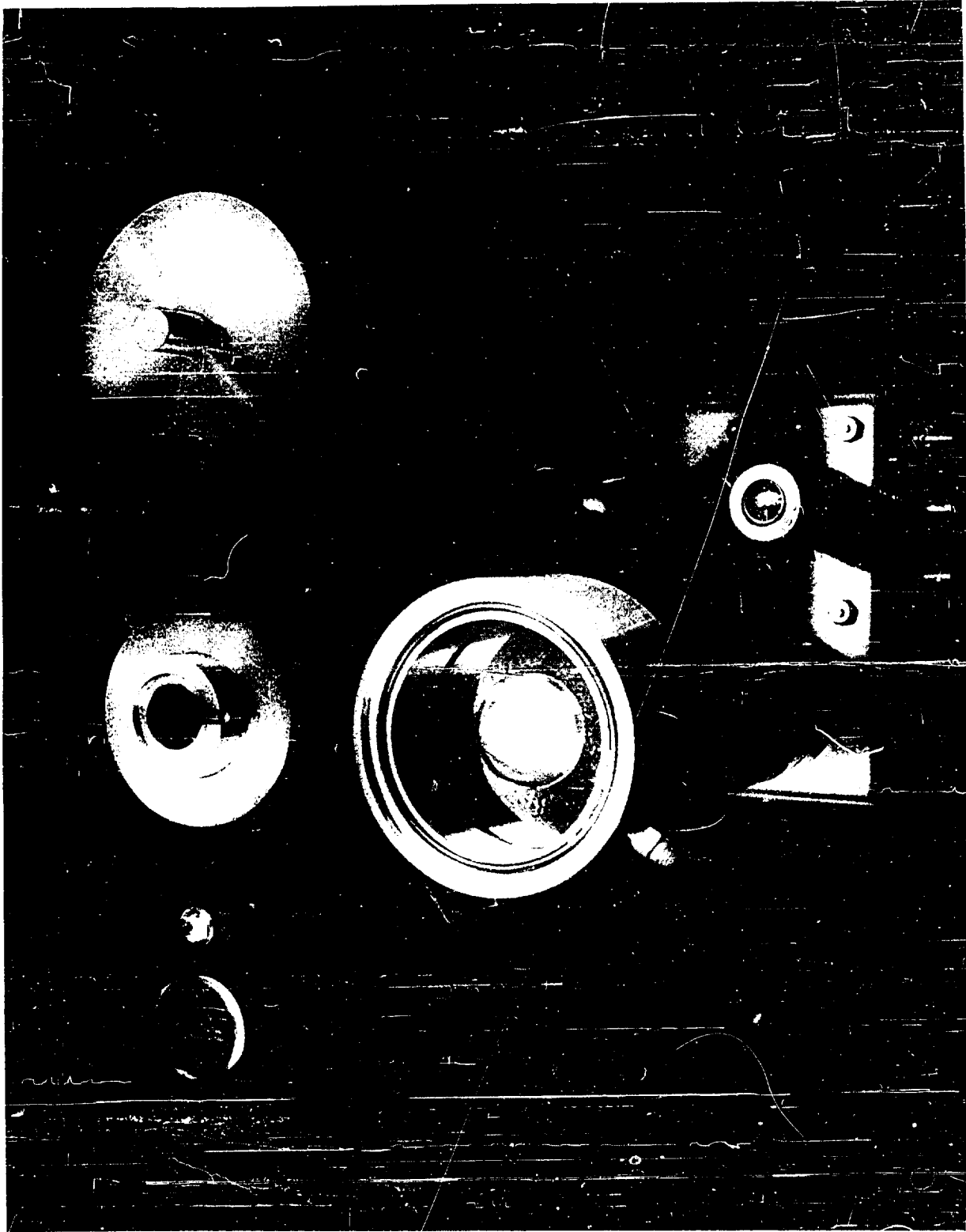


Figure 3. 37. Alpha Particle Spectrometer

Gamma ray and X-ray spectra were obtained using the Penco 100 Channel Pulse Height Analyzer and associated electronic equipment described earlier and three separate detectors. X-ray counting was done with a 1.1/4 inch diameter by 0.020 inch thick NaI(Tl) crystal obtained from the Crystals Division of Isotopes, Inc. coupled to a 2 inch diameter Dumont 6292 multiplier phototube with Dow Corning 10^6 centistoke silicone oil. This system was used to assay the 20 Kev ruthenium X-ray associated with the decay of rhodium-102. With 4 inches of lead shielding and the rhodium-102 source in direct contact with the crystal, the counting efficiency for the 20 Kev X-ray was 42.2 percent and the resolution was 39.3 percent. The photopeak background was about 2 counts per minute.

A second detector was employed for gamma ray spectroscopy of radio-chemically separated samples or unprocessed samples of relatively small mass. This detector consisted of a 1 3/4 inch diameter by 2 inch Harshaw NaI(Tl) well crystal coupled to a 2 inch diameter Dumont 6292 multiplier phototube with Dow Corning silicone grease and shielded by 4 inches of lead. The resolution of this crystal for the 0.661 Mev gamma ray of a cesium-137 source placed inside the well was 11 percent.

Spectroscopy of large soil samples was done with a third detector, an Isotopes, Inc. 3 inch diameter by 3 inch high cylindrical NaI(Tl) crystal mounted on a 3 inch diameter Dumont 6363 multiplier phototube with Dow Corning silicone grease. The crystal, phototube and preamplifier were housed in a 4 inch lead shield whose inside dimensions formed a 3 foot cube. The inside walls of the shield were lined with 0.005 inch of copper and 0.032 inch of cadmium to absorb

the lead X-rays generated in the shielding by the gamma rays from the source. The resolution of this 3" x 3" crystal for a cesium-137 point source mounted on the top face of the crystal was 8.6 percent.

Soil samples with volumes less than 400 cubic centimeters was contained in glass beakers and placed on top of the 3 inch diameter by 3 inch NaI(Tl) crystal for gamma spectrum analyses. For larger soil samples, a special plastic container was made to position the sample around as well as on top of the crystal. This container consisted of a 6 1/2 inch inside diameter by 7 inch cylinder with a 3 inch diameter by 3 inch high compartment protruding up from the bottom of the cylinder. The container was lowered over the NaI(Tl) crystal so that the crystal fit into the central compartment, and the soil was placed in the annular volume around and on top of the crystal. The height of soil above the crystal was adjusted to the width of the annular ring of soil around the crystal. The largest volume which could be accomodated with this arrangement was 2100 cubic centimeters. Two plastic inserts were made to fit inside the container which reduced the width of the annular ring around the central compartment. With the inserts in place, the height of soil above the crystal was always adjusted to the width of the annular ring as in the case of the container alone with no inserts. The sample volumes permitted, with the two inserts, were 920 and 400 cubic centimeters. The 3 inch diameter by 3 inch NaI(Tl) crystal, phototube, preamplifier and the plastic container along with its inserts are shown on top of the large lead cave in Figure 3.38.

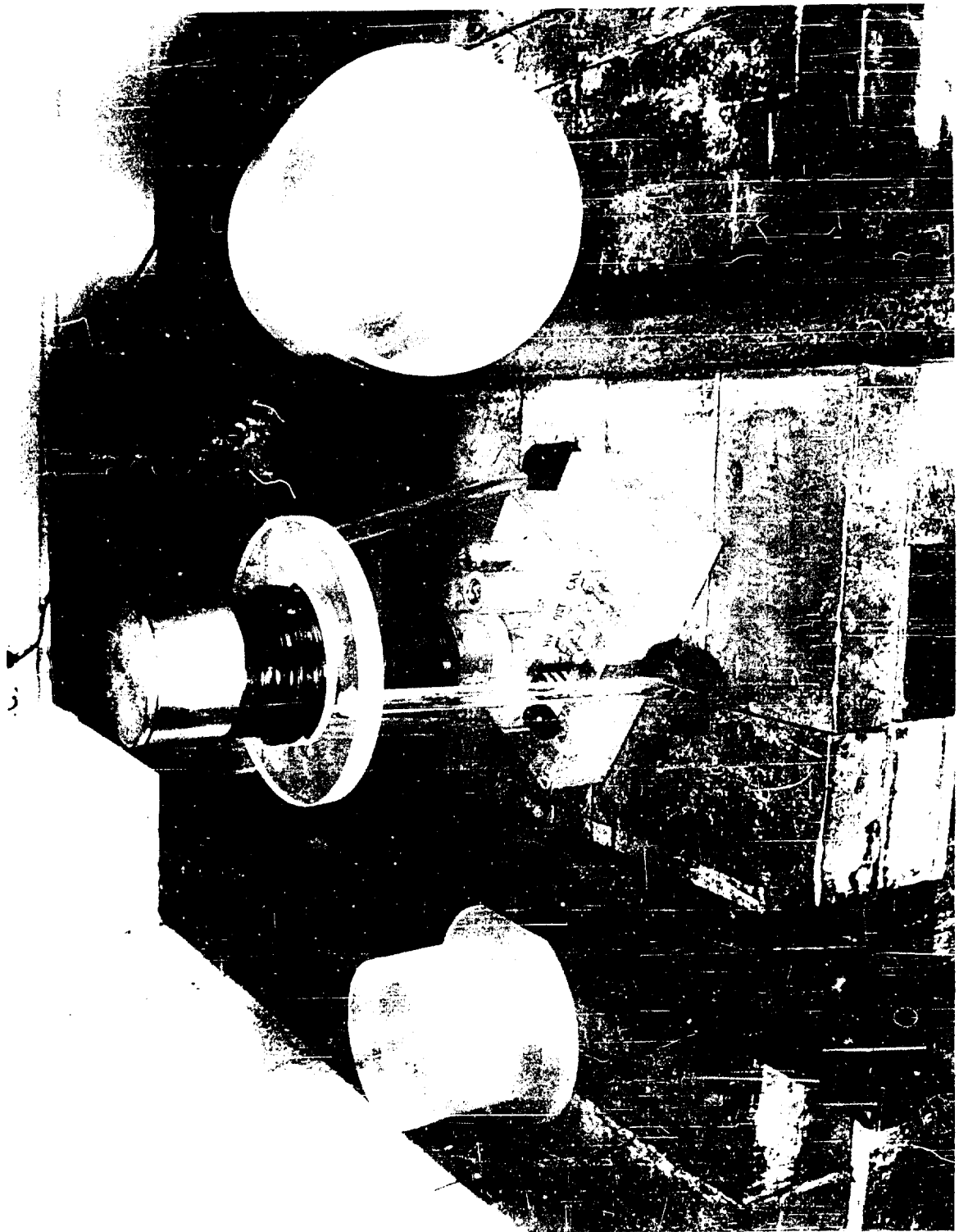
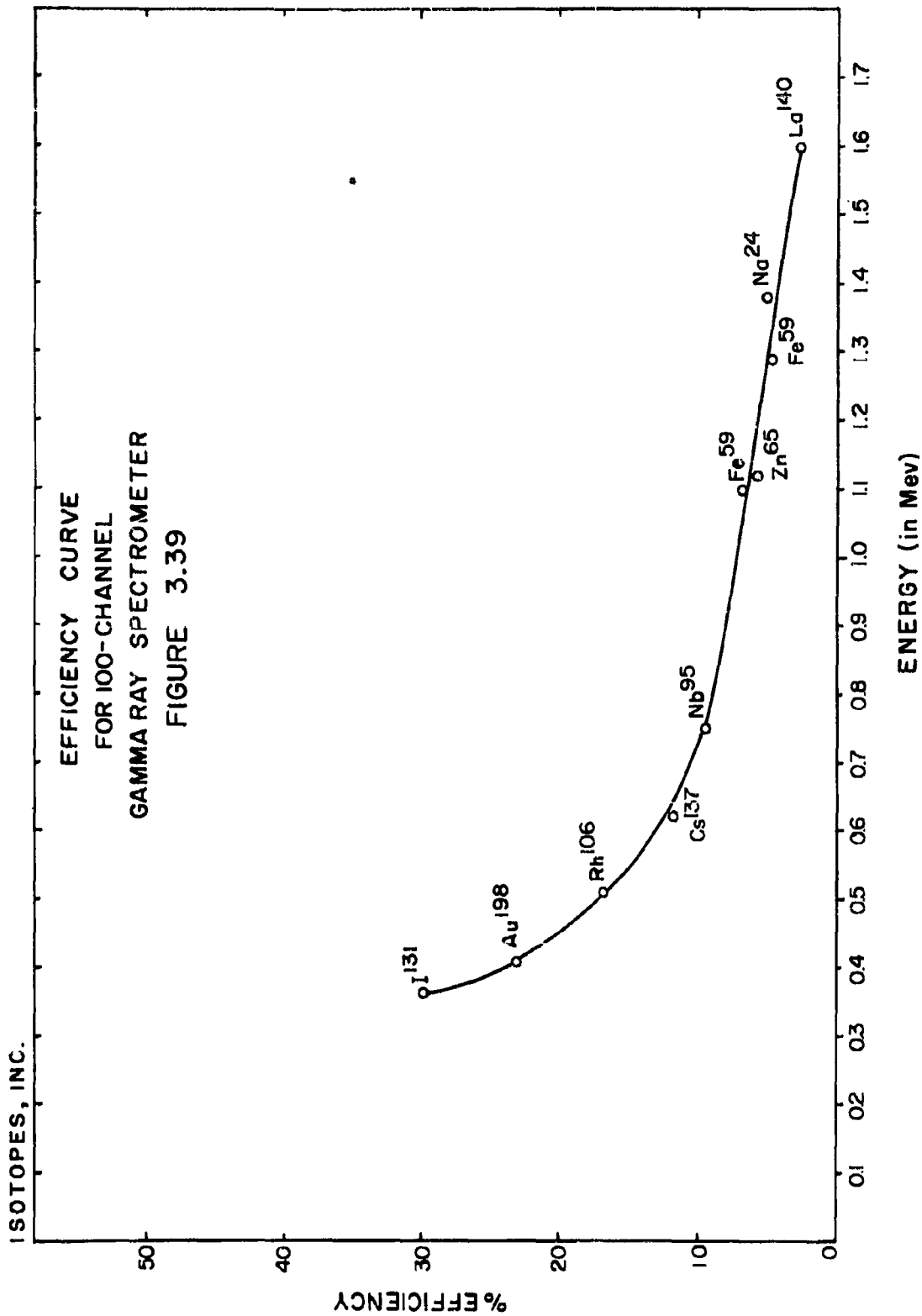


Figure 3.38. Bulk Spectrometry Facility

Counter Calibration and Accuracy

Each counting system employed in HASP was calibrated against standard solutions of the various radionuclides obtained from the National Bureau of Standards, Nuclear-Chicago Corp., Los Alamos Scientific Laboratory, Health and Safety Laboratory of the AEC, Westinghouse Electric Corp. and the Radiochemical Centre, United Kingdom Atomic Energy Authority. Self-absorption curves were prepared for each beta emitter when necessary. The standards were cross checked at Isotopes, Inc. by both 4π counting and point source defined geometry assay before being accepted. Recalibration of the radioassay equipment was conducted with these primary standards every 3 to 6 months; secondary standards were counted daily or before each use of the equipment to pinpoint any deviation from normal operation. A curve of the counting efficiency in the photopeak versus gamma ray energy for the 1 3/4 inch diameter by 2 inch NaI(Tl) well crystal was developed from the standard solutions and is presented in Figure 3.39. When standards of gamma emitting nuclides were not available, as in the case of beryllium-7, recourse was made to this calibration curve and the nuclear decay scheme of the particular radionuclide in question. Similarly when standards of beta emitting nuclides were not available, such standards were prepared at Isotopes, Inc. from spike solutions via 4π counting and point source defined geometry assay.

Rhodium-102 and tungsten-181 were two exceptions to this general policy of calibration. Both nuclides decay by electron capture, and the predominant emissions are the 22 and 67 Kev X-rays of ruthenium and tantalum, respectively.



These energies are far below the range of the spectrometer calibration curve shown in Figure 3.39. A theoretical counting efficiency for rhodium-102 on the thin X-ray crystal was calculated to be 28 percent employing modifications of the method described by Lazar³⁶. In these calculations, corrections were made for the decay scheme of rhodium-102 and the attenuation of the X-rays through the aluminum housing of the crystal. The well crystal of the gamma ray spectrometer was calibrated for tungsten-181 by reference to the DPM W¹⁸⁵/DPM¹⁸¹ ratio produced by the first shot at Operation Hardtack that generated tungsten radioisotopes. The ratios of the tungsten-185 disintegration rates to the counting rates in the tungsten-181 photopeak for seven HASP filter samples containing debris from this shot and no other radioactive-tungsten generating shots were corrected to shot date, and an average value of $\frac{\text{CPM W}^{181}}{\text{DPM W}^{185}}$ was obtained. The counting efficiency of the photopeak was calculated as follows:

$$\text{Counting Efficiency} = \frac{\text{CPM W}^{181}}{\text{DPM W}^{181}} \times 100 = \frac{\text{CPM W}^{181}}{\text{DPM W}^{185}} \times \frac{\text{DPM W}^{185}}{\text{DPM W}^{181}} \times 100 = 24.2\%$$

Most of the standard solutions received from external sources were certified to within ± 3 percent. The tungsten-185 standard from Los Alamos Scientific Laboratory was probably accurate to within ± 10 percent based upon an assay by four independent laboratories. Standards prepared at Isotopes, Inc. by 4π counting and gamma ray spectroscopy were accurate to within about ± 4 percent. A summary of all the radioassay techniques including the method and

Table 3. 17. Summary of Radioassay Techniques

Nuclide	Method of Calibration	% Error of Calibration	Counting Method	Counting Efficiency
Be ⁷	Gamma ray spectroscopy	4	Gamma ray spectroscopy	2%
Na ²²	NBS standard	3	End-window GM tube	20%
P ³²	Nuclear-Chicago standard	3	End-window GM tube	25%
Ca ⁴⁵	Defined geometry assay	5	End-window GM tube	7%
Sr ⁸⁹	4 γ and defined geometry assay	4	End-window GM tube	30%
Sr ⁹⁰	NBS and Nuclear-Chicago standard	3	End-window GM tube	20%
Y ⁹⁰	NBS and Nuclear-Chicago standard	3	End-window GM tube	25%
Y ⁹¹	4 γ and defined geometry assay	4	End-window GM tube	20%
Zr ⁹⁵	NBS standard (Nb ⁹⁵)	3	Gamma ray spectroscopy	10%
Rh ¹⁰²	Theoretical calculation	10	X-ray spectroscopy	28%
Cs ¹³⁷	Nuclear-Chicago standard	3	End-window GM tube	25%
Ba ¹⁴⁰	Defined geometry assay	5	Gamma ray spectroscopy End-window GM tube	5% 25%
Ce ¹⁴⁴	Radiochemical Centre standard	3	End-window GM tube with aluminum absorber	10%
W ¹⁸¹	Theoretical calculation	10	Gamma ray spectroscopy	15%
W ¹⁸⁵	Los Alamos standard	10	End-window GM tube	40%
Pu	Brookhaven National Laboratory standard	--	ZnS and CsI scintillation counting	

the estimated error of calibration, the counting method and counting efficiency for each nuclide is presented in Table 3.17. Although there were many beta counters employed in this program the relative counting efficiencies of the various counters were not widely different for each nuclide except for model CLL-4C which was a factor of about 1 1/2 more sensitive than the others. Consequently, the approximate counting efficiency for all counters with the exception of model CLL-4C for each nuclide is reported in Table 3.17.

QUALITY CONTROL

The quality control of the radiochemical analyses in HASP was based upon the monitoring of four areas:

1. reliability of the radiochemical procedures,
2. contamination levels,
3. accuracy and
4. precision.

Each radiochemical procedure was thoroughly investigated prior to its adoption for routine processing of samples. All procedures were implemented, whenever necessary, to yield reasonably high chemical recoveries. This criterion was established to increase the sensitivity of analysis and to provide higher probability of obtaining satisfactory reproducibility. Most chemical yields ranged between 50 and 80 percent; analyses were suspect when the chemical yield dropped below 50 percent, and no physical losses were reported during the sample processing.

The final verification of the reliability of each analysis under HASP was the determination of the radiochemical purity of the separated element. As indicated in each analytical procedure, this was done by either radioactive decay measurements, aluminum absorber counting to identify the energy of the beta emission or by alpha particle and gamma ray spectroscopy. Under this system of control, it was virtually impossible for any radionuclide other than the one being determined to contaminate the separated element to any significant level and go undetected.

The second area of concern in the HASP quality control program was the radioactive contamination level existing in the laboratories. Such radioactivity can result from cross contamination between samples or from minute residues from spike experiments. If a sample was contaminated with strontium-90 for example, the strontium-90 analysis of that sample would be high, but no indication of this contamination in the radiochemical purity check would be evident. On the other hand, if the cerium-144 fraction of this same sample was contaminated with strontium-90 after the major decontaminating steps in the cerium-144 analyses were completed, this contamination would be detected because the sample would not exhibit cerium-144 radiochemical purity. To monitor against any contamination, blank samples consisting of unexposed filter papers were processed periodically for strontium-89, strontium-90, cerium-144, tungsten-185 and plutonium since early 1959. All of the 116 blank samples reflected either no detectable radioactivity or, in a few cases, minute contamination which was insignificant with regard to the activity levels of the samples processed.

The third item in the quality control program was accuracy of analysis which is based almost exclusively on the calibration of the counting equipment. The subject of calibration has been discussed in the previous section and is summarized in Table 3.17. Interlaboratory calibrations were also carried out whenever the opportunity arose. The Health and Safety Laboratory of the AEC conducted a cross-calibration with some of the following laboratories: HASL, Isotopes, Inc., Nuclear Science and Engineering Corporation, Tracerlab, Los Alamos Scientific Laboratory, University of California Radiation Laboratory, U. S. Naval Research Laboratory and an Air Force laboratory. Table 3.18 gives a comparison of the analytical results obtained by Isotopes, Inc. and one of the above mentioned laboratories and, on the whole, indicates good agreement. In another interlaboratory calibration, different quadrants from the same HASP filter paper were analyzed by Isotopes, Inc. and an Air Force laboratory. The results of these analyses are shown in Table 3.19. The agreement between the laboratories is good although there appears to be some heterogeneity in radionuclide concentration between quadrants 1 and 2 as reported by Isotopes, Inc.

Table 3.20 gives the partial results of an additional interlaboratory comparison in which aliquots of a sample solution were distributed to the participating laboratories. Some nuclides were omitted as not being pertinent or representative of an adequate intercomparison. The agreement between laboratories shown in Table 3.20 is satisfactory although the tungsten-185 and cerium-144 results of Isotopes, Inc. appear slightly low. However, in both cases, at least one of the other laboratories also reports data very similar to the Isotopes, Inc. values.

A further evaluation of the accuracy of the HASP analytical procedures was made by analyzing a standard uranium-235 fission solution which had been irradiated in the Los Alamos thermal column. The results of these analyses along with the theoretical values calculated from Blomeke's fission yields³⁷ are shown in Table 3.21 and exhibit good agreement.

The fourth and final aspect of the quality control program under HASP was the precision of routine analyses. To monitor this area, many HASP sample solutions or spike solutions were split and analyses performed on two or more aliquots. One half of each split was usually assigned to a different analyst. Table 3.22 gives the results of this program in terms of the average percent standard deviation from the mean of all the duplicate analyses. These data were calculated by the following equations:

$$S = \pm 100 \frac{\sqrt{\frac{\sum_{i=1}^n X - X_i}{n-1}}}{\bar{X}} \quad (3.35)$$

where \bar{X} = Average value of the duplicate analysis

X = Individual analysis

n = 2 for most cases

S = Percent standard deviation of the duplicate analysis.

The average percent standard deviation was calculated by:

$$\text{Average \% Standard Deviation} = \frac{\sum_{i=1}^n S_i}{m} \quad (3.36)$$

where m is the total number of duplicate analyses performed.

Table 3. 18. Interlaboratory Calibration Number 1

Sample No.	DPM Reported by Isotopes, Inc.	DPM Reported by a Participating Laboratory
Cesium-137		
1	1200	1540
2	750	633
3	2790	2870
4	956	962
Cerium-144		
1	4770	4600
2	2900	2740
3	4000	3990
Zirconium-95		
1	938	820
2	2500	2530
3	1560	1850
Strontium-90		
1	194	200
2	427	417
3	905	856

Table 3. 19. Comparison of Quadrant Analyses Between Laboratories

Sample No.	DPM Reported by Isotopes, Inc.			Average	DPM Reported by Air Force Laboratory, Quadrant 3
	Quadrant 1	Quadrant 2			
329					
	Sr ⁸⁹	6.70 x 10 ⁵ ± 2.96%	4.94 x 10 ⁵ ± 8.58%	5.82 x 10 ⁵ ± 21.3%	6.80 x 10 ⁵ ± 0.83%
	Sr ⁹⁰	7.26 x 10 ³ ± 6.62%	6.36 x 10 ⁴ ± 3.33%	6.81 x 10 ³ ± 9.34%	6.68 x 10 ³ ± 2.54%
	Ba ¹⁴⁰	18.8 x 10 ⁵ ± 2.26%	---	18.8 ± 10 ⁵ ± 2.26%	18.3 x 10 ⁵ ± 4.32%
SF05 - Sr ⁹⁰	56,700 ± 1.4%	---	---	---	59,000
SF09 - Sr ⁹⁰	12,600 ± 3.3%	---	---	---	16,200
SF10 - Sr ⁹⁰	11,000 ± 3.5%	---	---	---	12,300
SF11 - Sr ⁹⁰	11,500 ± 2.8%	---	---	---	10,600

Table 3. 20. Interlaboratory Calibration Number 2

Nuclide	Isotopes, Inc.	Disintegrations Per Minute Per Milliliter Reported by				
		Lab No. 1	Lab. No. 2	Lab. No. 3	Lab. No. 4	Lab. No. 5
Sr ⁹⁰	1060 ± 2.8%	1138 ± 0.8%	1081 ± 2.6%	970 ± 5.2%	---	937 ± 4.0%
Cs ¹³⁷	2440 ± 1.2%	2268 ± 0.9%	---	2700 ± 3.7%	2575 ± 4.4%	2249 ± 1.6%
Cs ¹⁴⁴	5250 ± 2.1%	6472 ± 0.7%	6810 ± 1.6%	6400 ± 1.6%	5564 ± 10.3%	6160 ± 8.9%
W ¹⁸¹	293000 ± 0.2%	291800 ± 1.5%	271800 ± 0.4%	283000 ± 1.1%	---	170000 ± 5.9%
W ¹⁸⁵	91600 ± 3.6%	94000 ± 1.1%	118000 ± 1.4%	123000 ± 2.4%	108800 ± 15%	77900 ± 2.3%
Pu	26.0 ± 4.2%	25.78 ± 2.2%	27.30 ± 5.2%	---	---	---

In calculating the data in Table 3,22, the percent standard deviation of the low activity samples were included even if the counting statistics for each aliquot were large enough to overlap the value of the other aliquot. Consequently, the reported average percent standard deviation represents, in most cases, somewhat of an upper limit of the error.

Since the errors of the calibration of the counting equipment was usually less than ± 5 percent and the average percent standard deviation or reproducibility of analysis was about ± 5 to 6 percent, the overall error of the routine radiochemical analysis was approximately ± 7 percent. The uncertainty accompanying each radiochemical analysis reported under HASP represents one Poisson standard deviation of the counting error for that sample, and does not reflect the ± 7 percent overall error discussed above.

Table 3. 21. Analyses of Standard Uranium-235 Fission Solution

Nuclide	Observed DPM/ml	Theoretical DPM/ml
Sr ⁸⁹	$3.33 \times 10^4 \pm 10\%$	3.24×10^4
Zr ⁹⁵	$3.74 \times 10^4 \pm 3\%$	3.70×10^4
Cs ¹³⁷	$169 \pm 5.1\%$	179
Ba ¹⁴⁰	$1.82 \times 10^5 \pm 2.1\%$	1.80×10^5
Ce ¹⁴⁴	$7.41 \times 10^3 \pm 4\%$	7.68×10^3

Table 3. 22. Reproducibility of Radiochemical Analyses

Nuclide	No. of Duplicate Analyses	Average % Standard Deviation
Sr ⁸⁹	23	6.6
Sr ⁹⁰	57	5.1
Zr ⁹⁵	20	4.0
Cs ¹³⁷	16	5.0
Ba ¹⁴⁰	19	4.5
Ce ¹⁴⁴	18	2.7
W ¹⁸⁵	26	3.8
Pu	15	3.4

REFERENCES

1. Van den Akker, J. A., A Study of the Filtration and Permeability Characteristics of IPC 1478 Filter Paper, DASA 1168, 1960.
2. Reid, E. G., Notes on the analysis of effects upon the performance of air filters (1949)
3. Reid, E. G., Experimentally Determined Characteristics of IPC Filters and Supports, LAMS-2243 (TID-4500 AEC), 1958
4. cf. Scheidegger A. E., Physics of Fluid Flow Through Porous Media (The MacMillan Company, New York, 1957).
5. Stern, S. C., H. W. Zeller, and A. I. Schekman, J. Colloid Sci., 15, 546 (1960)
6. Ketelle B. H., G. E. Boyd, J. Am. Chem. Soc., 69, 2800 (1947).
7. Street, Jr. K., G. T. Seaborg, J. Am. Chem. Soc. 72, 2790 (1950).
8. Diamond R. M., K. Street, Jr., G. T. Seaborg, J. Am. Chem. Soc. 76, 1461 (1954).
9. Thompson, S. G., B. G. Harvey, G. R. Chopping, G. T. Seaborg, J. Am. Chem. Soc., 76, 6229 (1954)
10. Diamond R. M., J. Am. Chem. Soc., 77, 2978 (1955).
11. Iddings, G. M., Radiochemical Procedures in use at the University of California Radiation Laboratory, Livermore, edited by Manfred Lindner, UCRL-4377: 7 (1954)
12. Shuli T. T., Collected Radiochemical Procedures, U.S. A.E.C LA-1566, 22 (1953)
13. Prestwood R. J., Collected Radiochemical Procedures, U.S. A.E.C LA-1566, 27 (1953)
14. Banner N. A., H. A. Potratz, Collected Radiochemical Procedures, U. S. A. E.C., LA-1566, 31 (1953)
15. Hillebrand W. F., G. E. F. Lundell, H. A. Bright, J. I. Hoffman, Applied Inorganic Analysis, (John Wiley and Sons, Inc., New York, 1953), Second Edition, 694-709
16. Farabee L. B., Proceedings for the Radiochemical Analysis of Strontium and Barium in Human Urine, U. S. A. E. C. ORNL-1932 (Sept. 6, 1955)

17. Burgers W. H., Collected Radiochemical Procedures, U. S. AEC, LA-1566 , 37 (1953)
18. Steinberg F. P., Radiochemical Studies: The Fission Products, (McGraw-Hill Book Company, New York, 1951), Book I, p. 482
19. Turk E. H., A Modified Radiochemical Strontium Procedure, ANL-5184 (Dec. 1953)
20. Turk E. H., A Modified Radiochemical Strontium Procedure, ANL-5184 (Dec. 1953)
21. Stanley G. W., Collected Radiochemical Procedures, U. S. AEC LA-1566, 100 (1953)
22. Finston H. L., J. Miskel, Annual Review of Nuclear Science, 5, 286 (1955)
23. Stanley C. W., G. P. Ford, Radiochemical Studies: The Fission Products, (McGraw-Hill Book Company, New York, 1951) Book I.
24. Ballou N. E., Radiochemical Studies: The Fission Products, (McGraw-Hill Book Company, New York, 1951) Books III p. 1563-1573
25. Kalkstein M. I., Air Force Cambridge Research Laboratories, Bedford, Mass., Private Communications, (March 1961)
26. Turk E. H., Revised Radiochemical Iodine Analytical Procedure, ANL-5271, (1954)
27. Glendenin L. E., K. F. Flynn, R. E. Buchanan, E. P. Steinberg, Anal. Chem., 27, 59 (1955)
28. Prauch T., Radiochemical Section, Hot Laboratory Division, Brookhaven National Laboratory, Private Communication, 1958
29. Kleinberg J., Collected Radiochemical Procedures, LA-1721 (Sept. 1954)
30. Glendenin L. E., K. F. Flynn, R. E. Buchanan, E. P. Steinberg, Anal. Chem., 27, 59 (1955)
31. Prestwood R. S., Collected Radiochemical Procedures, Los Alamos Scientific Laboratory Report, LA-1721, (Sept. 10, 1954)
32. Phillips G., E. N. Jenkins, The Removal of Plutonium Before the Analyses of Mixed Fission Products, Inorg. Nuclear Chem., 4, 220 (1957)
33. Gleason, G. I., Taylor, J. D., and Tabern, D. L., Nucleonics, 8, No. 5, 12 (1951)
34. Burt, B., Nucleonics, 5, No. 2, 28 (1949)
35. Martinez, P. and Senville, F. E., Rev. Sci. Instr., 31, 974 (1960)

36. Lazar, H. H., Davis, R. C., and Bell, P. R., *Nucleonics*, 14, 52 (1956)
37. Blomeke, J. O., "Nuclear Properties of Uranium-235 Fission Products," ORNL-1783 (1955)

Appendix A

Recalibration
Of The
U-2 Particulate Samplers

Stanford University
June 29, 1961

Report prepared by


Elliott G. Reid

Summary

Recalibration of the U-2 air samplers used in Project HASP was carried out at Edwards AFB during the summer of 1960 in an effort to resolve the apparent paradox of disproportionality between the mass rates of air flow through the two samplers - as determined by the original calibration of 1958 - and the radioactivity of simultaneously collected pairs of samples.

Recalibration resulted in the finding that, under all conditions of flight, the flow rates for both samplers were substantially and non-uniformly smaller than those previously determined. On the other hand, the proportionality of sample activities to the mass flow rates determined during collection was accurately verified under a typical set of flight conditions.

As no evidence of consequential error in either calibration has been discovered - with possible exception of the scanty data obtained at the highest altitudes explored in 1958 - it would appear that the discrepancies between original and recalibration results probably reflect significant changes in sampler operating conditions which have thus far escaped detection.

Introduction

During the summer of 1958, flight tests were carried out at Laughlin AFB, under the writer's direction, for the purpose of determining the rates of flow through the air samplers of a U-2 airplane as functions of altitude and flight speed. This information was required for evaluation of the samples of radioactive material then being collected in the stratospheric survey known as Project HASP.

As the consequence of much inclement weather, the only occasional availability of qualified pilots, the time lost in airplane maintenance - and a series of delays and malfunctions of such capriciously varied origin as to defy belief - only one entirely satisfactory test flight was completed within the nominal five-week period of airplane "availability" for calibration purposes.

The data obtained from this single flight were, of course, disappointingly meagre, but when the deduced flow rates were found to be reasonably self-consistent and to approximate previously predicted values, they were tentatively accepted as valid. However, suspicion of their validity began to develop before many months had passed.

This suspicion originated when it was noticed that radiochemical analyses of pairs of samples simultaneously collected on Nose and Hatch filters were usually characterized by ratios of total activity which differed consistently from the corresponding ratios of flight-determined mass flow rates. As the results of sample analysis continued to accumulate, it became unmistakably evident that particulate material was not being collected in proportion to the flight-determined mass rates of air-flow thru the samplers.

It was therefore decided, early in 1960, to undertake recalibration tests with the object of dispelling this anomaly.

Arrangements were made to carry out the tests with the same airplane which had been used in 1958 and to do the work at Edwards AFB where the important advantages of dependably good weather and competent test pilots would be available.

The present report is devoted to description of the 1960 recalibration work and to the presentation and discussion of the results derived therefrom.

Objectives

The primary objective of the recalibration flights was, of course, to verify or correct the sampler flow rate characteristics which had been deduced from the scanty data obtained in the single test of 1958.

The most important secondary objective was to determine whether the activities of samples simultaneously collected by Nose and Hatch filters were directly proportional to the corresponding mass rates of air flow. This was to be accomplished by making flights of considerable duration at fixed values of speed and altitude, determining the sampler flow rates throughout the period of filter exposure, analyzing the collected material and comparing the ratio of sample activities with the ratio of mass flow rates.

A third objective was to measure, at various speeds and altitudes, the pressures which prevail in the forward and aft sections of sampler ducts when internal flow is blocked by substituting solid metal plates for the usual filters. This information was primarily desired for purposes of airborne sampler design but was thought to have potential value in the explanation of differences between the normal operating characteristics of dissimilar, or differently located, samplers.

The final objective, which had actually become rather superfluous by the time the flight tests began, was to substantiate the method used for flow rate determination by reconciling the rates of flow through perforated plates (whose characteristics are negligibly affected by variations of Reynolds number) with those for filters (whose characteristics vary widely with Reynolds number). However, during the calibration of filters for the present program, an opportunity was seized to test a particular sample in air of both normal and reduced densities; these carefully controlled experiments provided ample evidence of the kind sought in the flight testing of perforated plates.

Method and Instrumentation

As in the 1958 experiments, determination of the rates of air flow through the filter-obstructed sampler ducts was accomplished by using pre-calibrated filters as metering devices. The theory and application of this method are fully set forth in Reference 1; it should therefore suffice to note here that the only quantities which have to be measured in order to determine flow rates in flight are the pressure drop across the filter and the temperature and pressure of the air at its upstream face.

To measure these pressures during the recalibration tests, use was made of the duct-wall orifices and pressure lines originally installed in 1958. Only one (inconsequential) modification was made in this installation: An additional pair of orifices was incorporated in the Nose duct; they were located immediately forward and aft of the filter plane and at the port-side ends of horizontal diameters. Figure I and p. 1 of Fig. II illustrate the locations of samplers, duct orifices and the equipment bay in which the indicating instruments and recording camera were located.

The NASA color-film pressure recorders used in 1958 were replaced, in 1960, by standard aircraft types of air speed indicators. This change was made, primarily, to eliminate the troublesome temperature sensitivity of the NASA recorders but it resulted, also, in substantial improvements of the legibility and accuracy of recording. An additional benefit derived from the substitution was that it enabled the consolidation of all instruments required for the indication of both flight and duct operating conditions in an already available, well-illuminated "instrument theatre" and thus made possible the recording of all their indications on single frames of motion picture film. The convenience and remarkable clarity of the records thus obtained by the use of a 35 mm camera is illustrated by the sample reproduced herein as Fig. III. Figure IV[†] is a photograph of the instrument installation in equipment bay of the test airplane.

[†] This figure not reproduced in this report

Anticipation of the need to measure small values of Δp_1 and Δp_4 with greater accuracy than that attainable with a 400 km air speed indicator prompted the installation of 150 km instruments in parallel with the ones required for the measurement of greater pressure differences. The necessity of preventing the imposition of excessive pressure differences upon these low-range instruments required augmentation of the previously used protective valve installation; the three diagrams of Fig. II illustrate the operation of the revised duct-pressure measuring system.

Test Program

A complete outline of the recalibration flight test program, together with notes on its execution, will be found in Table 1.†

Attention is drawn to the fact that the flight plans for Flights No. 2, 4 and 5 are identical with those for Flights No. 3, 7, and 6, respectively. The precaution of duplicating all flights was adopted to preclude, in so far as possible, the acceptance of erroneous data and to facilitate the identification of equipment malfunctions.

Another detail which deserves special attention is that Flights No. 2 and 3 were, in reality, "double flights." As will be seen in the "Fuel" column of the table, each of these flights was begun with full fuel tanks. Upon completion of the runs scheduled for various altitudes in the "Heavy" condition, the airplane was returned to a relatively low altitude and cruised there until the fuel on board had been reduced to a quantity barely sufficient to provide a reserve for landing after completion of the scheduled "Light" runs. The purpose of carrying out these tests at extreme values of airplane gross weight was to determine whether the sampler flow rates which occurred at fixed values of altitude and indicated air speed would be appreciably altered by the changes of angle of attack required to maintain those conditions of flight as the gross weight varied between the normal operating limits.

One addition to the tabular record must be made here. Preliminary examination of the record of Flight No. 6 indicated that either the Nose sampler or associated instruments had malfunctioned or failed. As the Hatch record agreed satisfactorily with its counterpart of Flight No. 5 - and only Flight No. 7 remained to be completed - it was decided, after phone consultation with Maj. Stebbins, not to delay termination of the test

Tables and Figures marked with † are not reproduced in this report

program unless sampler failure was found to have occurred, because the uniformity with which flight conditions had been maintained in the sample-collecting Flight No. 5 made the recording of sampler pressures in Flight No. 7 appear a mere formality. When no evidence of sampler malfunction could be found, Flight No. 7 was carried out in accordance with schedule on the following day, but no effort was made to obtain a film record of flight conditions.

The origin of the mishap described above was finally identified in an interesting way. A post-test study of the behavior of the Δp_2 indicator during Flight No. 6 led to a tentative explanation of its puzzling behavior. It was deduced that the p_2 side of this instrument must have been subjected to cabin pressure. A phone call to the Lockheed plant brought forth the report that, upon disassembly of the test equipment, the p_2 pressure line was found to have been severed, within the equipment bay, presumably as the result of its disarrangement during installation of the Hatch panel.

Reduction of Data

General

As most of the recalibration data have been reduced in accordance with the methods which were used and explained in Ref. 1, comments will be limited here to those required for the clarification of previously unused methods.

The tabulations of Recorded Data (Tables 1-8)[†] differ from those of Ref. 1 only in the units of the initially recorded values. The translation of these values into terms of equivalent pressures was accomplished, in both cases, by the use of appropriate instrument calibration curves. The ones used in the present work are reproduced as Figures 15-22. †

The flow rate calculations for Flights No. 2 and 3 (Tables 9-12)[†] are entirely analogous to those in Table 4 of Ref. 1. They differ, however, in one quantitative detail: In the present instance, the test-samples' pressure loss ($\sigma\Delta p/\omega^2$) values have been adjusted to reflect the effect of known differences between the weights per unit area of actual filters and calibrated samples. (See Tables 23 and 24)[†] The calculations of Tables 9-12[†] were carried to completion in order that the effects of airplane gross weight variation on sampler flow rates might be appraised. Such appraisal was considered prerequisite to the establishment of a logical basis for the estimates described immediately below.

Calculation of "Standard Flow Rates"

The writer was asked to estimate, by use of the recalibration test data, the flow rates which might be expected to prevail at various speeds and altitudes if the U-2 samplers were fitted with filters of "average weight" and operated in the hypothetical Standard Atmosphere.* The requested estimates have been

*"Average weight" was fixed at 14.30g/ft² by long-term averaging of filter-stock inspection data.

made by use of the data obtained in Flights No. 2 and 3 in conjunction with appropriate corrections for the effects of changes in filter characteristics and air temperatures.

The data used for this purpose were (for the Nose sampler) those defined by the curves of Fig. 1 and (for the Hatch) the mean ordinates of corresponding curves of Figures 2 and 3. Mean values were used in the latter case because it appeared impractical to include separate estimates of the effects of weight variation. However, consideration of the inequality of the maximum altitudes attained in the heavy and light conditions dictated the definition of mean values of Hatch pressures by the fairing of curves toward coincidence with the light-weight values in the uppermost altitude range. (See Tables 15[†] and 16[†] and Fig. 4[†])

The corrections which have been applied to these data are based on the following assumptions:

- a) Under conditions of fixed air density and velocity at the filter face, pressure drop varies directly with filter "density," i.e. with filter weight per unit area.
- b) Variation of filter density (and, hence, resistance) has a secondary effect upon the ratio of duct velocity to flight speed. This is assumed to result in an additional variation of pressure drop across the filter which is approximately proportional to $(k_1/k_0)^{1/4}$. (k represents the pressure loss coefficient and is directly proportional to filter density, W/A). This empirical correction is of minor importance and has been included primarily to indicate that the effect which it represents has not been ignored.
- c) Air characteristics will be modified in conformity with the assumed prevalence of Standard-Atmosphere values of temperature, density and sound speed at the pressure altitudes at which the test data were obtained.

Correction in accordance with assumption (a) has been effected by the use of a filter calibration curve which corresponds to a density of 14.30g/ft^2 . The compatible results of the derivation of such characteristics from two sets of sample test data will be found in the right-hand columns of Tables 23† and 24;† they have been plotted in Fig. 30.

Correction in accordance with (b) has been accomplished by multiplying the test values of Δp_{fN} and Δp_{fH} by $(k_1/k_0)^{1/4}$, i.e. by $[14.30/(W/A)_{\text{test}}]^{1/4}$.

The replacement of observed air characteristics by Standard values has been carried out in accordance with the "U.S. Extension of the ICAO Standard Atmosphere, 1958" which, within the range of altitudes involved, cannot be distinguished from the "ARDC Model Atmosphere, 1959."

Pressures In Blocked Sampler Ducts

For convenience of comparison, significant pressure differences recorded in Table 7† have been reduced to pressure coefficients of a somewhat unorthodox, but useful, form. As will be seen in the lowest section of the table, these coefficients have been evaluated by dividing the recorded pressure differences (Δp) by q_c - a quantity sometimes loosely called the "compressible dynamic pressure." Actually, q_c represents the difference between static and stagnation pressures, i.e. $q_c = H - p$.

Determination of $(\sigma \Delta p / \omega^2)_c$ As $f(\sigma V / \omega)_f$ and $f(\sigma V / \omega)_p$

The auxiliary calculations of Tables 19† and 20 had to be performed in order to obtain the data required for reconciliation of the rates of flow thru filters and perforated plates.

The method envisaged was to utilize the forward sections of the sampler ducts as venturi meters and to correlate rates of flow with the associated reductions of pressure at the duct entrance orifices. Otherwise stated, it was postulated that, for each of the samplers, there must exist an unique and characteristic relationship of the form

$$(\sigma\Delta p/\omega^2)_e = f (\sigma V/\omega)_x$$

wherein Δp represents the entrance pressure reduction (Δp_1 or Δp_4) and V stands for velocity at the filter plane. (The subscripts f and p are used - in place of x - to identify data from filter and perforated plate tests, respectively.) Experimental verification of such a relationship would consist in showing that curves of

$$(\sigma\Delta p/\omega^2)_e \quad \text{vs} \quad (\sigma V/\omega)_f$$

and of $(\sigma\Delta p/\omega^2)_e \quad \text{vs} \quad (\sigma V/\omega)_p$

were identical.

Data for filter flow (obtained in Flight No. 2 - heavy weight) have been reduced to the required form in Table 19.† Table 20 contains analogous calculations which utilize the perforated plate data of Flight No. 5. The calculations themselves follow the pattern of preceding flow rate calculations.

"Adjusted" Filter Characteristics

The filters intended for use in the recalibration flights were cut - under the writer's observation - from adjacent sections of a 36 in. width roll of Knowlton filter stock. All large (Hatch) filters were cut from one edge of the material, identically numbered small (Nose) filters were cut from the other edge at opposite locations and similarly numbered samples were taken out of the material between each pair. By this method it was hoped to obtain samples whose characteristics would be truly representative of those of the adjacent pair of filters.

The weighing of filters and samples dashed this hope. The density (wt. per unit area) of each small filter proved to be greater than that of the identically numbered large one and the density of each sample was found to be less than that of either member of the corresponding filter pair.

As only small samples (5 in. diam.) could be calibrated in the available test equipment, the characteristics of the filters used in flight necessarily had to be deduced from sample test data.

To make appropriate corrections for the known differences between filter and sample densities, the test value of pressure drop at each air speed was multiplied by the ratio of filter density to sample density. The justification for such correction will be found in the results of the experimental work reported in Reference 2.

Sample test data and adjusted characteristics for each of the filters used in Flights No. 2, 3 and 4 will be found in Tables 22-24[†] and corresponding curves are identified as Figures 24-29.[†]

Results

1. The flow rates thru both samplers, at all speeds and altitudes, were found to be considerably smaller than those determined in 1958. Greater discrepancies were found in the case of the Nose than in that of the Hatch and these were minimum at high speeds in the case of the Nose and at low ones in that of the Hatch.
2. The ratio of the flow rates thru Hatch and Nose samplers, determined during sample collection, differed by less than three per cent from the ratio of the total activities of the samples.
3. When the sampler ducts were blocked by solid plates, stagnation pressures prevailed forward of the plate in the Nose sampler but not in the corresponding section of the Hatch duct; the pressures aft of the plates differed little from that of the ambient atmosphere in both samplers.
4. Satisfactory reconciliation of the rates of flow through filters and perforated plates was not achieved. Convincing similarity characterized the two sets of results for the Nose but a quantitative discrepancy of about fifteen per cent remains unexplained. Filter flow data for the Hatch were reasonably consistent but the plate data were unexplainably scattered.
5. Item 4 might have caused serious concern if the results of testing a filter in air of various densities had not become available during preparation for the recalibration tests. These results, however, provided unimpeachable evidence of the validity of the method of flow rate determination employed in both the 1958 and 1960 sampler calibrations.

Discussion

The extraordinary accuracy with which the raw data of Flight No. 2 were duplicated in Flight No. 3 is illustrated by Figures 1-3. In Fig. 1 it will be seen that each pressure curve for the Nose sampler is equally well defined by either set of data (for heavy or light weight) obtained in either of the two flights. In the case of the Hatch sampler, Figures 2 and 3 indicate the prevalence of a small but unmistakable effect of weight upon duct pressures; in these charts it will be noted that the pressures which correspond to the two extremes of weight are unequivocally defined by the data from both flights.

Such repeatability in flight test work must be exceedingly rare - if the present example is not actually unique; at least, no comparable verification by repetition of flight tests has come to the writer's attention during nearly forty years of aerodynamic research. This aspect of the recalibration work is emphasized because it warrants the placing of great confidence in the basic data from which the present sampler flow rates have been deduced.

The credit for this achievement belongs entirely to Captains Knapp and Jacobson - of the Edwards AFB Flight Test staff - who so meticulously flew the duplicate missions, and to Mr. George Holden - of the NASA Ames Research Center - who coddled a dozen instruments into performing so perfectly before the recording camera.

The pressures defined by the curves of Figures 1-3 have been used in the estimation of Standard Flow Rates for the Nose and Hatch samplers. In the case of the latter, these estimates have been based upon the mean ordinates of corresponding curves in Figures 2 and 3; this was believed to be justified by the smallness of the effects of weight variation and the fact that such extremes of weight as those reached in the tests are unlikely to occur during the routine sampling operations of Project HASP.

Estimated Standard Flow Rates for the test altitudes are graphically presented as functions of M and $V_{cal.}$ in Figures 5† and 6;† they are alternatively defined as continuous functions of altitude by contours of $V_{cal.} = \text{const.}$ (in the coordinates altitude vs flow rate) in Figures 7 and 8. Comparison of these charts with the analogous ones of Ref. 1 will disclose some rather large differences which might be seriously misleading if it were not recognized that such discrepancies are due, in part, to differences between the flow-resistance characteristics of the filters used in the 1958 and 1960 calibration flights (unusually light filters were used in 1958) and that the correction of 1960 results to Standard-Atmosphere conditions further invalidates such direct comparisons.

Rigorously comparable results of the two calibrations could be obtained only by correcting one set in such fashion as to obtain the flow rates which would have occurred under all of the conditions which actually prevailed during the other calibration. As it can be quite simply shown that correction for all known differences of test conditions would fail to effect even approximate reconciliation of the two calibrations, that laborious task has not been undertaken and the proof of substantial discrepancy is given below.

The uncorrected flow rates deduced from the data recorded in Flights No. 2 and 3 are available in Tables 9-12.† Assuming that the external form of the airplane and the internal forms of the sampler ducts remained unchanged between the times of original and present calibrations, the only reasons for discrepancy between 1958 and 1960 flow rates at equal speeds and altitudes would appear to be differences between the characteristics of the filters employed on those occasions and such differences of atmospheric temperatures at equal pressure heights as may have prevailed at those times. A fortunate coincidence serves to eliminate the latter as a factor of any consequence: The atmospheric temperature profile which was recorded at Laughlin AFB during the time of the single 1958 calibration

flight differed surprisingly little from those recorded at Edwards AFB on the days of Flights No. 2 and 3 of the 1960 series. All three were typical of tropical maritime air masses, i.e. characterized by tropopause heights and temperatures of the order of 55,000 ft and -70 to -80 deg. C. This leaves filter characteristics as the only apparent source of substantial discrepancy between 1958 and 1960 test flow rates.

In Fig. 9, curves of ^{1958 and 1960} test-determined volumetric flow rates (Q) vs flight speeds ($V_{cal.}$) for both samplers have been plotted for several altitudes. Here, then, are the discrepancies ostensibly due to nothing but differences between filter characteristics. Careful comparison of the calibration curves for the filters which were used (Fig. 20, Ref. 1 and Figures 26† and 27† of this report) indicates that the maximum reductions of 1958 flow rates which are explainable on the basis of the heavier Nose filter used in 1960 amount to 9 per cent whereas the corresponding value for the Hatch is about 5 per cent. As flow rate discrepancies as great as 35 and 15 per cent are shown by Fig. 9 for the Nose and Hatch, respectively, it is evident that not more than one-third of the maximum disparity between the results of the two calibrations can be ascribed to filter effects. It is also considered significant that the shapes of the calibration curves for the 1958 and 1960 filters are such as to warrant the expectation that flow rate discrepancies would increase with flight speed - and that Fig. 9 shows the opposite trend to characterize the performance of the Nose sampler.

Thus, unless one is to accept the hypothesis that at least one of the two calibrations is grossly inaccurate, it must be acknowledged that much of the disparity illustrated by Fig. 9 is the result of causes still unidentified. The writer concurs in the latter alternative but the time allotted for the completion of this report has been insufficient to enable the substantiation of his opinion.

One very gratifying and reassuring result of the recalibration was the excellent agreement found between the ratios of

sample activities and flow rates determined during collection. From Table 17,† the ratio of average mass flow rates per unit area during Flight No. 4 was found to be

$$(\sigma V)_{FH}/(\sigma V)_{FN} = 4.87/5.22 = 0.933$$

When this value is multiplied by the ratio of filter areas, i.e.

$$A_H/A_N = 2.507$$

the mass flow rate ratio turns out to be

$$\underline{M_H/M_N} = 0.933 \times 2.507 = \underline{2.339}$$

Laboratory analysis of the samples collected during this flight yielded the following ratio of total- β activities -

$$\underline{\beta_H/\beta_N} = \underline{2.396}$$

The percentage difference between these values is

$$\epsilon = 100 [1 - (2.396/2.339)] = 2.4 \text{ per cent}$$

It seems worth noting that the samples collected during Flight No. 7 were also analyzed and that the activity ratio was found in that case to be

$$\beta_H/\beta_N = 2.350$$

which is interpreted as excellent verification of the result obtained from Flight No. 4. Altho no flow rate data were recorded during Flight No. 7, it is reasonable to assume that the ratio determined in Flight No. 4 would have been closely duplicated since the same flight plan was followed and the filter weights differed negligibly from those in the previous sampling flight. On the basis of this assumption, the discrepancy between the flow rate and activity ratios for Flight No. 7 would be

$$\epsilon = 100 [1 - (2.350/2.339)] = 0.5 \text{ per cent}$$

The direct proportionality of sample activity to air mass flow rate thus appears to be satisfactorily verified.

The pressures in the blocked sampler ducts appears to warrant special comment in view of the still unexplained flow

rate discrepancies. These data, obtained in Flight No. 5, are presented in graphical form as Fig. 10.† The peculiar variation of the coefficient $\Delta p_{fH}/q_c$ with velocity and, particularly, its small values at large flight speeds are quite contrary to expectation - and unlike the characteristics of its Nose-counterpart, $\Delta p_{fN}/q_c$. The additional fact that stagnation pressure is not attained in the blocked Hatch duct (i.e. $\Delta p_5 \neq 0$, see Table 7) is a highly suspicious circumstance which would appear to merit further investigation.

The disappointing results of the perforated plate tests (Flight No. 5) are presented with no comment in addition to that made under Reduction of Data. The failure to effect complete reconciliation of filter and perforated plate flow rates is illustrated by Fig. 11.†

References

1. Reid, Elliott G.: Flight Calibration of the U-2 Particulate Samplers; Classified Report, April 1959.
2. Reid, Elliott G.: Experimentally Determined Characteristics of IPC Filters and Supports; Los Alamos Scientific Laboratory, LAMS-2243, 1958.
3. Ames Research Staff: Equations, Tables and Charts for Compressible Flow; NACA Technical Report No. 1135, 1953.
4. Minzner, R. A., W. S. Ripley and T. P. Condon: U.S. Extension to the ICAO Standard Atmosphere; U.S. Government Printing Office, 1958.

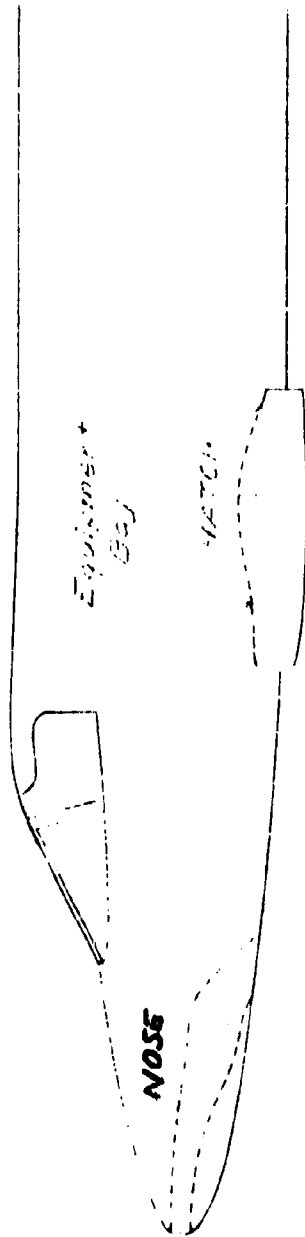
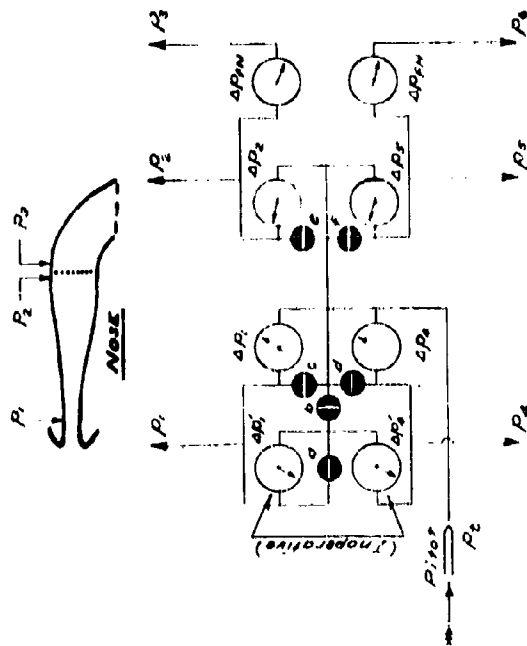
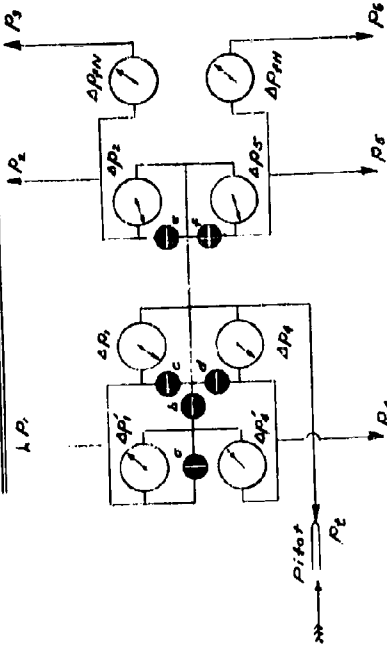


FIG. I- Sampler Locations

DUCT PRESSURE RECORDING SYSTEM



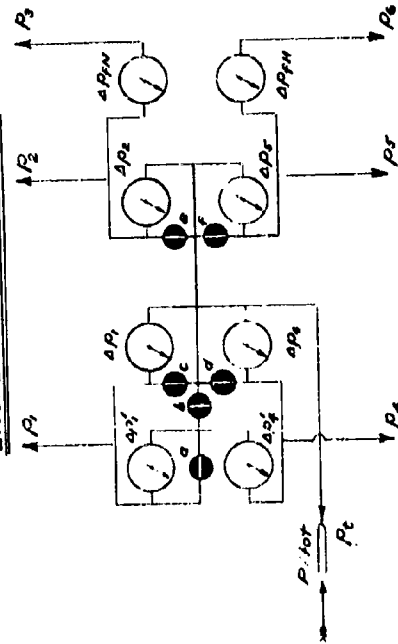
SENSITIVE RECORDING



NORMAL RECORDING CONFIGURATION

- P_t = Total pressure
 - $\Delta P_1 = P_2 - P_1$
 - $\Delta P_2 = P_3 - P_2$
 - $\Delta P_3 = P_4 - P_3$
 - $\Delta P_4 = P_5 - P_4$
 - $\Delta P_5 = P_6 - P_5$
 - $\Delta P_6 = P_5 - P_6$
- a - Poppet valve; normally open - solenoid closed; actuated by pilot's switch
- b - As in a - but normally closed
- c, d, e, f - Poppet valves; normally open - solenoid closed; actuated by entry-valve micro-switches

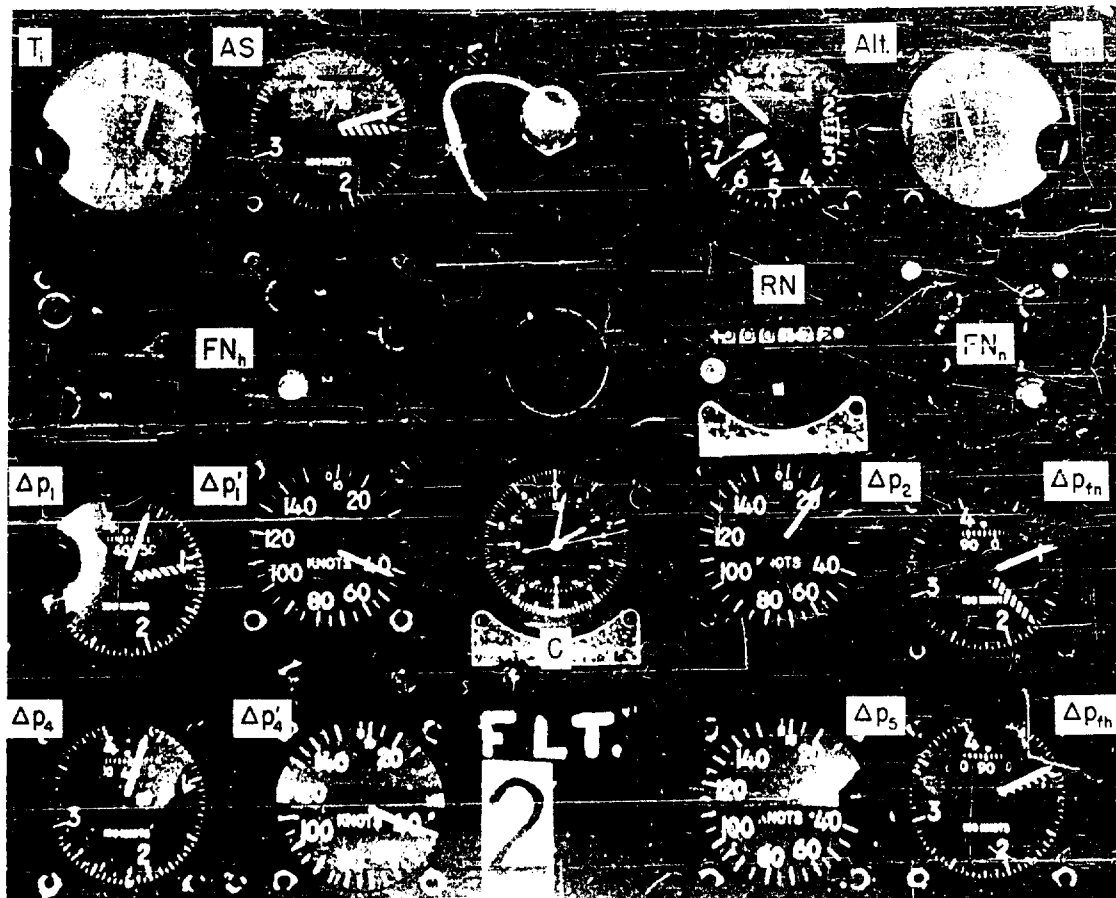
INOPERATIVE - BALANCED



Notes: Also balanced if positions of valves a, b are reversed - i.e. left in 'sensitive' positions

FIG. II - Plumbing, p. 2

FIG. I - Original Sketches Of 'Plumbing', p. 1



<u>Symbol</u>	<u>Quantity Measured</u>	<u>Reading</u>	<u>Corr. Value or Equivalent</u>
RN	Record Number	172	
C	Clock Time	2:02:13 PM	
T_i	Instrument temperature	15°C	16°C
AS	Calibrated air speed	104 kn	399 kn (true)
Alt.	Pressure altitude	66,880 ft	66,720 ft
$T_{a(t)}$	Outside air temperature (total)	-36°C	-35°C
FN_h	Filter number (Hatch)	2	2
FN_n	Filter number (Nose)	2	2
Δp_1	Duct inlet pressure (Nose)	42 kn	6.3 psf*
$\Delta p_1'$	Same; sensitive instrument	41.5 kn	6.4 " *
Δp_2	Pressure at filter face (Nose)	22 kn	1.7 " *
Δp_{fn}	Pressure drop across filter (Nose)	96 kn	30.4 "
Δp_4	Duct inlet pressure (Hatch)	39 kn	5.2 " *
$\Delta p_4'$	Same; sensitive instrument	40.5 kn	5.6 " *
Δp_5	Pressure at filter face (Hatch)	29 kn	3.4 " *
Δp_{fn}	Pressure drop across filter (Hatch)	91 kn	28.9 "

* Quantities so identified are deficiencies of local pressure with reference to total pressure.

Figure III Sample Record

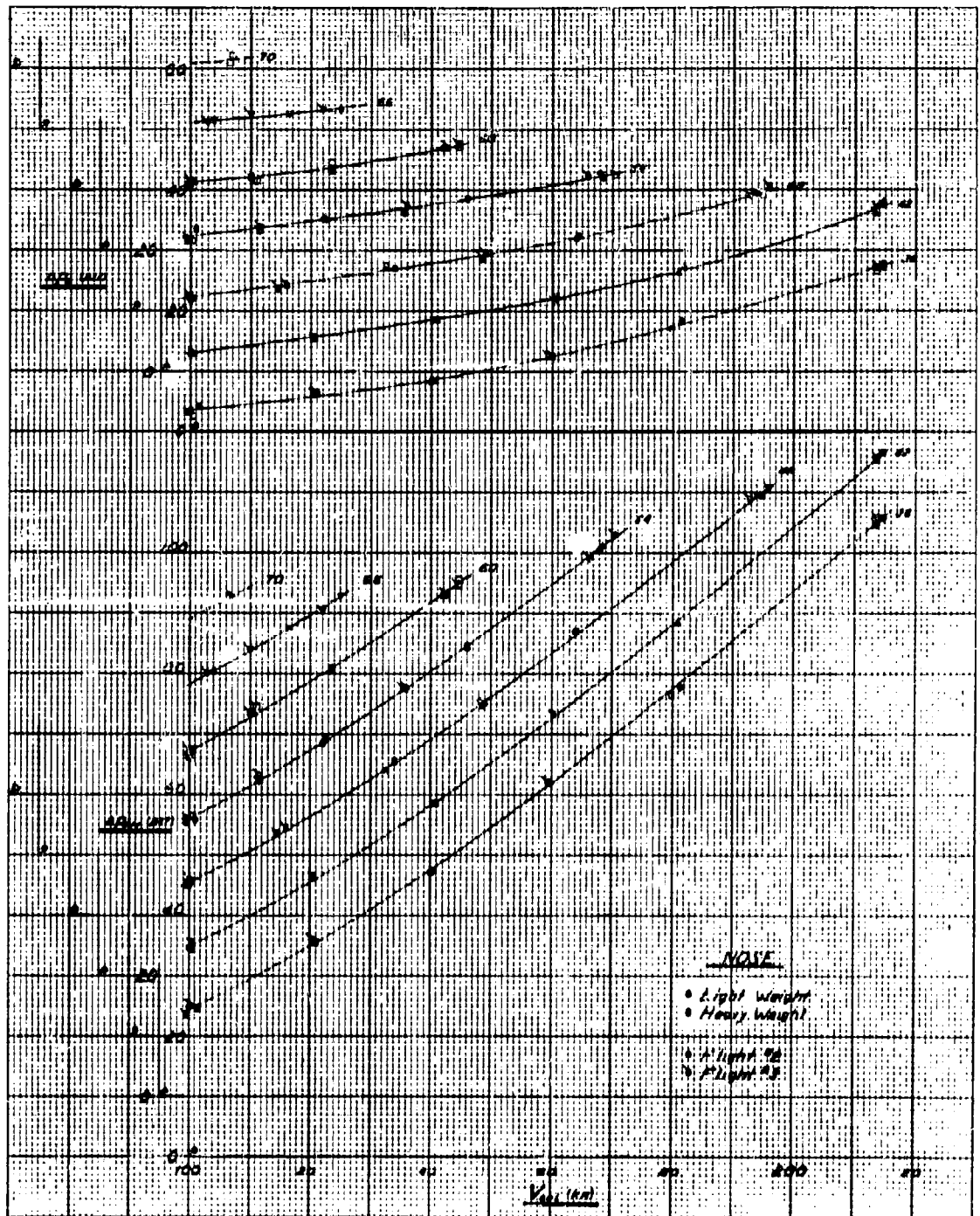
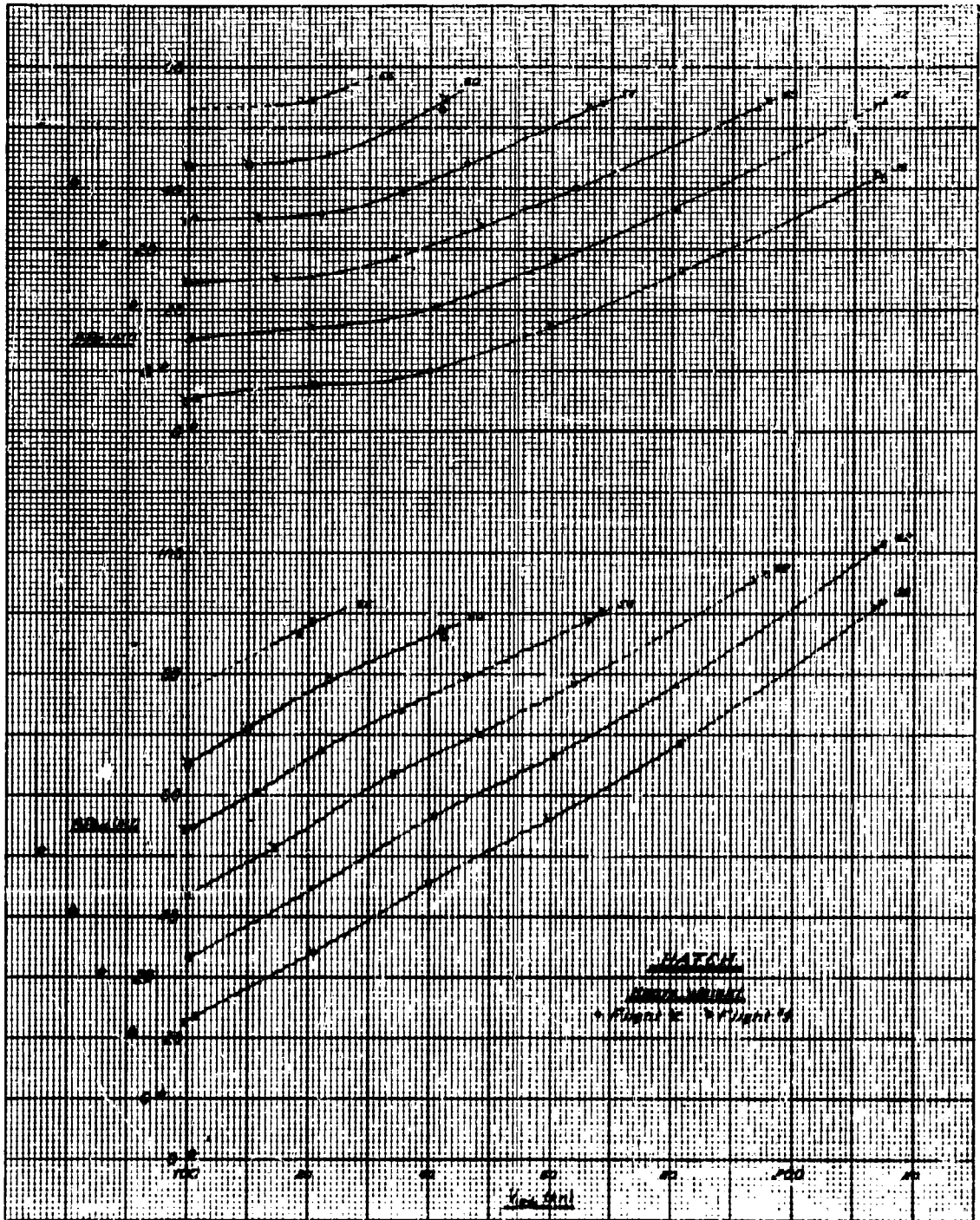
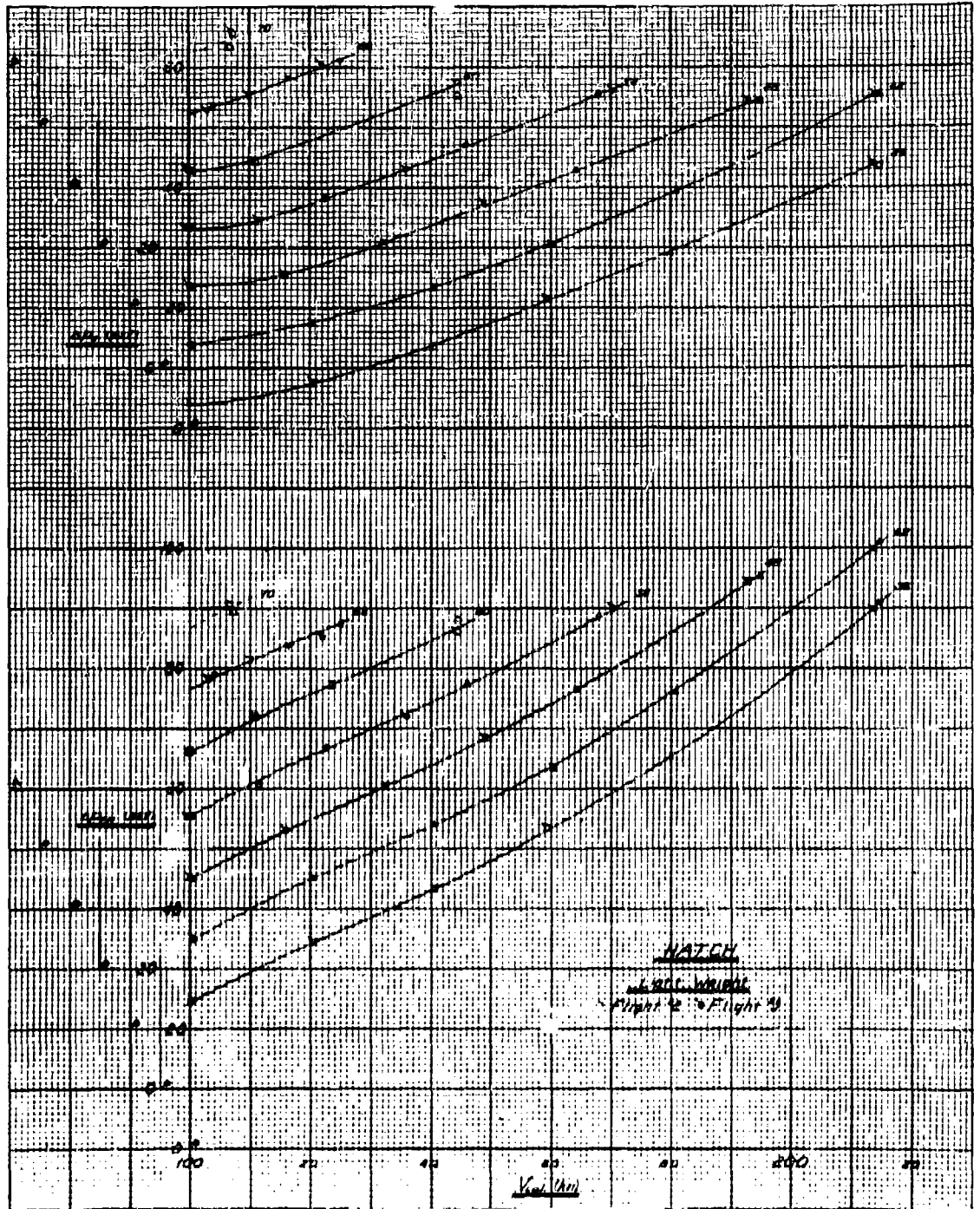


Fig. 1- Raw Data, Flights 2&3, Nose



Figs. 2,3- Raw Data, Flights 283, Hatch



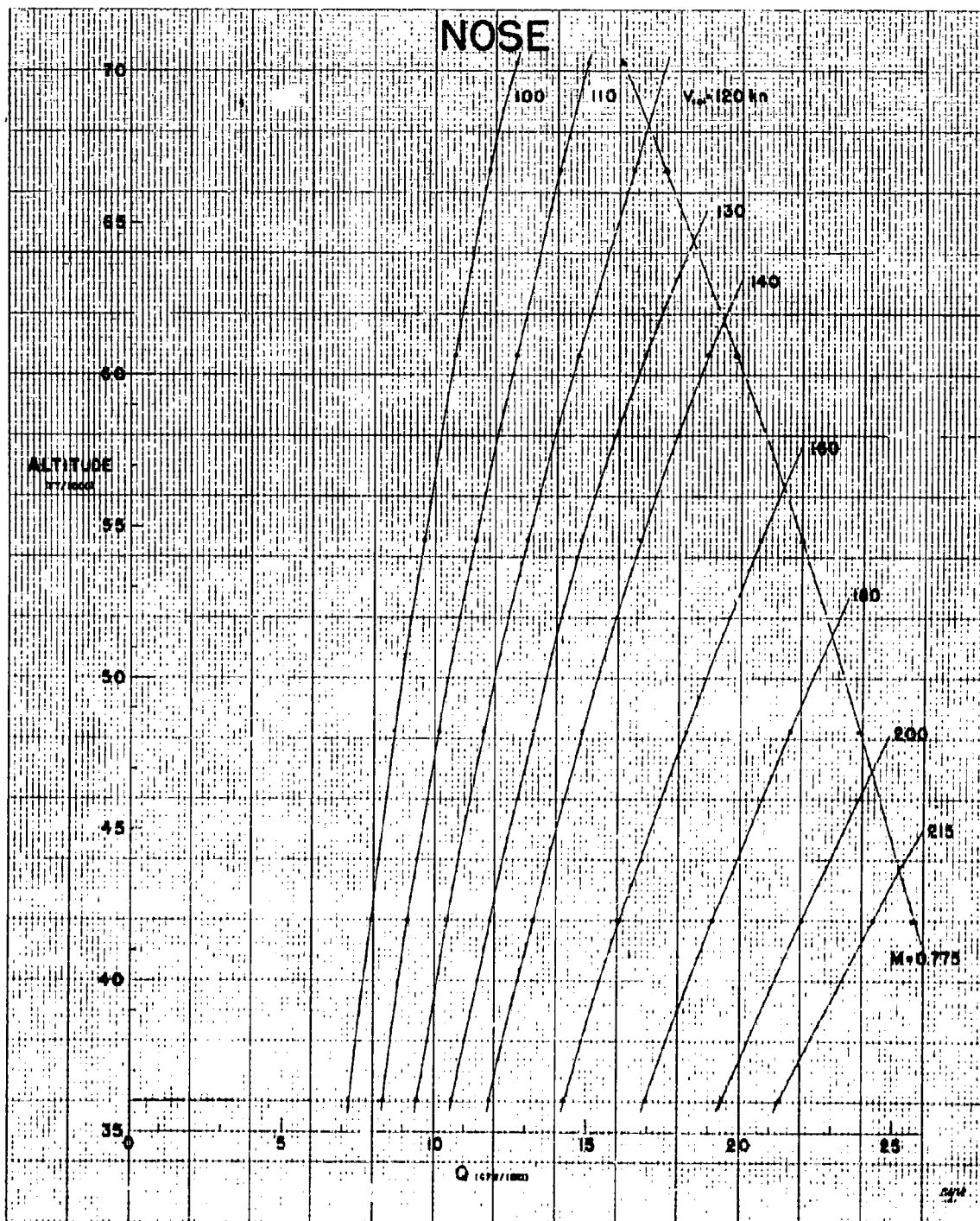


Fig. 7- Standard Flow Rates

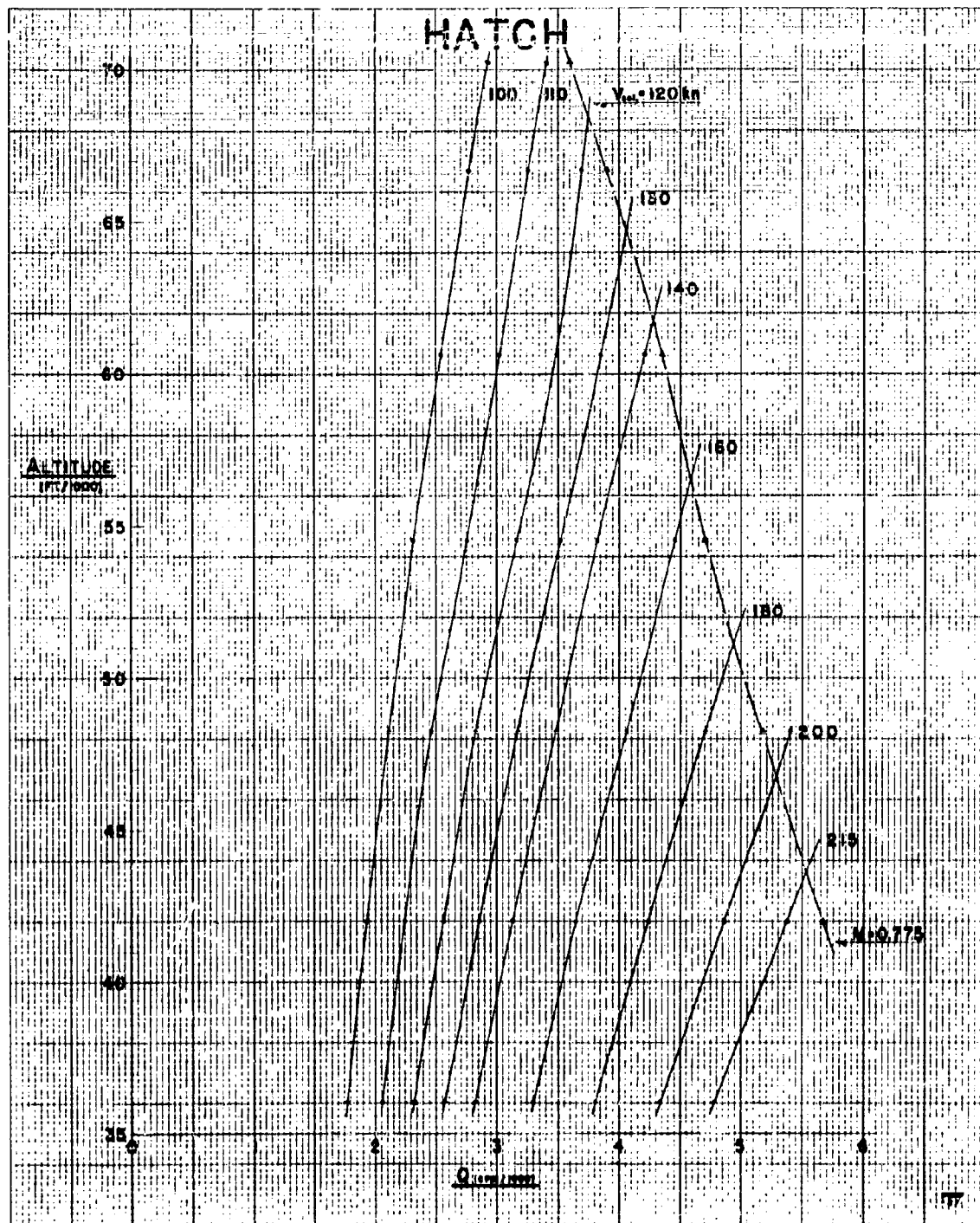


Fig. 8- Standard Flow Rates

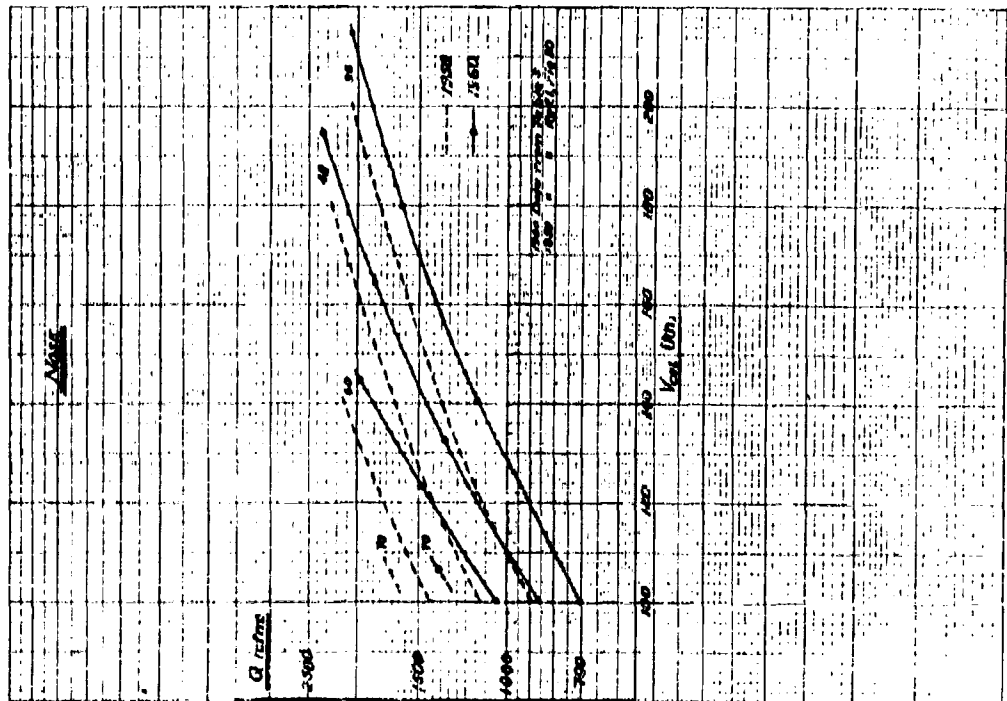
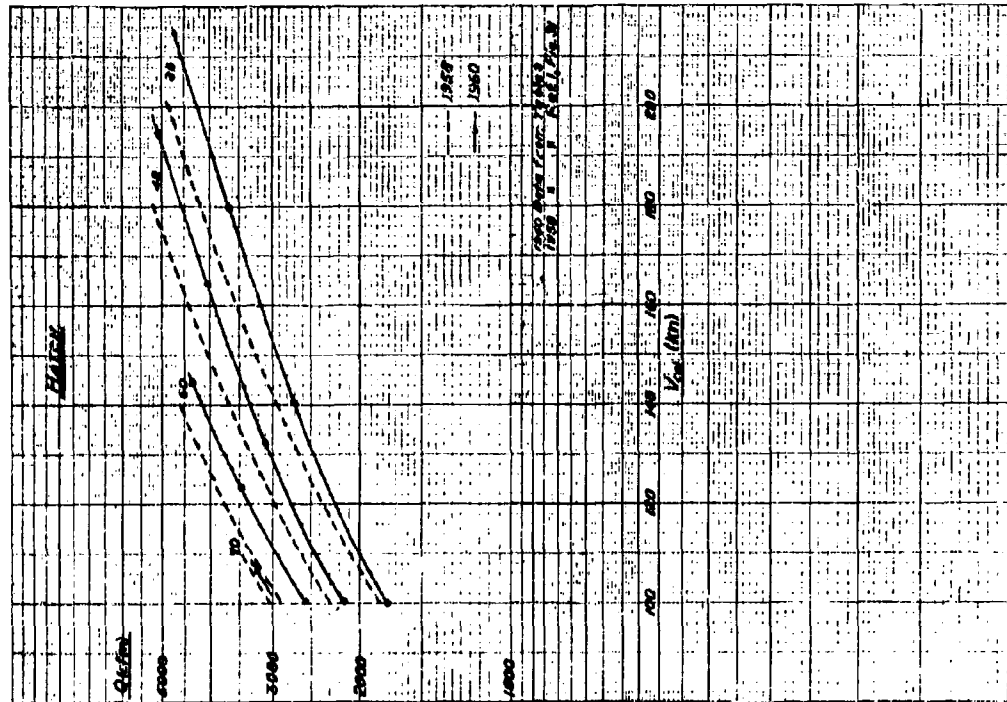
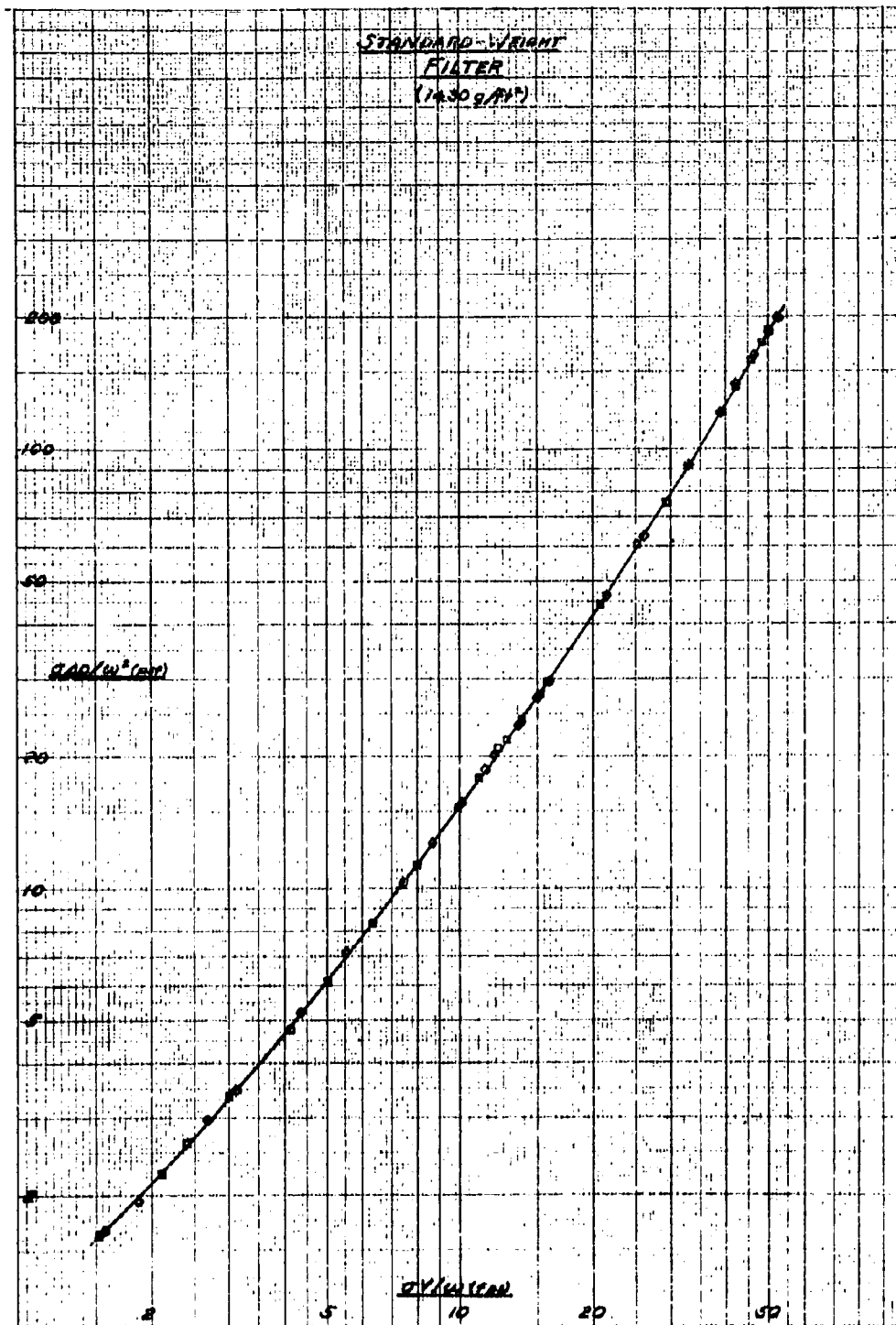


Fig. 9- Comparison Of Results



Notes on Table 13

Press. Alt.	Average of test run press. altitudes
V _{cal.}	Arbitrarily selected values
p	Standard value corresp. to press. alt.
q _c	" " " " V _{cal.}
H	H = p + q _c
p/H	Quotient
M	From Ref. 3; value corresp. to p/H
σ _{std}	From Ref. 4; value corresp. to press. alt.
T _{std}	" " " " " " " "
T/T _t	From Ref. 3; value corresp. to M
T _t	T _t = T/(T/T _t)
ω _f	Relative viscosity at T _t ; values from Ref. 4
ω _f ²	From ω

NOSE

Δp ₂	From Table 14†
p ₂	p ₂ = H - Δp ₂
σ _f	σ _f = 0.1362 p ₂ (psf)/T _t (°K)
Δp _{f0}	From Table 14
(κ ₁ /κ ₀) ^{1/4}	Correction to Δp _f explained in "Red. of Data"
Δp _{f1}	Value corrected to consistency with Std. Wt. Filter
(σΔp/ω ²) _f	Quotient
(σV/ω) _f	From proper filter calibr. chart; value corresp. to (σΔp/ω ²) _f
(σV) _f	(σV) _f = (σV/ω) _f x ω _f
Q ₀	Q ₀ = 32.922 (σV) _f
Q	Q = Q ₀ /σ

HATCH

Δp ₅	From Table 15 †
p ₅	p ₅ = H - Δp ₅
σ _f	σ _f = 0.1362 p ₅ (psf)/T _t (°K)
Δp _{f0}	From Table 16 †
(κ ₁ /κ ₀) ^{1/4}	See note, above
Δp _{f1}	" " " "

Subsequent calculations as in Nose section except that -

$$Q_0 (\text{Hatch}) = 82.524 (\sigma V)_{fH}$$

CALCULATION OF STANDARD FLOW RATES

AIRCLEAR (Mg/l) Filters - Std Atmosphere

	100	110	120	130	140	150	160	170	180	190	200	215	230	250
100	100	110	120	130	140	150	160	170	180	190	200	215	230	250
110	110	121	132	143	154	165	176	187	198	209	220	236	252	269
120	120	132	144	156	168	180	192	204	216	228	240	258	276	294
130	130	143	156	169	182	195	208	221	234	247	260	280	299	318
140	140	154	168	182	196	210	224	238	252	266	280	302	324	346
150	150	165	180	195	210	225	240	255	270	285	300	324	348	372
160	160	176	192	208	224	240	256	272	288	304	320	348	376	404
170	170	187	204	221	238	255	272	289	306	323	340	372	404	436
180	180	198	216	234	252	270	288	306	324	342	360	396	432	468
190	190	209	228	247	266	285	304	323	342	361	380	420	460	500
200	200	220	240	260	280	300	320	340	360	380	400	450	500	550
215	215	236	258	280	302	324	346	368	390	412	434	486	538	590
230	230	252	276	300	324	348	372	396	420	444	468	534	600	666
250	250	276	304	332	360	388	416	444	472	500	528	606	684	762

STANDARD FLOW RATES

	64,550				60,650				66,750				70,850				
	100	120	150	180	100	120	150	180	100	110	120	130	140	150	160	170	180
(GPM)	196	237	282	330	185	218	257	300	108.5	125	142	160	175	195	215	235	
(GPM)	340	413	492	578	340	413	492	578	340	413	492	578	672	721	779	838	
(GPM)	500	600	712	838	500	600	712	838	500	600	712	838	968	1035	1102	1170	
(GPM)	652	783	928	1088	652	783	928	1088	652	783	928	1088	1258	1335	1412	1490	
(GPM)	812	978	1158	1352	812	978	1158	1352	812	978	1158	1352	1552	1645	1738	1832	
(GPM)	980	1188	1412	1652	980	1188	1412	1652	980	1188	1412	1652	1872	1985	2098	2212	
(GPM)	1152	1392	1652	1932	1152	1392	1652	1932	1152	1392	1652	1932	2172	2295	2418	2542	
(GPM)	1332	1608	1908	2232	1332	1608	1908	2232	1332	1608	1908	2232	2492	2625	2758	2892	
(GPM)	1520	1832	2172	2552	1520	1832	2172	2552	1520	1832	2172	2552	2832	2975	3118	3262	
(GPM)	1712	2064	2432	2832	1712	2064	2432	2832	1712	2064	2432	2832	3132	3285	3428	3572	
(GPM)	1912	2304	2692	3112	1912	2304	2692	3112	1912	2304	2692	3112	3432	3595	3738	3882	
(GPM)	2120	2544	2972	3432	2120	2544	2972	3432	2120	2544	2972	3432	3732	3905	4048	4192	
(GPM)	2332	2792	3252	3742	2332	2792	3252	3742	2332	2792	3252	3742	4042	4225	4368	4512	
(GPM)	2552	3048	3528	4048	2552	3048	3528	4048	2552	3048	3528	4048	4342	4535	4678	4822	
(GPM)	2780	3304	3808	4352	2780	3304	3808	4352	2780	3304	3808	4352	4642	4845	4988	5132	
(GPM)	3012	3568	4092	4672	3012	3568	4092	4672	3012	3568	4092	4672	4962	5175	5318	5462	
(GPM)	3252	3832	4388	4992	3252	3832	4388	4992	3252	3832	4388	4992	5282	5505	5648	5792	
(GPM)	3500	4104	4688	5332	3500	4104	4688	5332	3500	4104	4688	5332	5622	5855	5998	6142	
(GPM)	3752	4384	4988	5672	3752	4384	4988	5672	3752	4384	4988	5672	5962	6205	6348	6492	
(GPM)	4012	4632	5252	5952	4012	4632	5252	5952	4012	4632	5252	5952	6242	6495	6638	6782	
(GPM)	4280	4928	5568	6252	4280	4928	5568	6252	4280	4928	5568	6252	6542	6805	6948	7092	
(GPM)	4552	5224	5888	6612	4552	5224	5888	6612	4552	5224	5888	6612	6902	7175	7318	7462	
(GPM)	4832	5528	6208	6932	4832	5528	6208	6932	4832	5528	6208	6932	7222	7505	7648	7792	
(GPM)	5120	5848	6548	7308	5120	5848	6548	7308	5120	5848	6548	7308	7602	7895	8038	8182	
(GPM)	5412	6168	6888	7688	5412	6168	6888	7688	5412	6168	6888	7688	7982	8285	8428	8572	
(GPM)	5712	6496	7232	8072	5712	6496	7232	8072	5712	6496	7232	8072	8372	8685	8828	8972	
(GPM)	6020	6832	7588	8472	6020	6832	7588	8472	6020	6832	7588	8472	8772	9095	9238	9382	
(GPM)	6332	7176	7952	8888	6332	7176	7952	8888	6332	7176	7952	8888	9182	9515	9658	9802	
(GPM)	6652	7528	8328	9312	6652	7528	8328	9312	6652	7528	8328	9312	9602	9945	10088	10232	
(GPM)	6980	7888	8708	9732	6980	7888	8708	9732	6980	7888	8708	9732	10022	10375	10518	10662	
(GPM)	7312	8248	9088	10172	7312	8248	9088	10172	7312	8248	9088	10172	10462	10825	10968	11112	
(GPM)	7652	8616	9472	10608	7652	8616	9472	10608	7652	8616	9472	10608	10892	11265	11408	11552	
(GPM)	8000	8992	9868	11052	8000	8992	9868	11052	8000	8992	9868	11052	11332	11715	11858	12002	
(GPM)	8352	9368	10268	11408	8352	9368	10268	11408	8352	9368	10268	11408	11682	12075	12218	12362	
(GPM)	8712	9752	10688	11872	8712	9752	10688	11872	8712	9752	10688	11872	12142	12545	12688	12832	
(GPM)	9080	10148	11108	12312	9080	10148	11108	12312	9080	10148	11108	12312	12582	13005	13148	13292	
(GPM)	9452	10544	11512	12752	9452	10544	11512	12752	9452	10544	11512	12752	13022	13455	13598	13742	
(GPM)	9832	10948	11932	13212	9832	10948	11932	13212	9832	10948	11932	13212	13482	13925	14068	14212	
(GPM)	10220	11352	12348	13732	10220	11352	12348	13732	10220	11352	12348	13732	14002	14455	14598	14742	
(GPM)	10612	11768	12772	14208	10612	11768	12772	14208	10612	11768	12772	14208	14482	14945	15088	15232	
(GPM)	11012	12192	13208	14692	11012	12192	13208	14692	11012	12192	13208	14692	14962	15435	15578	15722	
(GPM)	11420	12624	13652	15208	11420	12624	13652	15208	11420	12624	13652	15208	15482	15965	16108	16252	
(GPM)	11832	13056	14108	15752	11832	13056	14108	15752	11832	13056	14108	15752	16002	16495	16638	16782	
(GPM)	12252	13512	14588	16328	12252	13512	14588	16328	12252	13512	14588	16328	16482	17005	17148	17292	
(GPM)	12680	13968	15068	16932	12680	13968	15068	16932	12680	13968	15068	16932	17202	17715	17858	18002	
(GPM)	13112	14424	15548	17568	13112	14424	15548	17568	13112	14424	15548	17568	17682	18215	18358	18502	
(GPM)	13552	14888	16032	18192	13552	14888	16032	18192	13552	14888	16032	18192	18002	18545	18688	18832	
(GPM)	14000	15368	16548	18852	14000	15368	16548	18852	14000	15368	16548	18852	18882	19435	19578	19722	
(GPM)	14452	15848	17048	19508	14452	15848	17048	19508	14452	15848	17048	19508	19382	19945	20088	20232	
(GPM)	14912	16336	17552	20192	14912	16336	17552	20192	14912	16336	17552	20192	19882	20455	20598	20742	
(GPM)	15380	16848	18088	20912	15380	16848	18088	20912	15380	16848	18088	20912	20382	20965	21108	21252	
(GPM)	15852	17384	18648	21672	15852	17384	18648	21672	15852	17384	18648	21672	21082	21675	21818	21962	
(GPM)	16332	17944	19228	22472	16332	17944	19228	22472	16332	17944	19228	22472	21582	22185	22328	22472	
(GPM)	16820	18528	19832	23312	16820	18528	19832	23312	16820	18528	19832	23312	22082	22695	22838	22982	
(GPM)	17312	19136	20468	24192	17312	19136	20468	24192	17312	19136	20468	24192	22582	23205	23348	23492	
(GPM)	17812	19768	21128	25112	17812	19768	21128	25112	17812	19768	21128	25112	23082	23715	23858	24002	
(GPM)	18320	20424	21808	26072	18320	20424	21808	26072	18320	20424	21808	26072	23582	24225	24368	24512	
(GPM)	18832	21104	22512	27072	18832	21104	22512	27072	18832	21104	22512	27072	24082	24735	24878	25022	
(GPM)	19352	21808	23248	28112	19352	21808	23248	28112	19352	21808	23248	28112	24582	25245	25388	25532	
(GPM)	19880	22536	24008	29192	19880	22536	24008	29192	19880	22536	24008	29192	25082	25755	25898	26042	
(GPM)	20412	23288	24788	30312	20412	23288	24788	30312	20412	23288	24788	30312	25582	26265	26408	26552	
(GPM)	20952	24064	25592	31472	20952	24064	25592	31472	20952	24064	25592	31472	26082	26775	26918	27062	
(GPM)	21500	24864	26428	32672	21500	24864	26428	32672	21500	24864	26428	32672	26582	27285	27428	27572	
(GPM)	22052	25688	27288	33912	22052	25688	27288	33912	22052	25688	27288	33912	27082	27795	27938	28082	
(GPM)	22612	26536	28112	35192	22612	26536	28112	35192	22612	26536	28112	35192	27582	28305	28448	28592	
(GPM)	23180	27408	28968	36512	23180	27408	28968	36512	23180	27408	28968	36512	28082	28815	28958	29102	
(GPM)	23752	28															

Determination of (Cadm) As (10/10/10)

FLIGHT 15 - PERF. FLIGHT

	10	11	12	13	14	15	16	17	18	19	20	21	22	23	24	25	26	27	28	29	30	31	32	33	34	35	36	37	38	39	40	41	42	43	44	45	46	47	48	49	50	51	52	53	54	55	56	57	58	59	60	61	62	63	64	65	66	67	68	69	70	71	72	73	74	75	76	77	78	79	80	81	82	83	84	85	86	87	88	89	90	91	92	93	94	95	96	97	98	99	100	101	102	103	104	105	106	107	108	109	110	111	112	113	114	115	116	117	118	119	120
1000	1010	1020	1030	1040	1050	1060	1070	1080	1090	1100	1110	1120	1130	1140	1150	1160	1170	1180	1190	1200	1210	1220	1230	1240	1250	1260	1270	1280	1290	1300	1310	1320	1330	1340	1350	1360	1370	1380	1390	1400	1410	1420	1430	1440	1450	1460	1470	1480	1490	1500	1510	1520	1530	1540	1550	1560	1570	1580	1590	1600	1610	1620	1630	1640	1650	1660	1670	1680	1690	1700	1710	1720	1730	1740	1750	1760	1770	1780	1790	1800	1810	1820	1830	1840	1850	1860	1870	1880	1890	1900	1910	1920	1930	1940	1950	1960	1970	1980	1990	2000											
1000	1010	1020	1030	1040	1050	1060	1070	1080	1090	1100	1110	1120	1130	1140	1150	1160	1170	1180	1190	1200	1210	1220	1230	1240	1250	1260	1270	1280	1290	1300	1310	1320	1330	1340	1350	1360	1370	1380	1390	1400	1410	1420	1430	1440	1450	1460	1470	1480	1490	1500	1510	1520	1530	1540	1550	1560	1570	1580	1590	1600	1610	1620	1630	1640	1650	1660	1670	1680	1690	1700	1710	1720	1730	1740	1750	1760	1770	1780	1790	1800	1810	1820	1830	1840	1850	1860	1870	1880	1890	1900	1910	1920	1930	1940	1950	1960	1970	1980	1990	2000											

NOTE

MARKS

11.8 Marks

